



11.8-m Ridge off Mary Sachs Entrance (March 28, 2014)

2013-14 FREEZE-UP STUDY
OF THE
ALASKAN BEAUFORT AND CHUKCHI SEAS

Coastal Frontiers Corporation
882A Patriot Drive
Moorpark, CA 93021-3544
(818) 341-8133

Vaudrey & Associates, Inc.
1685 El Caserio Court
San Luis Obispo, CA 93401
(805) 544-9399

2013-14 FREEZE-UP STUDY OF THE ALASKAN BEAUFORT AND CHUKCHI SEAS

FINAL REPORT

Prepared for:

Shell Gulf of Mexico Inc. and Shell Offshore Inc.
Houston, Texas

U.S. Department of the Interior, Bureau of Safety and Environmental Enforcement
Washington, D.C.

Prepared by:

Coastal Frontiers Corporation
Moorpark, California

Vaudrey & Associates, Inc.
San Luis Obispo, California

November 2014

Expiration of Confidentiality: November 1, 2019

*This study was funded in part by the Bureau of Safety and Environmental Enforcement (BSEE), U.S. Department of the Interior, Washington, D.C., under Contract Number **E14PC00003**.*

This draft report has not been reviewed by the Bureau of Safety and Environmental Enforcement (BSEE), nor has it been approved for publication. Approval, when given, does not signify that the contents necessarily reflect the views and policies of the Bureau, nor does mention of trade names or commercial products constitute endorsement or recommendation for use.

EXECUTIVE SUMMARY

This report describes a joint-industry investigation of the ice conditions that prevailed in the Alaskan Beaufort and Chukchi Seas during the 2013-14 freeze-up season. The study was performed on behalf of Shell Gulf of Mexico Inc. and Shell Offshore Inc. (collectively, “Shell”) and the U.S. Department of the Interior, Bureau of Safety and Environmental Enforcement (“BSEE”), by Coastal Frontiers Corporation and Vaudrey & Associates, Inc.

The 2013-14 study was the fifth in a series of annual freeze-up investigations that began in 2009-10. It was designed to address five specific objectives:

1. Describe the ice conditions that evolve during the freeze-up and early winter seasons, including the development of the landfast ice zone and early shear zone;
2. Locate and map features of potential importance for offshore exploration and production activities, including ice movement lines, substantial leads (linear openings in the sea ice), polynyas (areal openings in the sea ice), first-year ridges and rubble fields, and multi-year floes;
3. Locate and map ice pile-ups on natural shorelines and man-made structures, and estimate the dimensions of these features;
4. Correlate significant changes in the ice canopy with the corresponding meteorological conditions;
5. Using the data acquired during the past five years, characterize present-day freeze-up processes and compare them with those documented in the 1980s.

The study was conducted using a combination of publicly-available data, proprietary data made available by Shell, and aerial reconnaissance missions. The acquisition of publicly-available meteorological data, ice charts, and satellite imagery began in September 2013, and continued through March 2014. Shell provided 40 high-resolution RADARSAT-2 images acquired from October 2013 through March 2014, as well as ice charts and the tracks of 21 telemetry buoys deployed on the sea ice in late February and early March. Shell’s willingness to contribute these data to the project at no cost is gratefully acknowledged.

Five aerial reconnaissance missions were undertaken in late March 2014 to supplement the remotely-sensed data obtained from other sources. The specific objectives were to obtain ground truth information for the satellite imagery, to investigate large-scale features

of interest identified in the imagery, and to document small-scale features that were beneath the resolution of the imagery.

The principal study findings are summarized below:

Findings for Entire Study Area

1. ***Air Temperatures:*** The air temperatures during the 2013-14 winter season were exceptionally warm. Based on the temperature data recorded at Barrow Airport, the past winter was the warmest in the last 44 years.
2. ***First-Year Ice Growth:*** The computed thickness of undeformed first-year ice at the end of the 2013-14 winter season was 152 cm in the Alaskan Beaufort Sea and 143 cm in the Chukchi, based on accumulations of 6,425 and 5,775 FDD at Deadhorse and Barrow Airports, respectively. These values are the lowest in the past five winters and, in the case of the Chukchi, the lowest in the past 44 winters. The highest values in recent winters, 176 cm in the Beaufort and 167 cm in the Chukchi, occurred in 2011-12.
3. ***Prediction of Freeze-Up:*** During the past five freeze-up seasons, the number of freezing degree days (FDD) at the time of freeze-up has varied widely in both the Beaufort and Chukchi Seas. This finding confirms that air temperature alone cannot be used to predict the date of freeze-up, and that other factors such as the sea surface temperature, wind conditions, and salinity must be taken into account.

Findings for Beaufort Sea

1. ***Late Summer:*** The ice cover in the Alaskan Beaufort Sea diminished throughout August and early September 2013. The minimum extent of the pack ice occurred on September 13th. Although 50% larger than in 2012, it nevertheless represented the sixth lowest value since the acquisition of satellite-based data began in 1979.
2. ***Freeze-Up:*** Freeze-up commenced in late September, when ice began to form in the semi-protected waters adjacent to the coast. Complete ice coverage in the nearshore region occurred on October 26th, followed by complete coverage in the Alaskan Beaufort Sea on November 20th. During the past five years, the average date of nearshore freeze-up was October 24th, while that of complete freeze-up was November 9th.
3. ***Wind Regime:*** Based on the average daily wind directions recorded at Deadhorse Airport from October 2013 through March 2014, westerlies prevailed more than 50% of the time in every month except January, and more than 60% of the time in November, February, and March. Over the entire six-month study period, westerlies

outnumbered easterlies by a ratio of 57 to 43%. The highest average monthly wind speed, 15 kt (8 m/s), occurred in January.

4. **Storm Events:** Storm events with average daily wind speeds exceeding 15 kt (8 m/s) occurred on twenty occasions encompassing 43 days. Nine of the events were easterlies, while eleven were westerlies. Both the total number of storms and total number of storm days were slightly higher than the average values over the past five freeze-up seasons (eighteen storms and 41 storm days per season).
5. **Landfast Ice:** The landfast ice zone remained narrow and poorly-developed until the end of December due to a predominance of westerly winds, a series of westerly storms, and a paucity of sustained easterly storms. The situation changed in January, when persistent easterly winds coupled with two prolonged easterly storms produced a substantial expansion past the 18-m isobath that stretched from Point Barrow to Barter Island. In February and March, the landfast ice edge advanced in response to easterly winds and retreated in response to westerly winds but tended to retreat no farther than the 18-m isobath due to the existence of a well-grounded shear zone.
6. **Ice Pile-Ups:** Forty-six ice pile-ups occurred in central portion of the Alaskan Beaufort Sea during the 2013-14 freeze-up season. Thirty-nine were located on natural barrier islands, four on man-made facilities, and three on the mainland shore. The heights ranged from 1 to 8 m, the encroachment distances from 0 to 20 m, the alongshore lengths from 50 to 2,600 m, and the ice block thicknesses from 30 to 60 cm.
7. **Multi-Year Ice:** Multi-year ice was present in the offshore portion of the Alaskan Beaufort Sea throughout freeze-up and early winter, but remained absent from the nearshore region except in the immediate vicinity of Point Barrow. During the past fourteen freeze-up seasons (2000-01 through 2013-14), large multi-year floes have invaded the nearshore region on only two occasions, 2001-02 and 2009-10. This finding suggests that the probability of an invasion in any given freeze-up season is less than 15%.

Findings for Chukchi Sea

1. **Freeze-Up:** Freeze-up in the Chukchi Sea began during the first week in October but proceeded slowly due to unseasonably warm temperatures that persisted through mid-November. Complete ice coverage in the nearshore region occurred on November 26th, followed by complete coverage in the entire Chukchi Sea north of Cape Lisburne on December 14th. These dates are the latest recorded in the past five years, with each exceeding the corresponding average value for the five-year period by ten days.

2. **Flash-Freeze Event:** On or about November 12th, a flash freeze created a small patch of ice centered 130 nm (241 km) west of Icy Cape. Although much smaller than that which formed off Wainwright in October 2013, it nevertheless marked the second documented occurrence of flash freezing in the Chukchi Sea over the past five freeze-up seasons.
3. **Wind Regime:** In sharp contrast to the Beaufort, easterly winds prevailed in the Chukchi in each month from October through March. Over the entire six-month period, easterlies outpaced westerlies by a margin of 61 to 39%. The highest average monthly speed, 14 kt (7 m/s), occurred in November and January.
4. **Storm Events:** Nineteen storm events were recorded from October through March. Twelve were easterlies, including five of the six storms that occurred after December 24th. The easterlies produced 29 storm-days, while the westerlies produced thirteen. Both the total number of storms and total number of storm days were slightly higher than the average values over the past five freeze-up seasons (sixteen storms and 40 storm days per season).
5. **Landfast Ice:** At the end of November, a narrow, discontinuous strip of landfast ice extended from Barrow to Peard Bay, and another narrow strip extended from Wainwright to the vicinity of Point Lay. The landfast ice zone remained narrow throughout December except for an advance to Blossom Shoals (off Icy Cape) that occurred at the end of the month. The ice remained grounded on this feature for the remainder of the study period. In mid-January, a prolonged easterly storm dislodged virtually all of the landfast ice north of the Nokotlek River Mouth. Subsequently, the ice waxed and waned in response to changing wind conditions, producing widths that ranged from negligible to 20 nm (37 km). At the end of March, the landfast ice was confined to a narrow strip that was located inside the 11-m isobath in most areas.
6. **Coastal Flaw Lead:** The distinctive flaw lead that opens off the Chukchi Sea coast in response to easterly winds was present on 57% of the days from December 2013 through March 2014. The frequency of occurrence peaked at 69% in January in response to a predominance of easterly winds and three easterly storms. The maximum width of 100 nm (185 km) occurred in February, at which time the lead encompassed all of the Burger and Crackerjack Prospects and parts of the Hanna Shoal and West Prospects. The maximum length, 250 nm (463 km), occurred on repeated occasions in February and March. The maximum persistence of 15 days took place from mid-February to early March.
7. **Nearshore vs. Offshore Ice Cover:** As in each of the past four years, a change in the nature of the ice canopy was noted on the seaward side of the coastal flaw lead during the aerial reconnaissance flights. Within about 50 nm (93 km) of the coast, where the

lead had caused a loss of confinement, the ice evidenced greater deformation indicative of collisions. Farther offshore, where the differential motion between individual floes had been limited by the more consolidated nature of the ice canopy, the ridges and rubble were more widely spaced.

8. ***Ice Pile-Ups:*** Twenty-two ice pile-ups were observed on the coast of the northeast Chukchi Sea during the 2013-14 freeze-up season. The highest concentration was located to the east of Icy Cape on the barrier islands that form the seaward boundary of Kasegaluk Lagoon. The pile-up heights, which varied from 1 to 3 m, were the smallest in the past five years. All 22 pile-ups encroached onto the subaerial beach, with encroachment distances ranging from 5 to 20 m, alongshore lengths from 100 to 7,800 m, and ice block thicknesses from 30 to 40 cm.
9. ***Multi-Year Ice Floes:*** Multi-year ice remained north of Point Barrow until mid-December. During the month that followed, multi-year floes were channeled into the region south and west of the Point on four occasions by a northeasterly extension of the coastal flaw lead. The last invasion, which occurred in mid-January, produced a significant southerly displacement of the multi-year ice edge. The ice continued to advance slowly to the south in February and March, crossing the 71° parallel in late February and reaching the vicinity of Icy Cape in mid-March. Large multi-year ice floes have invaded the region south and west of Point Barrow in nine of the past fourteen freeze-up seasons: 2000-01, 2001-02, 2003-04, 2005-06, 2008-09, 2009-10, 2010-11, 2011-12, and 2013-14. This finding suggests that the probability of an invasion in any given freeze-up season is about 65%.

Freeze-Up in Recent Years versus the 1980s

1. ***Air Temperatures:*** Since the 1970s, progressively warmer winter seasons have caused the number of freezing-degree days at Barrow to decline at an average rate of 44 per year. The greatest increase in temperature has occurred early in the freeze-up season, during the months of October and November.
2. ***Winds:*** Since the mid-1970s, the frequency of storm events during freeze-up has increased by more than 50%. However, the frequency of mid-winter storm events (January through April) is nearly identical to that in the early 1980s.
3. ***Freeze-Up:*** Freeze-up in the nearshore region currently tends to occur during the fourth week in October in the Alaskan Beaufort Sea, and third week in November in the northeastern Chukchi Sea. The former is about three weeks later than in the 1980s, while the latter is about one month later than in the 1970s.

4. ***First-Year Ice Growth:*** Based on air temperatures measured at Barrow Airport, the thickness of undeformed first-year ice attained during an average winter has decreased by nearly 10% (17 cm) since the early 1980s. However, a significant increase in snowfall may be causing a greater reduction in ice thickness due to its insulating effect. Other temperature-related factors, including reduced ice production in leads, decreased consolidation of ridges and rubble fields, and reduced ice strength, probably exert greater impacts on ice dynamics than reduced thickness.
5. ***Landfast Ice Development and Stability:*** In the Alaskan Beaufort Sea, the extent of the landfast ice zone to the west of Prudhoe Bay is similar to that observed in the 1980s but the ice develops more slowly. To the east of Prudhoe Bay, a stable, well-grounded shear zone is far less likely to develop during freeze-up and early winter. In the Chukchi, the narrow, ephemeral nature of the landfast ice zone noted in the 1980s continues to prevail today.
6. ***Coastal Flaw Lead:*** The frequencies with which the flaw lead and extended flaw lead occur off the Chukchi Sea coast have remained constant since the 1990s. Limited observations suggest that the width of the flaw lead may have increased since the 1980s, but the data are insufficient to confirm the existence of this trend.
7. ***Multi-Year Ice in the Alaskan Beaufort Sea:*** The probability of large multi-year ice floes invading the nearshore portion of the Alaskan Beaufort Sea in any given year is substantially less than in the 1980s. This trend may be explained in part by a reduction in the amount of multi-year ice comprising the permanent polar pack and an associated increase in the northerly retreat of the ice edge during the summer months, both of which have reduced the opportunities for pack floes to enter the nearshore area. In addition, warmer air temperatures and increased storm frequencies have decreased the likelihood that remnants of the shear zone will survive the summer melt season to become second-year floes. Nevertheless, as demonstrated in 2009-10, the possibility of multi-year ice encounters cannot be ruled out for developments in the nearshore region.
8. ***Multi-Year Ice in the Chukchi Sea:*** The probability of multi-year ice entering the Chukchi Sea to the south and west of Barrow has decreased since the 1980s, but to a lesser extent than in the Beaufort. Although the factors that have reduced the probability of invasions in the Beaufort also apply to the Chukchi, their impact has been partially offset by the ability of the coastal flaw lead to extend past Point Barrow until it intersects the southern boundary of the multi-year ice.
9. ***Pack Ice Movement:*** Based on the limited data acquired in recent years, the average drift rate of pack ice in the Alaskan Beaufort Sea during the early stages of freeze-up is about 5 nm/day (9 km/day). This value is comparable to that which prevailed in the 1980s.

TABLE OF CONTENTS

EXECUTIVE SUMMARY	i
TABLE OF CONTENTS	vii
LIST OF TABLES	ix
LIST OF FIGURES	xi
LIST OF PLATES	xvi
1. INTRODUCTION	1
2. PRIOR STUDIES	9
2.1 1980s Freeze-up Studies	9
2.2 2009-10 Freeze-Up Study	11
2.3 2010-11 Freeze-Up Study	13
2.4 2011-12 Freeze-Up Study	14
2.5 2012-13 Freeze-Up Study	16
3. DATA ACQUISITION AND ANALYSIS	19
3.1 Meteorological Data	19
3.2 Ice Charts	21
3.3 Satellite Imagery	24
3.4 Telemetry Buoys	26
3.5 Aerial Reconnaissance Missions	29
4. BEAUFORT SEA FREEZE-UP	37
4.1 Overview	37
4.2 Late Summer 2013	44
4.3 Early Freeze-Up	45
4.3.1 October 2013	45
4.3.2 November 2013	47
4.4 Late Freeze-Up	54
4.4.1 December 2013	54
4.4.2 January 2014	61
4.5 Mid-Winter	66
4.5.1 February 2014	66
4.5.2 March 2014	75
4.6 March Reconnaissance Flights	80
4.6.1 Lagoon Ice	80
4.6.2 Thermal Cracks	83
4.6.3 First-Year Ice Growth	83
4.6.4 Landfast Ice and Shear Zone	83
4.6.5 Leads	85
4.6.6 Ice Pile-Ups	91

TABLE OF CONTENTS

(continued)

4.6.7	Multi-Year Ice	92
4.6.8	Ice Conditions in Shell Prospects.....	92
5.	CHUKCHI SEA FREEZE-UP	97
5.1	Overview	97
5.2	Late Summer 2013	104
5.3	Early Freeze-Up	104
5.3.1	October 2013	104
5.3.2	November 2013	108
5.4	Late Freeze-Up.....	114
5.4.1	December 2013	114
5.4.2	January 2014	119
5.5	Mid-Winter.....	125
5.5.1	February 2014	125
5.5.2	March 2014	130
5.6	March Reconnaissance Flights.....	141
5.6.1	Lagoon Ice.....	141
5.6.2	Landfast Ice.....	141
5.6.3	Leads	144
5.6.4	Offshore Ice.....	144
5.6.5	Ice Pile-Ups	144
5.6.6	Multi-Year Ice.....	148
5.6.7	Ice Conditions in Shell Prospects.....	150
5.6.8	Katie's Floeberg.....	152
6.	FREEZE-UP IN RECENT YEARS VERSUS THE 1980s.....	155
6.1	Air Temperatures	155
6.2	Winds	159
6.3	Timing of Freeze-Up.....	163
6.4	First-Year Ice Growth	165
6.5	Landfast Ice.....	168
6.6	Coastal Flaw Lead.....	170
6.7	Multi-Year Ice.....	171
6.8	Pack Ice Movement.....	173
7.	SUMMARY AND CONCLUSIONS	175
8.	REFERENCES	180

APPENDIX A DRAWINGS (Bound Separately)

APPENDIX B DIGITAL DATA (DVD)

LIST OF TABLES

<u>Title</u>	<u>Page No.</u>
Table 1. Accumulated Freezing-Degree Days (<29°F) at Barrow and Deadhorse Airports in 2013-14.....	20
Table 2. Abbreviations for Ice Features	34
Table 3. Beaufort Sea Wind Characteristics, October 2013 – March 2014	37
Table 4. Beaufort Sea Storm Characteristics, October 2013–March 2014	39
Table 5. Beaufort Sea Computed Ice Thickness, October 2013-May 2014.....	40
Table 6. Ice Pile-Ups on Beaufort Sea Coast during 2013-14 Freeze-Up Season	41
Table 7. Beaufort Sea Multi-Year Ice Floe Speeds, November 2013 - March 2014	43
Table 8. Significance of Color Bands in Plots of Meteorological Conditions	47
Table 9. Chukchi Sea Wind Characteristics, October 2013 – March 2014	97
Table 10. Chukchi Sea Storm Characteristics, October 2013–March 2014.....	99
Table 11. Chukchi Sea Computed Ice Thickness, October 2013–June 2014	100
Table 12. Ice Pile-Ups on Chukchi Sea Coast during 2013-14 Freeze-Up Season	101
Table 13. Chukchi Sea Multi-Year Ice Floe Speeds, January 2014–March 2014	103
Table 14. Ice Cover in Shell’s Chukchi Sea Prospects during Freeze-Up.....	111
Table 15. Accumulated Freezing-Degree Days (<29°F) at Barrow, 1970-71 through 2013-14.....	156
Table 16. Beaufort Sea Wind Directions, 2009-10 through 2013-14	160
Table 17. Chukchi Sea Wind Directions, 2009-10 through 2013-14.....	160

LIST OF TABLES

(continued)

<u>Title</u>	<u>Page No.</u>
Table 18. Beaufort Sea Storms, 2009-10 through 2013-14	161
Table 19. Chukchi Sea Storms, 2009-10 through 2013-14	161
Table 20. Chronology of Freeze-Up in the Alaskan Beaufort Sea, 2009 through 2013	163
Table 21. Chronology of Freeze-Up in the Chukchi Sea, 2009 through 2013.....	164
Table 22. Computed Ice Thickness at Barrow, 1970-71 through 2013-14	166
Table 23. Beaufort Sea Ice Drift in November and December	174

LIST OF FIGURES

<u>Title</u>	<u>Page No.</u>
Figure 1. Study Area.....	2
Figure 2. Geographic Points of Interest in Central Beaufort Sea	6
Figure 3. Geographic Points of Interest in Western Beaufort Sea.....	7
Figure 4. Geographic Points of Interest in Chukchi Sea	8
Figure 5. Meteorological Data Recorded at Barrow Airport in February 2014	20
Figure 6. CIS Stage-of-Development Ice Chart of Beaufort Sea for January 13, 2014	22
Figure 7. NIC Ice Chart of Chukchi Sea for November 19, 2013.....	23
Figure 8. SIWAC Ice Chart of Beaufort Sea for December 30, 2013.....	24
Figure 9. CIS RADARSAT Mosaic of Beaufort Sea for January 24-27, 2014.....	25
Figure 10. RADARSAT-2 Image of Beaufort Sea Acquired on February 14, 2014 .	27
Figure 11. AVHRR Image of Beaufort and Chukchi Seas Acquired on February 15, 2014	28
Figure 12. MODIS Image of Beaufort and Chukchi Seas Acquired on February 24, 2014	28
Figure 13. Telemetry Buoy Trajectories in Beaufort Sea, February 24- March 31, 2014	30
Figure 14. Telemetry Buoy Trajectories in Chukchi Sea, February 26- March 31, 2014	31
Figure 15. Sea Ice Minimum Extent on September 13, 2013.....	44
Figure 16. Sea Ice Minimum Extent on September 16, 2012.....	45
Figure 17. Average Sea Ice Extent in September, 1979-2013.....	46
Figure 18. Meteorological Conditions at Deadhorse Airport in October 2013	46

LIST OF FIGURES

(continued)

<u>Title</u>	<u>Page No.</u>
Figure 19. NIC Ice Chart of Beaufort Sea for September 26, 2014	48
Figure 20. RADARSAT-2 Image of Beaufort Sea Acquired on October 31, 2013.....	49
Figure 21. Meteorological Conditions at Deadhorse Airport in November 2013	50
Figure 22. RADARSAT-2 Image of Beaufort Sea Acquired on November 14, 2013.....	51
Figure 23. Beaufort Sea Landfast Ice Edge in November 2013.....	53
Figure 24. Beaufort Sea Multi-Year Ice Floe Displacements in November 2013	55
Figure 25. Meteorological Conditions at Deadhorse Airport in December 2013.	56
Figure 26. Beaufort Sea Landfast Ice Edge in December 2013	57
Figure 27. RADARSAT-2 Image of Beaufort Sea Acquired on December 15, 2013.	59
Figure 28. Beaufort Sea Multi-Year Ice Floe Displacements in December 2013.....	60
Figure 29. Meteorological Conditions at Deadhorse Airport in January 2014	61
Figure 30. Beaufort Sea Landfast Ice Edge in January 2014	63
Figure 31. CIS Ice Chart of Beaufort Sea for January 13, 2014.....	64
Figure 32. RADARSAT-2 Image of Beaufort Sea Acquired on January 25, 2014.	65
Figure 33. Beaufort Sea Multi-Year Ice Floe Displacements in January 2014.....	67
Figure 34. Meteorological Conditions at Deadhorse Airport in February 2014	68
Figure 35. Beaufort Sea Landfast Ice Edge in February 2014	69
Figure 36. RADARSAT-2 Image of Beaufort Sea Acquired on February 18, 2014.	71

LIST OF FIGURES

(continued)

<u>Title</u>	<u>Page No.</u>
Figure 37. Beaufort Sea Multi-Year Ice floe Displacements in February 2014.....	72
Figure 38. Beaufort Sea Landfast Ice Edge and Telemetry Buoy Tracks in February 2014	73
Figure 39. Time Series of Telemetry Buoy Average Daily Speeds in Beaufort Sea in February 2014	74
Figure 40. Meteorological Conditions at Deadhorse Airport in March 2014	75
Figure 41. Beaufort Sea Landfast Ice Edge and Telemetry Buoy Tracks in March 2014	77
Figure 42. RADARSAT-2 Image of Beaufort Sea Acquired on March 17, 2014	78
Figure 43. Beaufort Sea Multi-Year Ice Floe Displacements in March 2014.....	79
Figure 44. Time Series of Telemetry Buoy Average Daily Speeds in Beaufort Sea, March 2014	81
Figure 45. Frequency of Occurrence of Chukchi Sea Flaw Lead, December 2013 - March 2014	102
Figure 46. NIC Ice Chart for September 3, 2013, Showing Tongue of Ice off Point Franklin	105
Figure 47. Meteorological Conditions at Barrow Airport in October 2013	106
Figure 48. RADARSAT-2 Image of Chukchi Sea Acquired on October 30, 2013	107
Figure 49. Meteorological Conditions at Barrow Airport in November 2013	108
Figure 50. RADARSAT-2 Image of Chukchi Sea Acquired on November 15, 2013	110
Figure 51. Chukchi Sea Landfast Ice Edge in November 2013	112

LIST OF FIGURES

(continued)

<u>Title</u>	<u>Page No.</u>
Figure 52. RADARSAT-2 Image of Chukchi Sea Acquired on November 29, 2013	113
Figure 53. Meteorological Conditions at Barrow Airport in December 2013.....	114
Figure 54. RADARSAT-2 Image of Chukchi Sea Acquired on December 6, 2013	116
Figure 55. Chukchi Sea Landfast Ice Edge in December 2013.....	117
Figure 56. AVHRR Image of Chukchi Sea Acquired on December 23, 2013.....	118
Figure 57. Meteorological Conditions at Barrow Airport in January 2014.....	119
Figure 58. Chukchi Sea Landfast Ice Edge in January 2014.....	121
Figure 59. RADARSAT-2 Image of Chukchi Sea Acquired on January 20, 2014	122
Figure 60. AVHRR Image Acquired on January 7, 2014	123
Figure 61. Chukchi Sea Multi-Year Ice Floe Displacements in January 2014	124
Figure 62. Meteorological Conditions at Barrow Airport in February 2014.	125
Figure 63. Chukchi Sea Landfast Ice Edge in February 2014.....	127
Figure 64. AVHRR Image of Chukchi Sea Acquired on February 17, 2014.....	128
Figure 65. RADARSAT-2 Image of Chukchi Sea Acquired on February 26, 2014	129
Figure 66. Chukchi Sea Multi-Year Ice Floe Displacements in February 2014	131
Figure 67. Chukchi Sea Landfast Ice Edge and Telemetry Buoy Tracks in February 2014	132
Figure 68. Meteorological Conditions at Barrow Airport in March 2014.....	133
Figure 69. Chukchi Sea Landfast Ice Edge in March 2014.....	134

LIST OF FIGURES

(continued)

<u>Title</u>	<u>Page No.</u>
Figure 70. RADARSAT-2 Image of Chukchi Sea Acquired on March 29, 2014....	136
Figure 71. Chukchi Sea Multi-Year Ice Floe Displacements in March 2014	137
Figure 72. Chukchi Sea Landfast Ice Edge and Telemetry Buoy Tracks in March 2014	138
Figure 73. Time Series of Telemetry Buoy Average Daily Speeds in Chukchi Sea, March 2014	140
Figure 74. Annual Cumulative Freezing-Degree Days (<29°F) at Barrow, 1970-71 through 2013-14.....	157
Figure 75. Differences between Recent Monthly Air Temperatures and Long-Term Average Values at Barrow.....	158
Figure 76. Yearly Storm Count at Barrow during the Open-Water and Freeze-Up Seasons, 1950-2004.....	162
Figure 77. Computed Ice Thickness: Recent Winters vs. 1970s and 1980s.....	167
Figure 78. Annual Snowfall at Barrow during Freeze-Up (October 1 – March 31), 1969-70 through 2013-14.....	168
Figure 79. AVHRR Image Acquired on March 12, 2001, Showing Multi-Year Ice Floes Entering Coastal Flaw Lead	172

LIST OF PLATES

<u>Title</u>	<u>Page No.</u>
Plate 1. Aero Commander 690 at Deadhorse Airport	32
Plate 2. Bell 412 Helicopter at 11.8-m Ridge off Mary Sachs Entrance	32
Plate 3. Flat Ice in Simpson Lagoon between Oliktok Point and Spy Island Drillsite.....	82
Plate 4. 5-m Pile-Up on Southwest End of Pole Island with 2-m Rubble in Stefansson Sound	82
Plate 5. 1-m High Thermal Crack in Stefansson Sound.....	84
Plate 6. Ice Thickness Measurement in Mikkelsen Bay	84
Plate 7. 11.8-m Grounded Ridge on Sivulliq Development Prospective Pipeline Route with Brooks Range in Background	86
Plate 8. 11.8-m Grounded Ridge on Sivulliq Development Prospective Pipeline Route Showing Evidence of Ice Override	86
Plate 9. 1.4-m Ice Blocks on Landward Side of 11.8-m Grounded Ridge.....	87
Plate 10. 6-m Ridge and Extensive Rubble Field on Stamukhi Shoal	87
Plate 11. 20-m Ridge on Weller Bank	88
Plate 12. Wide Expanse of Flat Ice on South Side of Stamukhi Shoal.....	88
Plate 13. Extensive Rubble Field with Heights to 5 m off Cross Island.....	89
Plate 14. 3-m Rubble Adjacent to Landfast Ice Edge in Camden Bay	89
Plate 15. Small Lead Located 20 nm (37 km) off Narwhal Island	90
Plate 16. Polynya Located 23 nm (43 km) off Brownlow Point.....	90
Plate 17. Extended Flaw Lead 15 nm (28 km) Northeast of Point Barrow	91
Plate 18. 8-m Pile-Up that Encroached 20 m onto Northwest Corner of STP Pad	93

LIST OF PLATES

(continued)

<u>Title</u>	<u>Page No.</u>
Plate 19. 5-m Pile-Up that Encroached 10 m onto Southwest Tip of Narwhal Island	93
Plate 20. Flat Ice in Leffingwell Lagoon with Rubble Field outside Mary Sachs Entrance in Background.....	94
Plate 21. 3-m Rubble and Inactive Shear Line in Landfast Ice 3 nm off Mary Sachs Entrance in Background.....	94
Plate 22. 1-to-3-m Rubble and Refreezing Lead at Seaward End of Sivulliq Development Pipeline Route.....	95
Plate 23. Flat First-Year Ice Interspersed with 2-m Ridges and Rubble in Southwestern Portion of Harrison Bay Prospects	95
Plate 24. 5-m Ridges and Rubble with Scattered First-Year Floes in Northeastern Portion of Harrison Bay Prospects	96
Plate 25. Flat Ice in Kasegaluk Lagoon East of Icy Cape.....	142
Plate 26. Mixture of Flat and Deformed Ice in Landfast Ice Zone off Wainwright.....	142
Plate 27. Flat Ice Interspersed with Ridges Northwest of Icy Cape.....	143
Plate 28. 5-m Rubble Grounded on Blossom Shoal.....	143
Plate 29. Coastal Flaw Lead off Barrow	145
Plate 30. Coastal Flaw Lead off Point Lay	145
Plate 31. Small Refreezing Lead in Burger Prospects	146
Plate 32. Extensive Accumulation of 3-m Rubble 40 nm West of Barrow	146
Plate 33. Intermittent 3-m Ridges and Rubble 80 nm West of Barrow	147
Plate 34. 3-m Ice Pile-Up on Barrier Island 5 nm East of Icy Cape	147
Plate 35. 2-m Pile-Up on Barrier Island off Mouth of Nokotlek River	148

LIST OF PLATES

(continued)

<u>Title</u>	<u>Page No.</u>
Plate 36. Multi-Year Floe with 5-m Ridge 20 nm West of Wainwright.....	149
Plate 37. Cracked Multi-Year Floe 80 nm West of Barrow.....	149
Plate 38. Multi-Year Floes in Landfast Ice off Barrow	150
Plate 39. First-Year Ice with 3-m Ridges and Rubble at East Edge of Hanna Shoal Prospects.....	151
Plate 40. First-Year Ice with Intermittent 3-m Ridges and 2-m Rubble in Southeastern Portion of Burger Prospects	151
Plate 41. Multiple Leads and Broken Ice in Central Portion of Burger Prospects	152
Plate 42. Mixture of First-Year Rubble and Multi-Year Floes Comprising Katie's Floeberg.....	153
Plate 43. 8-m Rubble on Northeast Side of Katie's Floeberg	154

2013-14 FREEZE-UP STUDY OF THE ALASKAN BEAUFORT AND CHUKCHI SEAS

1. INTRODUCTION

This report describes an investigation of the ice conditions that prevailed in the Alaskan Beaufort and Chukchi Seas during the 2013-14 freeze-up season. The study was performed as a joint-industry project on behalf of Shell Gulf of Mexico Inc. and Shell Offshore Inc. (collectively, “Shell”), and the U.S. Department of the Interior, Bureau of Safety and Environmental Enforcement (“BSEE”), by Coastal Frontiers Corporation and Vaudrey & Associates, Inc.

As shown in Figure 1, the study area includes the nearshore portion of the Beaufort Sea from Barter Island on the east to Point Barrow on the west, and the northeastern portion of the Chukchi Sea bounded by the shoreline between Point Barrow and Point Lay, the 74°N parallel, and the 168°W meridian. The boundaries in the Beaufort Sea were selected to encompass Shell’s prospects in Camden and Harrison Bays as well as all existing oil and gas developments operated by others, while those in the Chukchi were selected to encompass Hanna Shoal and Shell’s Burger and Crackerjack prospects.

Despite their proximity, the ice regimes in the Beaufort and Chukchi Seas differ markedly due to factors that include geography, meteorology, and oceanography. Whereas the Beaufort Sea coast is oriented east southeast-west northwest, the Chukchi coast trends northeast-southwest (Figure 1). As a result, the easterly winds that occur frequently in both regions tend to push the ice along the Beaufort Sea coast but away from the Chukchi coast. In the Beaufort, the alongshore winds coupled with flat nearshore slopes produce such extensive landfast ice growth that the ice seasons (freeze-up, winter, and break-up) are defined in large part by the condition of this ice. In the Chukchi, the growth of landfast ice is limited not only by the offshore winds but also by a nearshore sea bottom that tends to be relatively steep. As a result, the seasons are blurred by near-constant ice motion and the recurring formation of new ice adjacent to a small strip of landfast ice that clings to the shoreline.

The pronounced difference in ice regimes that characterizes freeze-up and mid-winter also prevails during the break-up and summer seasons. Whereas the Beaufort Gyre transports pack ice from east to west in the Beaufort Sea, the Alaska Coastal Current carries

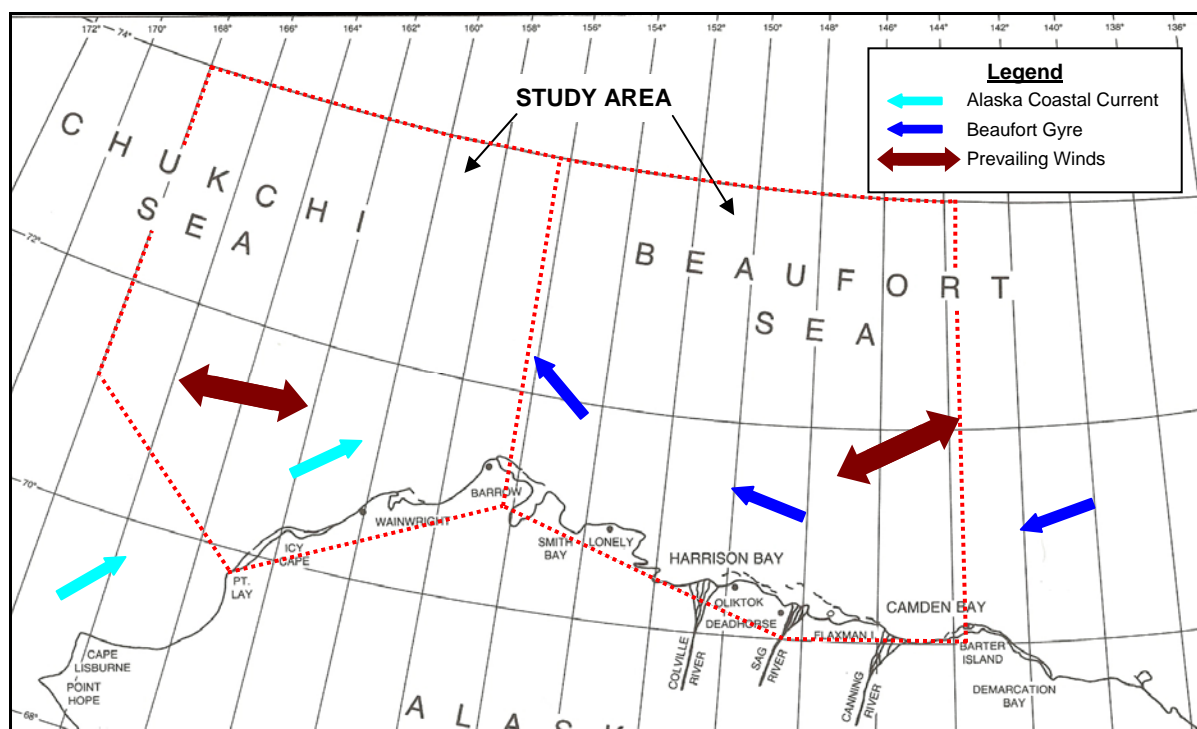


Figure 1. Study Area

warm water north from the Bering Sea (Figure 1) and contributes to the retreat of the ice edge in the Chukchi.

During freeze-up, the ice cover in the study area consists primarily of thin, flexible sheets of newly-formed ice. It also may contain thicker, stronger multi-year floes that have moved into the region after surviving one or more summer melt seasons. Frequent storms tend to disturb the first-year ice before it attains sufficient thickness to resist displacement. As a result, the multi-year floes can travel great distances and attain relatively high speeds in open water. Potential concerns for oil and gas facilities include impact loads on fixed structures such as man-made islands and platforms, displacement of floating structures such as drillships, and ice gouging at the sites of subsea pipelines.

In addition to substantial ice movements, the storms during freeze-up and early winter can produce significant pile-up events when the ice encounters fixed objects such as natural shorelines, shoals, and man-made islands. The storms also can cause substantial deformation of the first-year ice, leading to the formation of ridges and rubble fields.

The foregoing phenomena, along with the curtailment of vessel navigation and the increasing viability of the ice sheet as a platform for transportation and construction, imply that an understanding of freeze-up is essential for the safe design and operation of offshore

oil and gas facilities. To this end, six freeze-up studies were conducted as joint-industry projects from 1980-81 through 1985-86 (Vaudrey, 1981a; 1982a; 1983; 1984; 1985a; 1986). Each study was largely observational in nature, and included aerial surveys undertaken at intervals of two to three weeks from early October until early December. In some instances, an additional aerial survey was made at the end of January to record late-freeze-up ice movements caused by storms that occurred after the early-December visit. The primary objectives of these annual studies were twofold: (1) observe and record major ice movement events and their effects on man-made structures, and (2) document the size and distribution of multi-year floes, the locations of major first-year ridges and rubble fields, and the zonation of the nearshore ice.

Between 1986 and 2008, freeze-up processes in the Alaskan Beaufort and Chukchi Seas were investigated primarily through the analysis of satellite imagery (Vaudrey, 1988-1992; Eicken, *et al.*, 2006). The resulting information, although useful in its own right, lacked some of the detail provided by the earlier observational studies. Specifically, items such as the character of multi-year ice floes and the locations and characteristics of ice pile-ups could not be extracted from the satellite-based data. To remedy this shortcoming, Shell (a participant in the original freeze-up studies) and BSEE (known previously as the Minerals Management Service and subsequently as the Bureau of Ocean Energy Management, Regulation, and Enforcement) commissioned studies of the 2009-10, 2010-11, 2011-12, and 2012-13 freeze-up seasons that combined remote sensing with on-site observations. Each project included an analysis of meteorological data, ice charts, and satellite imagery in concert with a series of aerial reconnaissance missions conducted in early February to document the conditions at the end of freeze-up (when processes such as nearshore rubble formation and ice encroachment onto the shoreline typically have slowed or ceased; Coastal Frontiers and Vaudrey, 2010; 2011; 2012a; 2013). The latter two studies also included reconnaissance flights in late November to observe the conditions that prevailed early in the freeze-up period (when emergency response measures could become necessary to address a drilling incident that occurred late in the open-water season).

To expand the database on the nature and interannual variability of present-day freeze-up processes, a program similar to those conducted during the prior four years was undertaken in 2013-14. The scope of work was designed to address five specific objectives:

1. Describe the ice conditions that evolve during the freeze-up and early winter seasons, including the development of the landfast ice zone and early shear zone;
2. Locate and map features of potential importance for offshore exploration and production activities, including ice movement lines, substantial leads (linear

openings in the sea ice) and polynyas (areal openings in the sea ice), first-year ridges and rubble fields, and multi-year ice floes;

3. Locate and map ice pile-ups on natural shorelines and man-made structures, and estimate the dimensions of these features;
4. Correlate significant changes in the ice canopy with the corresponding meteorological conditions;
5. Using the data acquired since 2009-10, characterize present-day freeze-up processes and compare them with those in the 1980s.

The acquisition of publicly-available meteorological data, ice charts, and satellite imagery began in September 2013 and continued through March 2014. These data were supplemented with ice charts, 40 high-resolution RADARSAT-2 images acquired from October 2013 through March 2014, and the tracks of 21 telemetry buoys deployed on the sea ice in late February and early March, all of which were provided by Shell. Shell's willingness to contribute these data to the project at no cost is gratefully acknowledged.

The original plan of study called for reconnaissance flights to be conducted in November and February, with the former intended to document the conditions that prevailed early in the freeze-up season and the latter intended to document those at the end. Unfortunately, however, both sets of flights were precluded by delays in the issuance of contractual approval. The necessary authorization was received on March 28th, allowing two fixed-wing flights and one helicopter flight to be conducted in the Beaufort along with two fixed-wing flights in the Chukchi by month-end. While flights in November and February would have been preferable from the standpoint of documenting the conditions during freeze-up, the late-March missions nevertheless provided valuable information that could be used to refine and expand the data derived previously using remote sensing techniques.

The remainder of this report provides a detailed account of the 2013-14 Freeze-Up Study. To provide historical context, the findings of the ten prior joint-industry studies (1980-81 through 1985-86 and 2009-10 through 2012-13) are summarized in Section 2. Data acquisition and analysis are discussed in Section 3, which covers the aerial reconnaissance missions in addition to the data obtained from all other sources. Section 4 describes the progression of freeze-up in the Beaufort in 2013-14, while Section 5 provides comparable information for the Chukchi. In Section 6, present-day freeze-up processes are characterized and compared with those in the 1980s. Conclusions are presented in Section 7, followed by references in Section 8. Figures, tables, and plates are interspersed with the text, while three large-format drawings that portray the observations made during

the aerial reconnaissance flights are provided in Appendix A. The digital data files that were used in conducting the study are provided on a DVD in Appendix B. The DVD also contains a digital version of this report (including Appendix A).

The horizontal datum for all geographic coordinates presented in the text and the accompanying graphical products is the North American Datum of 1983 (NAD 83). Some of the graphical products also include a grid referenced to the Universal Transverse Mercator (UTM) Datum, NAD 83, with units of meters. UTM Zone 6N is used in the central Beaufort Sea, UTM Zone 5N in the western Beaufort Sea, and UTM Zone 4N in the Chukchi Sea.

The vertical datum is Mean Sea Level (MSL). MSL lies only 11 cm above Mean Lower Low Water (MLLW) at Prudhoe Bay, 9 cm at Barrow, and 8 cm at Point Hope (National Ocean Service, 2013). For purposes of this report, the differences between MSL and MLLW (which represents the vertical datum for all National Ocean Service nautical charts of the region) are assumed to be negligible.

Units are provided in the SI system, with three exceptions: (1) distances are provided in nautical miles (nm) to maintain consistency with the use of geographic coordinates; (2) wind speeds are provided in knots (kt), again to maintain consistency with the use of geographic coordinates; and (3) freezing degree days (“FDD”) are provided using the Fahrenheit rather than Celsius scale to provide greater resolution and maintain consistency with past freeze-up reports. In the case of nautical miles and knots, the corresponding values in SI units are provided in parentheses.

Throughout this report, the locations of ice features are referenced to geographic features that include bays, rivers, lagoons, points of land, natural and man-made islands, and coastal villages. For ease of reference, these geographic features are shown in Figures 2 (Central Beaufort Sea), 3 (Western Beaufort Sea), and 4 (Chukchi Sea).

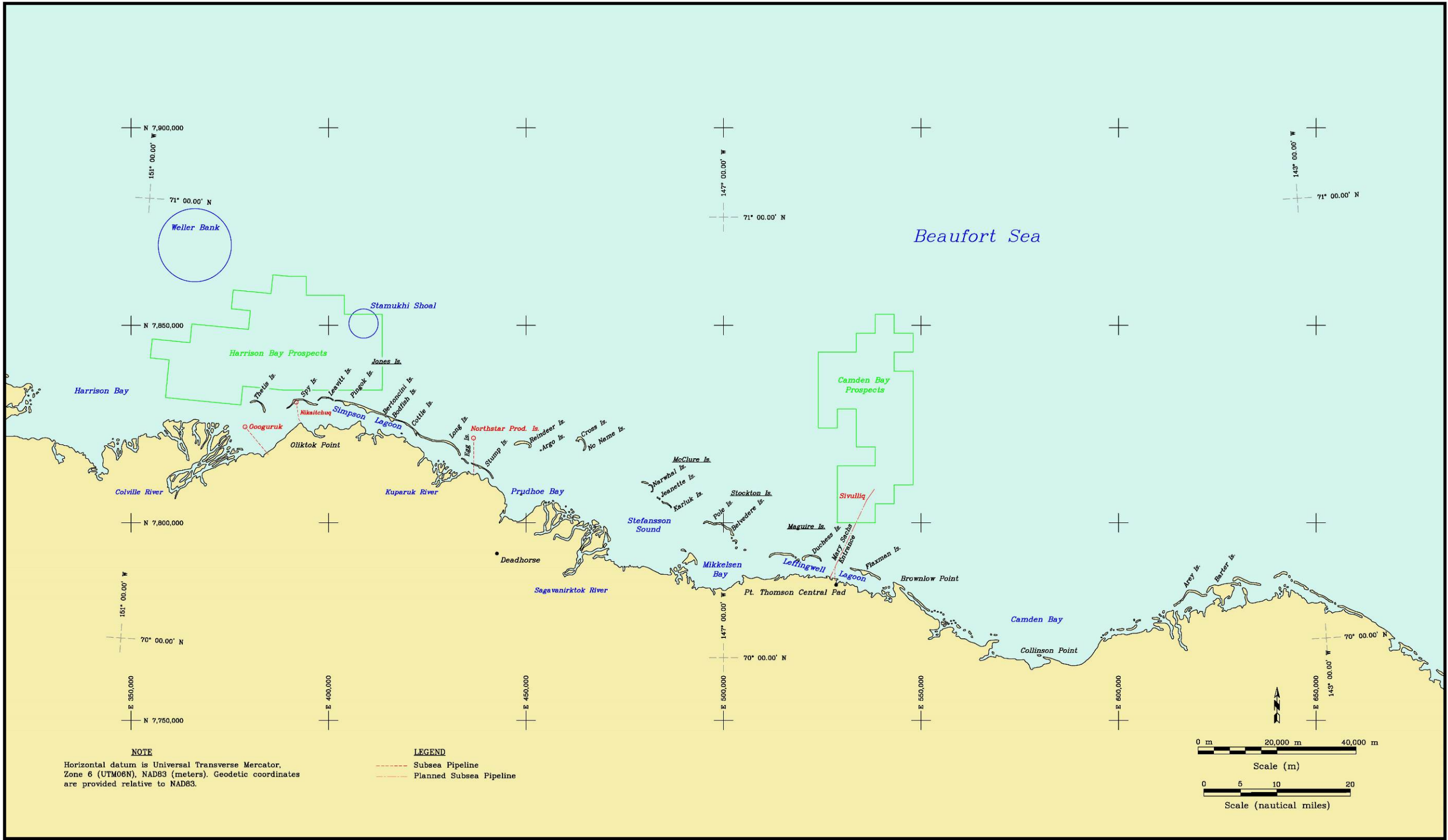


Figure 2. Geographic Points of Interest in Central Beaufort Sea

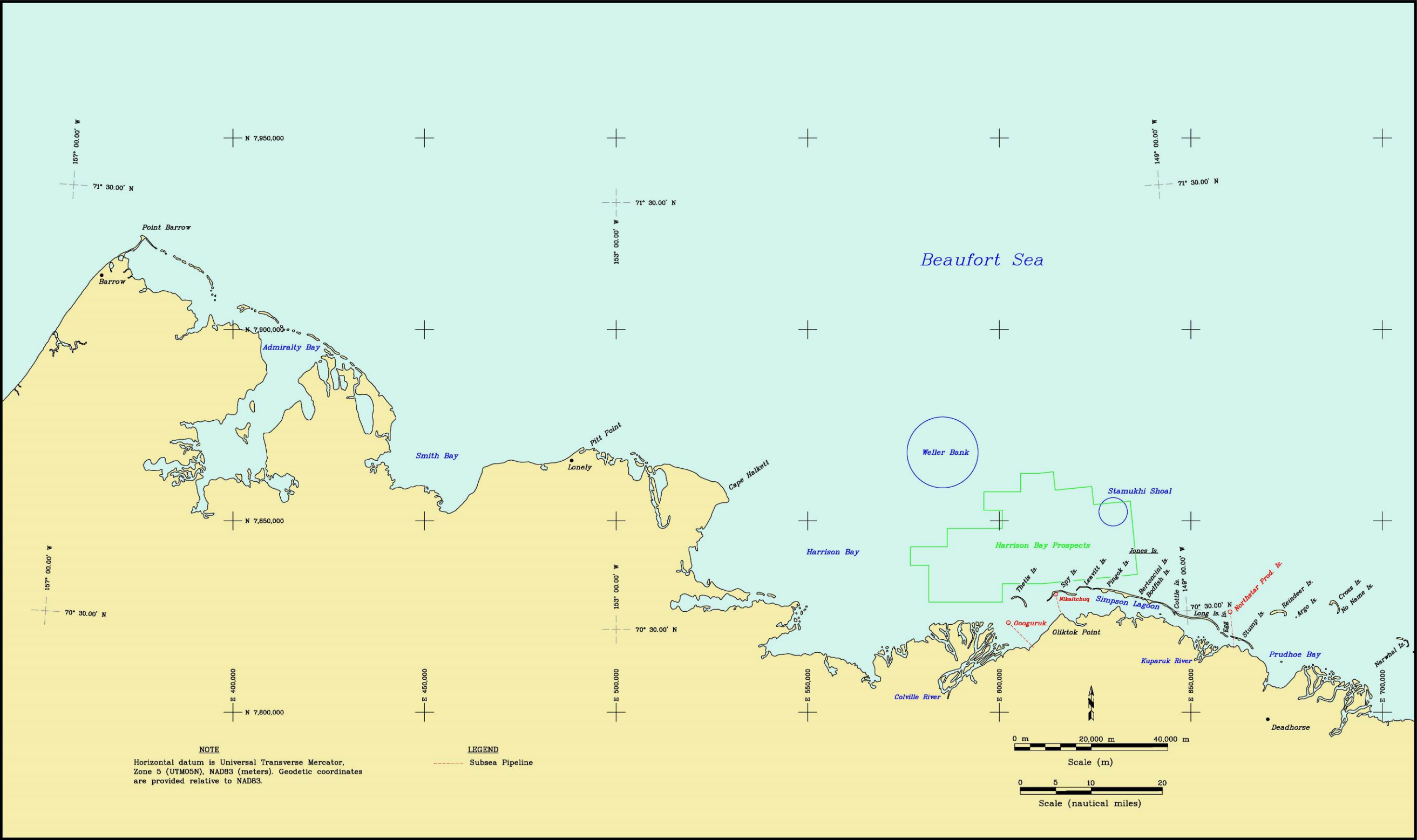


Figure 3. Geographic Points of Interest in Western Beaufort Sea

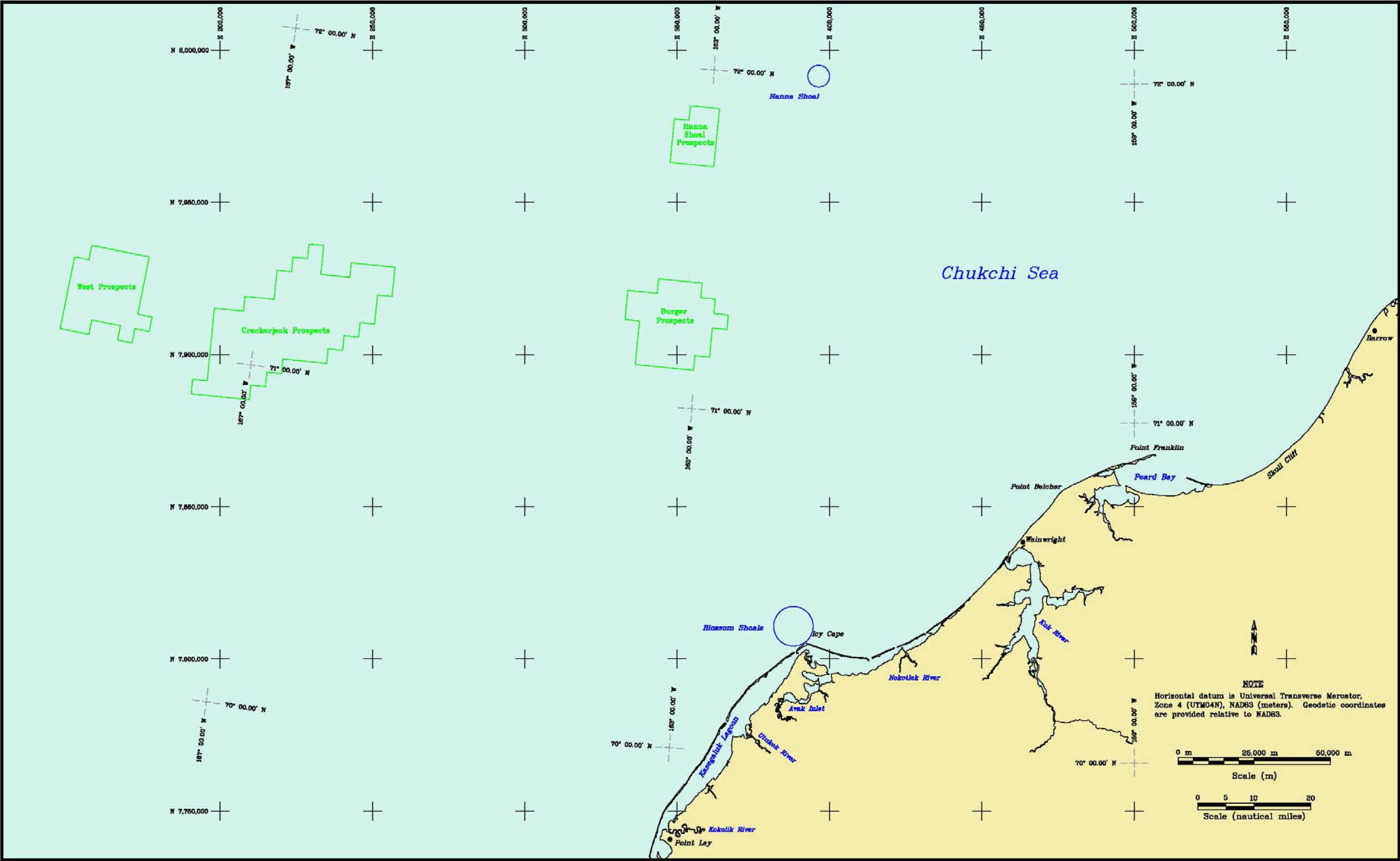


Figure 4. Geographic Points of Interest in Chukchi Sea

2. PRIOR STUDIES

As indicated in Section 1, six annual freeze-up studies were conducted as joint industry programs from 1980-81 through 1985-86 (Vaudrey, 1981a; 1982a; 1983; 1984; 1985a; 1986). More recently, joint industry freeze-up studies were undertaken in 2009-10, 2010-11, 2011-12, and 2012-13 (Coastal Frontiers and Vaudrey, 2010; 2011; 2012a; 2013). The methods and results of these ten prior studies are summarized in the subsections that follow.

2.1 1980s Freeze-Up Studies

The freeze-up studies conducted in the 1980s were made available to the present project through the courtesy of Shell (Reece, 2009). The primary objectives of each study were twofold: (1) observe and record major ice movement events and their effects on man-made structures, and (2) document the size and distribution of multi-year floes, the locations of major first-year ridges and rubble fields, and the zonation of the nearshore ice. Each study included a series of aerial surveys conducted at two- to three-week intervals from early October until early December to monitor the progression of freeze-up.

The first three studies (1980-81 through 1982-83) were limited to the central Beaufort Sea, from Cape Halkett on the west to Flaxman Island on the east. The last three studies (1983-84 through 1985-86) were expanded significantly to include the entire region between Icy Cape in the Chukchi Sea and Barter Island in the Beaufort Sea. Occasionally, the reconnaissance flights continued east of Barter Island to the Canadian border. Each of the three studies commencing in 1983, 1984 and 1985 included an additional trip at the end of January to record late freeze-up ice movements caused by storms occurring after the early-December visit. The progress of the freeze-up season was documented by reporting the ice conditions observed during each successive trip. Meteorological data, including wind speed and direction as well as air temperature, were acquired from coastal or near-coastal reporting stations at Deadhorse, Barrow, and Barter Island.

Key findings from the freeze-up studies of the 1980s are presented below:

Beaufort Sea: 1980s

- **Initiation of Freeze-Up:** Freeze-up occurred in the nearshore Beaufort Sea between late September and early October, generally coinciding with the accumulation of 40 to 50 FDD. Warming trends in October retarded initial ice growth by 7 to 10 days in 1983 and 1985 and by almost three weeks in 1984.

- **Landfast Ice and Shear Zone Development:** Persistent easterly winds in the Beaufort Sea created a grounded shear zone that provided stability for the landfast ice. In contrast, intermittent westerly winds during freeze-up fostered movement of the ice cover and prevented landfast ice stability. Freeze-up seasons without westerlies tended to have well-established shear zones and stable landfast ice.
- **Ice Pile-Ups and Rubble Pile Formation:** The primary cause of ice pile-ups on natural shorelines and man-made facilities was found to be a reversal in the wind direction, especially during the first two months after freeze-up. Two such ice movement sequences were documented during the six-year study period. The first, in November 1981, was caused by a westerly that loosened the landfast ice followed by an easterly that drove the ice back into the shoreline. The second, in mid-October 1982, resulted from an easterly that created a lead offshore of the temporary fast ice followed by a strong westerly that dislodged the fast ice and drove it up the slopes and onto the work surfaces of man-made exploration islands.

Wind reversals also tended to create significant rubble piles offshore, especially on Stamukhi Shoal and Weller Bank in the Beaufort Sea. Several large rubble piles located 10 to 15 nm (19 to 28 km) northwest of Seal Exploration Island (the current location of Northstar Production Island) in water depths of 10 to 12 m were observed after a strong southwesterly in late December 1983.

- **Multi-Year Ice:** Significant concentrations of multi-year ice were noted in the nearshore portion of the central Beaufort Sea during three of the six freeze-up seasons studied. The most extensive invasion occurred in late September 1980, when concentrations of 3 to 5 tenths occurred 2 to 3 nm (4 to 6 km) offshore of the barrier islands from Cross to Flaxman. During the summer of 1983, mild winds and cold air temperatures produced a substantial concentration of second-year ice in the nearshore region in early October. Two years later, in October 1985, most of the multi-year ice lay north of a line that roughly paralleled the coast 15 to 20 nm (28 to 37 km) offshore. During the remaining three freeze-up seasons, (1981, 1982, and 1984), multi-year ice in the nearshore region was confined to localized belts and patches of small floes and isolated ridge fragments grounded in the shear zone.

Chukchi Sea: 1980s

- **Initiation of Freeze-Up:** In 1983, freeze-up near Barrow occurred around October 1st. This early date appears to have resulted, at least in part, from the cooling and stabilizing influence of old ice present in the region. In 1984 and

1985, the nearshore waters of the Chukchi remained ice free until late October and mid-October, respectively.

- **Landfast Ice:** Landfast ice development along the Chukchi coast was found to be very limited in extent due to the predominance of easterly winds. These winds repeatedly opened a coastal flaw lead that, in turn, promoted ice production when refreezing occurred in the lead.
- **Ice Pile-Ups:** As in the Beaufort Sea, storm reversals during the freeze-up season were found to cause shoreline pile-ups along the Chukchi coast, especially near Barrow and Point Belcher. However, an absence of strong winds in 1983 and a paucity of abrupt wind reversals in both 1984 and 1985 minimized the number of pile-ups observed on the Chukchi coast.
- **Multi-Year Ice:** Cold air temperatures and a lack of strong winds during the summer of 1983 produced a significant concentration of second-year ice north of the 71°N parallel in the Chukchi Sea in early October. In November 1984, a 2- to 3-tenths concentration of multi-year ice in the western Beaufort Sea was advected into the northern Chukchi. It remained north of the 71°N parallel through late January 1985, and was located well offshore of the prevailing 10- to 20-nm (19- to 37-km) wide coastal flaw lead. The multi-year floes typically ranged from 300 to 600 m in diameter, with a maximum extent of 4 km. In October 1985, the multi-year ice in the Chukchi attained higher concentrations and moved closer to the coast than in the Beaufort.

2.2 2009-10 Freeze-Up Study

The scope and methods of the 2009-2010 Freeze-Up Study, which were adopted with only minor modifications in 2010-11, 2011-12, and 2012-13, are described in detail by Coastal Frontiers and Vaudrey (2010). Significant findings are as follows:

Beaufort Sea: 2009-10

- **Initiation of Freeze-Up:** Freeze-up in the nearshore portion of Beaufort Sea occurred during the third week in October.
- **Landfast Ice and Shear Zone Development:** An intense easterly storm in late December created a grounded shear zone to the west of Prudhoe Bay that remained intact through midwinter. In contrast, westerly winds in January 2010 removed much of the landfast ice off the barrier islands to the east of Prudhoe Bay, and the ice remained dynamic through mid-February.

- **Ice Pile-Ups:** Ice pile-ups were observed on or adjacent to six natural barrier islands and one man-made island during the reconnaissance flights conducted in early February. The estimated pile-up heights ranged from 1 to 16 m. The largest pile-up exceeded 2 km in length.
- **Multi-Year Ice:** For the first time since 2001-02, multi-year ice floes invaded the nearshore waters of the Alaskan Beaufort Sea. The floes remained 10 to 20 nm (19 to 37 km) offshore as they migrated toward the west and ultimately entered the Chukchi Sea.

Chukchi Sea: 2009-10

- **Initiation of Freeze-Up:** Freeze-up proceeded more slowly than in the Beaufort, with the ice edge advancing to the south and west during the month of November. By the end of the month, ice covered the Chukchi Sea north of Cape Lisburne and east of 169°W.
- **Landfast Ice:** Alternating periods of easterly and westerly winds repeatedly dislodged the nearshore ice between Barrow and Point Lay, causing the freeze-up process to start anew. As a result, most of the coast lacked a shear zone with sufficient grounding to stabilize the offshore boundary of the landfast ice, and the ice remained susceptible to removal during easterly storms.
- **Coastal Flaw Lead:** The distinctive flaw lead that forms off the Chukchi Sea coast opened and closed repeatedly in response to easterly (offshore) and westerly (onshore) winds. The width of the lead varied substantially, depending on the duration and intensity of the easterly winds. A maximum width of 40 to 50 nm (74 to 93 km) was noted during a 25-day period from mid-February to early March, and again during a 10-day period in late March.
- **Ice Pile-Ups:** Nineteen ice pile-ups were observed on the Chukchi Sea coast during the February reconnaissance flights, including three that encroached substantial distances onto the beach. The most significant pile-up extended 150 m alongshore and attained a maximum height of 15 m. The maximum heights of the other pile-ups ranged from 4 to 10 m.
- **Multi-Year Ice:** The multi-year ice that entered the northern Chukchi Sea from the western Beaufort split into two separate branches that persisted through mid-winter: (1) a northern branch that remained above the 71.5°N parallel in the eastern and central Chukchi before dipping south, and (2) a southern branch that extended southwest from Barrow to the vicinity of the 70°N parallel.

2.3 2010-11 Freeze-Up Study

Key findings of the 2010-11 Freeze-Up Study (Coastal Frontiers and Vaudrey, 2011) are summarized below:

Beaufort Sea: 2010-11

- **Initiation of Freeze-Up:** Freeze-up in the nearshore portion of Beaufort Sea occurred during the second week in October.
- **Landfast Ice and Shear Zone Development:** The landfast ice zone remained narrow and unstable during the 2010-11 freeze-up season due to a lack of both easterly storms and sustained easterly winds. In the western Beaufort, the landfast ice edge passed through Weller Bank but had not reached its other typical anchor point on Stamukhi Shoal at the end of January. In the central Beaufort, the landfast ice edge at the end of January was located in close proximity to the barrier islands east of Prudhoe Bay and within 10 nm (19 km) of the shoreline in Camden Bay.
- **Ice Pile-Ups:** Only one ice pile-up was observed in the Alaskan Beaufort Sea in 2010-11. It was located at the Oooguruk Offshore Drillsite in the shallow waters of the Colville River Delta, and consisted of 10- to 15-cm thick plates that were stacked against the south corner and southwest side in multiple waves with heights to 3 m. The pile-up did not encroach beyond the waterline of the island's gravel-bag armor.
- **Multi-Year Ice:** In contrast to 2009-2010, large multi-year ice floes did not invade the nearshore region of the Alaskan Beaufort Sea during the 2010-11 freeze-up season. Between November 2010 and mid-February 2011, such floes remained north of the 71°N parallel in the eastern Beaufort and the 72°N parallel in the western Beaufort. However, grounded fragments of old ice with diameters ranging from 1.0 to 5.5 m were observed on the shorelines of many of the barrier islands. The fragments were derived from a band of grounded ice that persisted in the nearshore area between Flaxman Island and Smith Bay throughout the 2010 open-water season.

Chukchi Sea: 2010-11

- **Initiation of Freeze-Up:** Freeze-up in the Chukchi Sea began during the first week in October but progressed slowly due to above-normal air temperatures and a prolonged easterly storm that dislodged the newly-formed landfast ice from the coast in mid-month. Complete ice coverage in the region north of Cape Lisburne and east of the 169°W meridian occurred during the first week in December.

- **Landfast Ice:** Except in Peard Bay, Kasegaluk Lagoon, and the semi-protected area east of Point Franklin, the landfast ice that developed off the coast between Barrow and Point Lay was confined to a narrow strip that remained unstable through mid-February 2011. A paucity of westerly storms through mid-January limited the production of grounded rubble, thereby leaving the nearshore ice susceptible to break-out and removal during periods of easterly winds.
- **Coastal Flaw Lead:** The coastal flaw lead was detected on five occasions during the 2010-11 freeze-up season: late December, early January, late January, and twice in the first half of March. The dimensions of the lead varied substantially, from an estimated 50 nm (93 km) long by 5 nm (9 km) wide in late December to 140 nm (259 km) long by up to 60 nm (111 km) wide in late January. The feature's persistence also varied, from as little as several days during each appearance in March to about a week in early January.
- **Ice Pile-Ups:** Twenty-seven ice pile-ups were observed on the Chukchi Sea coast in February 2011, representing eight more than in 2010. The largest pile-ups were located between Point Belcher and Wainwright, where one ice pile attained both the maximum estimated height of 8 m and the maximum estimated encroachment distance of 40 m onto the beach. The longest ice pile, stretching 2,300 m alongshore with a height of 3 m, also occurred in this region.
- **Multi-Year Ice:** Large multi-year ice floes remained well offshore throughout the 2010-11 freeze-up season, with the southern boundary located approximately 60 nm (111 km) off Point Barrow at the end of December and 180 nm (333 km) at the end of March. Nevertheless, fragments of old ice embedded in first-year floes were observed in Shell's Burger Prospects in February 2011. They comprised less than 5% of the ice cover, with maximum horizontal dimensions that ranged from one hundred to several hundred meters.

2.4 2011-12 Freeze-Up Study

The results of the 2011-12 Freeze-Up Study (Coastal Frontiers and Vaudrey, 2012a) are summarized below:

Beaufort Sea: 2011-12

- **Initiation of Freeze-Up:** Freeze-up began during the second week in October, when ice began to form adjacent to the coast. Complete ice coverage in the nearshore region occurred on October 26th, followed soon thereafter by complete freeze-up in the Alaskan Beaufort Sea on November 1st.

- **Landfast Ice and Shear Zone Development:** After remaining narrow in November, the landfast ice zone grew dramatically in December in response to three easterly storms. The ice remained firmly grounded on Weller Bank and Stamukhi Shoal through mid-winter, but failed to achieve stability to the east of Prudhoe Bay seaward of the 11-m isobath.
- **Ice Pile-Ups:** Ten ice pile-ups occurred in the central portion of the Alaskan Beaufort Sea during the 2011-12 freeze-up season. Nine were located on natural barrier islands and one on Northstar Production Island. The heights ranged from 2 to 7.6 m, the encroachment distances from 0 to 20 m, and the alongshore lengths from 200 to 1,200 m.
- **Multi-Year Ice:** Except in the immediate vicinity of Point Barrow, multi-year ice remained well offshore in the Alaskan Beaufort Sea throughout the 2011-12 freeze-up season.

Chukchi Sea: 2011-12

- **Initiation of Freeze-Up:** As in 2010-11, freeze-up in the Chukchi Sea commenced during the first week in October but developed slowly in the weeks that followed. Complete coverage in the region north of Cape Lisburne occurred on November 30th.
- **Landfast Ice:** The landfast ice in the northeast Chukchi Sea remained unstable and discontinuous until January, when a predominance of westerly winds coupled with two westerly storms produced a narrow but continuous strip between Barrow and Point Lay. This strip persisted throughout February despite the frequent occurrence of easterly winds, indicating that it had become well-grounded during the westerly winds in January.
- **Coastal Flaw Lead:** The coastal flaw lead was present during a significant portion of the 2011-12 freeze-up season, including more than half of the months of December and February. The width typically ranged from 10 to 30 nm (19 to 56 km) but expanded to as much as 60 nm (111 km) in December. The length typically varied between 120 and 180 nm (222 and 334 km) but equaled or exceeded 200 nm (371 km) on several occasions.
- **Ice Pile-Ups:** Thirty-one ice pile-ups were detected on the coast between Point Barrow and Point Lay. The highest concentrations were located on the Point Franklin spit and on the barrier islands that bracket Icy Cape. The heights ranged from 3 to 18 m, the encroachment distances from 0 to 40 m, and the alongshore lengths from 100 to 5,400 m. All of the maximum dimensions were associated

with a massive pile-up that overtopped the 15-m high bluff at Skull Cliff and spilled 3 m onto the tundra.

- **Multi-Year Ice:** Large multi-year ice floes began streaming into the region south and west of Point Barrow in mid-December when they encountered a northeasterly extension of the coastal flaw lead that caused them to turn to the southwest. This pattern of southwesterly movement, which persisted through mid-winter, included another episode of the flaw lead entraining multi-year floes in late March. Between December and March, floes with diameters from 100 m to more than 20 km attained concentrations as high as 90%, and moved as far south as the 68°N parallel.
- **Grounded Ice Features:** Two grounded ice features believed to be ice island fragments that originated at Ellesmere Island were discovered off the Chukchi Sea coast in February 2012. The larger of the two, located approximately 3 nm (6 km) off Point Belcher in a charted water depth of 32 m, was estimated to be 80 m long, 40 m wide and 20 m above sea level.

2.5 2012-13 Freeze-Up Study

Key findings from the 2012-13 Freeze-Up Study (Coastal Frontiers and Vaudrey, 2013) are as follows:

Beaufort Sea: 2012-13

- **Initiation of Freeze-Up:** Ice began to form in the brackish waters off river deltas and in semi-protected bays and lagoons during the second week in October. Freeze-up in the nearshore region took place on November 5th; basin-wide freeze-up occurred one week later on the 12th.
- **Ice Fracture Event:** From late January through late March, the ice canopy in the Beaufort Sea was disturbed by a massive fracture event that ultimately stretched from Point Barrow on the west to Banks Island on the east. Energized by sustained easterly winds and a series of easterly storms, the event caused large pieces of the pack ice to break free and rotate to the west.
- **Landfast Ice and Shear Zone Development:** The landfast ice zone remained narrow and poorly-developed through mid-December, but expanded dramatically from mid-December through late January in response to the same sustained easterly winds and storms that caused the fracture event. In mid-March, the fracture event encompassed the outer portion of the landfast ice, and the seaward edge retreated to the vicinity of the 18-m isobath.

- **Ice Pile-Ups:** Thirty eight ice pile-ups were noted in the central portion of the Alaskan Beaufort Sea, consisting of thirty-four on barrier islands, three on Northstar Production Island, and one on the mainland shore. The heights ranged from 2 to 10 m, the encroachment distances from 0 to 10 m, and the alongshore lengths from 100 to 2,200 m
- **Multi-Year Ice:** As in 2010-11 and 2011-12, multi-year ice failed to invade the nearshore portion of the Alaskan Beaufort Sea during the 2012-13 freeze-up season.

Chukchi Sea: 2012-13

- **Initiation of Freeze-Up:** Freeze-up began during the second week in October with the formation of ice in Kasegaluk Lagoon, the Kuk River Inlet, and Peard Bay. Complete ice coverage in the nearshore region occurred on November 15th, followed by complete coverage in the entire Chukchi Sea north of Cape Lisburne on November 28th.
- **Flash-Freeze Event:** On October 31st, a flash freeze occurred in a large area off Wainwright bounded by the 71° and 72.5°N parallels, and the 160° and 165°W meridians. The ice patch, which was surrounded by open water, covered all of the Hanna Shoal Prospects and portions of the Burger Prospects.
- **Landfast Ice:** At the end of November, a narrow strip of landfast ice extended from Barrow to the vicinity of Wainwright, and another narrow strip encircled Icy Cape. During the next four months, in the absence of westerly storms, the landfast ice zone alternated between a narrow, continuous strip and an even narrower, discontinuous strip.
- **Coastal Flaw Lead:** The coastal flaw lead remained open for about half of the month of December, three quarters of the month of January, the entire month of February, and half of the month of March. During the 46-day period from January 31st through March 17th, it never closed. Driven by a combination of sustained easterly winds, easterly storms, and the massive ice fracture event in the Beaufort, the lead attained a maximum width of 150 nm (278 km) while stretching from Cape Lisburne to well northeast of Point Barrow.
- **Ice Pile-Ups:** Thirty-two ice pile-ups were observed on the Chukchi Sea coast between Point Barrow and Point Lay, with the highest concentration located on the barrier islands that lie to the south of Icy Cape. The pile-ups were relatively small by recent standards, with heights ranging from 2 to 4 m, encroachment distances from 0 to 8 m, and alongshore lengths from 100 to 3,800 m.

- **Multi-Year Ice:** As in the case of the Beaufort, multi-year ice remained absent from the region south and west of Point Barrow during the 2012-13 freeze-up season.

3. DATA ACQUISITION AND ANALYSIS

As outlined in Section 1, the 2013-14 Freeze-Up Study was conducted using a combination of remotely-sensed data and on-site observations. This section describes the sources of data and methods of analysis. The discussion is divided into the following five categories: meteorological data (Section 3.1), ice charts (Section 3.2), satellite imagery (Section 3.3), telemetry buoy data (Section 3.4), and aerial reconnaissance missions (Section 3.5). Digital data files are provided on the DVD that constitutes Appendix B.

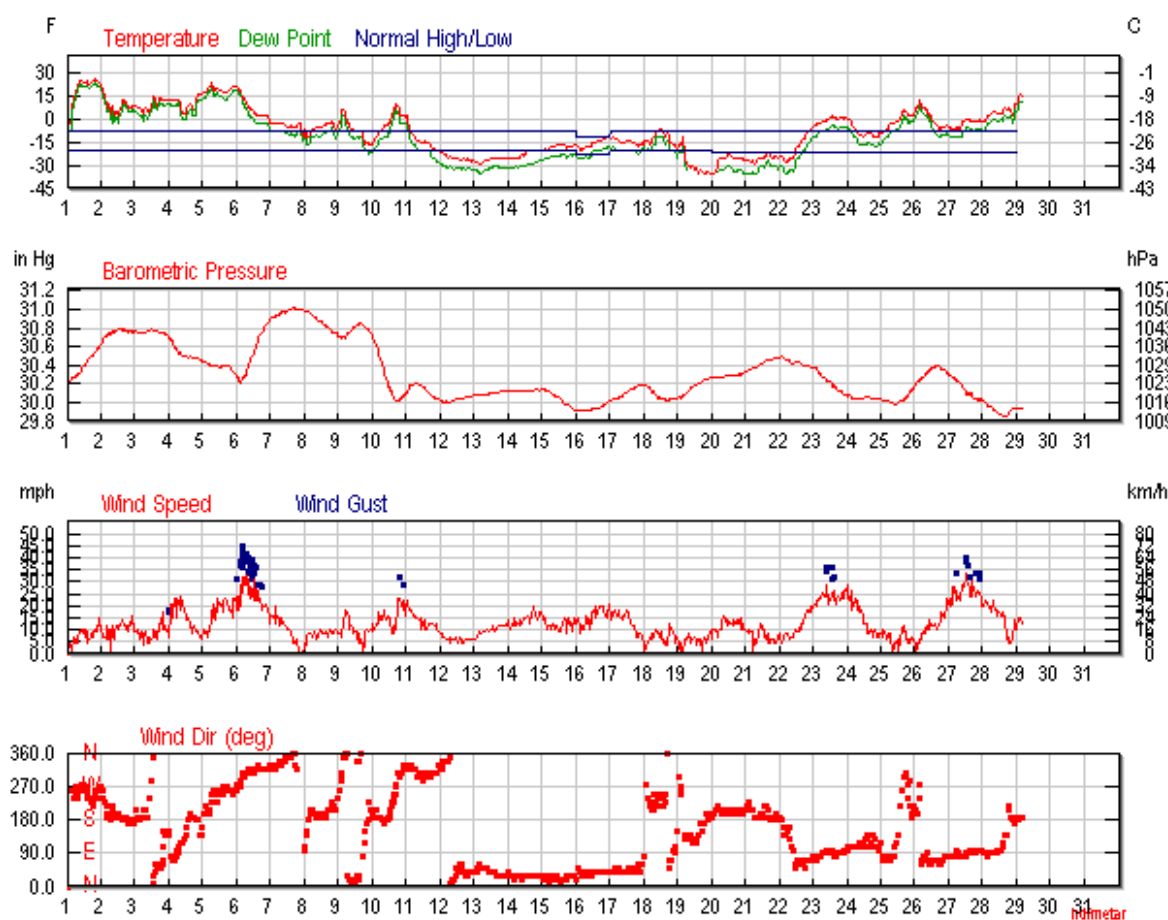
3.1 Meteorological Data

Meteorological data were obtained from two publicly-available sources: the Weather Underground (2014) and the National Ocean Service (2014). The following data were downloaded from the Weather Underground website for the Barrow and Deadhorse Airports for the nine-month period from September 2013 through May 2014:

- Monthly tabulations of daily air temperature, wind speed and direction, dew point, humidity, barometric pressure, visibility, and precipitation (compiled in an Excel spreadsheet in Appendix B);
- Monthly plots of air temperature, barometric pressure, wind speed, and wind direction (included as GIF files in Appendix B, with a representative example shown in Figure 5).

The wind data were used to identify storm events and changes in wind direction that impacted the ice canopy. Such impacts included the accumulation or loss of landfast ice, the opening or closing of the Chukchi Sea coastal flaw lead, and the generation of ice pile-ups. Although the monthly plots developed by the Weather Underground provide a useful overview of the wind conditions (*e.g.*, Figure 5), the tabulated values of sustained wind speed and wind direction were replotted to obtain better resolution while displaying the wind speeds in knots rather than miles per hour. These plots appear in Sections 4 and 5.

The air temperature data were used to derive freezing degree days (FDD), which were computed for each day as the difference between the freezing point of seawater (29°F; -2°C) and the mean air temperature. Days in which the temperature exceeded 29°F produced negative FDD. The daily values were summed over the period that produced the maximum number of accumulated FDD: September 22nd through June 2nd at Barrow Airport, and September 22nd through May 27th at Deadhorse Airport. The results are shown in Table 1.



Source: Weather Underground, 2014

Figure 5. Meteorological Data Recorded at Barrow Airport in February 2014

Table 1. Accumulated Freezing-Degree Days (<29°F) at Barrow and Deadhorse Airports in 2013-14

Site	Sep	Oct	Nov	Dec	Jan	Feb	Mar	Apr	May
Barrow	34	161	799	1786	2889	3897	4945	5696	5775
Deadhorse	27	239	1025	2089	3254	4450	5637	6390	6425

Note: FDD accumulation at Barrow extended through June 2, 2014.

To supplement the data obtained from the Weather Underground, monthly plots of air temperature, sea water temperature, barometric pressure, wind speed, and wind direction measured at the Prudhoe Bay West Dock Seawater Treatment Plant were downloaded from the National Ocean Service website (2013) for the period from October 2013 through March 2014. The plots are included as PNG files in Appendix B.

3.2 Ice Charts

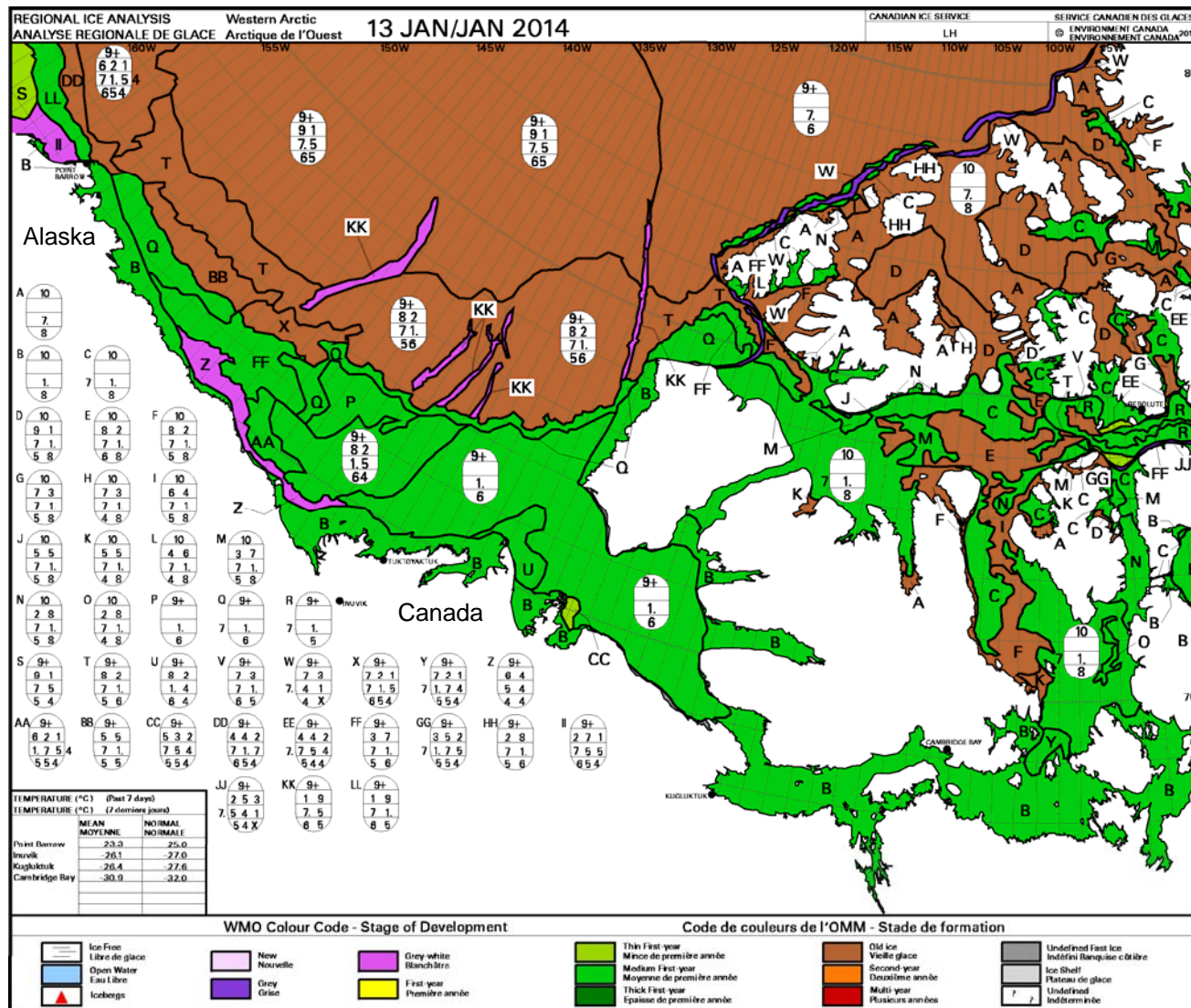
Ice charts were downloaded from two publicly-available sources: the Canadian Ice Service (CIS; 2014) and the National Ice Center (NIC; 2014). Although the charts from both organizations provide similar information, the CIS products incorporate greater detail by virtue of separate displays for ice concentration and stage of development. However, coverage is limited to the Beaufort Sea and extreme northeast portion of the Chukchi. The NIC produces separate charts for the Beaufort and the entire Chukchi.

Twenty-six pairs of ice charts showing concentration and stage of development were obtained from the CIS for the period from October 7, 2013, through March 31, 2014. The charts, which were issued on a weekly basis, are provided as GIF files in Appendix B. A sample stage-of-development chart for January 13, 2014, when multi-year ice was present at Point Barrow, is included as Figure 6.

Eighty-two ice charts covering the period from September 2, 2013, through April 3, 2014, were obtained from the NIC, consisting of 40 Beaufort Sea charts and 42 Chukchi Sea charts. The charts typically were issued twice per week prior to the occurrence of complete ice cover in each basin, and once per week thereafter. A representative example that displays the Chukchi Sea on November 19th, one week prior to the occurrence of nearshore freeze-up, is provided as Figure 7. PDF files of all of the NIC charts are included in Appendix B.

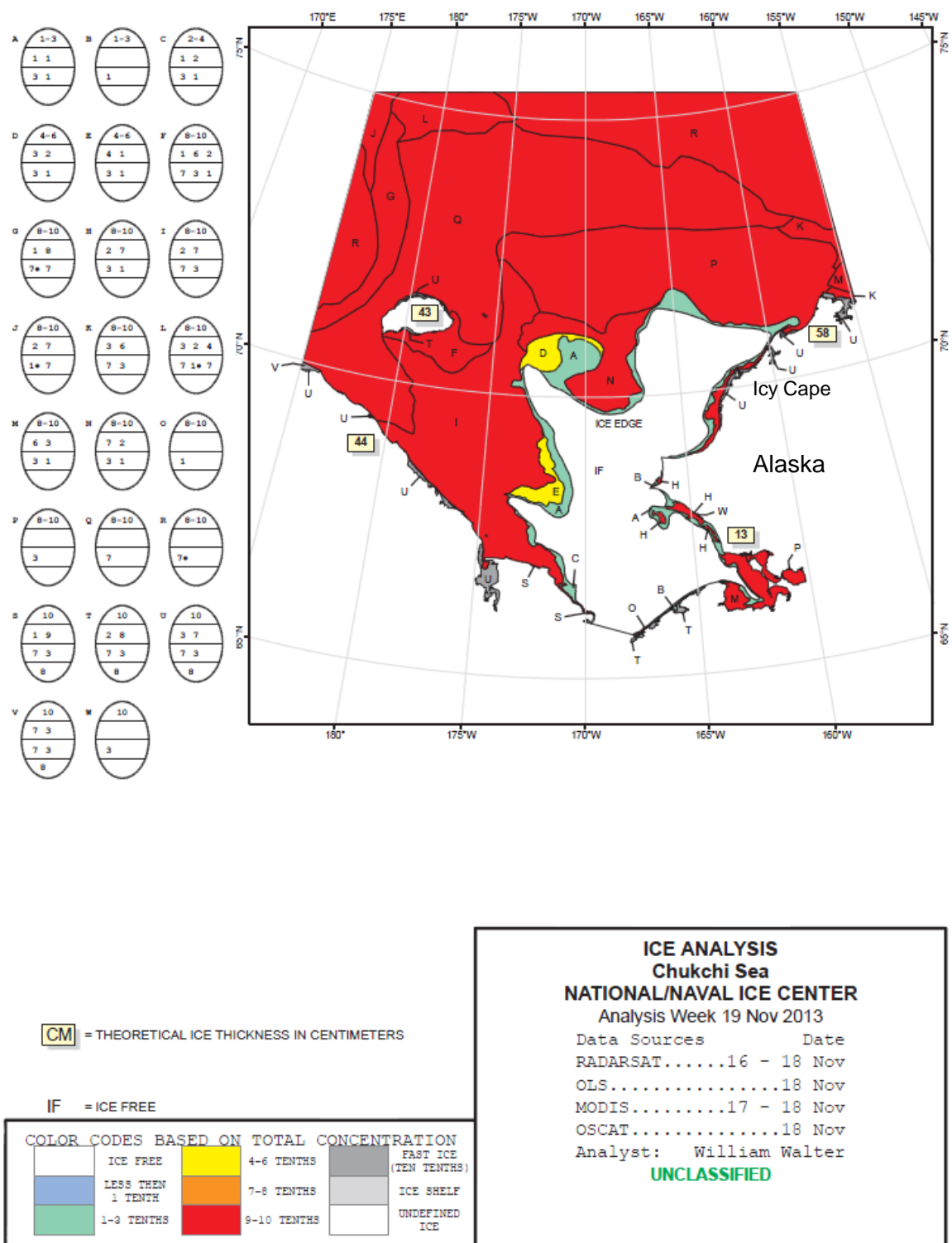
Additional insight into the condition of the ice canopy was obtained from nineteen sets of ice charts for the Beaufort and Chukchi Seas developed by the Shell Ice & Weather Advisory Center (SIWAC) for the period from October 9, 2013, through March 29, 2014. These charts, which were released into the public domain two weeks after their preparation, provide detailed information about the ice conditions in the nearshore region. Figure 8 presents the SIWAC Beaufort Sea ice chart from December 30th, when a substantial band of landfast ice stretched from Point Barrow to the vicinity of the Sivulliq Development project area. PNG files of all of the SIWAC charts are also included in Appendix B.

The ice charts from the three organizations were used to track the evolution of freeze-up on a coarse scale, particularly during the early stages of the process. They were not sufficiently detailed to support the investigation of fine-scale features such as individual ice floes and ice movement lines. The CIS stage-of-development charts and the SIWAC charts also were used to monitor the southern boundary of multi-year ice.



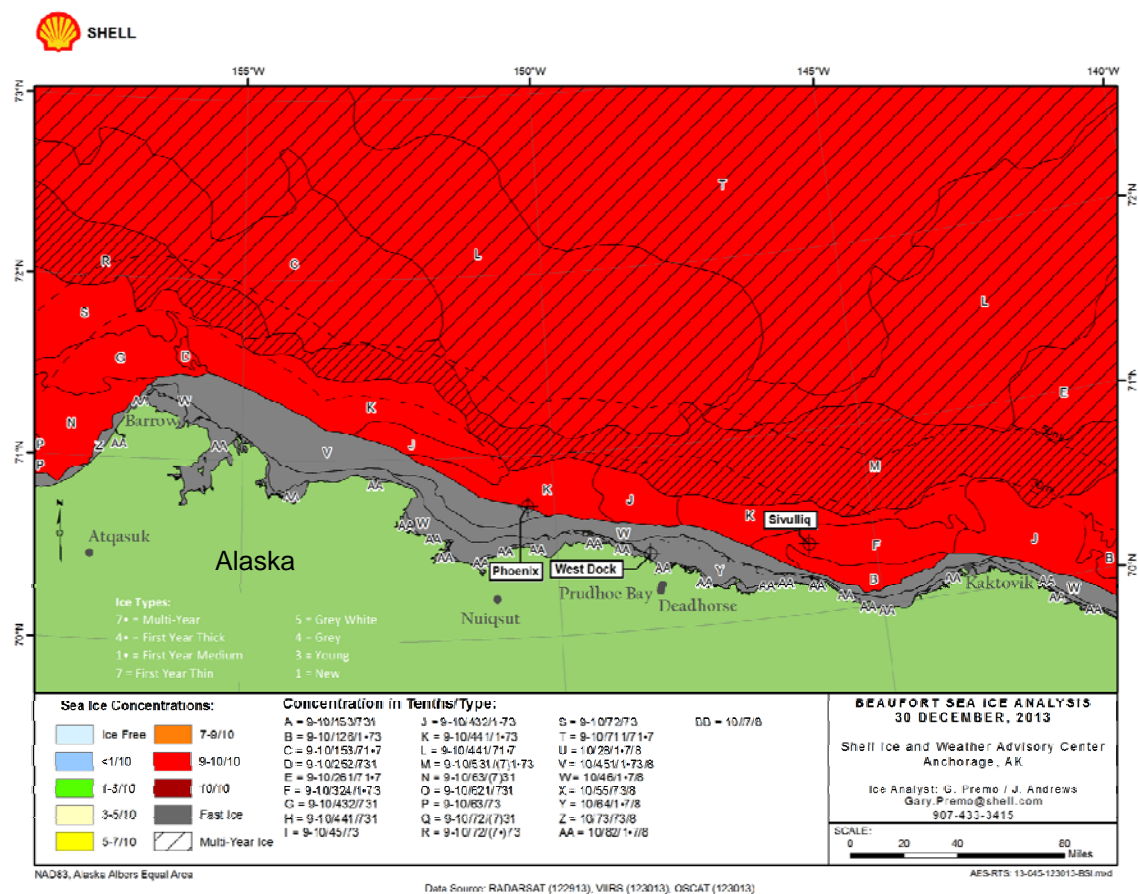
After: Canadian Ice Service, 2014

Figure 6. CIS Stage-of-Development Ice Chart of Beaufort Sea for January 13, 2014



After: National Ice Center, 2014

Figure 7. NIC Ice Chart of Chukchi Sea for November 19, 2013



After: Shell Ice & Weather Advisory Center, 2014

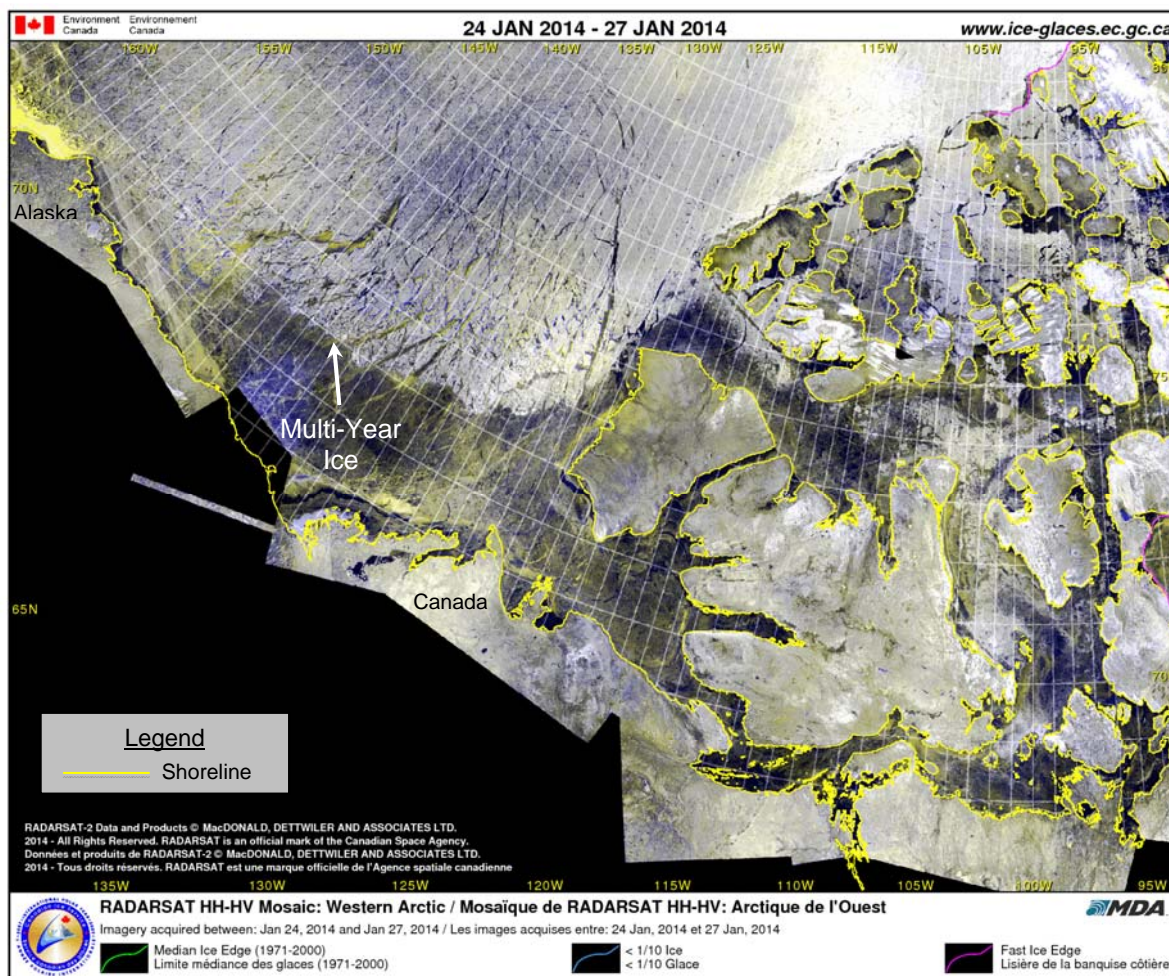
Figure 8. SIWAC Ice Chart of Beaufort Sea for December 30, 2013

3.3 Satellite Imagery

Three different types of satellite imagery were used to study the ice conditions that prevailed during the 2013-14 freeze-up season: RADARSAT-2, AVHRR (Advanced Very High Resolution Radiometer), and MODIS (Moderate Resolution Imaging Spectroradiometer). The RADARSAT-2 imagery served as the primary source of ice data, while the AVHRR imagery played a supplemental role. The MODIS imagery was used only sparingly.

General information about the progress of freeze-up was obtained from 26 publicly-available RADARSAT mosaics compiled by the CIS (2014) for the period from October 7, 2013, through March 31, 2014. The mosaics, which were produced on a weekly basis, are provided as GIF files in Appendix B. Although the resolution was inadequate to support detailed analysis, the composite images provided useful information on synoptic-scale ice

conditions. A representative example showing multi-year ice extending south to the 72nd parallel in the Alaskan Beaufort Sea is provided in Figure 9 (CIS, 2014).



After: Canadian Ice Service, 2014

Figure 9. CIS RADARSAT Mosaic of Beaufort Sea for January 24-27, 2014

The most useful RADARSAT-2 images were provided by Shell, which supplied 20 high-resolution, geo-referenced scenes for each of the Beaufort and Chukchi Seas. The images of the Beaufort were acquired between October 8, 2013, and March 28, 2014 while those of the Chukchi were acquired between October 9th and March 29th. The images were obtained using the ScanSAR Wide beam mode, which provides a nominal resolution of 100 m over a nominal area of 270 x 270 nm (500 x 500 km; MacDonald, Dettweiler and Associates Ltd., 2014). These characteristics were sufficient not only to track the general evolution of the ice cover during freeze-up and early winter, but also to support detailed investigations of features and phenomena that included the landfast ice edge, individual multi-year ice floes, leads, and ice movements over extended periods of time.

The licensing agreement for the RADARSAT-2 images prohibits the distribution of the original geo-referenced TIFF files. Accordingly, each scene is provided in Appendix B in JPG format. Figure 10 provides a sample image of the western Beaufort Sea acquired on February 28th. An extensive band of landfast ice is evident in the nearshore region, while a dense accumulation of multi-year ice lies well offshore.

One hundred and fifty AVHRR images obtained between October 30, 2013, and March 31, 2014, were downloaded from the National Weather Service Alaska Region Headquarters (2014) to bridge the chronological gaps between RADARSAT-2 scenes. The images are provided as JPG files in Appendix B. A representative image in Figure 11 shows the coastal flaw lead in the Chukchi Sea on February 15, 2014.

The utility of the AVHRR imagery was limited by the sensor's 1-km resolution and inability to penetrate cloud cover. Notwithstanding these drawbacks, the high frequency of image capture (multiple scenes per day subject to suitable weather conditions) allowed large-scale changes in the ice canopy to be tracked on a short-term basis. The imagery was particularly useful in identifying periods when the coastal flaw lead opened in the Chukchi.

MODIS imagery, like AVHRR imagery, was acquired to supplement the RADARSAT-2 scenes. Unfortunately, the sensor's maximum resolution of 250 m was outweighed by its inability to penetrate cloud cover, its dependence on light in the visible spectrum, and its inability to image the region above 72°N. In addition, the failure of a disk storage device resulted in the loss of most images obtained between January 2011 and mid-December 2013 (NASA, 2014a). As a result, useful scenes were confined to the period between February 3rd (when sufficient daylight became available for image acquisition) and March 31st. The 56 images that were downloaded from the MODIS Rapid Response website (NASA, 2014b) are provided as JPG files in Appendix B. Figure 12 presents an image acquired on February 24th that shows ice forming in the flaw lead off the Chukchi coast following the conclusion of a brief easterly storm.

3.4 Telemetry Buoys

During the 2009-10 through 2012-13 freeze-up seasons, Shell installed telemetry buoys to monitor ice motion off Camden and Harrison Bays in the Beaufort Sea (Coastal Frontiers and Vaudrey, 2010; 2011; 2012a; 2013). In 2013-14, Shell acquired such data by participating in the International Arctic Buoy Programme (IABP). The primary objective of the IABP is to acquire meteorological and oceanographic data in the Arctic Ocean through a network of drifting telemetry buoys (Polar Science Center, 2014a).

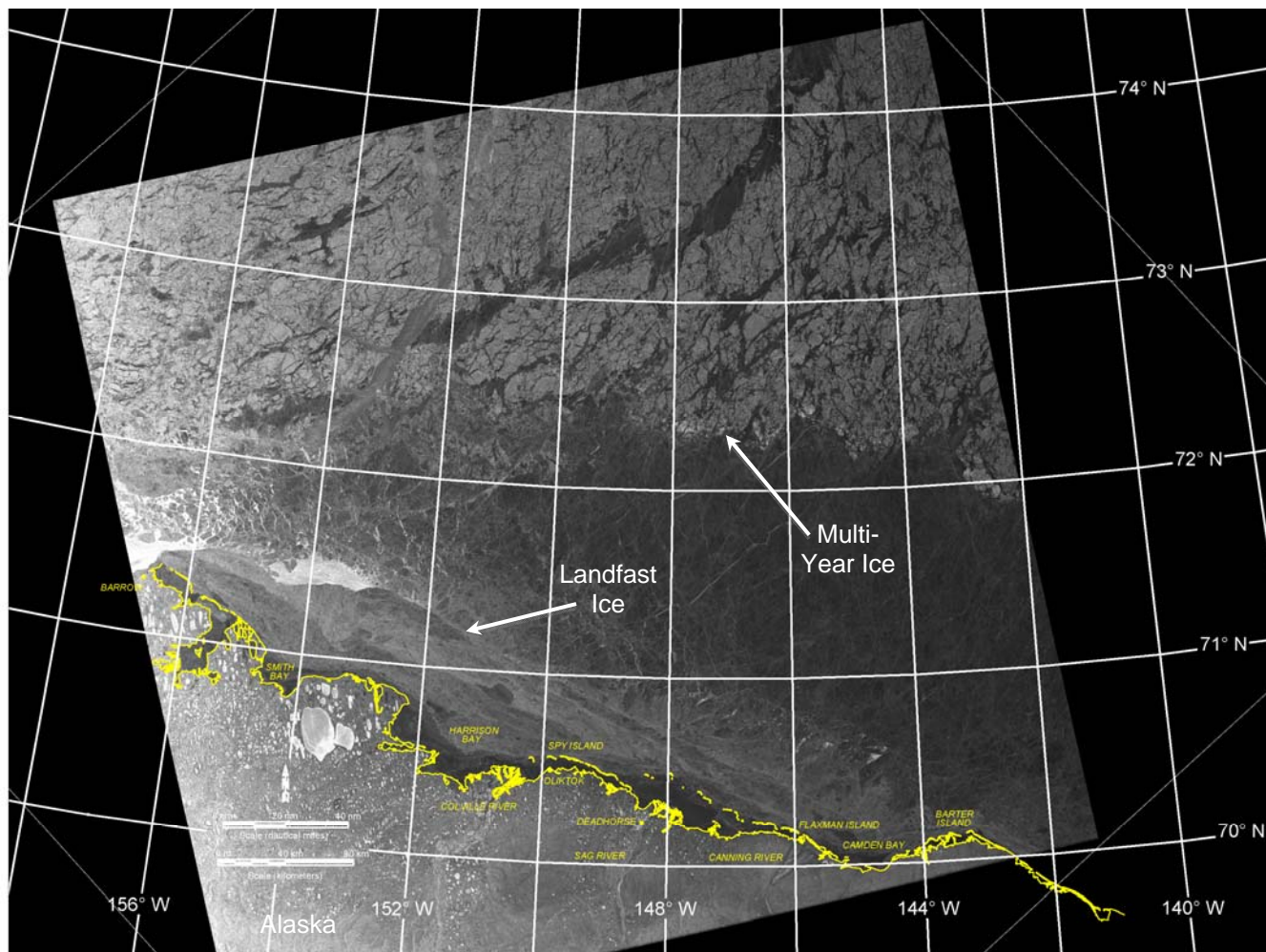
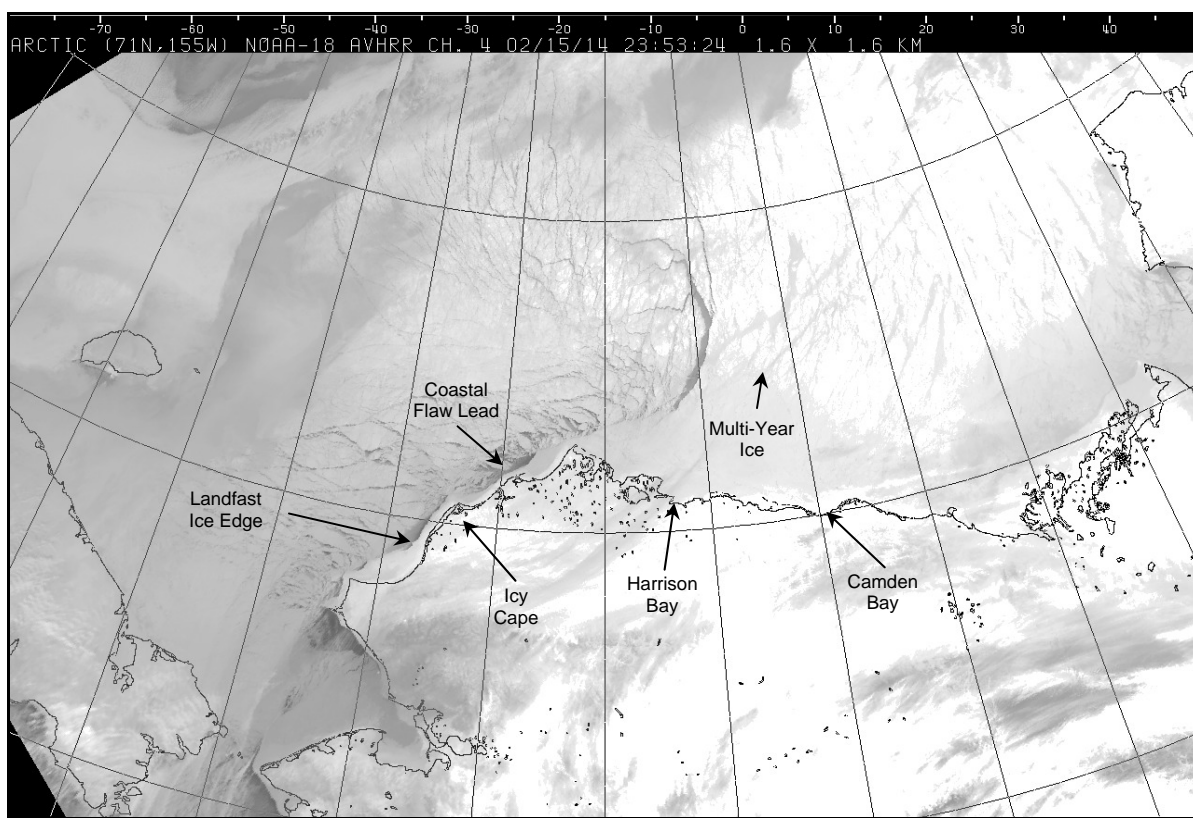


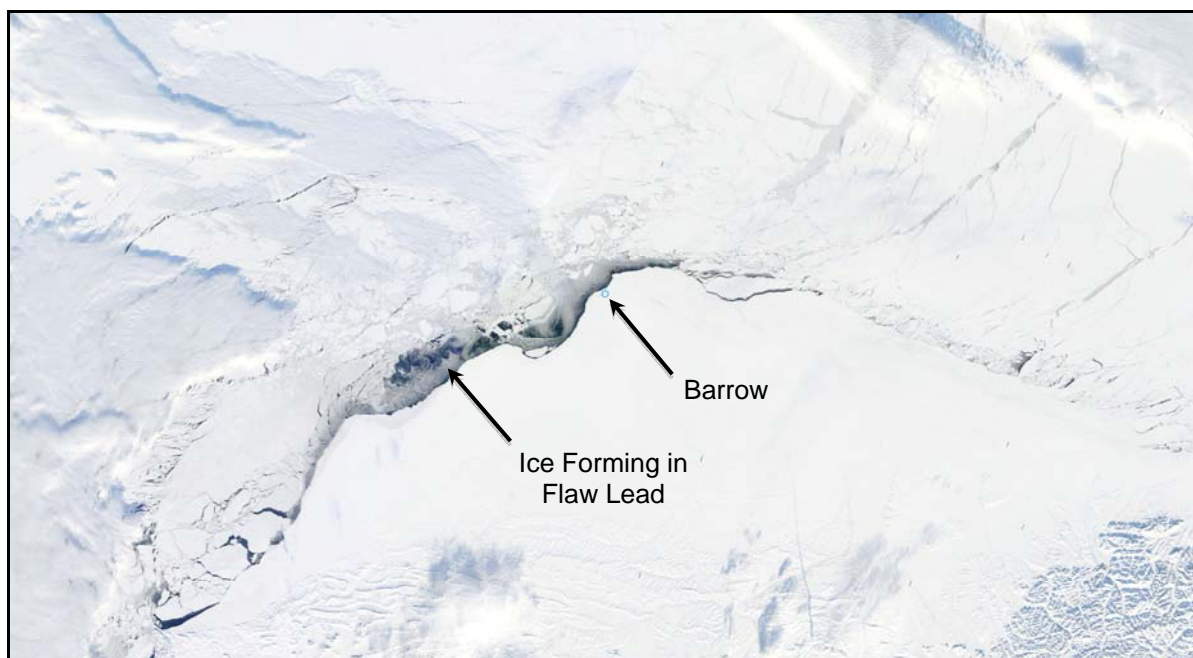
Image Source: RADARSAT-2 Data and Products © MacDonald Dettweiler and Associates Ltd., 2014 – All Rights Reserved

Figure 10. RADARSAT-2 Image of Beaufort Sea Acquired on February 28, 2014



Source: National Weather Service, 2014

Figure 11. AVHRR Image of Beaufort and Chukchi Seas Acquired on February 15, 2014



Source: NASA, 2014b

Figure 12. MODIS Image of Beaufort and Chukchi Seas Acquired on February 24, 2014

Under the auspices of the IABP, 21 telemetry buoys were deployed in the study area in late February and early March 2014. Fourteen were located in the Beaufort, with five off the east side of Camden Bay, four off the east side of Harrison Bay, two on Weller Bank, one off Smith Bay, and two to the east of Point Barrow (Figure 13). Seven buoys were deployed in the Chukchi, consisting of four on multi-year ice floes to the northwest of Point Barrow and three in Peard Bay (Figure 14). Hourly buoy positions were transmitted via satellite and compiled on a website maintained by the University of Washington's Polar Science Center (2014b). Shell contributed the data to this project in the interest of developing a more complete understanding of ice dynamics.

The trajectories shown in Figures 13 and 14, along with those presented in Sections 4 and 5, were constructed from the daily position of each buoy at midnight. The nearshore buoys in both basins tended to remain stationary, indicating that they were located in the zone of landfast ice. The offshore buoys, in contrast, experienced significant displacements.

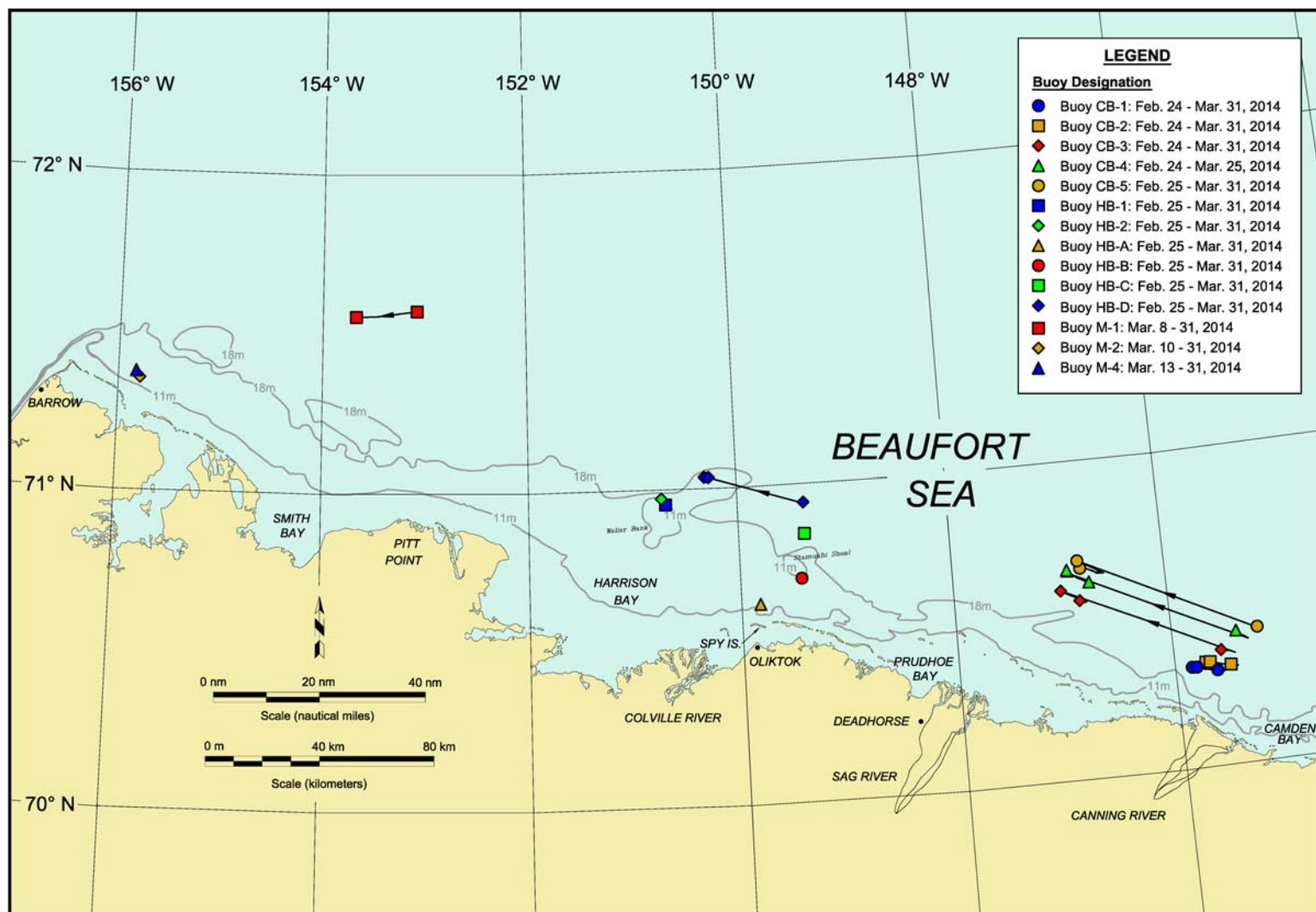
The hourly position data for the twenty one telemetry buoys are tabulated in an Excel spreadsheet that appears in Appendix B. As in past years, the information proved to be extremely useful in defining the boundary between stationary landfast ice and mobile pack ice, and also in correlating ice movements with wind events.

3.5 Aerial Reconnaissance Mission

Five aerial reconnaissance missions, consisting of three in the Beaufort and two in the Chukchi, were undertaken in late March 2014 to supplement the remotely-sensed data obtained from other sources. The specific objectives were as follows:

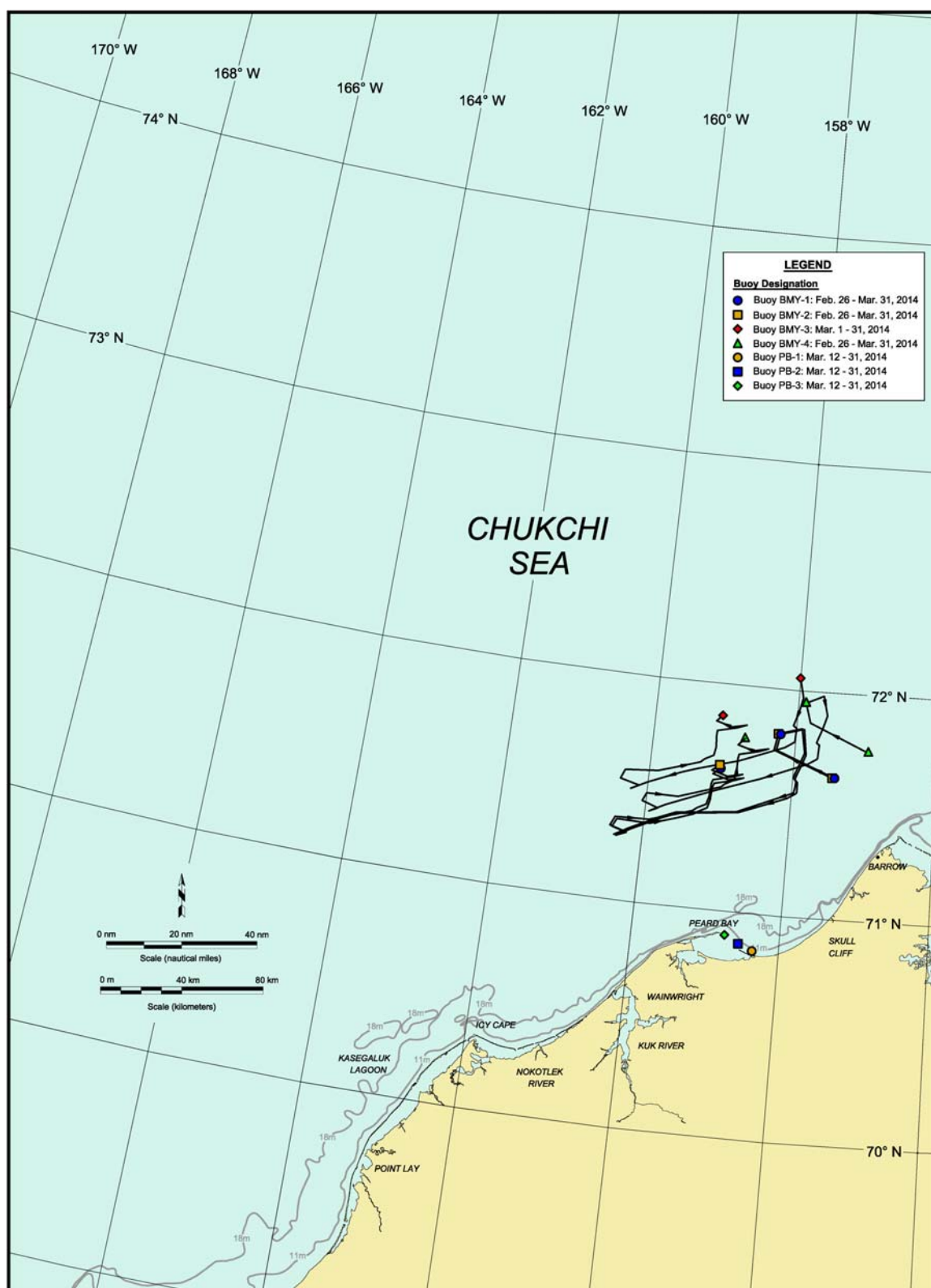
- Obtain ground truth information to confirm and expand upon the conclusions drawn from satellite imagery;
- Investigate major features identified in the satellite imagery, such as leads, landfast ice and well-developed shear lines; detect, investigate, and document small-scale features that were beneath the resolution of the satellite imagery, including ridges, rubble fields, and shoreline pile-ups.

Both flights in the Chukchi and two of the three flights in the Beaufort were conducted using an Aero Commander 690 (Plate 1). This fixed-wing aircraft offered the benefits of an extended range, an ability to fly at relatively slow speeds, a high wing that permitted unobstructed views of the ice below, and a moderate cost per flight hour. The remaining flight over the Beaufort Sea was conducted using a Bell 412 helicopter (Plate 2), which



Data Source: Polar Science Center, 2014b

Figure 13. Telemetry Buoy Trajectories in Beaufort Sea, February 24 - March 31, 2014



Data Source: Polar Science Center, 2014b

Figure 14. Telemetry Buoy Trajectories in Chukchi Sea, February 26 - March 31, 2014



Plate 1. Aero Commander 690 at Deadhorse Airport



Plate 2. Bell 412 Helicopter at 11.8-m Ridge off Mary Sachs Entrance

provided invaluable opportunities to hover over and, if warranted, land at features of interest. The primary disadvantages of the helicopter were its limited range and high cost per flight hour.

Each flight path was mapped using a Garmin GPSMap 196. To improve the accuracy of the position data, differential corrections broadcast in real time via satellite by the U.S. Government's Wide Area Augmentation System (WAAS) were received by the GPS unit when available. Static position checks conducted at North Slope survey monuments in the past have indicated that the accuracy attainable with WAAS is about 1 m. When operated in the stand-alone mode, the GPS accuracy typically is on the order of 10 m.

The GPS position data were displayed on a base map of the study area in real time using a laptop computer and Hypack survey software. This arrangement allowed the field crew both to direct the aircraft to locations of interest identified in advance from the satellite imagery, and to record the locations of small-scale features noted during the flight.

The flight paths are shown in Drawings CFC-917-01-001, -002, and -003 (Appendix A). The drawings display the locations of ice features observed during the flights as well as those of photographs and videos taken during the flights. Each photo has been assigned a unique identification number such as "B1-19" and each video a unique identification number such as "C2-V12". The first letter, "B" or "C", indicates whether the flight was conducted in the Beaufort or Chukchi; the number after the letter indicates which flight was involved; and the number that follows the hyphen indicates the order in which the photo or video was obtained during that flight. Hence, "B2-17" designates the 17th photograph acquired during the second Beaufort Sea reconnaissance flight.

The photographs are provided in digital form in Appendix B, with the file names corresponding to the identification numbers shown on the drawings. The ice features observed during the flights are denoted on the drawings using the abbreviations listed in Table 2, while the objective and path of each flight are summarized below:

Beaufort Sea Flight No. 1 ("B1" on Drawing CFC-917-01-001)

The first reconnaissance flight was undertaken with the Aero Commander on March 28th to observe the ice conditions in the central Beaufort Sea. The route and flight time were as follows:

- Deadhorse Airport
- Barrier islands from Cross to Duchess (heading east)
- Sivulliq Development prospective pipeline route

Table 2. Abbreviations for Ice Features

Ice Feature	Abbreviation
Active Shear Line	ASL
First-Year Ice (> 30 cm)	FY
Inactive Shear Line	ISL
Landfast Ice Edge	LFI
Lead	LD
Multi-Year Ice (concentration)	MY (_%)
Nilas (< 10 cm)	NLS
Open Water	OW
Pile-Up (height, encroachment, m)	P/U (_,_m)
Polynya	PLY
Refrozen Lead	RFL
Ridge (height, m)	RDG (_,m)
Rubble (height, m)	RBL (_,m)
Thermal Crack	TCK
Undeformed Ice	UDI
Young Ice (10-30 cm)	YNG

Note: The prefixes “i” and “m” are used to indicate intermittent features and multiple features, respectively (*i.e.*, “iRBL” indicates intermittent rubble).

- Transit east across southern Camden Bay
- Barter Island
- Transit northwest across northern Camden Bay
- Camden Bay Prospects
- Transit west at distances of 15 to 30 nm (28 to 56 km) offshore
- Stamukhi Shoal
- Harrison Bay Prospects
- Weller Bank
- Harrison Bay Prospects
- Spy Island Drillsite
- Barrier islands from Spy to Long (heading east)
- Northstar Production Island

- Reindeer and Argo Islands
- Deadhorse Airport
- Flight time = 2.7 hr.

Beaufort Sea Flight No. 2 (“B2” on Drawing CFC-917-01-001)

The reconnaissance flight on March 29th, the sole helicopter mission, was undertaken to investigate features of interest noted during the prior fixed-wing flight in the central Beaufort. The itinerary was as follows:

- Deadhorse Airport
- Northstar Production Island
- Reindeer and Argo Islands
- Transit south across Stefansson Sound to avoid fog
- Endicott Project
- Mainland coast from Endicott Project to Mikkelsen Bay (heading east)
- Land on ice in Mikkelsen Bay to measure ice thickness
- Mainland coast from Mikkelsen Bay to Point Thomson (heading east)
- Southern half of Sivulliq Development prospective pipeline route
- Land on ice to measure ridge characteristics
- Barrier islands from Duchess to Jeanette (heading west)
- Transit southwest across Stefansson Sound to avoid fog
- Deadhorse Airport
- Flight time = 2.6 hr.

Beaufort Sea Flight No. 3 (“B3” on Drawing CFC-917-01-002)

A fixed-wing flight was undertaken with the Aero Commander 690 on March 30th to observe the ice conditions in the western Beaufort Sea. The flight proceeded in the manner outlined below:

- Deadhorse Airport
- West Dock Causeway
- Barrier islands from Stump to Thetis (heading west)
- Oooguruk Offshore Drillsite
- Harrison Bay Prospects
- Weller Bank
- Transit northwest at distances of 20 to 30 nm (37 to 56 km) offshore
- Transit west to Point Barrow
- Barrow Airport
- Flight time = 1.6 hr.

Chukchi Sea Flight No. 1 (“C1” on Drawing CFC-917-01-003)

A second fixed-wing flight was undertaken with the Aero Commander 690 on March 30th to observe nearshore ice conditions and shoreline pile-ups between Barrow and Point Lay, a region where pipelines from the offshore prospects conceivably could make landfall. The flight described the following path:

- Barrow Airport
- Coast from Barrow to Point Lay (heading southwest)
- Transit north until 20 nm (37 km) from Point Lay
- Transit northeast at distances of 10 to 22 nm (19 to 41 km) offshore
- Barrow Airport
- Flight time = 2.8 hr.

Chukchi Sea Flight No. 2 (“C2” on Drawing CFC-917-01-003)

The final reconnaissance flight was undertaken with the Aero Commander 690 on March 31st to observe the ice conditions in the offshore portion of the northeast Chukchi Sea. Primary emphasis was placed on visiting Hanna Shoal and the Burger and Hanna Prospects. It should be noted that the Hanna Shoal Prospects are located 20 to 40 nm (37 to 74 km) southwest of Hanna Shoal itself (Figure 4). This wide-ranging flight proceeded in the following manner:

- Barrow Airport
- Transit northwest
- Hanna Shoal
- Transit southwest
- Hanna Shoal Prospects
- Transit west to vicinity of 163.5° meridian
- Transit south and then east
- Burger Prospects
- Transit east with diversion to northeast to follow multi-year ice
- Barrow Airport
- Flight time = 3.2 hr.

As in each of the four prior freeze-up studies (Coastal Frontiers and Vaudrey, 2010; 2011; 2012a, 2013), the reconnaissance flights in 2013-14 provided invaluable opportunities to confirm and refine the findings derived from satellite imagery, and to expand upon those findings with respect to small-scale features and processes.

4. BEAUFORT SEA FREEZE-UP

Section 4.1 provides an overview of the 2013-14 freeze-up season in the Alaskan Beaufort Sea. Sections 4.2 through 4.5 then present a month-by-month analysis of the conditions that prevailed from October 2013 through March 2014. The findings of the aerial reconnaissance flights undertaken at the end of March are discussed in Section 4.6.

4.1 Overview

Air Temperatures: As in each of the prior four years, the air temperatures recorded at Deadhorse Airport remained above normal during most of October. Above-normal temperatures also prevailed in November and January, while the average monthly values approached normal in September, December, February and March. The longest period of below-normal temperatures, an 11-day stretch that occurred in mid-February, was bracketed by above-normal temperatures at the beginning and end of the month.

Winds: Wind conditions during the 2013-14 freeze-up season are summarized in Table 3, which is based on the average daily speeds and directions recorded at Deadhorse Airport. Westerlies prevailed more than 50% of the time in every month except January, and more than 60% of the time in November, February, and March. Easterlies occurred on 58% of the days in January. Over the entire six-month period, westerlies prevailed 57% of the time versus 43% for easterlies. The average monthly speeds ranged from a maximum of 15 kt (8 m/s) in January to a minimum of 8 kt (4 m/s) in October and March.

Table 3. Beaufort Sea Wind Characteristics, October 2013 – March 2014

Month	Days		Average Speed (kt)
	Easterly	Westerly	
October	15	16	8
November	10	20	12
December	13	18	13
January	18	13	15
February	11	17	10
March	11	20	8
Total Days	78	104	n/a
Frequency (%)	43	57	n/a

Note: Table 3 is based on the average daily values recorded at Deadhorse Airport.

Storms: The characteristics of all storms with a daily average sustained wind speed exceeding 15 kt (8 m/s) at Deadhorse Airport are presented in Table 4 for the six-month period from October 2013 through March 2014. Of the twenty events, nine were easterlies and eleven were westerlies. December and January were the stormiest months, with twelve and fifteen days of storm activity, respectively. At the other end of the spectrum, October contained only two days of storm activity and March none. The highest sustained wind speed (29 kt; 15 m/s) and longest duration (10 days) were associated with an easterly storm that began on December 28th and continued through January 6th.

Ice Cover: Freeze-up commenced in late September, when ice began to form in the semi-protected waters adjacent to the coast. Complete ice coverage in the nearshore region occurred on October 26th. Complete coverage in the entire Alaskan Beaufort Sea took place more than three weeks later, on November 20th.

Ice Thickness: The thickness of undeformed first-year ice at the end of each month was estimated using the relationship of Lebedev (Bilello, 1960) in concert with the accumulated freezing degree days (FDD) at Deadhorse shown in Table 1. The relationship is as follows:

$$t = 0.94(\Sigma FDD)^{0.58} \quad (1)$$

where:

$$\begin{aligned} t &= \text{ice thickness in cm} \\ \Sigma FDD &= \text{accumulated freezing-degree days relative to } 29^{\circ}\text{F} \end{aligned}$$

(Although Lebedev originally calculated FDD relative to 32°F, ice thickness measurements in the Beaufort Sea obtained by Vaudrey and Associates, Inc., have indicated that Equation (1) provides more accurate results if FDD are referenced to 29°F.)

The computed values of ice thickness for the 2013-14 winter season are provided in Table 5, which indicates that undisturbed first-year ice attained a maximum thickness of 152 cm on May 27th. Subsequent to that date, the average daily air temperatures remained above 29°F.

Landfast Ice: Although landfast ice began to form in mid-October, its development remained stunted until the end of December due to a predominance of westerly winds (Table 3), a series of westerly storms, and a paucity of sustained easterly storms (Table 4). The situation changed in January, however, when persistent easterly winds coupled with two prolonged easterly storms produced a substantial expansion anchored by a well-grounded shear zone. At the end of the month, the seaward edge was located well outside the 18-m

Table 4. Beaufort Sea Storm Characteristics, October 2013 – March 2014¹

Month	Day	Duration (days)	Maximum Wind Speed (kt) ²	
			Easterly	Westerly
October	8	1	16	
	10	1		17
November	10-12	3		28
	14-19	6		22
	22	1	19	
December	1	1		22
	6-7	2	19	
	8	1		24
	9	1	20	
	16	1		17
	24-25	2		22
January	Dec 28-Jan 6	10	29	
	10-11	2		19
	15	1		17
	18	1	28	
	21-25 ³	5	25	
February	6	1		20
	11	1		16
	23	1	17	
	27	1	23	
March	-	-	-	-
Total Duration		43		
Total Number of Events			9	11

Notes:

- ¹ Table 4 includes all storm events with a daily average sustained wind speed exceeding 15 kt (8 m/s) at Deadhorse Airport.
- ² “Maximum Wind Speed” refers to highest daily average sustained wind speed that occurred during each storm event.
- ³ Daily average wind speed decreased to 8 kt (4 m/s) on January 22nd but freshened to 25 kt (13 kt) on January 23rd.

Table 5. Beaufort Sea Computed Ice Thicknesses, October 2013 – May 2014¹

Date	FDD	Accumulated FDD	Ice Thickness ² (cm)
31 October 2013	212	239	23
30 November 2013	786	1,025	52
31 December 2013	1,064	2,089	79
31 January 2014	1,165	3,254	102
28 February 2014	1,196	4,450	123
31 March 2014	1,187	5,637	141
30 April 2014	753	6,390	151
27 May 2014	35	6,425	152

Notes:

¹ Table 5 is based on the average daily air temperature data recorded at Deadhorse Airport.

² Ice thickness is computed from accumulated FDD using method of Lebedev (Bilelo, 1960).

isobath from the vicinity of Point Barrow to the vicinity of Barter Island. Thereafter, during the months of February and March, the landfast ice edge advanced in response to easterly winds and retreated in response to westerly winds but tended to retreat no farther than the 18-m isobath.

Ice Pile-Ups: As shown in Table 6, 46 ice pile-ups formed in the central portion of the Alaskan Beaufort Sea during the 2013-14 freeze-up season. Thirty nine were located on natural barrier islands, two on Northstar Production Island, one on Goose Exploration Island, one on the Prudhoe Bay West Dock Causeway Seawater Treatment Plant (STP) Pad, and three on the mainland shore. The heights ranged from 1 to 8 m, the encroachment distances from 0 to 20 m (measured from the waterline), and the alongshore lengths from 50 to 2,600 m. Due to the late-March timing of the reconnaissance flights, the ice blocks that comprised the pile-ups were partially obscured by drifted snow. The thicknesses appeared to range from 30 to 60 cm, however.

It is likely that the pile-ups occurred during three different periods, each of which contained strong winds that changed direction abruptly:

- November 9th through 10th, when the winds shifted from southeasterly to southwesterly and freshened to a peak of 24 kt (12 m/s), creating pile-ups on southerly, southwesterly, and westerly exposures;

Table 6. Ice Pile-Ups on Beaufort Sea Coast during 2013-14 Freeze-Up Season

No.	Location	Formation Date	Arrived From	Length¹ (m)	Height² (m)	Encroachment³ (m)
1	Thetis Is.	Nov 9-10	SW	100	2	3
2	Thetis Is.	Nov 14	NW	1,500	4	20
3	Thetis Is.	Nov 9-10	S	500	2	5
4	Thetis Is.	Nov 9-10	S	200	1	5
5	Spy Is.	Nov 14	NW	200	3	10
6	Spy Is.	Dec 8	N	100	3	5
7	Leavitt Is.	Dec 8	NE	100	3	0
8	Leavitt Is.	Dec 8	NE	100	2	0
9	Pingok Is.	Dec 8	NE	400	3	5
10	Cottle Is.	Dec 8	NE	1300	1	0
11	Long Is.	Dec 8	NE	500	2	5
12	Long Is.	Nov 9-10	W	100	2	5
13	West Dock	Nov 14	NW	250	8	20
14	Northstar Prod.	Nov 9-10	SW	100	4	0
15	Northstar Prod.	Dec 8	N	300	5	3
16	Reindeer Is.	Nov 14	NW	300	3	10
17	Reindeer Is.	Nov 9-10	SW	2,600	2	15
18	Reindeer Is.	Dec 8	NE	200	2	5
19	Argo Is.	Nov 9-10	S	400	3	15
20	Cross Is.	Dec 8	NE	300	1	5
21	Cross Is.	Dec 8	NE	300	2	5
22	Narwhal Is.	Nov 9-10	SW	300	5	10
23	Narwhal Is.	Dec 8	NE	1,000	2	0
24	Narwhal Is.	Dec 8	NE	1,100	5	20
25	Jeanette Is.	Nov 9-10	SW	50	3	0

(continued)

**Table 6. Ice Pile-Ups on Beaufort Sea Coast during 2013-14 Freeze-Up Season
(continued)**

No.	Location	Formation Date	Arrived From	Length¹ (m)	Height² (m)	Encroachment³ (m)
26	Jeanette Is.	Nov 9-10	SW	50	4	0
27	Jeanette Is.	Nov 9-10	SW	100	5	0
28	Jeanette Is.	Nov 9-10	S	500	4	15
29	Jeanette Is.	Nov 9-10	S	900	5	5
30	Pole Is.	Nov 9-10	SW	1,000	5	10
31	Pole Is.	Dec 8	NE	400	4	10
32	Pole Is.	Nov 14	NW	150	3	0
33	Pole Is.	Nov 9-10	SW	1,900	3	10
34	Pole Is.	Nov 9-10	SW	1,000	1	0
35	Pole Is.	Nov 9-10	SW	1,200	3	10
36	Belvedere Is.	Dec 8	NE	500	6	20
37	Belvedere Is.	Nov 9-10	SW	200	5	20
38	Belvedere Is.	Nov 9-10	SW	200	5	20
39	Challenge Is.	Dec 8	N	1,100	5	20
40	Alaska Is.	Dec 8	NE	1,300	2	5
41	Alaska Is.	Nov 9-10	S	1,100	2	0
42	Duchess Is.	Nov 14	NW	100	2	5
43	Brownlow Point	Dec 8	NE	2,500	3	0
44	Goose Is.	Nov 9-10	W	100	3	3
45	Point Gordon	Nov 9-10	W	200	1	0
46	Point Hopson	Nov 9-10	W	200	1	0

Notes:

¹ "Length" indicates alongshore extent of pile-up.

² "Height" indicates maximum height of pile-up relative to MSL.

³ "Encroachment" indicates distance ice advanced onto subaerial beach.

- November 14th, when the winds shifted from southerly to slightly north of west and freshened to 17 kt (9 m/s), creating pile-ups on northwesterly exposures;
- December 8th, when a 24-kt (12-m/s) westerly quickly veered through north to become a 20-kt (10-m/s) easterly, creating pile-ups on northerly and northeasterly exposures.

Multi-Year Ice: Multi-year was present in the offshore portion of the Alaskan Beaufort Sea throughout freeze-up and early winter, but remained absent from the nearshore region except in the immediate vicinity of Point Barrow. At the U.S.-Canadian Border, the southern boundary was located in the vicinity of the 72° parallel for most of the October-March study period but moved as far south as the 71°20' parallel for brief periods in late December and mid-January. Off Point Barrow, the boundary remained above the 72° parallel through mid-December. It then advanced to the south during the month that followed, reaching the Point in mid-January. From mid-January through March, it oscillated in a narrow range located 10 to 40 nm (19 to 74 km) offshore.

Ice Movement: The movements of eight multi-year ice floes were tracked using RADARSAT-2 images, and an average monthly speed was computed for each floe for which the period of record in the Beaufort Sea equaled or exceeded sixteen days. In keeping with the westerly set of the Beaufort Gyre, all of the floes experienced net displacements to the west during freeze-up and early winter. The greatest displacements and highest speeds occurred in January, the sole month in which easterly winds predominated. As shown in Table 7, the average monthly speeds ranged from 1.2 to 7.7 nm/day (2.2 to 14.3 km/day). The average monthly value was 3.3 nm/day (6.1 km/day).

Table 7. Beaufort Sea Multi-Year Ice Floe Speeds, November 2013 - March 2014

Month	No. of Floes	Average Monthly Speed (nm/day)		
		Maximum	Minimum	Average
November	4	2.5	1.2	1.8
December	4	3.4	1.5	2.0
January	4	7.7	4.0	6.2
February	4	5.5	2.7	4.3
March	2	2.7	2.2	2.4
Average				3.3

Note: Monthly speeds were derived for periods that ranged from 16 to 34 days.

4.2 Late Summer 2013

The ice cover in the Alaskan Beaufort Sea diminished throughout August and early September, due in part to melting in the nearshore zone and in part to the northward migration of the Arctic pack ice. In the nearshore zone, the last vestiges of the winter ice canopy disappeared in mid-August. On September 12th, the edge of the pack ice (where the ice concentration exceeded 0%) was located approximately 110 nm (204 km) off Barter Island and 175 nm (324 km) off Point Barrow (NIC, 2014).

The minimum extent of the pack ice, 5.10 million km² (Figure 15), occurred on September 13th (National Snow & Ice Data Center, 2013a; “extent” refers to the area in which ice covers at least 15% of the ocean surface). Although 50% larger than in 2012, when the minimum extent of 3.41 km² was the lowest recorded since the acquisition of satellite-based data began in 1979 (Figure 16), it nevertheless represented the sixth lowest in the period of record. A comparison of Figures 15 and 16 indicates that the rebound that occurred in 2013 was concentrated off Alaska and Canada. As a result, the separation between the Beaufort Sea coast and the edge of the pack ice at the beginning of the 2013-14 freeze-up season was less than half that which existed a year earlier.



After: National Snow & Ice Data Center, 2013a

Figure 15. Sea Ice Minimum Extent on September 13, 2013



After: National Snow & Ice Data Center, 2012

Figure 16. Sea Ice Minimum Extent on September 16, 2012

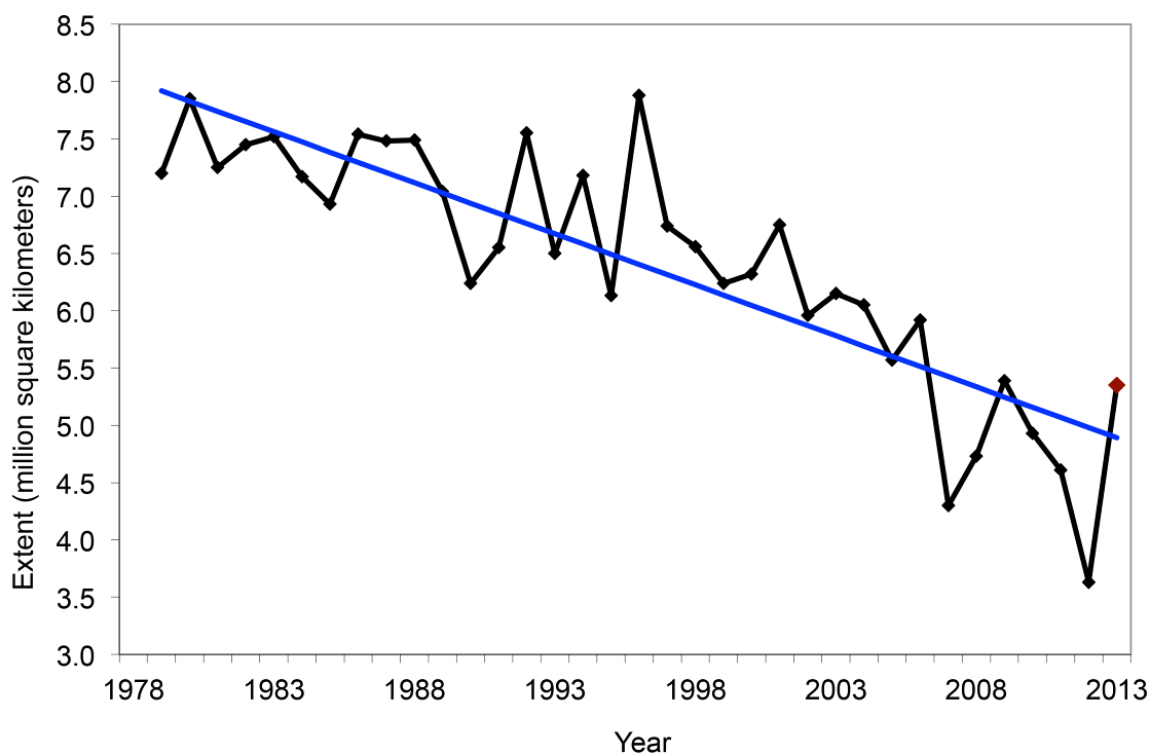
Notwithstanding substantial interannual variations, the extent of the Arctic sea ice in September has declined at an average rate of 13.7% per decade since 1979 (Figure 17). Also noteworthy is the fact that the average ice extents recorded during the past seven Septembers represent the lowest values in the historical record.

4.3 Early Freeze-Up

4.3.1 October 2013

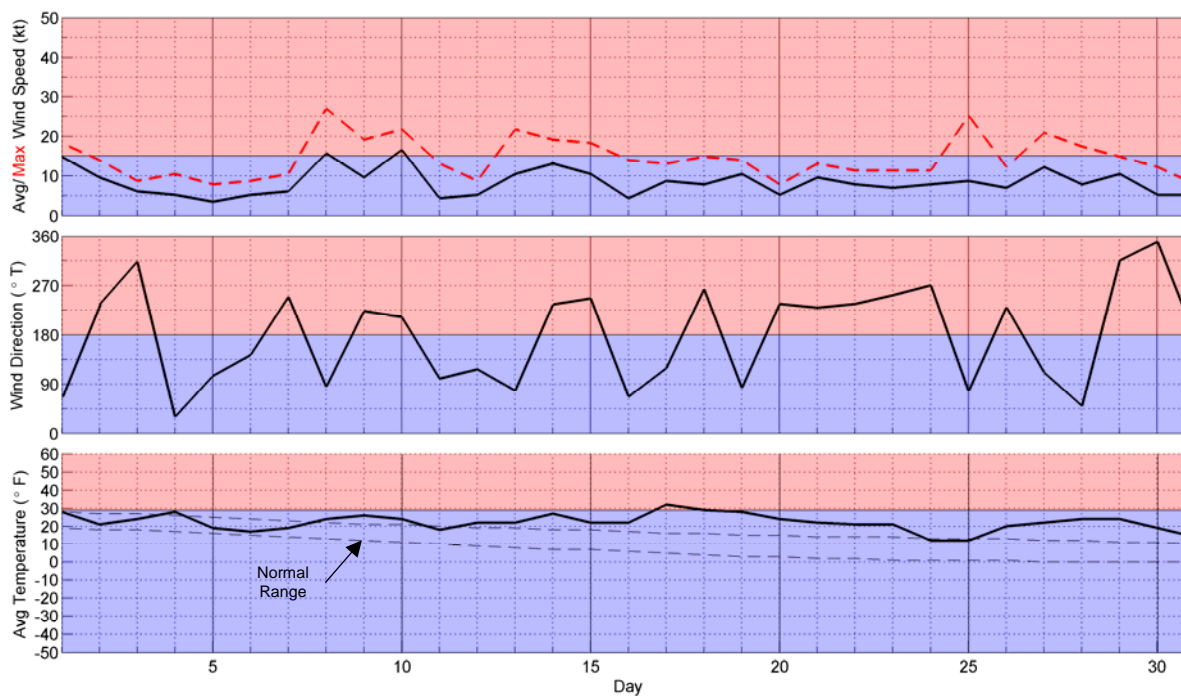
Meteorological Conditions: The daily values of average sustained wind speed, maximum sustained wind speed, average wind direction, and average air temperature at Deadhorse Airport are shown in Figure 18 along with the normal range of air temperatures defined by the average values of the daily highs and lows from 1971 through 2000. The significance of the red and blue color bands in this and all subsequent meteorological plots is indicated in Table 8. Unless stated otherwise, the wind speeds discussed in the text refer to the daily average values rather than the daily maximum values.

As in each of the past four years, the air temperatures remained above normal for most of the month of October. The wind speeds were relatively low, with the directions reflecting



Source: National Snow & Ice Data Center, 2013b

Figure 17. Average Sea Ice Extent in September, 1979-2013



Source: Weather Underground, 2014

Figure 18. Meteorological Conditions at Deadhorse Airport in October 2013

Table 8. Significance of Color Bands in Plots of Meteorological Conditions

Parameter	Band Color	
	Blue	Red
Wind Speed	≤ 15 kt	> 15 kt (Storm)
Wind Direction	Easterly	Westerly
Air Temperature	$\leq 29^{\circ}\text{F}$ (Freezing Point of Seawater)	$> 29^{\circ}\text{F}$

a near-equal split between westerly (16 days) and easterly (15 days). Storm activity was limited to two brief, back-to-back events (Table 4):

- October 8th: one-day easterly with maximum speed of 16 kt (8 m/s);
- October 10th: one-day westerly with maximum speed of 17 kt (9 m/s).

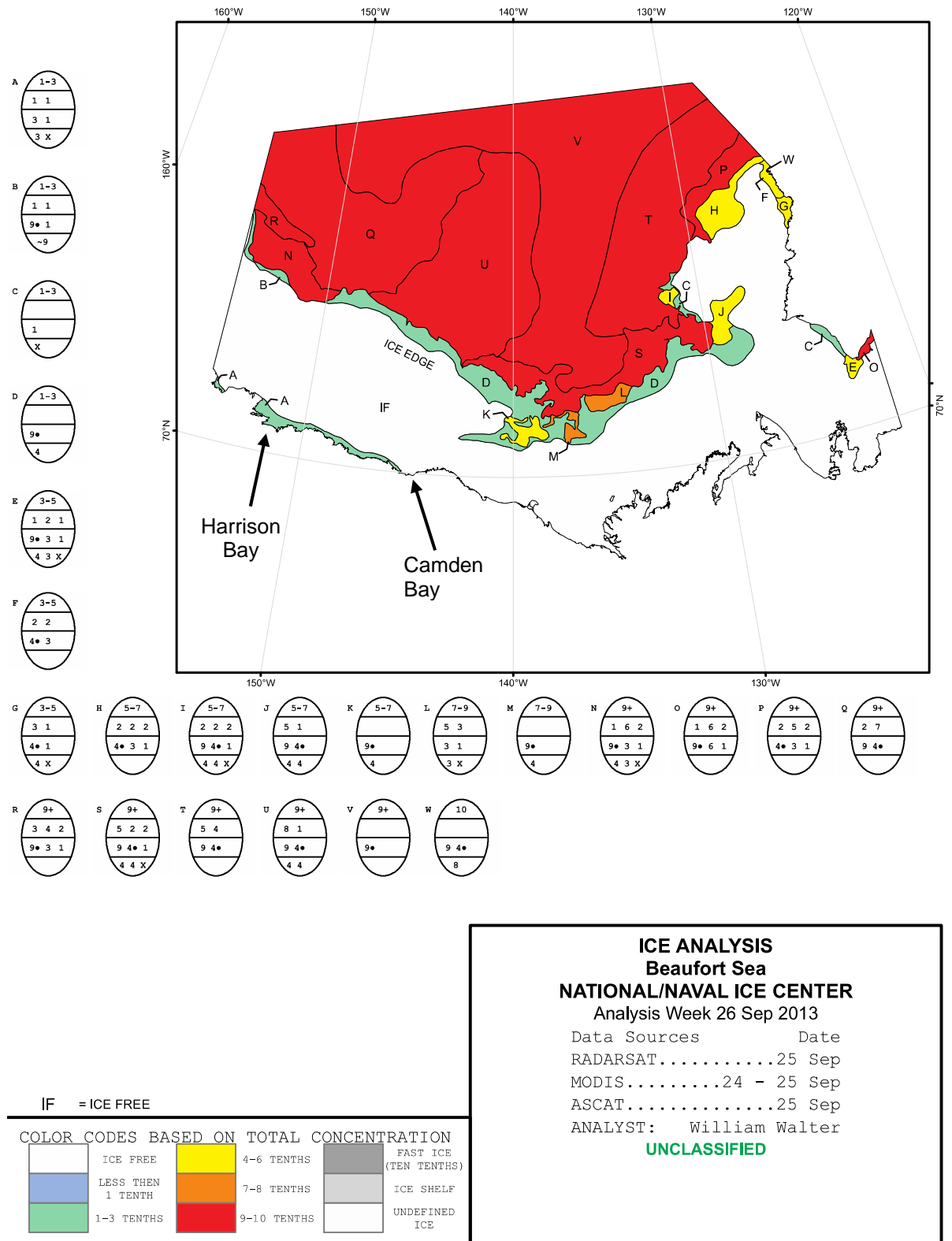
Ice Cover: Freeze-up in the Alaskan Beaufort Sea began in late September, when ice began to form in the brackish waters off river deltas and in semi-protected bays and lagoons (Figure 19). The first-year ice canopy developed slowly until mid-October, when the pace quickened in response to sub-freezing temperatures coupled with an absence of storm events (Figure 18). Ice charts prepared by SIWAC (2014), the NIC (2014) and the CIS (2014) indicate that complete freeze-up occurred in the nearshore region on or about October 26th. The temperature data recorded at Deadhorse Airport through this date produced an accumulated total of 197 FDD. (Note: for the purpose of establishing a date for freeze-up, the “nearshore region” is defined as the area that typically becomes covered with landfast ice.)

Ice Thickness: As indicated in Table 5, the computed thickness of undisturbed first-year ice was 23 cm at the end of October.

Multi-Year Ice: In a pattern analogous to that last noted in 2009, multi-year ice remained present in the northern reaches of the Alaskan Beaufort Sea throughout the summer and fall of 2013. At the end of October, the southern boundary paralleled the coast approximately 80 nm (148 km) offshore (Figure 20).

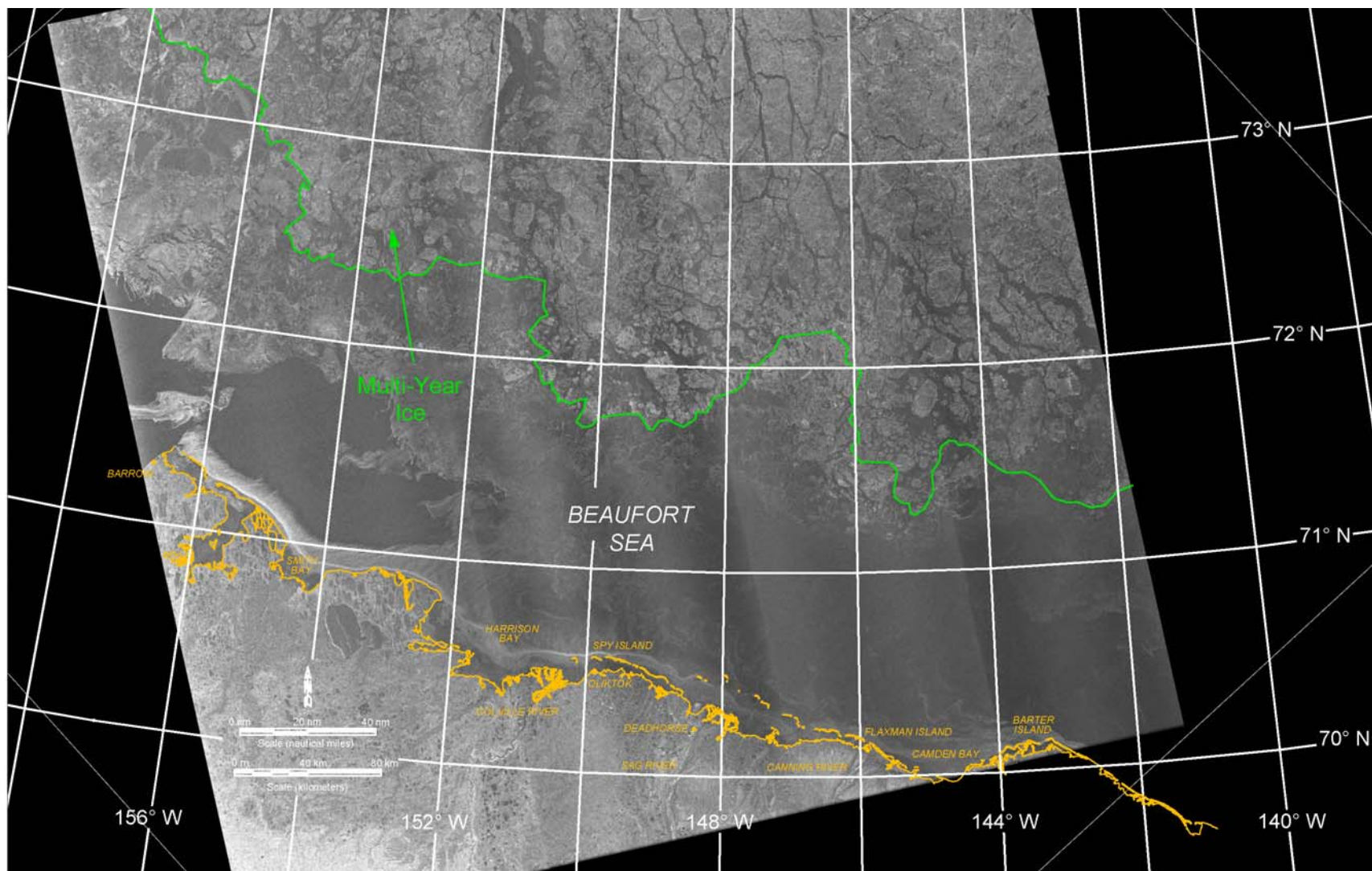
4.3.2 November 2013

Meteorological Conditions: The meteorological conditions that prevailed at Deadhorse Airport in November are shown in Figure 21. The air temperatures trended



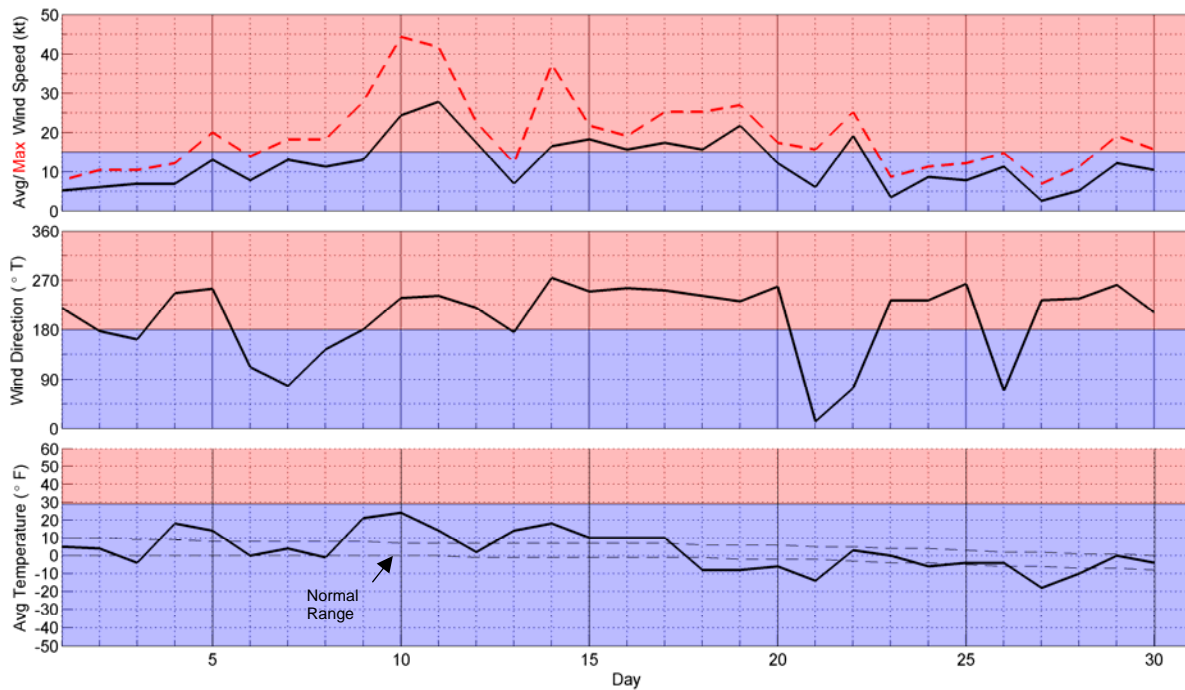
After: NIC, 2014

Figure 19. NIC Ice Chart of Beaufort Sea for September 26, 2014



Source: RADARSAT-2 Data and Products © MacDonald Dettweiler and Associates Ltd., 2013 – All Rights Reserved

Figure 20. RADARSAT-2 Image of Beaufort Sea Acquired on October 31, 2013



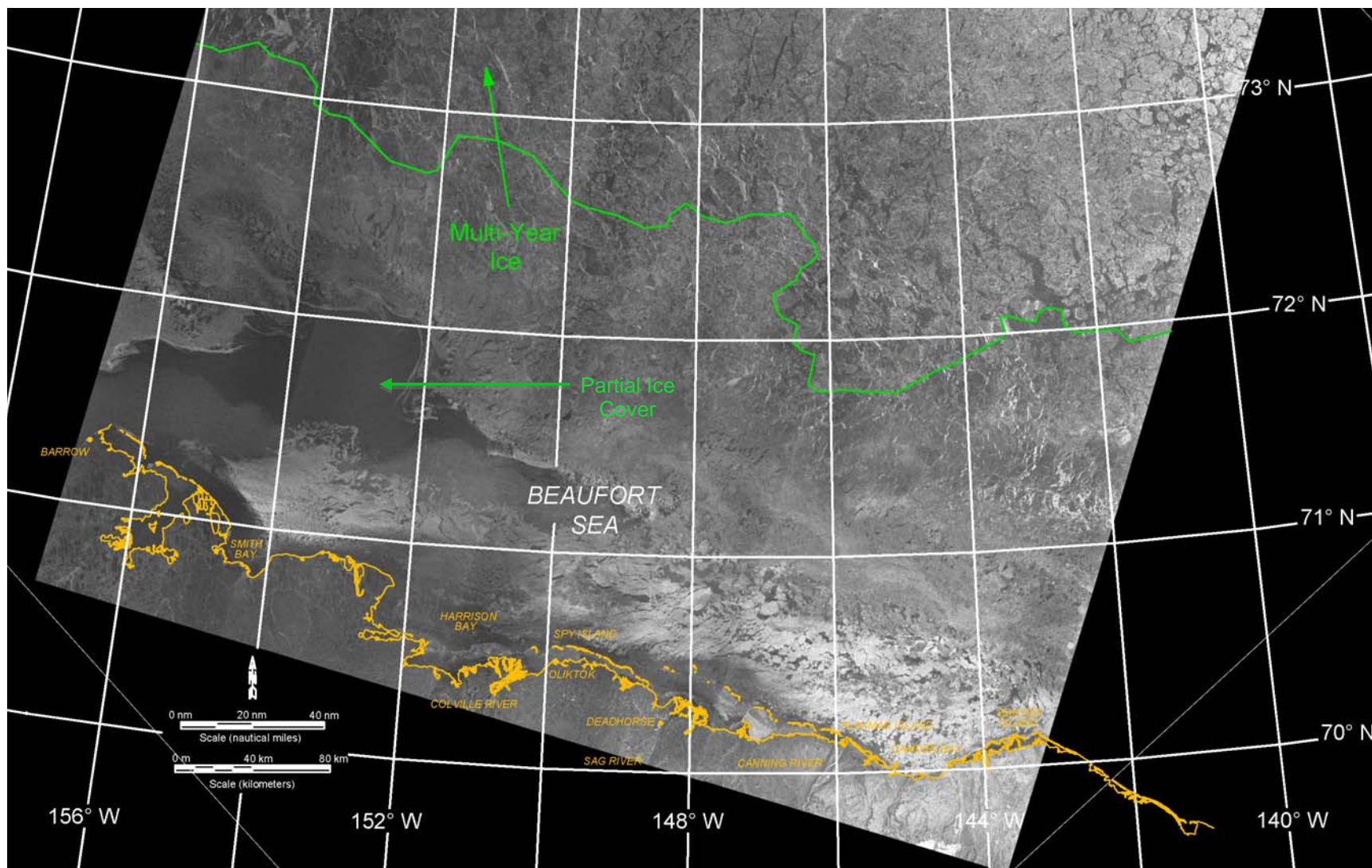
Source: Weather Underground, 2014

Figure 21. Meteorological Conditions at Deadhorse Airport in November 2013

above normal through the 17th before oscillating between normal and subnormal for the remainder of the month. Westerlies outnumbered easterlies by a ratio of 2:1 (20 of 30 days), and the average monthly speed was substantially higher than in October (12 kt versus 8 kt; 6 m/s versus 4 m/s). The storm population consisted of two prolonged westerly events and one brief easterly (Table 4):

- November 10th-12th: three-day westerly with maximum speed of 28 kt (14 m/s);
- November 14th-19th: six-day westerly with maximum speed of 22 kt (11 m/s);
- November 22nd: one-day easterly with maximum speed of 19 kt (10 m/s).

Ice Cover: During the first two weeks in November, the ice canopy closed in the region to the east of Harrison Bay, but a tongue of partial ice cover persisted to the west (Figure 22). Based on the ice charts compiled by the NIC (2014), complete freeze-up in the Alaskan Beaufort Sea occurred on or about November 20th in response to sub-zero temperatures coupled with the end of the westerly storm that had persisted for the prior six days (Figure 21). A total of 678 FDD had accumulated at Deadhorse Airport through this date. During the remainder of the month, which was marked by light to moderate winds and relatively low temperatures, the nascent ice canopy remained intact.



Source: RADARSAT-2 Data and Products © MacDonald Dettweiler and Associates Ltd., 2013 – All Rights Reserved

Figure 22. RADARSAT-2 Image of Beaufort Sea Acquired on November 14, 2013

Ice Thickness: The calculated thickness of undisturbed first-year ice increased from 23 cm at the beginning of the month to 52 cm at the end (Table 5).

Landfast Ice: The successive locations of the landfast ice edge as interpreted from RADARSAT-2 images obtained on November 1st, 14th, and 28th are shown in Figure 23. At the beginning of the month, landfast ice was confined to the semi-protected waters in bays and lagoons. In keeping with the relatively warm air temperatures and frequent occurrence of westerly winds that prevailed in October, exposed areas such as the region to the north of the barrier islands were completely devoid of landfast ice.

During the first two weeks in November, the landfast ice zone grew modestly in Harrison Bay and in the narrower lagoons between Oliktok Point and Flaxman Island but remained nearly static in the more exposed areas due to the disruptive influence of the westerly storm that occurred from the 10th through 12th. Another westerly storm occurred from the 14th through 19th, but the relatively cold temperatures, modest westerly wind speeds, and brief easterly storm that followed caused the landfast ice zone to expand to the vicinity of the 11-m isobath by month-end.

Ice Pile-Ups: As indicated in Section 4.1, 46 ice pile-ups were noted in the central portion of the Beaufort Sea when reconnaissance flights were conducted at the end of March 2014. Based on a review of the wind and temperature data acquired at Deadhorse Airport (Figure 21), it is likely that 23 of these features occurred on November 9th and 10th when the winds shifted from southeasterly to southwesterly and freshened to a peak of 24 kt (12 m/s). The pile-ups occurred on shorelines with southerly, southwesterly, and westerly exposures, including many on the lagoon side of the barrier islands from Thetis to Alaska.

An additional six pile-ups are believed to have occurred on November 14th when the winds shifted from southerly to slightly north of west and freshened to 17 kt (9 m/s), creating pile-ups on northwesterly exposures. The tallest pile-up discovered during the 2013-14 Freeze-Up Study, with a height of 8 m and an encroachment of 20 m past the waterline, occurred on the northwest corner of the West Dock Causeway Seawater Treatment Plant (STP) Pad during this event.

Additional information regarding the pile-ups, including photographs, will be provided in Section 4.6.6.

Multi-Year Ice: The southern boundary of the multi-year ice remained roughly parallel to the coast during the first half of November but moved north from approximately 80 nm (148 km) offshore at the beginning of the month to 120 nm (222 km) at mid-month

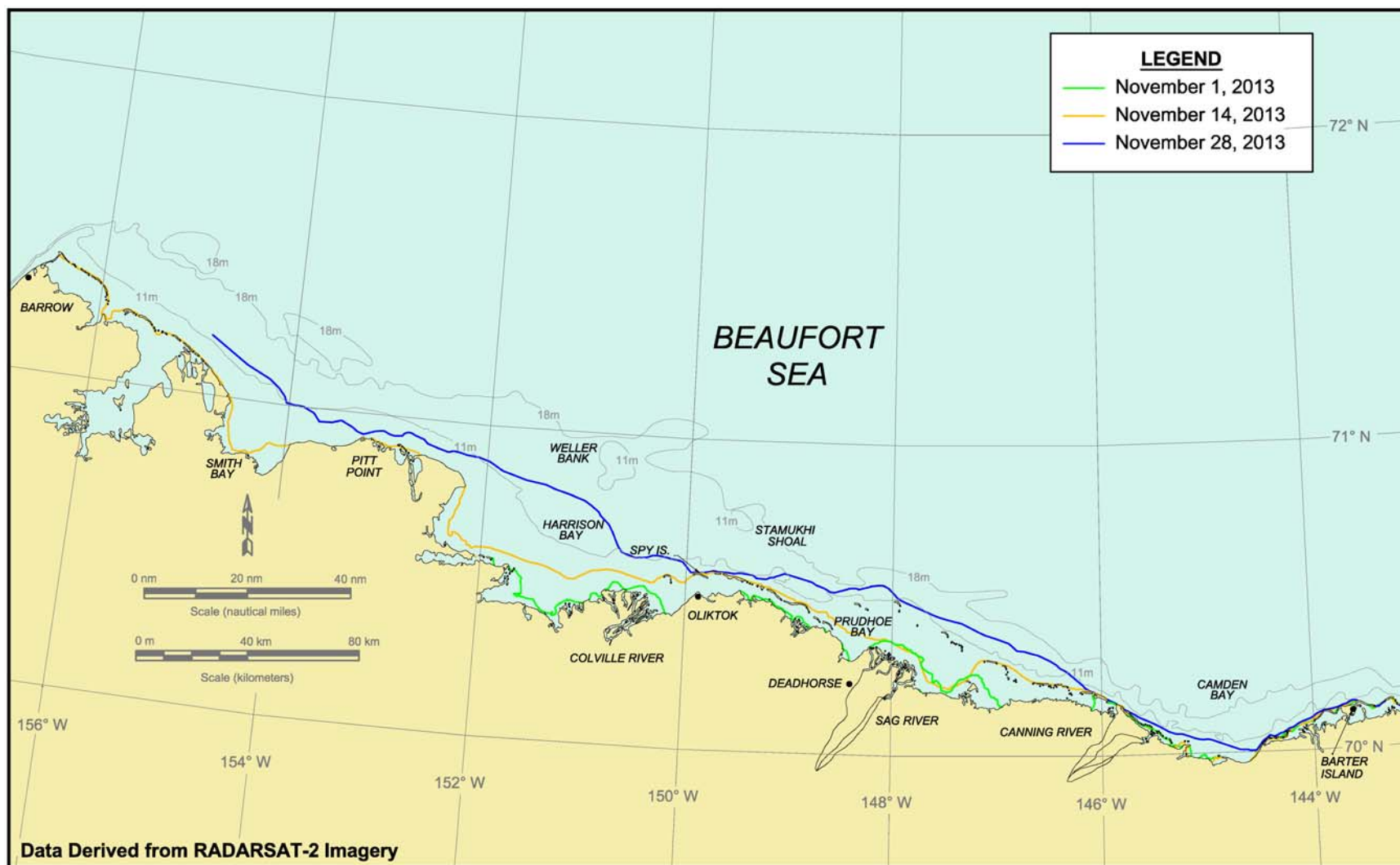


Figure 23. Beaufort Sea Landfast Ice Edge in November 2013

(Figure 22). This trend was reversed during the second half, producing a boundary that lay 90 nm (167 km) off Barter Island and only about 40 nm (74 km) off Smith Bay.

Ice Movement: Ice movement rates were quantified by tracking the progress of four multi-year floes in successive RADARSAT-2 images. As shown in Figure 24, Floes A and B were identified in the images obtained on November 1st, 14th, and 28th. Due to differences in the coverage provided by each image, Floes C and D were evident on the 1st and 28th but not on the 14th. The diameters of these floes ranged from 7 to 23 km.

In keeping with the absence of sustained easterly winds and the occurrence of a strong westerly storm from the 10th through 12th, Floes A and B experienced small net displacements to the north during the first half of the month. This pattern reflects a balance between the westward-setting Beaufort Gyre (Figure 1) and the countervailing influence of westerly winds. During the second half of the month, both floes moved to the west southwest as the Gyre was re-established. The speeds between successive images ranged from 0.7 to 4.9 nm/day (1.3 to 9.1 km/day), while the average speed over the course of the month (computed on the basis of the net displacement) was 2.3 nm/day (4.3 km/day) for Floe A and 2.5 nm/day for Floe B.

Floes C and D, which were located farther from the southern boundary of the multi-year ice and therefore more constrained by other floes, experienced modest southerly displacements over the course of the month. The average speeds were only 1.4 nm/day (2.6 km/day) for Floe C and 1.2 nm/day (2.2 km/day) for Floe D.

4.4 Late Freeze-Up

4.4.1 December 2013

Meteorological Conditions: The wind and temperature data recorded at Deadhorse Airport in December 2013 are provided in Figure 25. The air temperatures remained well above normal through the 9th, peaking at 27°F (-3°C) on the 7th. From the 10th through month-end, the temperatures oscillated between normal and sub-normal.

As in November, westerly winds predominated over easterlies by a wide margin (18 of 31 days). The monthly average speed, 13 kt (7 m/s), reflected the occurrence of six full storm events plus the beginning of another storm that continued into January. The six full storms, consisting of four westerlies and two easterlies (Table 4), are summarized below:

- December 1st: one-day westerly with maximum speed of 22 kt (11 m/s);
- December 6th-7st: two-day easterly with maximum speed of 19 kt (10 m/s);

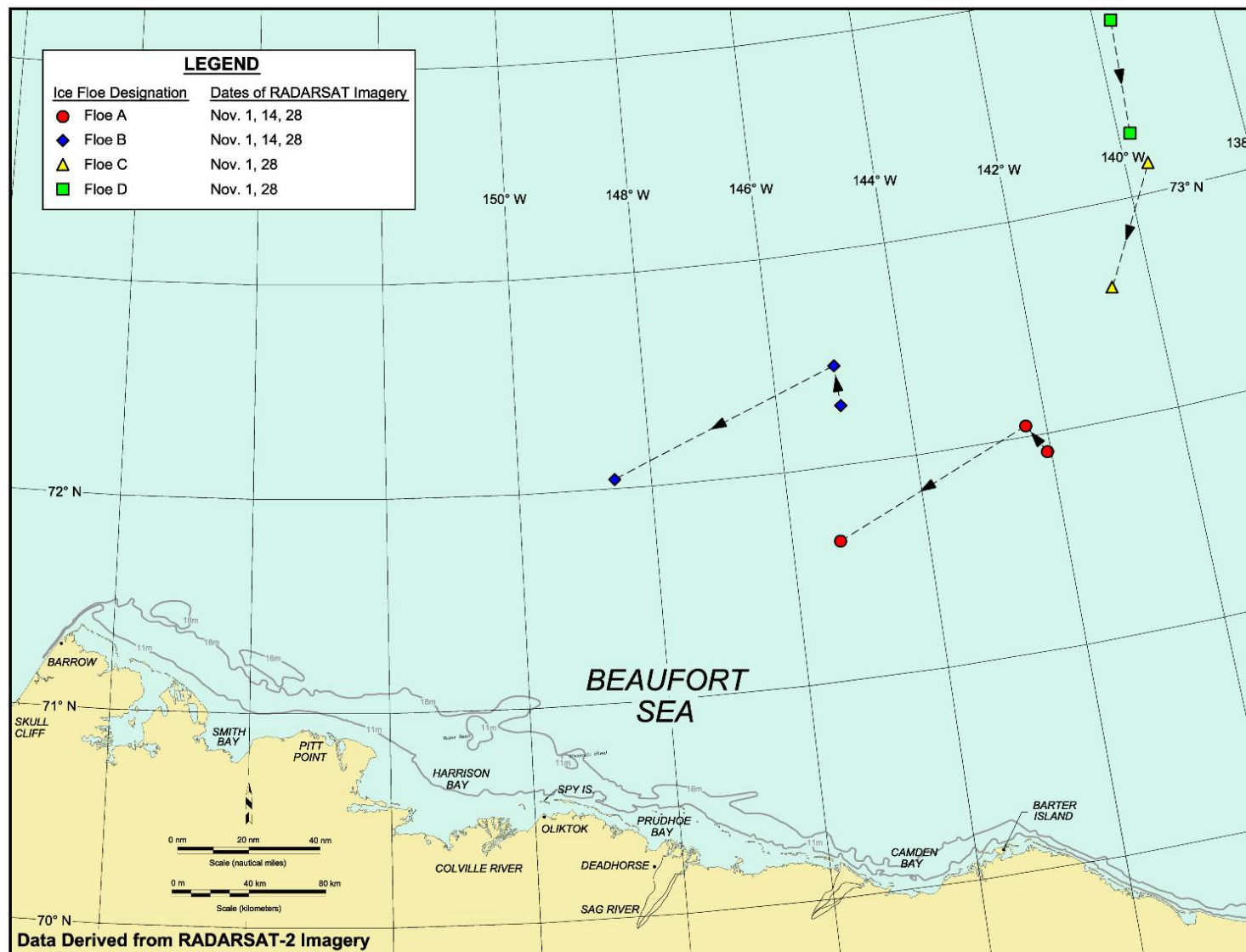
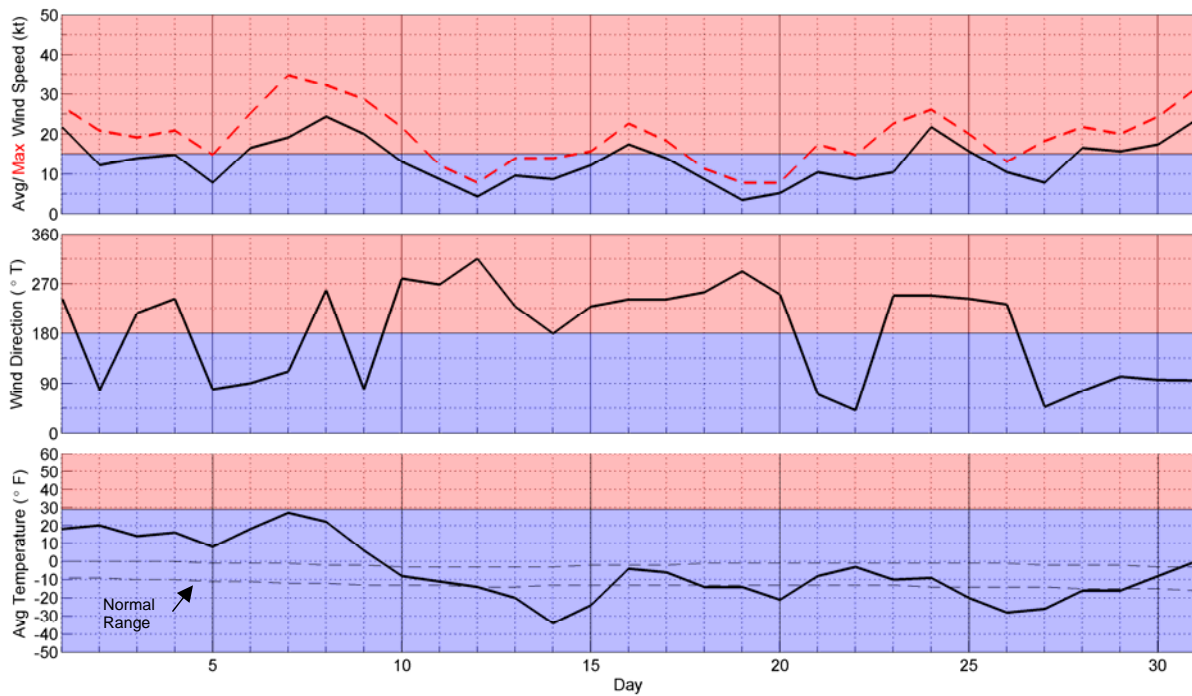


Figure 24. Beaufort Sea Multi-Year Ice Floe Displacements in November 2013



Source: Weather Underground, 2014

Figure 25. Meteorological Conditions at Deadhorse Airport in December 2013

- December 8th: one-day westerly with maximum speed of 24 kt (12 m/s);
- December 9th: one-day easterly with maximum speed of 20 kt (10 m/s);
- December 16th: one-day westerly with maximum speed of 17 kt (9 m/s);
- December 24th-25th: two-day westerly with maximum speed of 22 kt (11 m/s).

Another easterly storm that began on December 28th and continued through January 6th will be included in the discussion of meteorological conditions in January (Section 4.4.2).

Ice Thickness: The calculated thickness of undisturbed first-year ice increased by 24 cm over the course of the month, from 52 to 79 cm.

Landfast Ice: The locations of the landfast ice edge were estimated from RADARSAT-2 images obtained on December 4th, 15th, and 29th. The results are presented in Figure 26, which also shows the ice edge on November 28th.

Between November 28th and December 4th, the landfast ice retreated in response to westerly winds that peaked at 22 kt (11 m/s) on the 1st (Figure 26). It then remained stationary from the 4th through the 15th, a period in which, despite the occurrence of two brief easterly storms, expansion was precluded by a predominance of westerly winds and

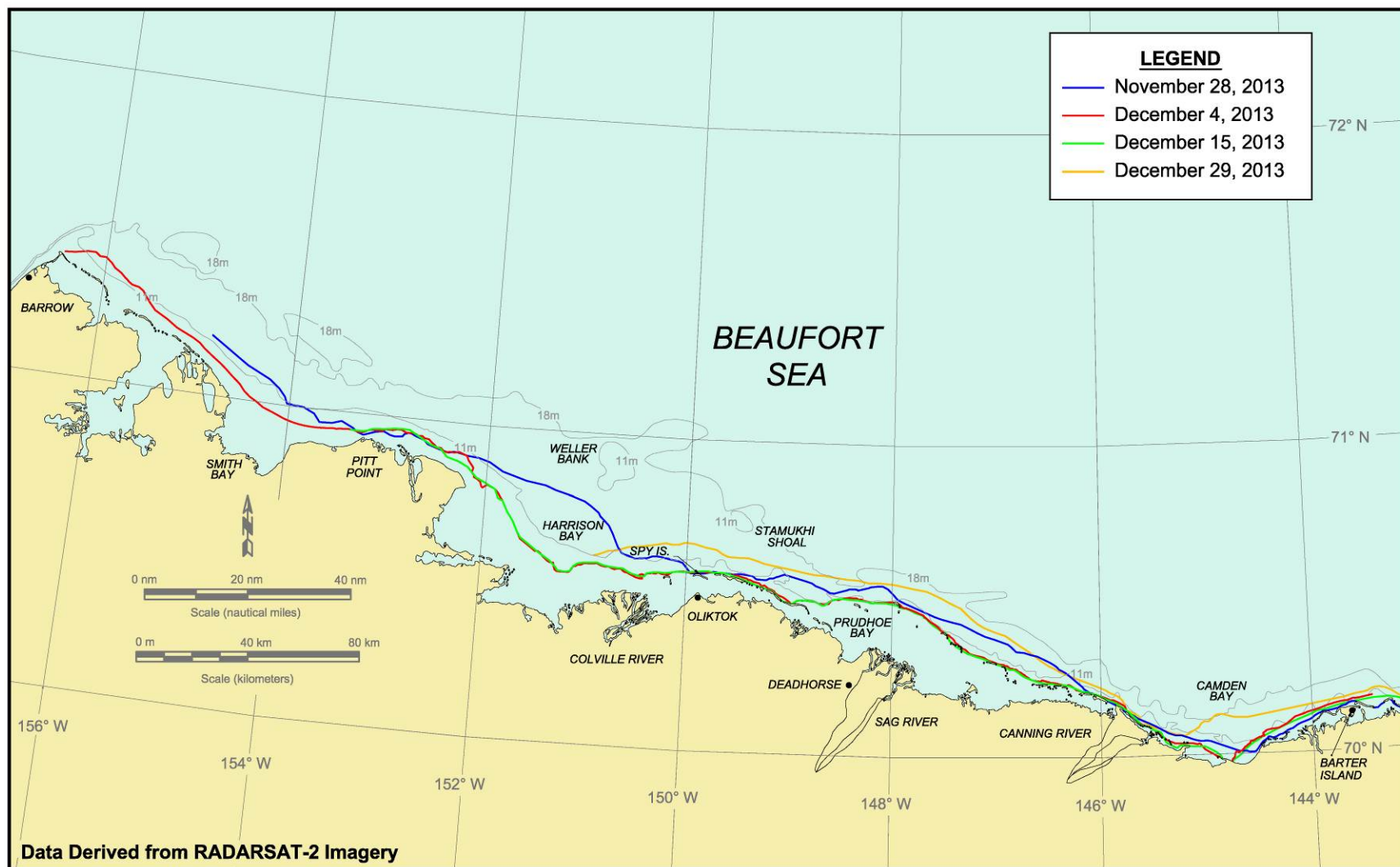


Figure 26. Beaufort Sea Landfast Ice Edge in December 2013

one westerly storm. Slight expansion followed between the 15th and 29th, suggesting that the landfast ice that existed at the beginning of this period was sufficiently well-grounded to resist displacement during the westerly storms that occurred on the 16th and the 24th through 25th. It then expanded to the north in response to the easterly storm that began on the 28th.

Ice Pile-Ups: Of the 46 ice pile-ups observed in the central portion of the Beaufort Sea during the March reconnaissance flights (Section 4.1), 29 are believed to have occurred in November (Section 4.3.2). The remaining 17 pile-ups, all of which were located on shorelines with northerly or northeasterly exposures, probably formed on December 8th when a 24-kt (12-m/s) westerly quickly veered through north to become a 20-kt (10-m/s) easterly (Figure 25).

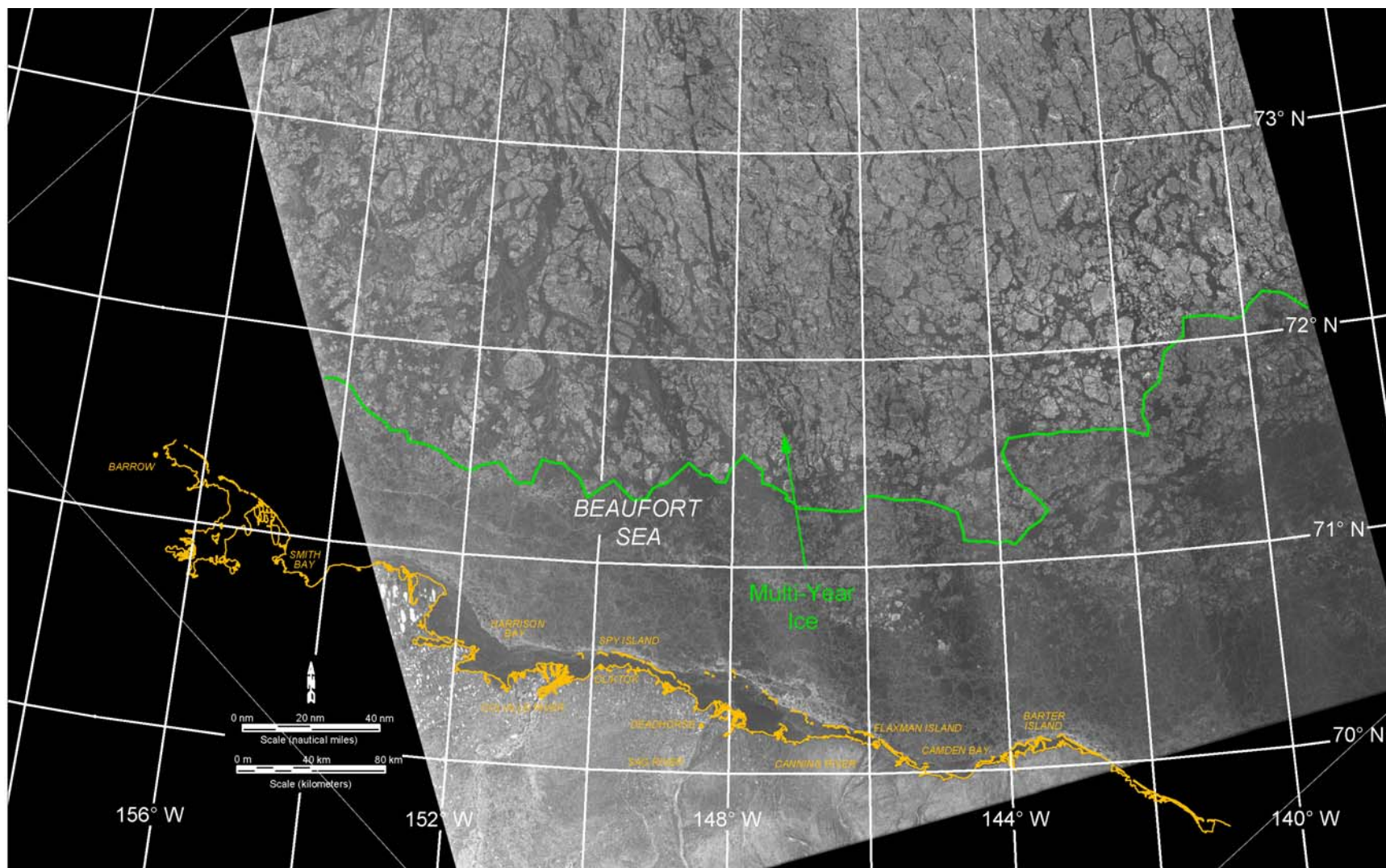
Multi-Year Ice: During the first half of December, the multi-year ice edge off Point Barrow moved north from its initial location near the 72° parallel. This trend was reversed in the second half, with the ice edge ultimately returning to the vicinity of its starting point. Farther east, from Harrison Bay to Barter Island, the ice edge remained between 71°N and 71°30' N throughout the month (Figure 27).

Ice Movement: Ice movement was quantified by comparing the positions of six multi-year floes over various periods bracketed by RADARSAT-2 images obtained on November 28th and December 29th. Four of the floes (A, B, C, and D) had been tracked in November, while two new floes were added in mid-December (Floes E and F, with diameters of 10 and 8 km, respectively). The tracking period for each floe was determined by the extent to which it could be identified in the bracketing images as well as intermediate scenes obtained on December 4th and 15th. The results are presented in Figure 28.

Floes A, C, and D, for which positions were obtained on both November 28th and December 29th, experienced net displacements to the southwest over the course of the month. The average monthly speeds ranged from 1.5 to 1.7 nm/day (2.8 to 3.2 km/day) – extremely low values indicating that the Beaufort Gyre was neutralized by a predominance of westerly winds that included four westerly storm events.

When the trajectories of all six floes are considered together, the following three components are evident:

- Nov 28th–Dec 4th: southerly motion in response to a westerly storm;
- Dec 4th–15th: westerly motion in response to two easterly storms;
- Dec 15th–29th: southeasterly motion in response to two westerly storms.



Source: RADARSAT-2 Data and Products © MacDonald Dettweiler and Associates Ltd., 2013 – All Rights Reserved

Figure 27. RADARSAT-2 Image of Beaufort Sea Acquired on December 15, 2013

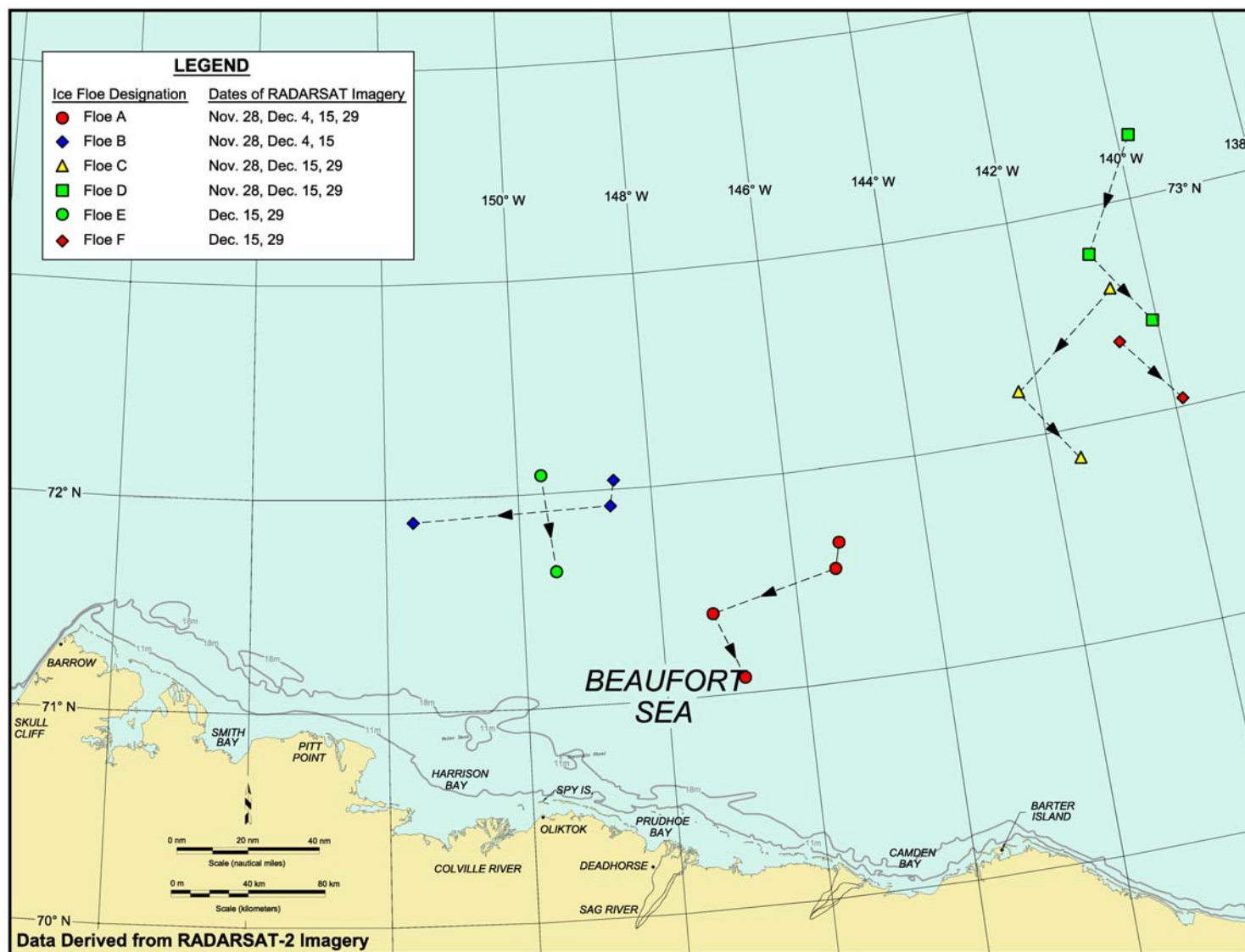
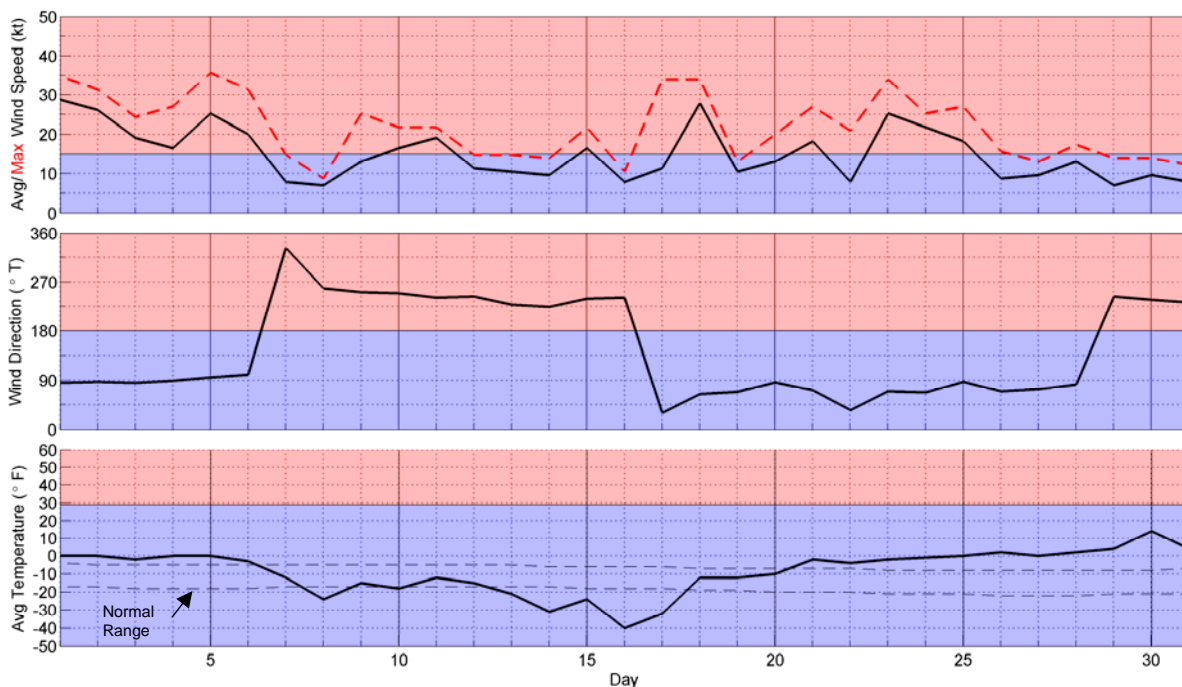


Figure 28. Beaufort Sea Multi-Year Ice Floe Displacements in December 2013

The average speeds recorded between successive images varied from a low of 1.2 nm/day (2.2 km/day for Floes A and B between November 28th and December 4th) to a high of 5.5 nm/day (10.2 km/day for Floe B between December 4th and 15th).

4.4.2 January 2014

Meteorological Conditions: Figure 29 presents the wind and temperature data recorded at Deadhorse Airport in January 2014. The air temperatures remained above normal from the 1st through 6th, ranged from normal to sub-normal from the 7th through 20th, and then surged above normal for the remainder of the month.



Source: Weather Underground, 2014

Figure 29. Meteorological Conditions at Deadhorse Airport in January 2014

As in 2012-13, January proved to be the windiest month of the 2013-14 freeze-up season. The average monthly speed was 15 kt (8 m/s). It also was the only month in which easterly winds predominated (18 of 31 days). The storm population consisted of three easterlies and two westerlies:

- Dec 28th - Jan 6th: ten-day easterly with maximum speed of 29 kt (15 m/s).
- January 10th-11th: two-day westerly with maximum speed of 19 kt (10 m/s)
- January 15th: one-day westerly with maximum speed of 17 kt (9 m/s);
- January 18th: one-day easterly with maximum speed of 28 kt (14 m/s);
- January 21st-25th: five-day easterly with maximum speed of 25 kt (13 m/s).

The easterly storm that began on December 28th and continued through January 6th was the most severe of the six-month study period, with a duration of ten days and a maximum sustained wind speed of 29 kt (15 m/s).

Ice Thickness: The calculated thickness of undisturbed first-year ice increased from 79 cm at the beginning of January to 102 cm at the end, a gain of 23 cm.

Landfast Ice: Figure 30 illustrates the locations of the landfast ice edge derived from RADARSAT-2 images obtained on December 29th and January 8th, 18th, and 25th. During the 10-day period between the first two images, the landfast ice edge remained nearly stationary from just east of Stamukhi Shoal to Barter Island, but registered a substantial advance off Harrison Bay. This gain, which caused the landfast ice zone to reach its traditional anchor points on Weller Bank and Stamukhi Shoal, resulted from the prolonged easterly storm that persisted from December 28th through January 6th (Table 4).

The landfast ice edge on January 18th bore a close resemblance to that on the 8th, the most prominent exception being a modest retreat that occurred between Stamukhi Shoal and Prudhoe Bay. The loss is consistent with the predominance of westerly winds and the two westerly storms that occurred during the intervening 10-day period.

Another significant increase in the extent of the landfast ice zone occurred between January 18th and 25th. In this case, the driving force was provided by two easterly storms: a one-day event on the 18th and a five-day event that began on the 21st and ended on the 25th. At the conclusion of the second storm, the landfast ice edge lay well seaward of the 18-m isobath from the vicinity of Point Barrow to Barter Island. As discussed by Mahoney, *et al.*, (2012), this type of “stable extension” occurs when the landfast ice edge is maintained not by grounding but by compression with minimal shear. A similar feature was noted a year earlier, in January 2013 (Coastal Frontiers and Vaudrey, 2014)

Multi-Year Ice: The CIS ice charts (2014) indicate that the multi-year ice edge off Point Barrow moved south during the first part of January, ultimately reaching the Point on the 13th (Figure 31). It then retreated slightly to the vicinity of the 71°30' parallel, where it remained during the second half of the month (Figure 32).

From just east of Point Barrow to Barter Island, the multi-year ice edge hovered between the 71 and 72° parallels throughout the month of January. On the 25th, it was located 15 nm (28 km) off Point Barrow, 70 nm (130 km) off Prudhoe Bay, and 100 nm (185 km) off Barter Island (Figure 32).

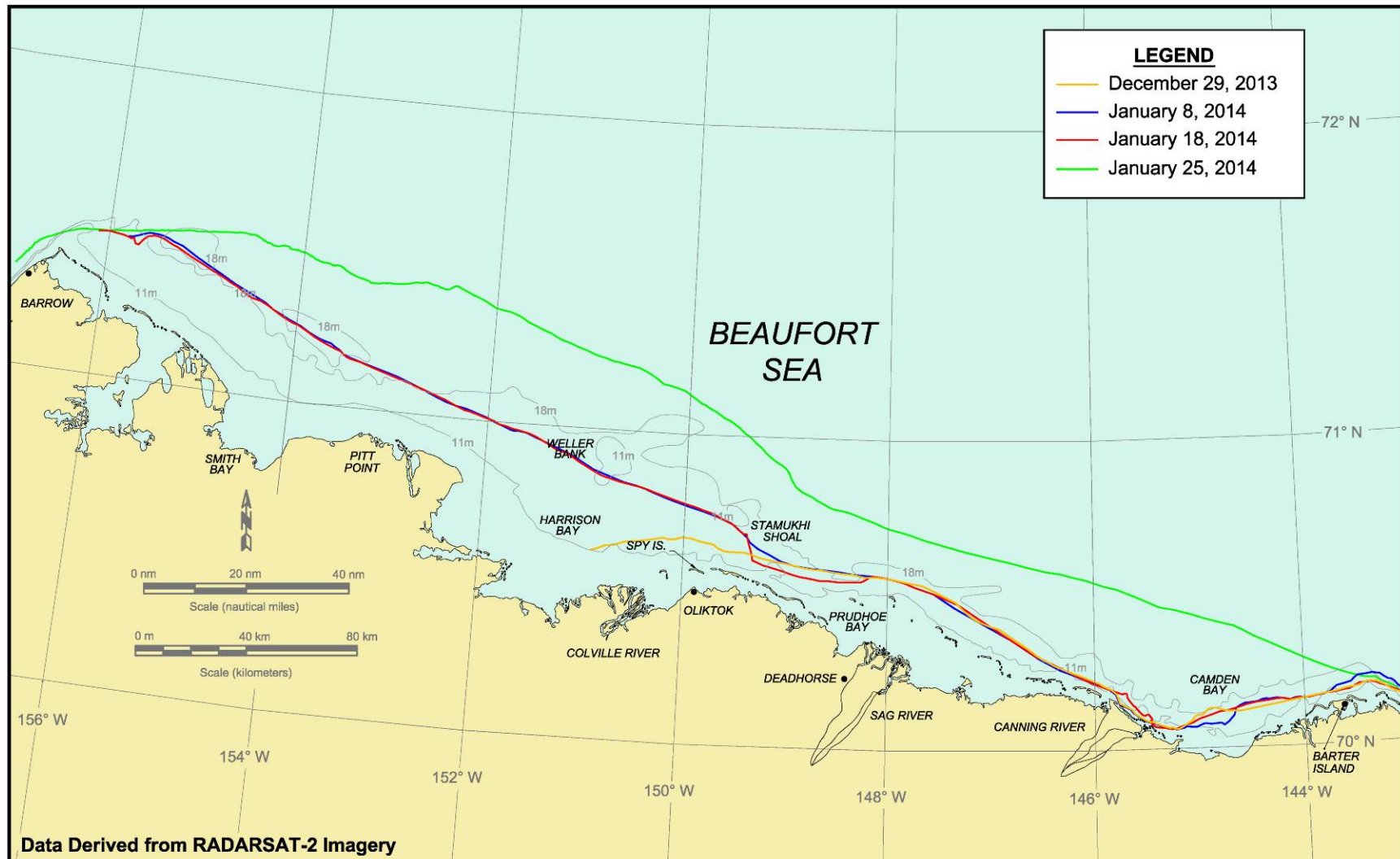
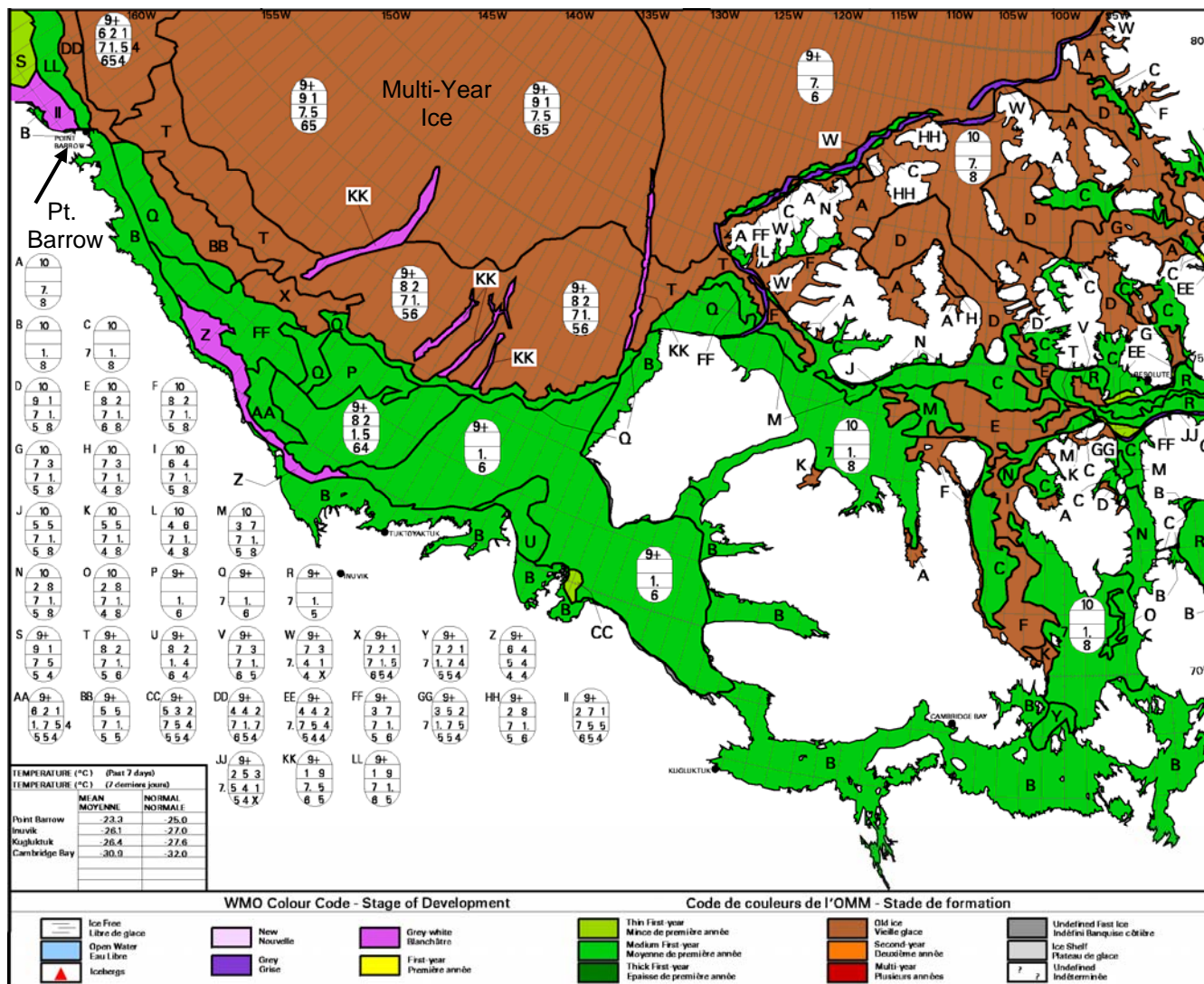
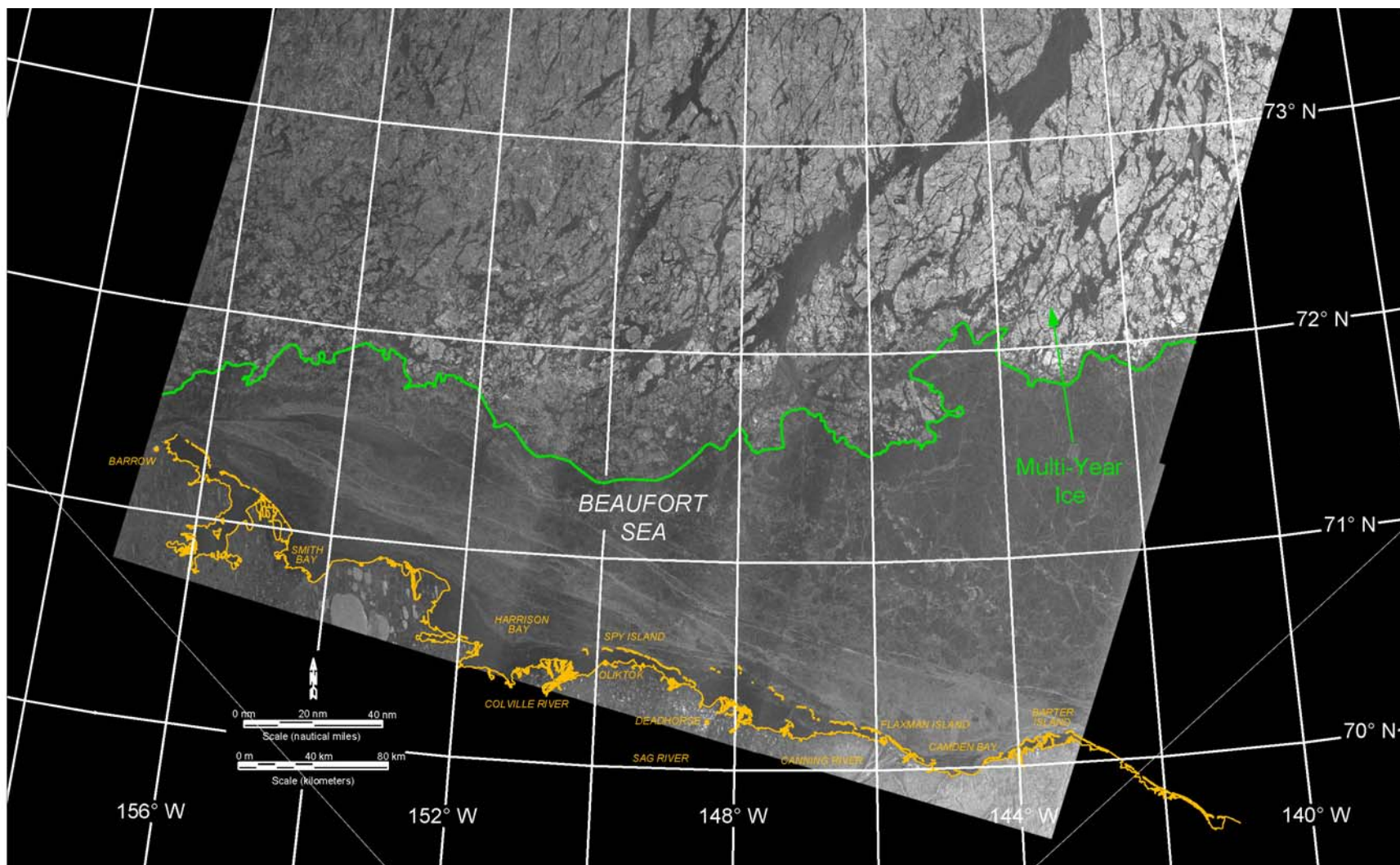


Figure 30. Beaufort Sea Landfast Ice Edge in January 2014



After: NIC, 2014

Figure 31. CIS Ice Chart of Beaufort Sea for January 13, 2014



Source: RADARSAT-2 Data and Products © MacDonald Dettweiler and Associates Ltd., 2014 – All Rights Reserved

Figure 32. RADARSAT-2 Image of Beaufort Sea Acquired on January 25, 2014

Ice Movement: Four of the multi-year floes tracked in December (Floes C, D, E, and F) and one new floe (Floe G, with a diameter of 7 km) were used to investigate ice movement rates in January based on RADARSAT-2 images obtained on December 29th and January 8th, 9th, 18th, and 25th. In the case of Floe E, which moved into the Chukchi Sea in early January, the tracking period attributable to the Beaufort was terminated on January 9th. The trajectories of the five floes are shown in Figure 33.

In keeping with the predominance of easterly winds and easterly storms in January, all five floes experienced substantial net displacements to the west. In the case of the four floes for which position data are available on December 29th and January 25th (Floes C, D, F, and G), the average monthly speeds ranged from 4.0 to 7.7 nm/day (7.4 to 14.3 km/day). The lowest speed was associated with Floe G, which was the northernmost feature and therefore the most constrained by adjoining multi-year floes. The other three features, which were located near the southern boundary of the multi-year ice, attained average monthly speeds from 6.5 to 7.7 nm/day (12.0 to 14.3 km/day).

The movements of the floes mirrored the wind conditions, as summarized below:

- Dec 29th– Jan 8/9th: rapid westerly motion in response to easterly winds and a prolonged easterly storm;
- Jan 8/9th–18th: sluggish southeasterly motion in response to westerly winds and two westerly storms ;
- Jan 18th–29th: a return to rapid westerly motion in response to easterly winds and two easterly storms.

The minimum speed between successive images, 2.6 nm/day (4.8 km/day), was recorded by Floes C and F in response to the westerly winds and storms that dominated the ten-day period between January 8th and 18th. The maximum speed, 15.2 nm/day (28.2 km/day) for Floe C, reflected the return to easterly winds and storms that occurred between the 18th and 25th.

4.5 Mid-Winter

4.5.1 February 2014

Meteorological Conditions: The meteorological conditions recorded at Deadhorse Airport in February 2014 are displayed in Figure 34. The air temperatures began the month above normal, dropped below normal in mid-month, and then rose above normal at the end. The net result was an average monthly temperature that approximated the long-term average value.

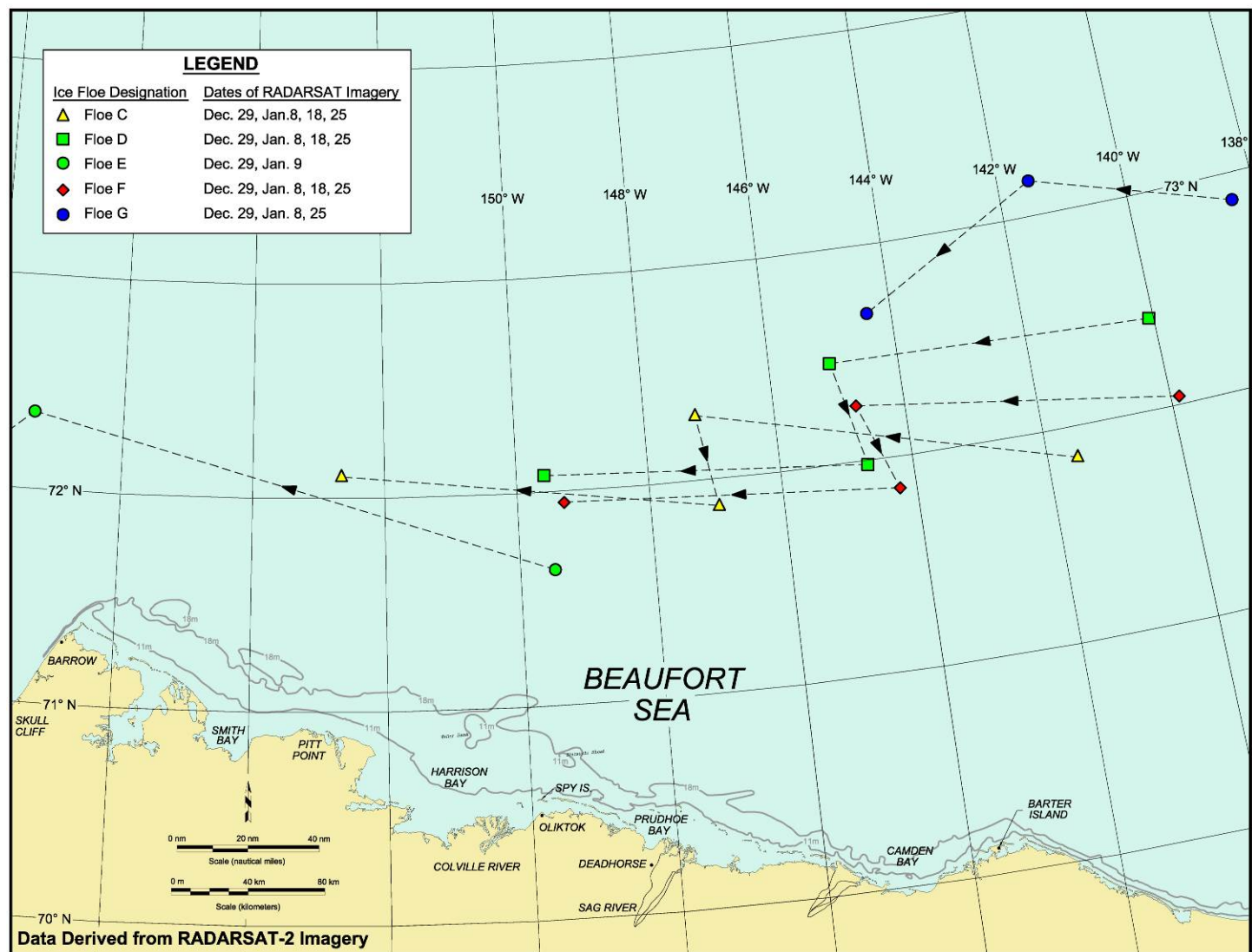
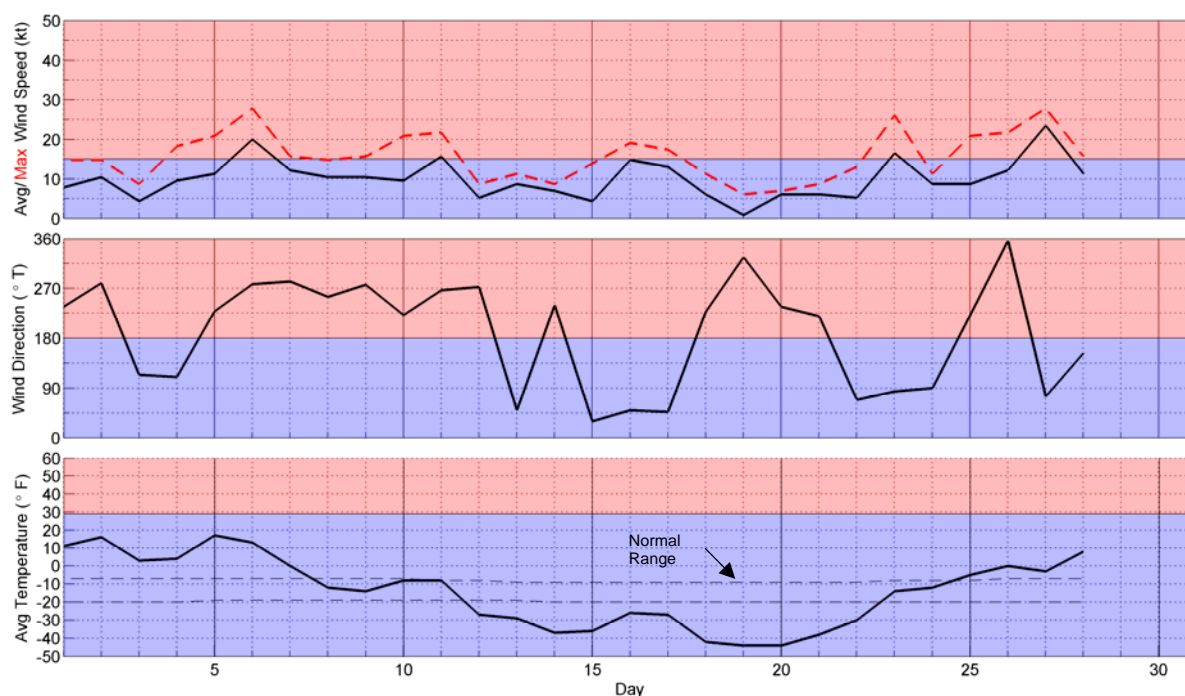


Figure 33. Beaufort Sea Multi-Year Ice Floe Displacements in January 2014



Source: Weather Underground, 2014

Figure 34. Meteorological Conditions at Deadhorse Airport in February 2014

The wind direction switched between easterly and westerly on nine occasions, but as in the case of each month except January, westerlies predominated (17 of 28 days). The average monthly speed, 10 kt (5 m/s) was only two thirds of that recorded in January. The storm population consisted of two one-day westerlies followed by two one-day easterlies:

- February 6th: one-day westerly with maximum speed of 20 kt (10 m/s);
- February 11th: one-day westerly with maximum speed of 16 kt (8 m/s);
- February 18th: one-day easterly with maximum speed of 17 kt (9 m/s);
- February 27th: one-day easterly with maximum speed of 23 kt (12 m/s);

Ice Thickness: The calculated thickness of undisturbed first-year ice increased by 21 cm, from 102 to 123 cm.

Landfast Ice: Figure 35 presents the locations of the landfast ice edge derived from RADARSAT-2 images obtained on January 25th, February 18th, and February 28th. During the period between the first two images, which contained frequent changes in wind direction and two brief westerly storms, the landfast ice edge remained essentially stable to the east of Spy Island but retreated by up to 20 nm (37 km) to the west. Subsequently, from the 18th to the 28th, the ice edge rebounded between Weller Bank and Smith Bay but retreated by up to 15 nm (28 km) in Camden Bay. Both of the retreats represented losses of the stable

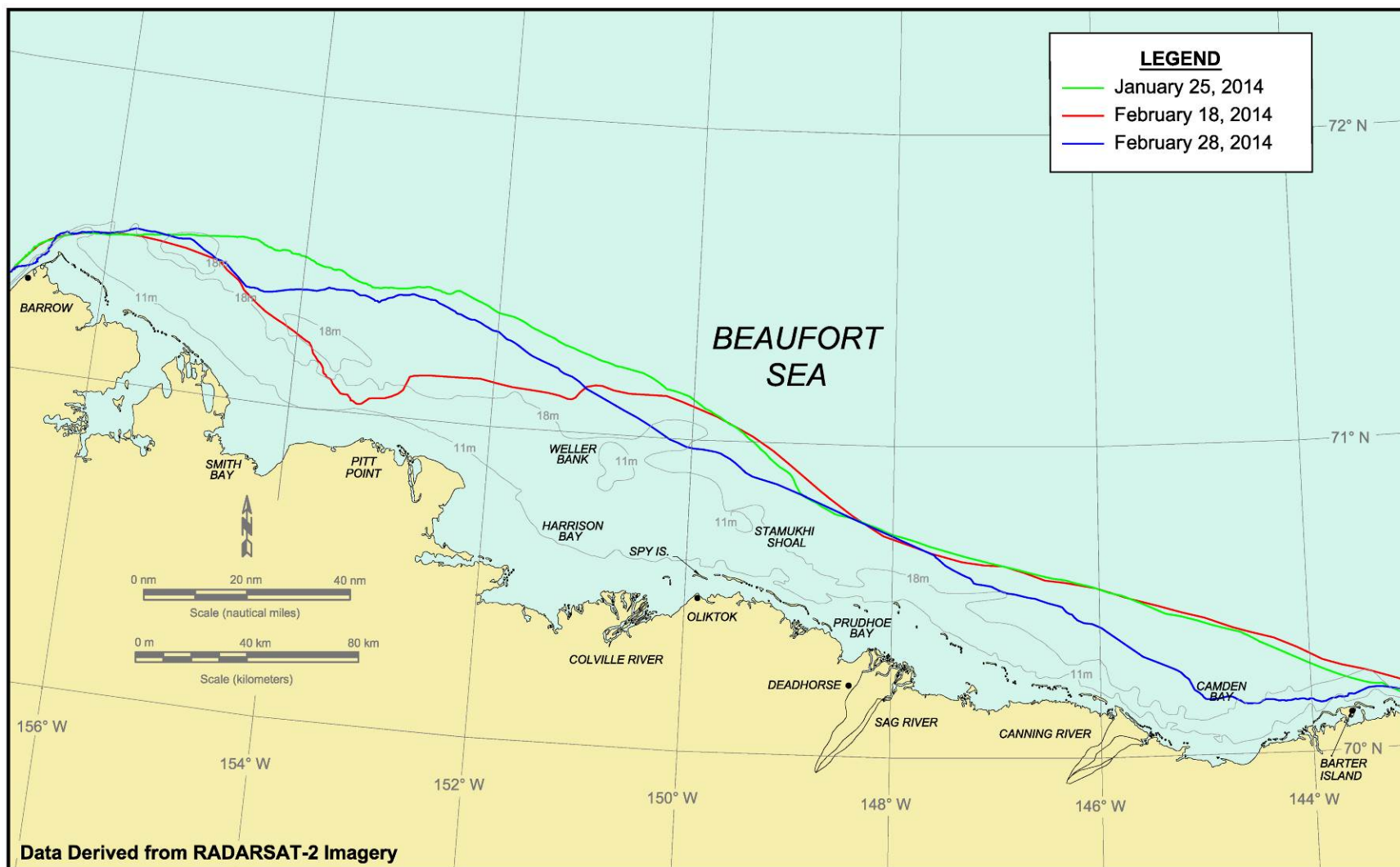


Figure 35. Beaufort Sea Landfast Ice Edge in February 2014

extensions that had been maintained by compression (rather than grounding) in January (Figure 30).

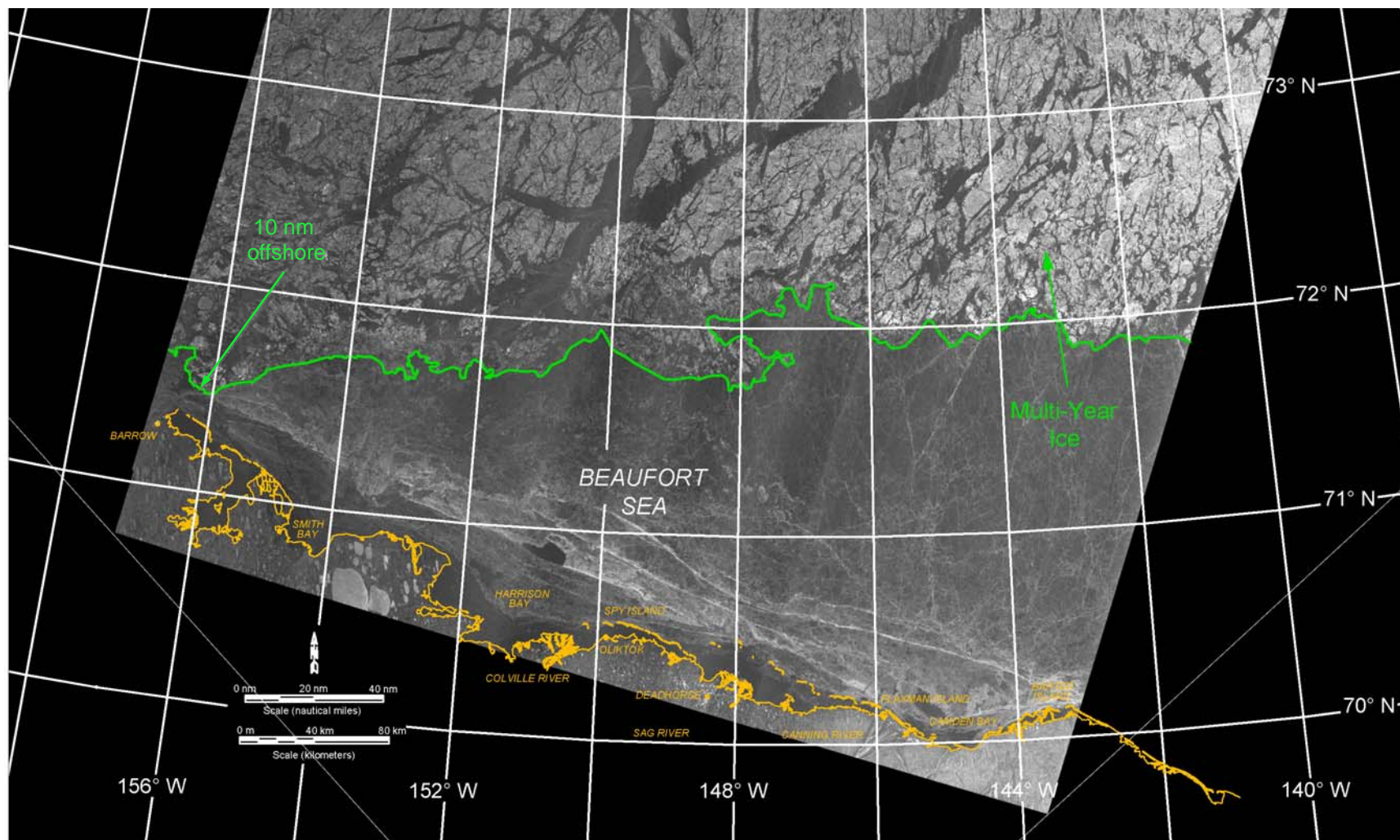
Multi-Year Ice: The weekly CIS ice charts (2014) along with the two RADARSAT-2 images obtained on the 8th and 28th indicate that the multi-year ice edge tended to maintain an east-west orientation between the 71°30' and 72°30' parallels throughout the month of February. The closest approach to coast occurred at Point Barrow, where the distance offshore ranged from 10 to 40 nm (19 to 74 km; Figure 36).

Ice Movement: Ice movement rates in February were investigated using four of the multi-year floes tracked in January (Floes C, D, F, and G) and one new multi-year floe (Floe H, with a diameter of 9 km). The five floes were identified in RADARSAT-2 images obtained on January 25th and February 16th, 18th, and 28th. Because Floes C, D, and F moved into the Chukchi over the course of the month, the tracking period for Floe C attributable to the Beaufort was terminated on the 16th, while that for Floes D and F was terminated on the 18th (Figure 37).

As in January, all five floes experienced net displacements to the west. The speeds were substantially lower, however, reflecting the resurgence of westerly winds that occurred in February (Figure 34). In the case of Floe G, the sole feature for which the tracking period extended from January 25th to February 28th, the average monthly speed was a modest 2.7 nm/day (5.0 km/day). The minimum and maximum speeds between successive images, 1.9 and 5.5 nm/day (3.5 and 10.2 km/day), both occurred between January 25th and February 18th. The former was recorded by Floe G, which was well-embedded in the multi-year ice; the latter was recorded by Floe F, which was located at the southern boundary.

Ice movement rates also were derived from eleven telemetry buoys installed in the Beaufort Sea on February 24th and 25th (Section 3.4). As shown in Figure 38, five were located off the east side of Camden Bay (CB-1 through -5), four off the east side of Harrison Bay (HB-A through -D), and two in the rubble that had formed on Weller Bank (HB-1 and -2). Hourly position data for each buoy were available from the time of installation through month-end.

The tracks described by the eleven buoys are illustrated in Figure 38, while the daily average speeds are plotted in Figure 39. Both figures are based on the positions reported at midnight of each day. Of the six buoys associated with Harrison Bay and Weller Bank, all except the seawardmost were located within the landfast ice zone and remained stationary. Buoy HB-D, which was located outside the landfast ice zone, moved to the west-northwest



Source: RADARSAT-2 Data and Products © MacDonald Dettweiler and Associates Ltd., 2014 – All Rights Reserved

Figure 36. RADARSAT-2 Image of Beaufort Sea Acquired on February 18, 2014

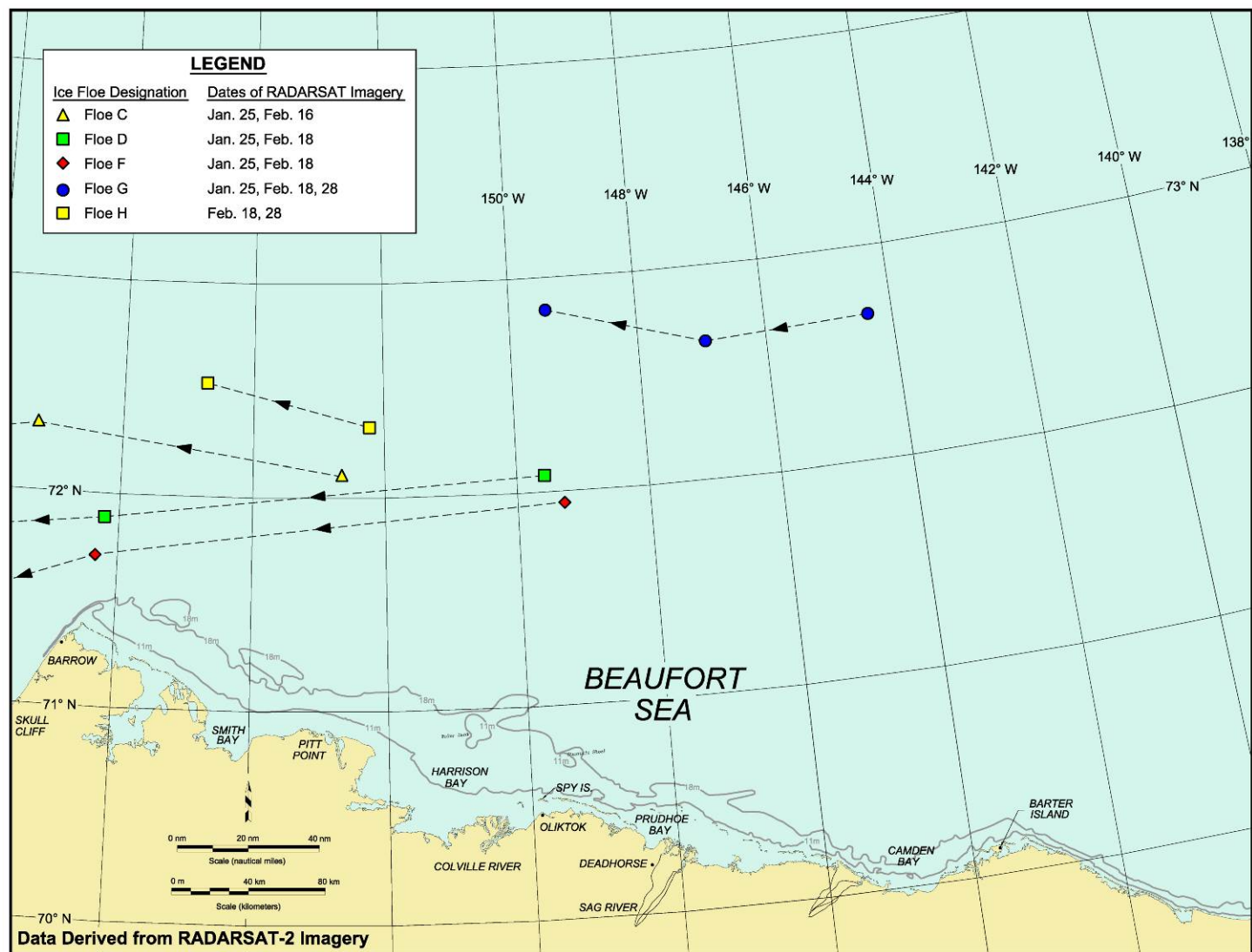


Figure 37. Beaufort Sea Multi-Year Ice Floe Displacements in February 2014

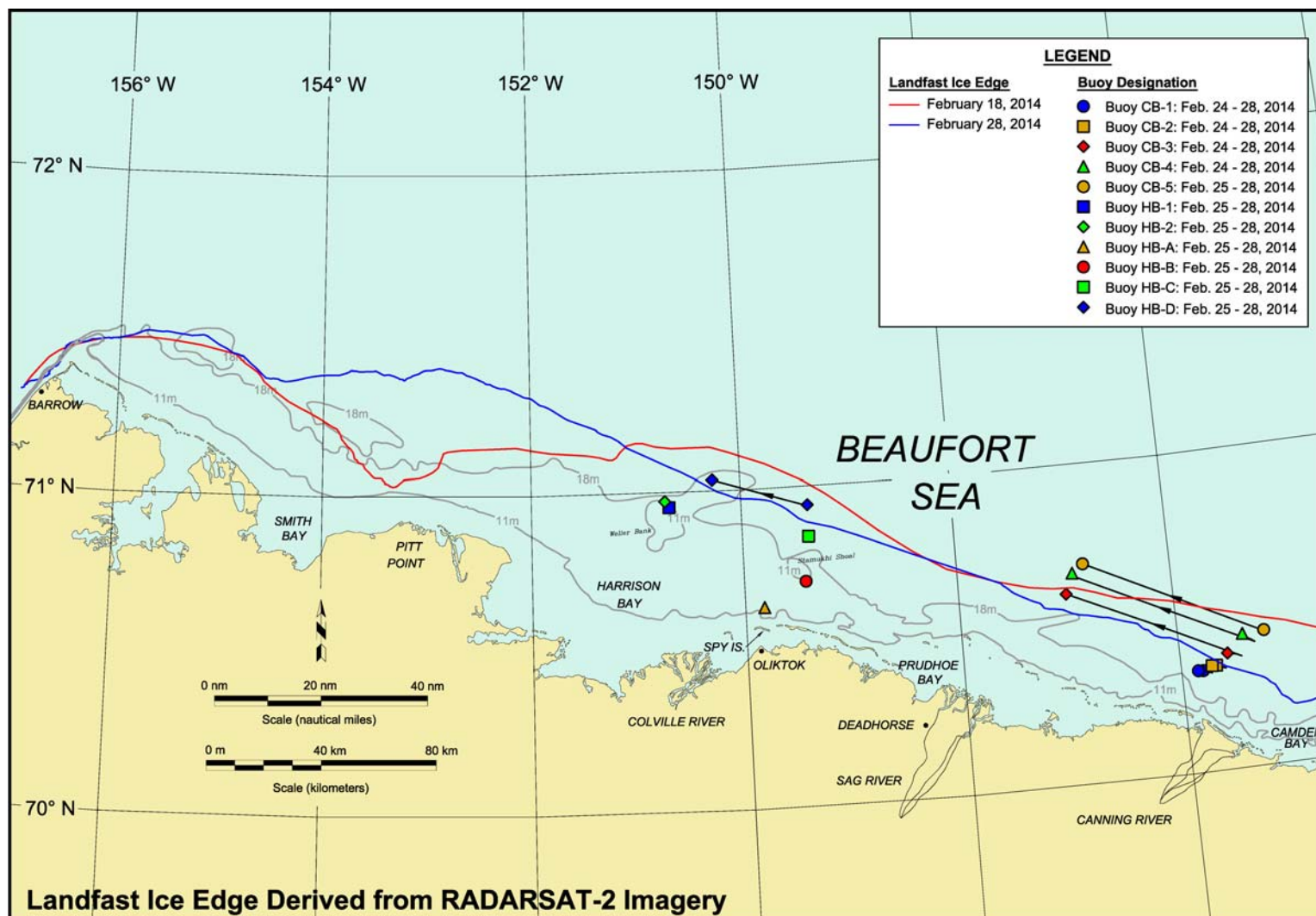


Figure 38. Beaufort Sea Landfast Ice Edge and Telemetry Buoy Tracks in February 2014

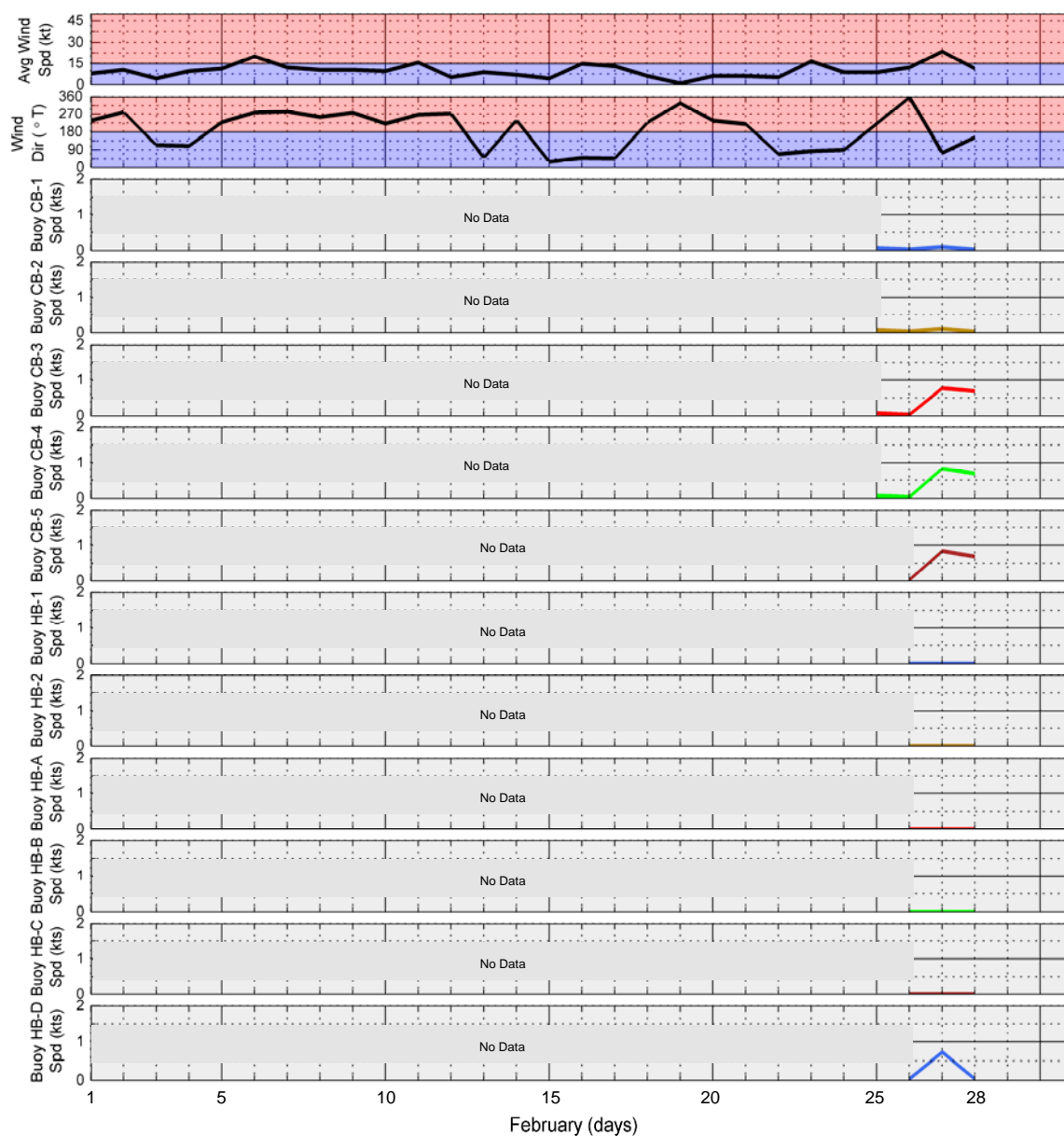


Figure 39. Time Series of Telemetry Buoy Average Daily Speeds in Beaufort Sea, February 2014

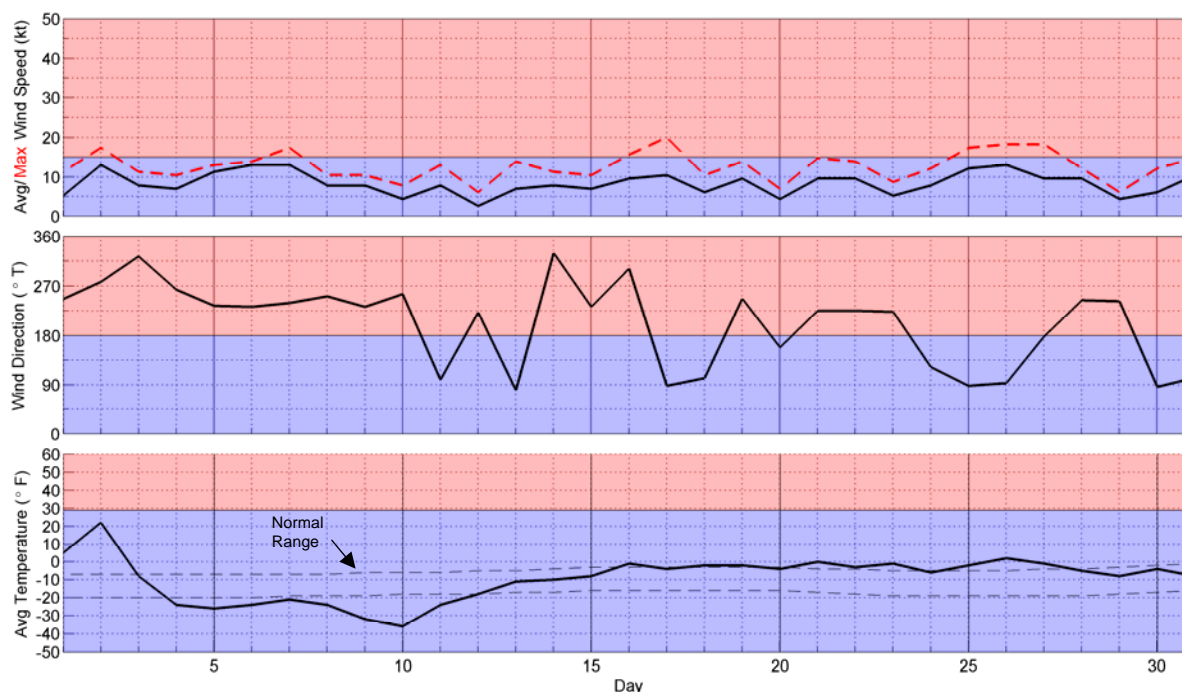
at an average daily speed of 0.73 kt (0.38 m/s) during the 23-kt (12 m/s) easterly storm that occurred on February 27th.

Of the five buoys in Camden Bay, the two closest to shore (Buoys CB-1 and -2) remained within the landfast ice zone from deployment on February 24th through month-end. Each moved approximately 2.5 nm (4.6 km) to the west during the easterly storm that took place on February 27th, probably reflecting compression of the landfast ice.

In contrast, Buoys CB-3, -4, and -5 were located outside the landfast ice zone and experienced substantial displacements to the west-northwest on the 27th and 28th. The average daily speeds peaked on the 27th, with values of 0.77 kt (0.40 m/s) for CB-3, 0.83 kt (0.43 m/s) for CB-4, and 0.85 kt (0.44 m/s) for CB-5 (Figure 39). The 0.85-kt value for Buoy CB-5 proved to be the highest recorded in the Beaufort Sea during the 2013-14 Freeze-Up Study. The corresponding average daily wind speed at Deadhorse Airport was 23 kt (12 m/s; Figure 34), producing a wind factor (ratio of ice speed to wind speed) of 3.7%. Substantially higher wind factors have been noted in previous freeze-up studies, including a maximum value of 6.7% in March 2013 (Coastal Frontiers and Vaudrey, 2013).

4.5.2. March 2014

Meteorological Conditions: Figure 40 presents the wind and temperature data recorded at Deadhorse Airport in March 2014. The air temperatures tended to be warmer than normal, with subnormal readings limited to an eight-day stretch that began on the 4th and ended on the 11th. The wind conditions were mild, with an average monthly speed of 8 kt (4 m/s) and no storm events. Westerlies prevailed during the first ten days of the month, followed by frequent wind shifts that produced eleven changes between easterly and westerly. The net result was a strong predominance of westerlies (20 of 31 days).



Source: Weather Underground, 2014

Figure 40. Meteorological Conditions at Deadhorse Airport in March 2014

Ice Thickness: The calculated thickness of undisturbed first-year ice increased by 18 cm, from 123 cm at the beginning of the month to 141 cm at the end.

Landfast Ice: Figure 41 presents the locations of the landfast ice edge derived from RADARSAT-2 images obtained on February 28th and March 7th, 14th, 17th, and 28th. In keeping with the absence of storm events and the well-grounded nature of the shear zone, the ice edge remained stable for most of the month. The only changes of note were: (1) a retreat of up to 10 nm (19 km) that occurred to the east of Prudhoe Bay at the beginning of the month during a period of westerly winds and (2) an advance of up to 18 nm (33 km) that occurred to the west of Prudhoe Bay at the end of the month during a period of mixed easterly and westerly winds.

Multi-Year Ice: Except in the vicinity of Point Barrow, the multi-year ice edge tended to remain in a narrow band between 72° and 72°30' N for the entire month of March. Off Point Barrow, multi-year ice approached within 15 nm of the coast (71°38' N) on the 17th (Figure 42) before returning to the 72° N parallel at the end of the month (NIC, 2014).

Ice Movement: Ice movement data in March were obtained from two of the multi-year floes tracked previously (Floes G and H), the eleven telemetry buoys installed in late February, and three new buoys installed in the western Beaufort during the second week in March (M-1, M-2, and M-4). The ice floe trajectories, which were derived from RADARSAT-2 images obtained on February 28th and March 7th, 14th, 16th, 17th, and 28th, are shown in Figure 43; the buoy trajectories, which were developed from the positions reported at midnight of each day, are shown in Figure 41.

The two multi-year ice floes described similar trajectories that resulted in modest westerly displacements over the course of the month. Floe G, which remained in the Beaufort, attained an average monthly speed of only 2.2 nm/day (4.1 km/day). Floe H moved at an average speed of 2.7 nm/day (5.0 km/day) between February 28th and March 16th before moving into the Chukchi. These low values are consistent with the predominance of westerly winds and absence of easterly storms discussed above.

The minimum speed between successive images, 0.9 nm/day (1.7 km/day) by Floe G, occurred at the beginning of the month (February 28th – March 7th) in response to prolonged westerly winds (Figure 40). The maximum speed, 6.7 nm/day (12.4 km/day) by Floe H, occurred between March 12th and 16th. Although westerly winds predominated at Deadhorse during this short period, the floe moved toward the west-southwest – an apparent

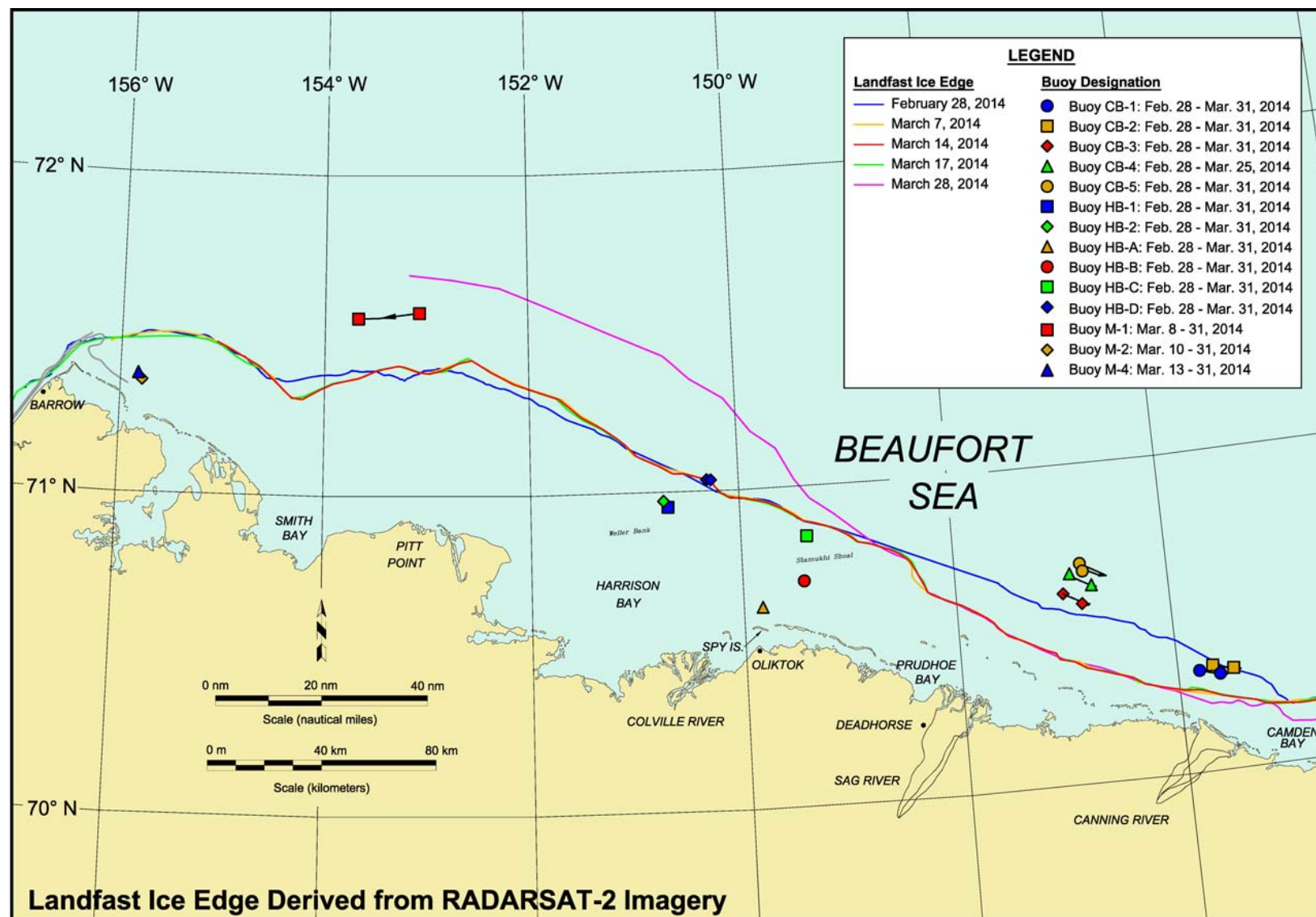
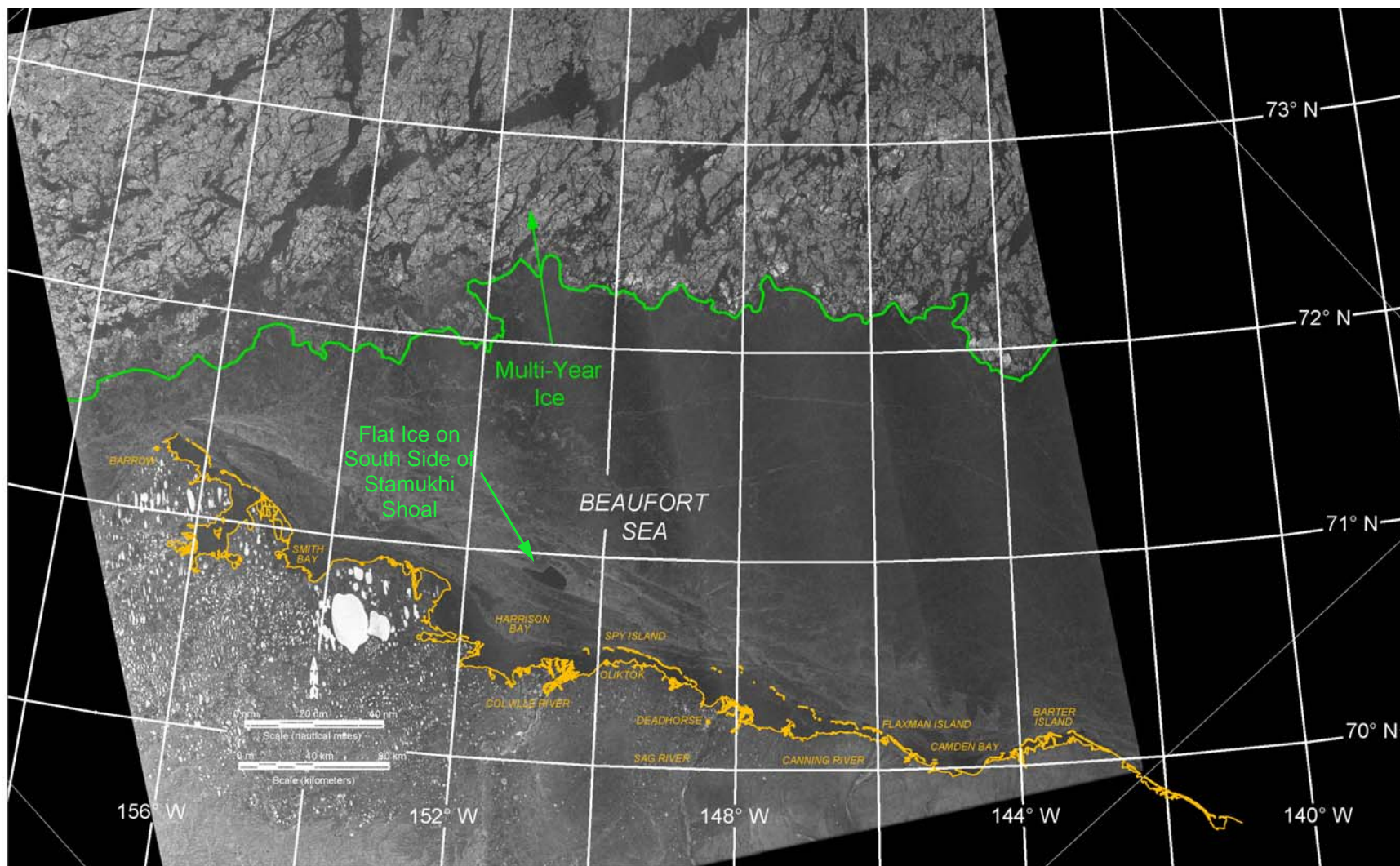


Figure 41. Beaufort Sea Landfast Ice Edge and Telemetry Buoy Tracks in March 2014



Source: RADARSAT-2 Data and Products © MacDonald Dettweiler and Associates Ltd., 2014 – All Rights Reserved

Figure 42. RADARSAT-2 Image of Beaufort Sea Acquired on March 17, 2014

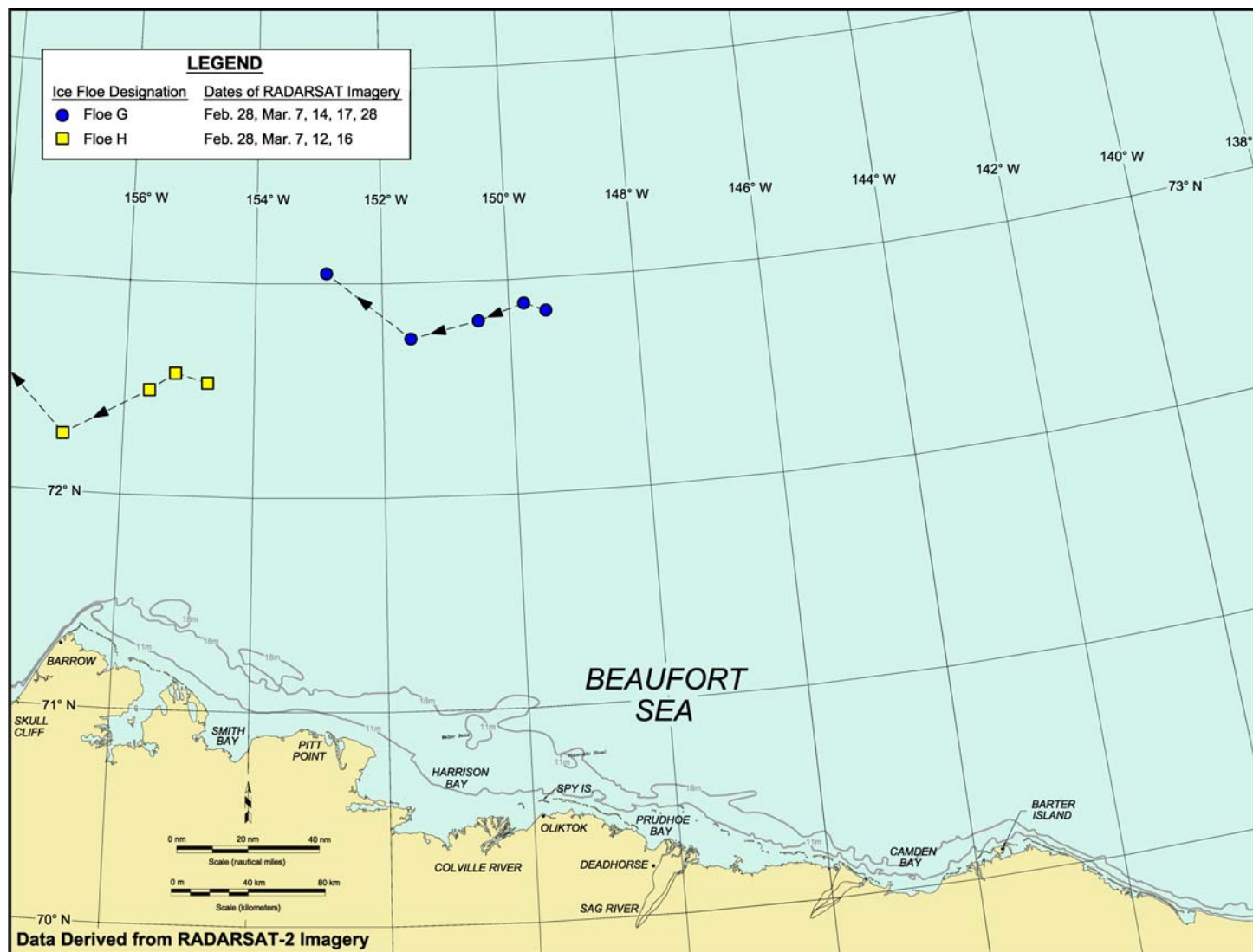


Figure 43. Beaufort Sea Multi-Year Ice Floe Displacement in March 2014

paradox that may be explained by the fact that the easterly winds prevailed at Barrow throughout this period (Figure 67 in Section 5.5.2).

The displacements and speeds of the fourteen telemetry buoys ranged from small to negligible in March (Figures 41 and 44). The six buoys in the vicinity of Harrison Bay, along with two new buoys deployed to the east of Point Barrow in March (Buoys M-2 and -4), remained stationary within the landfast ice zone. Buoy M-1, deployed outside the landfast ice zone off Smith Bay on March 8th, moved 11.5 nm (21.3 km) to the west-southwest on the 11th and 12th before coming to rest for the remainder of the month. The maximum daily average speed, 0.31 kt (0.16 m/s), occurred on the 11th (Figure 44).

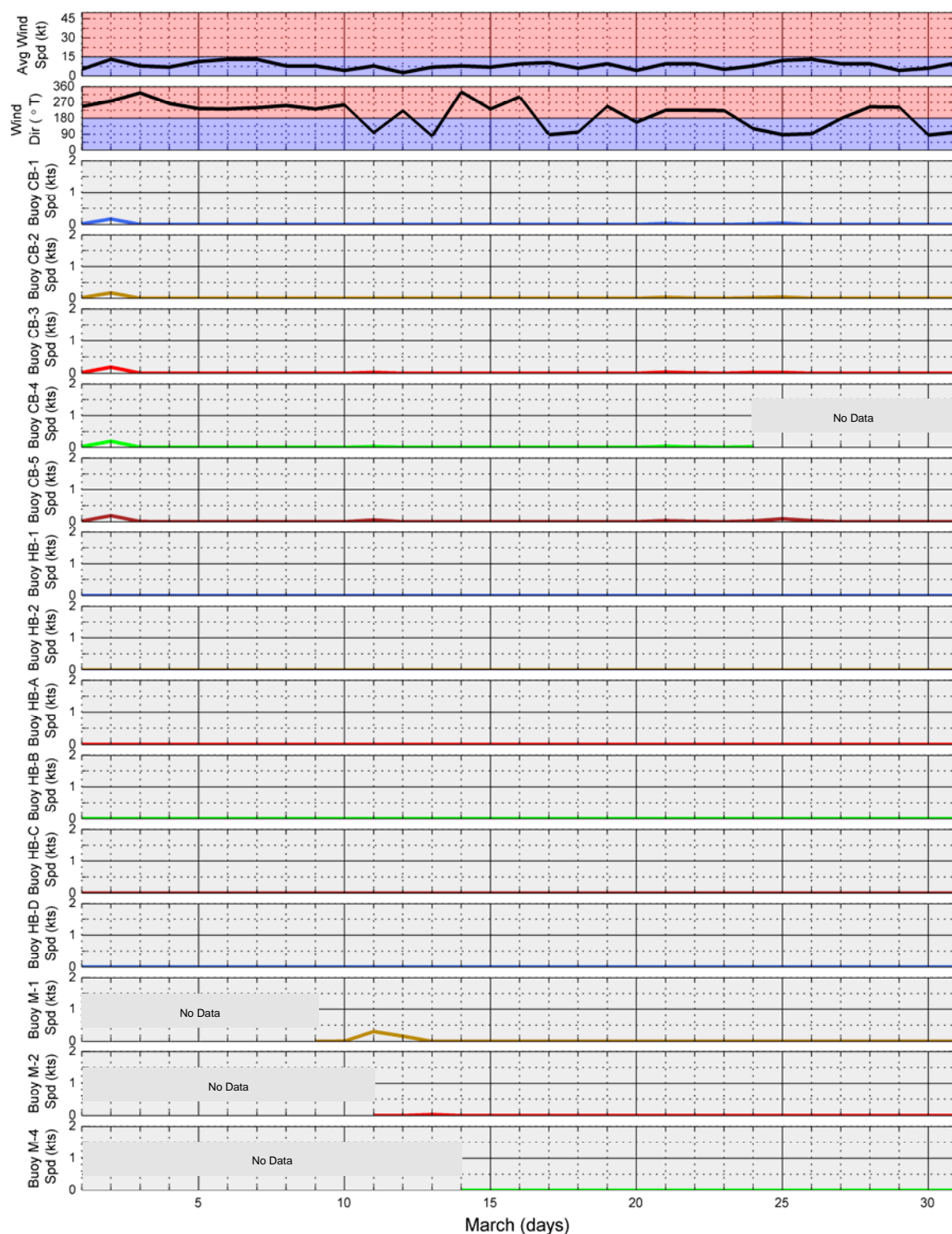
All five Camden Bay buoys were located outside the landfast ice zone that developed in early March, and all five responded to the 13-kt (7-m/s) westerly winds on the 2nd by moving to the southeast at speeds of 0.17 to 0.19 kt (0.09 to 0.10 m/s). Small displacements to the northwest at speeds less than or equal to 0.10 kt (0.05 m/s) followed in response to the easterly winds that occurred later in the month (Figure 44), producing net displacements for the month that ranged from 1 to 4 nm (2 to 7 km).

4.6 March Reconnaissance Flights

As discussed in Section 3.5, three aerial reconnaissance missions were undertaken in the Alaskan Beaufort Sea at the end of March to document the ice conditions that prevailed at the conclusion of the study period. Beaufort Sea Flight Nos. 1 and 2 (Flights “B1” and “B2” on Drawing CFC-917-01-001) were conducted in the central Beaufort, while Beaufort Sea Flight No. 3 (Flight “B3” on Drawing CFC-917-01-002) traversed the western Beaufort.

4.6.1 Lagoon Ice

The ice in semi-protected basins that included Simpson Lagoon, Gwydyr Bay, Prudhoe Bay, Mikkelsen Bay, and Leffingwell Lagoon was primarily flat and featureless (Plate 3). In Stefansson Sound, however, flat ice in the southern portion transitioned into intermittent rubble with heights of 1 to 2 m in the northern portion (Plate 4). The rubble resulted from a loss of confinement during southerly winds, and probably formed in November at the same time that the shoreline pile-ups discussed in Section 4.3.2 were created. Similar ice conditions – flat ice in the lagoon areas except the northern portion of Stefansson Sound – were noted in 2012-13 (Coastal Frontiers and Vaudrey, 2013), suggesting that Stefansson Sound is more prone to a loss of confinement due to its greater width. Loss of confinement can occur in other lagoon areas, however, as evidenced by a 2-m pile-up on the southeastern tip of Long Island that was caused by ice arriving from the west (Table 6).



Note: Wind data from Deadhorse Airport

Figure 44. Time Series of Telemetry Buoy Average Daily Speeds in Beaufort Sea, March 2014



Plate 3. Flat Ice in Simpson Lagoon between Oliktok Point and Spy Island Drillsite (looking southeast on March 28, 2014)

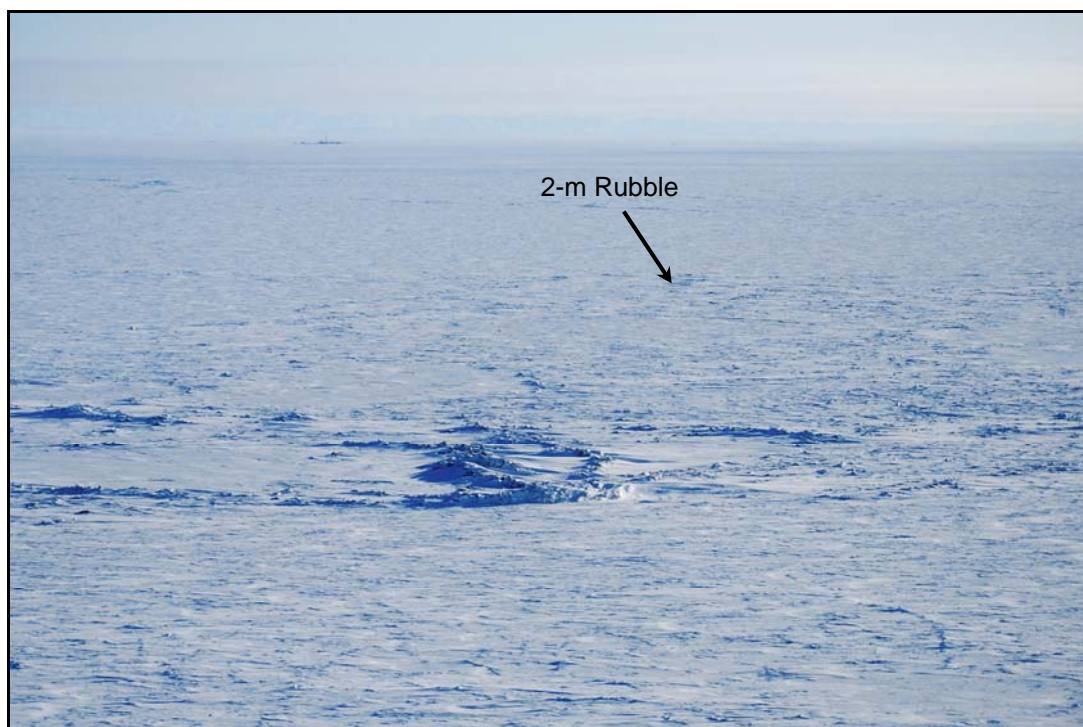


Plate 4. 5-m Pile-Up on Southwest End of Pole Island with 2-m Rubble in Stefansson Sound (looking southeast on March 28, 2014)

4.6.2 Thermal Cracks

Six large thermal cracks were observed during the flights, consisting of three between Prudhoe Bay and Long Island, and three in Stefansson Sound between Prudhoe Bay and Mikkelsen Bay. The heights of the associated ridges ranged from 0.5 to 1 m. The longest crack extended from the Sagavanirktok Delta more than 8 nm (15 km) to the southeast (Plate 5; Drawing CFC-917-01-001).

Thermal cracks have been observed in Stefansson Sound in each of the past four years (2010-11 through 2013-14; Coastal Frontiers and Vaudrey, 2011; 2012a; 2013). They also formed in this region in 1982, at which time they disrupted ice road operations during the construction of Shell's Tern Island (Vaudrey, 1982b).

As discussed in the 2010-11 Freeze-Up Study report (Coastal Frontiers and Vaudrey, 2011), such cracks tend to form when a rapid drop in air temperature precedes a rapid rise. The drop causes contraction and cracking of the ice sheet, which are followed by refreezing and then compression and extrusion of the refrozen slush into a ridge as the temperature rises. Based on a review of the temperature data at Deadhorse Airport, the cracks noted during the March aerial reconnaissance missions may have formed between December 7th and 16th. Over the course of this period, the average daily temperature dropped from +27 to -34°F (-3 to -37°C) and then rose to -4°F (-20°C).

4.6.3 First-Year Ice Growth

During the helicopter flight on March 29th (Section 3.5), the field crew landed in Mikkelsen Bay to measure the thickness of undisturbed first-year ice (Plate 6). The objective was to provide a basis for verifying or refining the ice thickness computations developed using the method of Bilello (1960; Section 4.1). Two independent measurements were obtained, yielding values of 135 and 142 cm. The mean value, 138.5 cm, was nearly identical to the predicted value of 140 cm for this date.

4.6.4 Landfast Ice and Shear Zone

When the reconnaissance flights were undertaken at the end of March, the landfast ice zone extended to the vicinity of the 18-m isobath to the east of Prudhoe Bay and well past the 18-m isobath to the west (Figure 41). Although the flight paths were largely contained within this zone, the seaward boundary observed while following the Sivulliq Development prospective pipeline route and again while crossing Camden Bay evidenced close agreement with that derived from the March 28th RADARSAT-2 image (Drawing CFC-917-01-001; Figure 41).

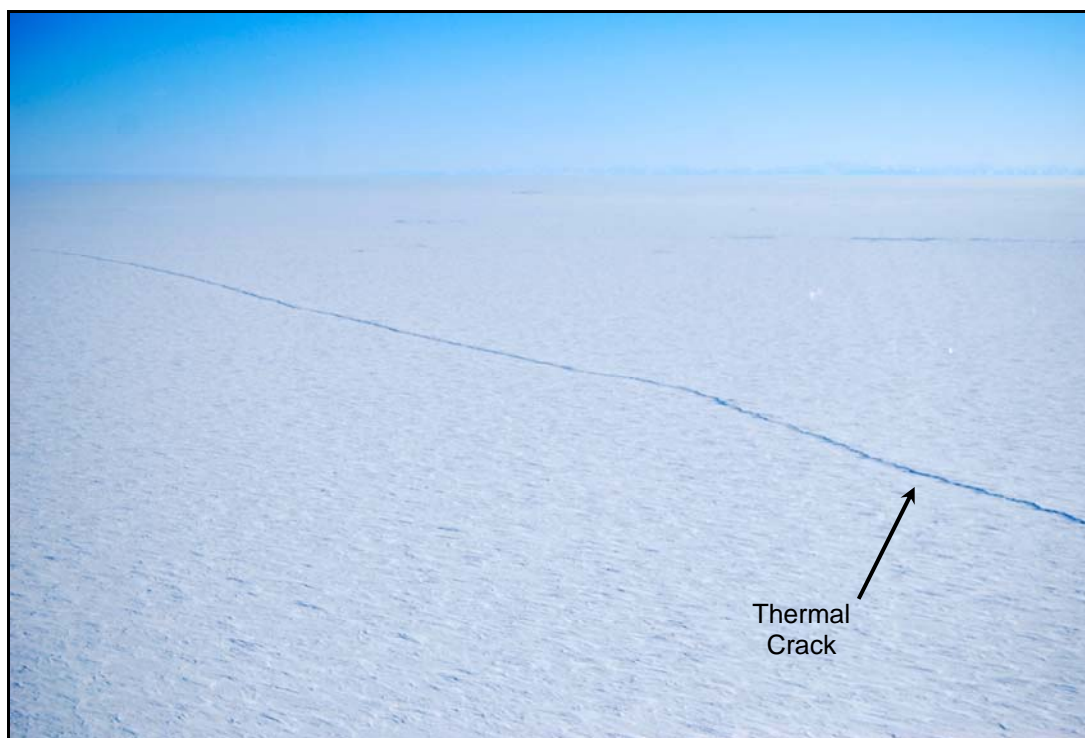


**Plate 5. 1-m High Thermal Crack in Stefansson Sound
(looking southeast on March 29, 2014)**



Plate 6. Ice Thickness Measurement in Mikkelsen Bay (March 29, 2014)

In keeping with the timing of the flights, which was substantially later than in any of the four prior freeze-up studies, the landfast ice was found to be securely anchored by an extensive and well-grounded shear zone. The extent of the grounding was particularly evident in the case of a massive ridge that marked the edge of the landfast ice on the Sivulliq Development prospective pipeline route. As suggested by Plate 7, it formed initially as a shear ridge. Subsequently, when subjected to compression by the pack ice, it was sufficiently well-grounded not only to resist displacement but also to cause the encroaching ice to fracture and override the original crest (Plate 8). The maximum height of this composite feature was measured at 11.8 m when the helicopter landed nearby on March 29th. The overriding ice blocks were 1.4 m thick, suggesting the override event had occurred in the recent past (Plate 9).

Regional characteristics of the landfast ice observed during the reconnaissance flights are summarized below:

- **Harrison Bay:** As in past years, the landfast ice was anchored by large expanses of grounded ridges and rubble on Stamukhi Shoal and Weller Bank. These features attained a maximum height of 6 m on the former (Plate 10), and 20 m on the latter (Plate 11). An unexpected discovery was an area of flat, nearly-featureless ice on the south side of Stamukhi Shoal measuring up to 5 nm (9.3 km) wide and 15 nm (27.8 km) long (Plate 12). Based on a review of the RADARSAT-2 images, this feature probably formed during the December 28th – January 6th easterly storm when ice grounded on the north side of the shoal. The protected area in the lee of the grounded ice then froze without disturbance and remained intact for the remainder of the study period (Figure 42).
- **Barrier Islands:** The barrier islands in the central Beaufort Sea were fronted by a wide band of grounded ridges and rubble. The deformed ice typically extended about 5 nm (9.3 km) offshore, with heights to 5 m (Plate 13) that occasionally reached 8 m.
- **Camden Bay:** The landfast ice in Camden Bay was less consolidated than in most other areas, with a number of cracks and small refreezing leads evident. Although flat ice was present in some areas, ridges and rubble with typical heights of 3 to 5 m were commonplace (Plate 14).

4.6.5 Leads

In the central Beaufort, the ice canopy outside the landfast ice zone contained a number of small leads and polynyas that were local rather than regional in extent. Representative examples are provided in Plates 15 and 16.



Plate 7. 11.8-m Grounded Ridge on Sivulliq Development Prospective Pipeline Route with Brooks Range in Background (looking south on March 28, 2014)

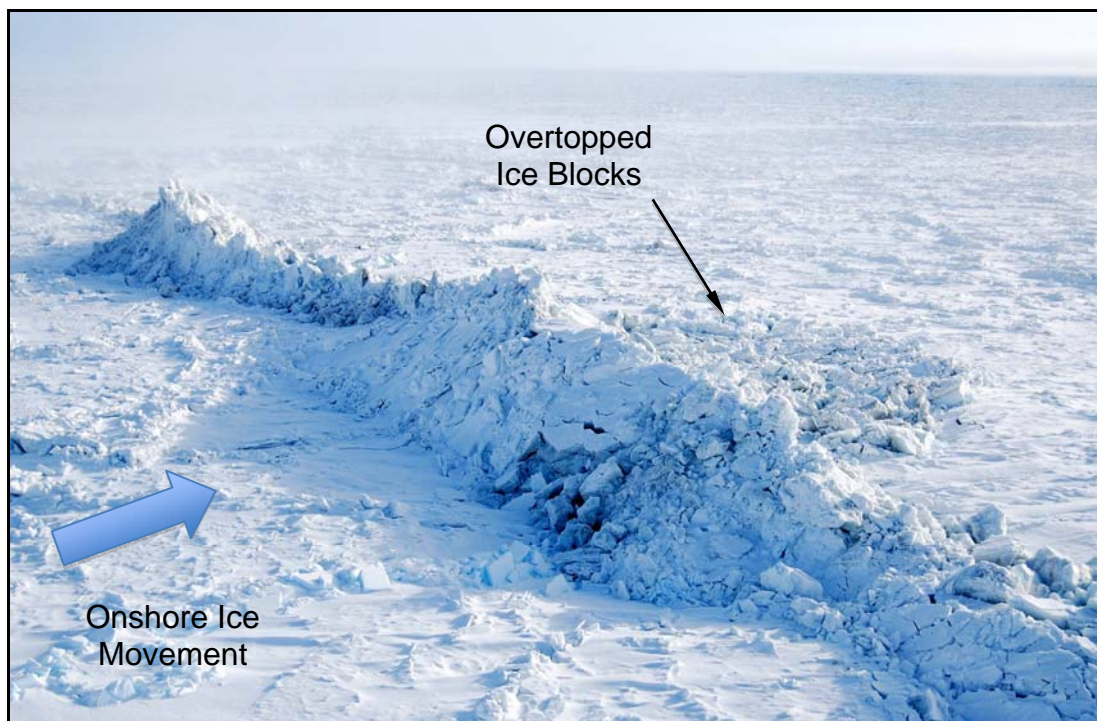
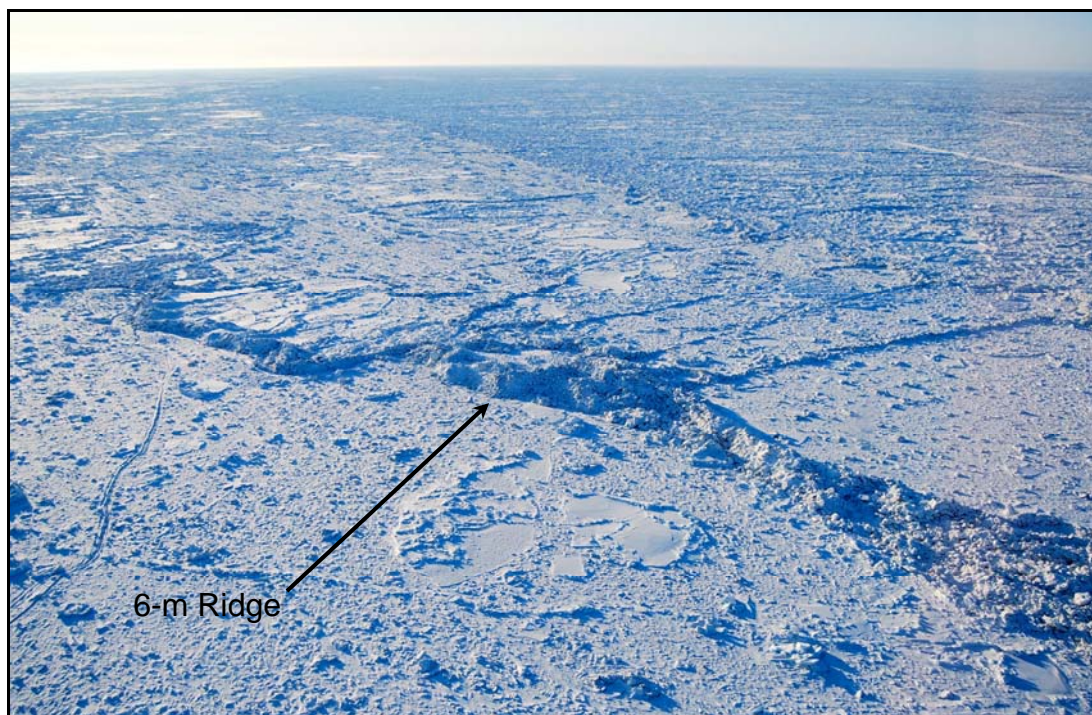


Plate 8. 11.8-m Grounded Ridge on Sivulliq Development Prospective Pipeline Showing Evidence of Ice Override (looking southeast on March 29, 2014)



**Plate 9. 1.4-m Ice Blocks on Landward Side of 11.8-m Grounded Ridge
(looking north on March 29, 2014)**



**Plate 10. 6-m Ridge and Extensive Rubble Field on Stamukhi Shoal
(looking southeast on March 28, 2013)**



Plate 11. 20-m Ridge on Weller Bank (looking north on March 30, 2014)



**Plate 12. Wide Expanse of Flat Ice on South Side of Stamukhi Shoal
(looking southwest on March 28, 2014)**



**Plate 13. Extensive Rubble Field with Heights to 5 m off Cross Island
(looking northeast on March 28, 2014)**



**Plate 14. 3-m Rubble Adjacent to Landfast Ice Edge in Camden Bay
(looking southeast on March 28, 2014)**



**Plate 15. Small Lead Located 20 nm (37 km) off Narwhal Island
(looking west on March 28, 2014)**



**Plate 16. Polynya Located 23 nm (43 km) off Brownlow Point
(looking west on March 28, 2014)**

In the western Beaufort, the only substantial lead observed during the reconnaissance flight on March 30th was an extension of the coastal flaw lead that typically develops off the Chukchi Sea coast in response to easterly winds (Section 2). Plate 17 illustrates this “extended flaw lead” (Coastal Frontiers and Vaudrey, 2012a) as it existed 15 nm (28 km) northeast of Point Barrow.



**Plate 17. Extended Flaw Lead 15 nm (28 km) Northeast of Point Barrow
(looking northwest on March 30, 2014)**

4.6.6. Ice Pile-Ups

Forty-six ice pile-ups were noted in the central Beaufort Sea during the March reconnaissance flights (Table 6). As discussed in Section 4.1, it is surmised that 23 of these features formed on November 9th and 10th when the winds shifted from southeasterly to southwesterly, six on November 14th when the winds shifted from southerly to slightly north of west, and the remaining seventeen on December 8th when the winds shifted from westerly to easterly. The pile-ups occurred on shorelines with exposure to the southwest, northwest, and northeast quadrants, including many on the south-facing beaches of the barrier islands.

The maximum heights of the pile-ups varied from 1 to 8 m above MSL, while the alongshore lengths varied from 50 to 2,600 m. Thirty-two of the 46 pile-ups extended past

the waterline onto the subaerial beach, with encroachment distances ranging from 3 to 20 m. Thirty-nine were located on barrier islands, three on the mainland shore, and four on man-made facilities.

The tallest pile-up, with a height of 8 m, encroached 20 m onto the gravel bags that protect the northwest corner of the West Dock Causeway Seawater Treatment Plant (STP) Pad. As shown in Plate 18, the pile-up reached the elevation of the pad work surface but did not spill onto it.

Plate 19 illustrates a pile-up representative of those observed on the barrier islands. Located on the southwest tip of Narwhal Island, it was 5-m high, 300 m long, and encroached 10 m onto the subaerial beach.

4.6.7. Multi-Year Ice

No multi-year ice floes were observed during the three Beaufort Sea reconnaissance flights, which were conducted well south of the multi-year ice edge.

4.6.8 Ice Conditions in Shell Prospects

As discussed in Section 4.6.4, a massive ridge marked the boundary between landfast ice and mobile pack ice on Shell's prospective pipeline route for the Sivulliq Development at the time of the reconnaissance flights (Plates 7 and 8). The ridge was located approximately 5 nm (9 km) outside Mary Sachs Entrance.

As in each of the past five winters, the lagoon ice in Leffingwell Lagoon (between the mainland shore and Mary Sachs Entrance) was flat and undeformed (Plate 20). Farther offshore, between Mary Sachs Entrance and the edge of the landfast ice, 3-m rubble was interspersed with small first-year floes and inactive shear lines (Plate 21). The maximum ridge height in this region was estimated to be 5 m. From the landfast ice edge to the seaward end of the prospective pipeline route, a distance of 7 nm (13 km), the ice was less deformed, with rubble heights of 1 to 3 m (Plate 22). An active shear line was present along with a series of refreezing leads.

Shell's Harrison Bay Prospects were located in the landfast ice zone when the flights were undertaken. The ice was well-consolidated, with no open leads. Deformation tended to increase with distance to the northeast. As shown in Plate 23, flat first-year ice was interspersed with ridges and rubble typically 2 to 3 m high in the southwestern portion. Ridges and rubble predominated in the northeastern portion, with heights to 5 m to the west of Stamukhi Shoal (Plate 24) and 6 m on the shoal itself (Plate 10).



**Plate 18. 8-m Pile-Up that Encroached 20 m onto Northwest Corner of STP Pad
(looking south on March 30, 2014)**



**Plate 19. 5-m Pile-Up that Encroached 10 m onto Southwest Tip of Narwhal Island
(looking southeast on March 28, 2014)**



Plate 20. Flat Ice in Leffingwell Lagoon with Rubble Field outside Mary Sachs Entrance in Background (looking north on March 29, 2014)



Plate 21. 3-m Rubble and Inactive Shear Line in Landfast Ice 3 nm off Mary Sachs Entrance (looking northeast on March 28, 2014)



Plate 22. 1- to 3-m Rubble and Refreezing Lead at Seaward End of Sivulliq Development Pipeline Route (looking southwest on March 28, 2014)



Plate 23. Flat First-Year Ice Interspersed with 2-m Ridges and Rubble in Southwestern Portion of Harrison Bay Prospects (looking west on March 28, 2014)



Plate 24. 5-m Ridges and Rubble with Scattered First-Year Floes in Northeastern Portion of Harrison Bay Prospects (looking southwest on March 28, 2014)

5. CHUKCHI SEA

Section 5.1 presents a brief overview of the 2013-14 freeze-up season in the northeast Chukchi Sea. As in the case of Section 4.1, emphasis is placed on summary tables. An analysis of the conditions that prevailed from late summer 2013 through March 2014 follows in Sections 5.2 through 5.7.

5.1 Overview

Air Temperatures: As in each of the past four freeze-up seasons, the air temperatures at Barrow Airport ranged from normal to well above normal in October 2013. This pattern continued for the next five months, with elevated temperatures occurring frequently and subnormal temperatures infrequently. When compared with the long-term averages derived for the period from 1971-72 through 1999-2000, the air temperatures in October, February, and March were particularly high.

Winds: Wind conditions during the 2013-14 freeze-up season are summarized in Table 9, which is based on the average daily speeds and directions recorded at Barrow Airport. In sharp contrast to the Beaufort, where westerlies outnumbered easterlies in five of the six months (Section 4.1), easterlies prevailed in the Chukchi in each month from October through March. Over the entire period, easterlies outpaced westerlies by a margin of 61% to 39%. The average monthly speeds ranged from a low of 8 kt (4 m/s) in March to a high of 14 kt (7 m/s) in November and January.

Table 9. Chukchi Sea Wind Characteristics, October 2013 – March 2014

Month	Days		Average Speed (kt)
	Easterly	Westerly	
October	22	9	9
November	16	14	14
December	17	14	11
January	22	9	14
February	15	13	11
March	19	12	8
Total Days	111	71	n/a
Frequency (%)	61	39	n/a

Note: Table 9 is based on the average daily wind speeds and directions recorded at Barrow Airport.

Storms: The characteristics of all storms with a daily average sustained wind speed exceeding 15 kt (8 m/s) at Barrow Airport are presented in Table 10 for the six-month period from October 2013 through March 2014. Twelve of the nineteen events were easterlies, including five of the six storms that occurred after December 24th. November and January were the stormiest months, with thirteen and twelve storm-days, respectively. At the opposite end of the spectrum, there were no storm-days in March and only two in November. The highest sustained wind speed, 26 kt (13 m/s), occurred during the December 28th- January 6th easterly storm, which also proved to be the longest storm event of the study period.

Ice Cover: Ice began to form in the protected waters of Kasegaluk Lagoon, the Kuk River Inlet, and Peard Bay during the first week in October. Complete coverage of these areas did not occur until the end of the month due to unseasonably warm air temperatures. After moving slowly to the south during the first three weeks of October, the pack ice advanced rapidly during the final ten days. At month-end, it was located in the vicinity of the 72° parallel off Point Barrow and the 71° parallel off Point Franklin. The coast was ice-free.

During the first half of November, the ice edge retreated slightly to the north under the influence of warm air temperatures and winds from the southeast and southwest quadrants. This trend was reversed during the second half, when a rapid march to the south occurred in response to colder temperatures and winds from the northeast and northwest quadrants. Freeze-up in the nearshore region occurred on November 26th, followed by complete freeze-up in the entire Chukchi Sea north of Cape Lisburne on December 14th.

On or about November 12th, a flash freeze created a small patch of ice centered 130 nm (241 km) west of Icy Cape. Although much smaller than that which formed off Wainwright in October 2013 (Coastal Frontiers and Vaudrey, 2014), it nevertheless marked the second documented occurrence of flash freezing in the Chukchi Sea over the past five freeze-up seasons.

Ice Thickness: The thickness of undeformed first-year ice at the end of each month was estimated using the relationship of Lebedev (Bilello, 1960) in concert with the accumulated freezing degree days (FDD) at Barrow shown in Table 1. The method of calculation is identical to that presented for the Beaufort Sea in Section 4.1. The results are provided in Table 11, which indicates that undisturbed first-year ice attained a thickness of approximately 143 cm at the beginning of June.

Table 10. Chukchi Sea Storm Characteristics, October 2013 – March 2014¹

Month	Day	Duration (days)	Maximum Wind Speed (kt) ²	
			Easterly	Westerly
October	8	1	23	
	27	1	16	
November	5	1		19
	7-9 ³	3	22	
	10-11	2		26
	14-17 ⁴	4		21
	22-23	2	18	
December	Nov 30-Dec 1	2		19
	6	1	20	
	7	1		18
	8-9	2	24	
	21	1	16	
	24	1		16
January	Dec 28-Jan 6 ⁵	10	26	
	18	1	22	
	21-25	5	24	
February	5-6	2		21
	23	1	21	
	27	1	23	
March	-	-	-	-
Total Duration		42		
Total Number of Events			12	7

Notes:

- ¹ Table 10 includes all storm events with a daily average sustained wind speed exceeding 15 kt at Barrow Airport.
- ² “Maximum Wind Speed” refers to highest daily average sustained wind speed that occurred during each storm event.
- ³ Daily average wind speed decreased to 15 kt on November 8th but freshened to 17 kt on November 9th.
- ⁴ Daily average wind speed decreased to 15 kt on November 15th but freshened to 17 kt on November 16th.
- ⁵ Daily average wind speed decreased to 15 kt on December 29th and 30th but freshened to 18 kt on December 31st.

Table 11. Chukchi Sea Computed Ice Thicknesses, October 2013 – June 2014¹

Date	FDD	Accumulated FDD	Ice Thickness ² (cm)
31 October 2013	127	161	18
30 November 2013	638	799	45
31 December 2013	987	1,786	72
31 January 2014	1,103	2,889	96
28 February 2014	1,008	3,897	114
31 March 2014	1,048	4,945	131
30 April 2014	751	5696	142
2 June 2014	79	5775	143

Notes:

¹ Table 11 is based on the average daily temperature data recorded at Barrow Airport.

² Ice thickness is computed from accumulated FDD using method of Lebedev (Bilello, 1960).

Landfast Ice: Landfast ice began to form in early November in the semi-protected waters of Peard Bay, the Kuk River Inlet, and the Utukok River Inlet. By the end of the month, a narrow, discontinuous strip extended from Barrow to Peard Bay, and another narrow strip from Wainwright to the vicinity of Point Lay. The landfast ice zone remained narrow throughout December except for an advance to Blossom Shoals (off Icy Cape) that occurred at the end of the month. The ice remained grounded on this feature for the remainder of the study period.

During the third week in January, a prolonged easterly storm dislodged virtually all of the landfast ice north of the Nokotlek River Mouth. In February and March, the ice waxed and waned in response to changing wind conditions, producing widths that ranged from negligible to 20 nm (37 km). At the end of March, the landfast ice was confined to a narrow strip that remained inside the 11-m isobath in most areas.

Ice Pile-Ups: Twenty-two ice pile-ups occurred on the coast of the northeast Chukchi Sea during the 2013-14 freeze-up season. The highest concentration was located to the east of Icy Cape on the barrier islands that form the seaward boundary of Kasegaluk Lagoon. As shown in Table 12, the pile-up heights ranged from 1 to 3 m, the encroachment distances from 5 to 20 m (measured from the waterline), and the alongshore lengths from 100 to 7,800 m. As in the case of the Beaufort, the ice blocks that comprised the pile-ups were partially obscured by drifted snow. The block thicknesses were estimated to be 30 to 40 cm.

Table 12. Ice Pile-Ups on Chukchi Sea Coast during 2013-14 Freeze-Up Season

No.	Region	Formation Date	Arrived From	Length ¹ (m)	Height ² (m)	Encroachment ³ (m)
1	Barrow-Peard Bay	Dec 7	W	700	3	5
2	Barrow-Peard Bay	Dec 7	W	1,300	3	15
3	Barrow-Peard Bay	Dec 7	W	7,800	3	20
4	Barrow-Peard Bay	Dec 7	W	700	3	20
5	Pt. Franklin-Kuk R.	Dec 7	W	2,300	3	10
6	Pt. Franklin-Kuk R.	Dec 7	W	3,900	2	5
7	Pt. Franklin-Kuk R.	Dec 7	W	2,600	2	5
8	Pt. Franklin-Kuk R.	Dec 7	W	2,500	2	10
9	S of Kuk River	Dec 7	W	100	1	5
10	S of Kuk River	Dec 7	W	400	2	5
11	S of Kuk River	Dec 7	W	1,900	1	5
12	E of Icy Cape ⁴	Dec 7	W	800	1	5
13	E of Icy Cape ⁴	Dec 7	W	1,500	2	15
14	E of Icy Cape ⁴	Dec 7	W	1,500	2	10
15	E of Icy Cape ⁴	Dec 7	W	1,800	2	10
16	E of Icy Cape ⁴	Dec 7	W	700	2	10
17	E of Icy Cape ⁴	Dec 7	W	100	2	5
18	E of Icy Cape ⁴	Nov 21-22	NE	1,900	3	5
19	E of Icy Cape ⁴	Nov 21-22	NE	1,900	3	5
20	E of Icy Cape ⁴	Nov 21-22	NE	800	3	5
21	S of Icy Cape ⁵	Dec 7	W	600	1	5
22	S of Icy Cape ⁵	Dec 7	W	1,900	1	10

Notes:

¹ “Length” indicates alongshore extent of pile-up.

² “Height” indicates maximum height of pile-up relative to MSL.

³ “Encroachment” indicates distance ice advanced onto subaerial beach.

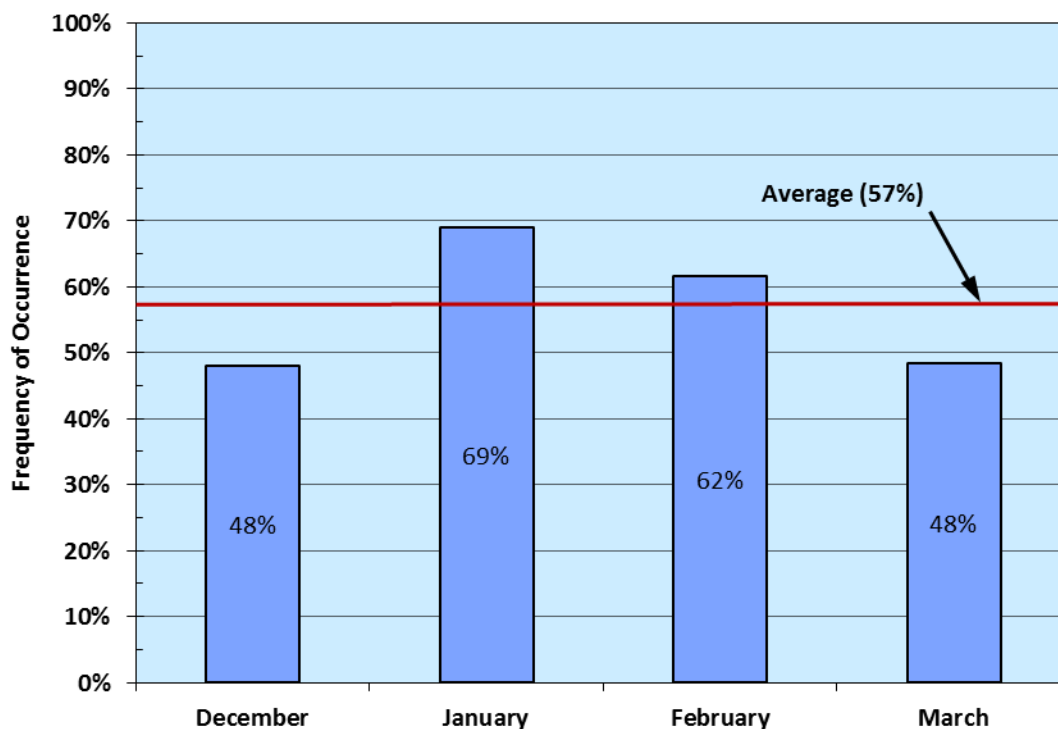
⁴ Pile-up occurred on barrier islands east of Icy Cape.

⁵ Pile-up occurred on barrier islands south of Icy Cape.

The pile-ups probably resulted from two abrupt wind-shifts that occurred in mid-November and early December:

- November 21st through 22nd, when the winds backed from southerly to northeasterly and freshened to a peak of 18 kt (9 m/s), creating three pile-ups on the northeast-facing beaches to the east of Icy Cape;
- December 7th, when the winds veered from easterly to westerly and freshened to a peak of 18 kt (9 m/s), creating nineteen pile-ups on northwest-facing beaches throughout the study area.

Coastal Flaw Lead: During the four-month period from December 2013 through March 2014, the flaw lead that forms off the Chukchi Sea coast in response to easterly winds was present on 57% of the days for which useful satellite images are available (Figure 45). The frequency of occurrence peaked at 69% in January in response to a predominance of easterly winds (Table 9) and three easterly storms (Table 10). The maximum width, 100 nm (185 km), occurred in February while the maximum length, 250 nm (463 km), occurred on repeated occasions in February and March. The maximum persistence of 15 days took place from mid-February to early March.



Note: Useful images were available for 92% of the four-month period.

Figure 45. Frequency of Occurrence of Chukchi Sea Flaw Lead, December 2013 - March 2014

Multi-Year Ice: Multi-year ice was present in the Chukchi Sea throughout the study period, but remained north of the 72° parallel until the end of November. After a brief advance to the vicinity of 71°30' N, the southern boundary returned to the 72° parallel in mid-December. During the month that followed, the coastal flaw lead extended northeast of Point Barrow to such an extent that it reached the multi-year ice and diverted multi-year floes to the southwest on four occasions that lasted from one to five days. The last of these, which occurred in mid-January, produced a significant southerly displacement of the multi-year ice edge into the region south and west of Point Barrow. The ice continued to advance slowly to the south in February and March, crossing the 71° parallel in late February and reaching the vicinity of Icy Cape in mid-March.

Ice Movement: As in the case of the Beaufort, ice movement was investigated using multi-year ice floes that appeared in successive RADARSAT-2 images. Six of the eight floes tracked in the Beaufort (Section 4.1) moved into the Chukchi over the course of the study period, and one additional floe was identified in the Chukchi alone. The average monthly speeds, which were computed over periods of 16 to 31 days, ranged from 0.2 to 6.1 nm/day (1.5 to 11.0 k/day; Table 13). The average monthly value was 2.6 nm/day (4.8 km/day)

Table 13. Chukchi Sea Multi-Year Ice Floe Speeds, January 2014 - March 2014

Month	No. of Floes	Average Monthly Speed (nm/day)		
		Maximum	Minimum	Average
January	2	6.1	5.9	6.0
February	1	1.0	1.0	1.0
March	4	1.9	0.2	0.8
Average				2.6

Note: Speeds were derived from periods ranging from 16 to 31 days (depending on the availability of RADARSAT-2 images).

All of the floes that remained north of Point Barrow, with full exposure to the Beaufort Gyre, experienced net displacements to the west. The speeds were highest in January, a month marked by a predominance of easterly winds and three easterly storms as indicated above. In March, three floes that were located at or below the latitude of Point Barrow, and therefore sheltered from the Beaufort Gyre, moved first to the southwest and then back to the northeast in the region dominated by the coastal flaw lead. Although the net displacements over the course of the month were small, the speeds between successive images were high when opening of the flaw lead caused a loss of confinement.

5.2 Late Summer 2013

During the month of August, the coast of the northeast Chukchi Sea remained ice-free. Farther offshore, the ice retreated to the north. By the first week in September, large areas of open water prevailed to the north of Point Barrow and west of Wainwright. However, as shown in Figure 46, a tongue of ice trending northwest-southeast extended to within 50 nm (93 km) of Icy Cape. The ice continued to retreat until mid-September, when the southern boundary was located near the 74° parallel approximately 180 nm (278 km) off Point Barrow.

The second half of September was marked by a reversal of this trend: at month-end, the ice edge off Point Barrow had advanced to the 73°30' parallel. Although ice began to form in Kasegaluk Lagoon in response to the sub-freezing temperatures that occurred between the 22nd and 27th, it failed to survive the warmer temperatures that followed at the end of the month.

5.3. Early Freeze-Up

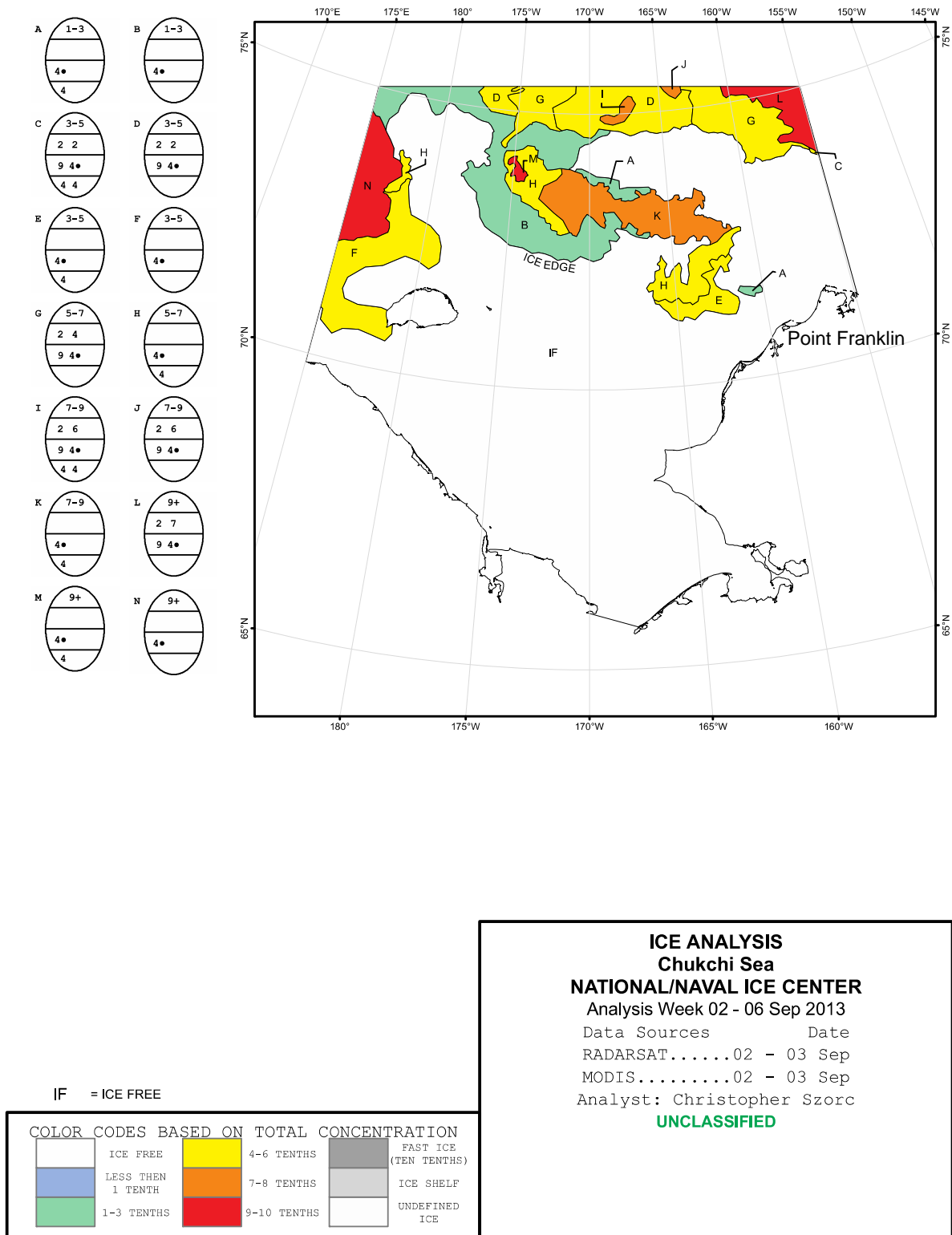
5.3.1. October 2013

Meteorological Conditions: The daily values of average and maximum sustained wind speed, average wind direction, and average air temperature at Barrow Airport are shown in Figure 47. As in Section 4, the red and blue color bands in this and all subsequent meteorological plots are intended to denote the ranges of parameters defined in Table 8. Unless indicated otherwise, the wind speeds discussed in the text refer to the daily average values of the sustained speed rather than the daily maximum values.

As in each of the past four freeze-up seasons (Coastal Frontiers and Vaudrey, 2013), the daily average air temperatures in October 2013 tended to exceed the corresponding long-term average values for the period from 1971-72 through 1999-2000 by a wide margin. The average temperature for the month, 25°F (-4°C), was a full 10°F (6°C) higher than the long-term average.

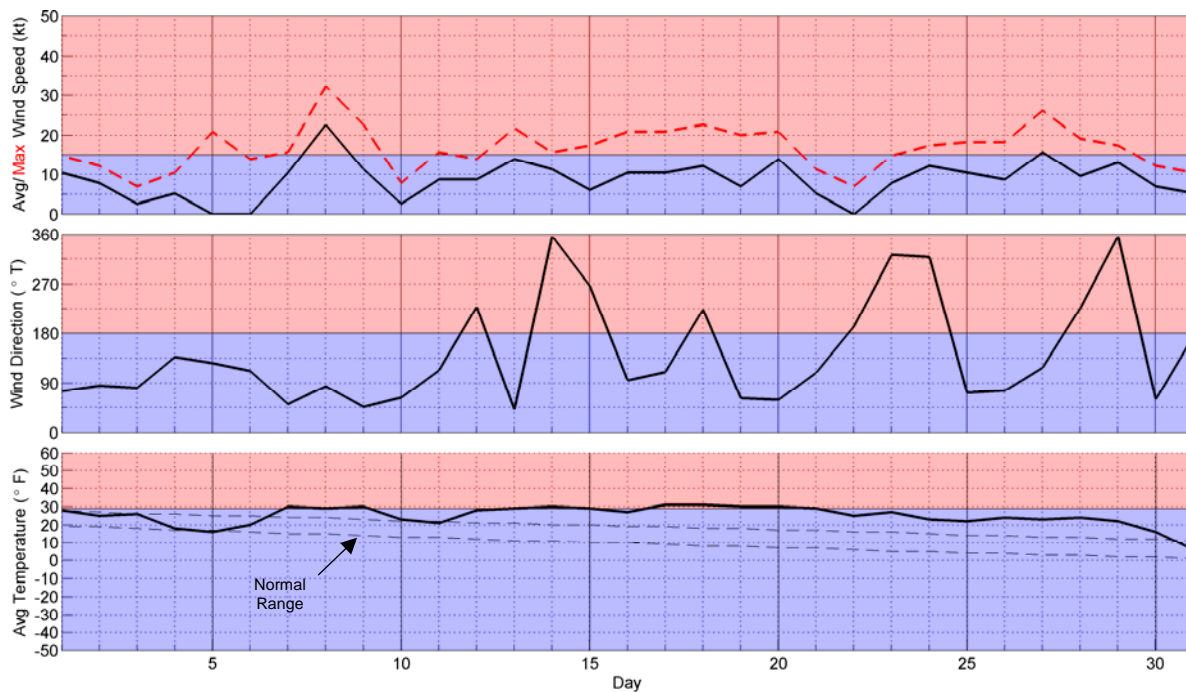
Easterly winds predominated, occurring on 22 of the 31 days (Table 9). The average speed for the month was relatively low, at 9 kt (5 m/s). Storm events were limited to two brief easterlies:

- October 8th: one-day easterly with maximum speed of 23 kt (12 m/s);
- October 27th: one-day easterly with maximum speed of 16 kt (8 m/s).



After: National Ice Center, 2014

Figure 46. NIC Ice Chart for September 3, 2013 Showing Tongue of Ice off Point Franklin



Source: Weather Underground, 2014

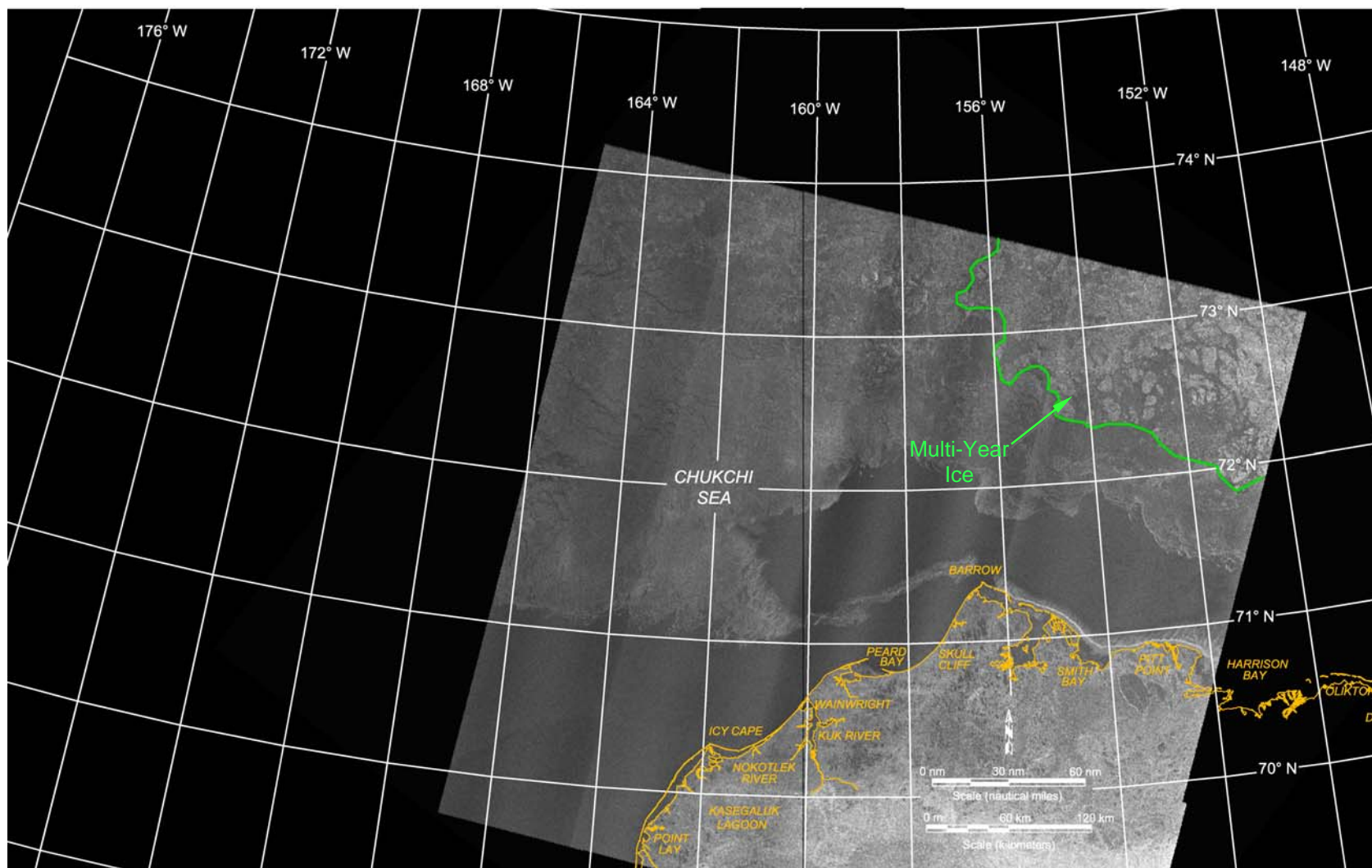
Figure 47. Meteorological Conditions at Barrow Airport in October 2013

Ice Cover: Based on a review of RADARSAT-2 imagery and NIC ice charts (2014), ice began to form in the protected waters of Kasegaluk Lagoon, the Kuk River Inlet, and Peard Bay during the first week in October. Complete coverage of these areas did not occur until the end of the month, however, due to the unseasonably warm temperatures that prevailed during the intervening period.

After moving slowly to the south during the first three weeks of October, the pack ice advanced rapidly during the final ten days. At month-end, it was located in the vicinity of the 72° parallel off Point Barrow and the 71° parallel off Point Franklin. A narrow tongue of ice extended northeast from offshore of Peard Bay to the vicinity of Point Barrow, but the coast itself remained ice-free (Figure 48).

Ice Thickness: The thickness of undisturbed first-year ice at the end of October was approximately 18 cm (Table 11).

Multi-Year Ice: Multi-year ice was present in the northern portion of the Alaskan Chukchi Sea throughout October, but remained well offshore. At the end of the month, the southern boundary was located in the vicinity of the 73° parallel off Point Barrow (Figure 48).

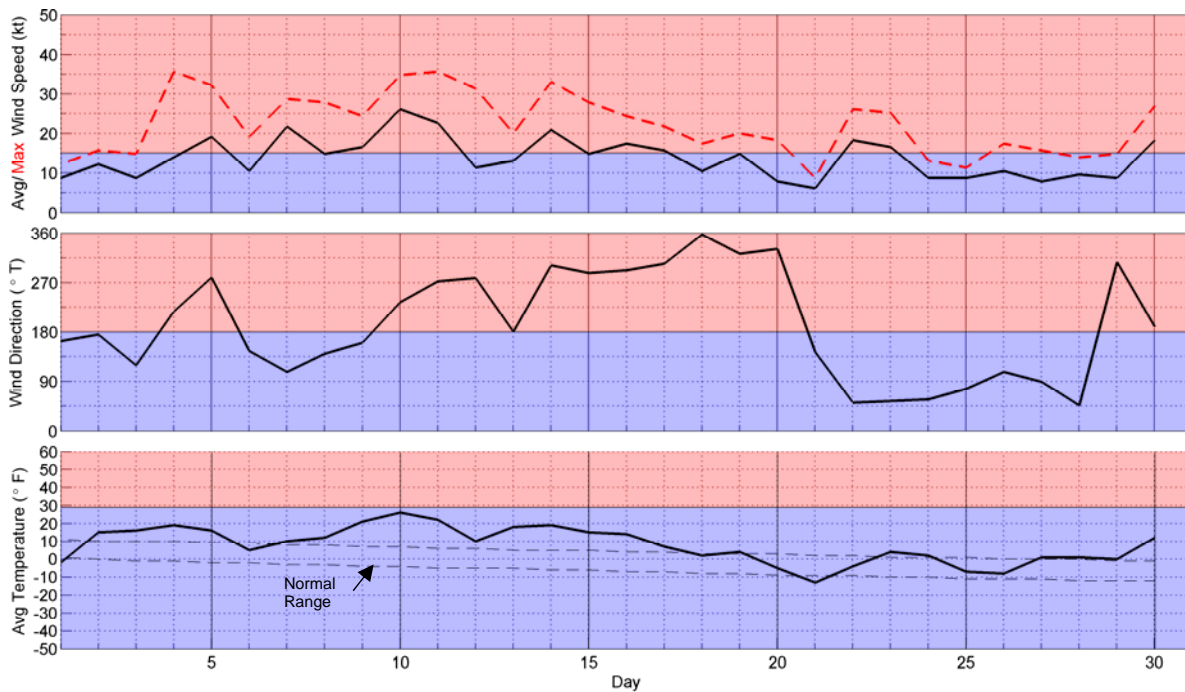


Source: RADARSAT-2 Data and Products © MacDonald Dettweiler and Associates Ltd., 2013 – All Rights Reserved

Figure 48. RADARSAT-2 Image of Chukchi Sea Acquired on October 30, 2013

5.3.2. November 2013

Meteorological Conditions: The wind and temperature data acquired at Barrow Airport in November are shown in Figure 49. The average daily air temperature exceeded the normal range on 21 of the 30 days, and fell below on only two occasions. Elevated temperatures were especially common from the 2nd through 19th.



Source: Weather Underground, 2014

Figure 49. Meteorological Conditions at Barrow Airport in November 2013

Easterly winds prevailed over westerlies by the narrowest of margins: 16 vs. 14 days (Table 9). The average speed for the month, 14 kt (7 m/s), equaled that in January and represented the highest value recorded during the six-month study period. The storm population consisted of two easterlies and three westerlies:

- November 5th: one-day westerly with maximum speed of 19 kt (10 m/s);
- November 7th-9th: three-day easterly with maximum speed of 22 kt (11 m/s);
- November 10th-11th: two-day westerly with maximum speed of 26 kt (13 m/s);
- November 14th-17th: four-day westerly with maximum speed of 21 kt (11 m/s);
- November 22nd-23rd: two-day easterly with maximum speed of 18 kt (9 m/s).

Another westerly storm that began on November 30th and peaked on December 1st will be included in the discussion of meteorological conditions in December (Section 5.4.1).

Ice Cover: During the first half of November, a period marked by warm temperatures and winds from the southeast and southwest quadrants (Figure 49), the ice edge retreated slightly to the north. This reversal of the southerly advance that occurred in late October is evident from a comparison of Figures 48 and 50.

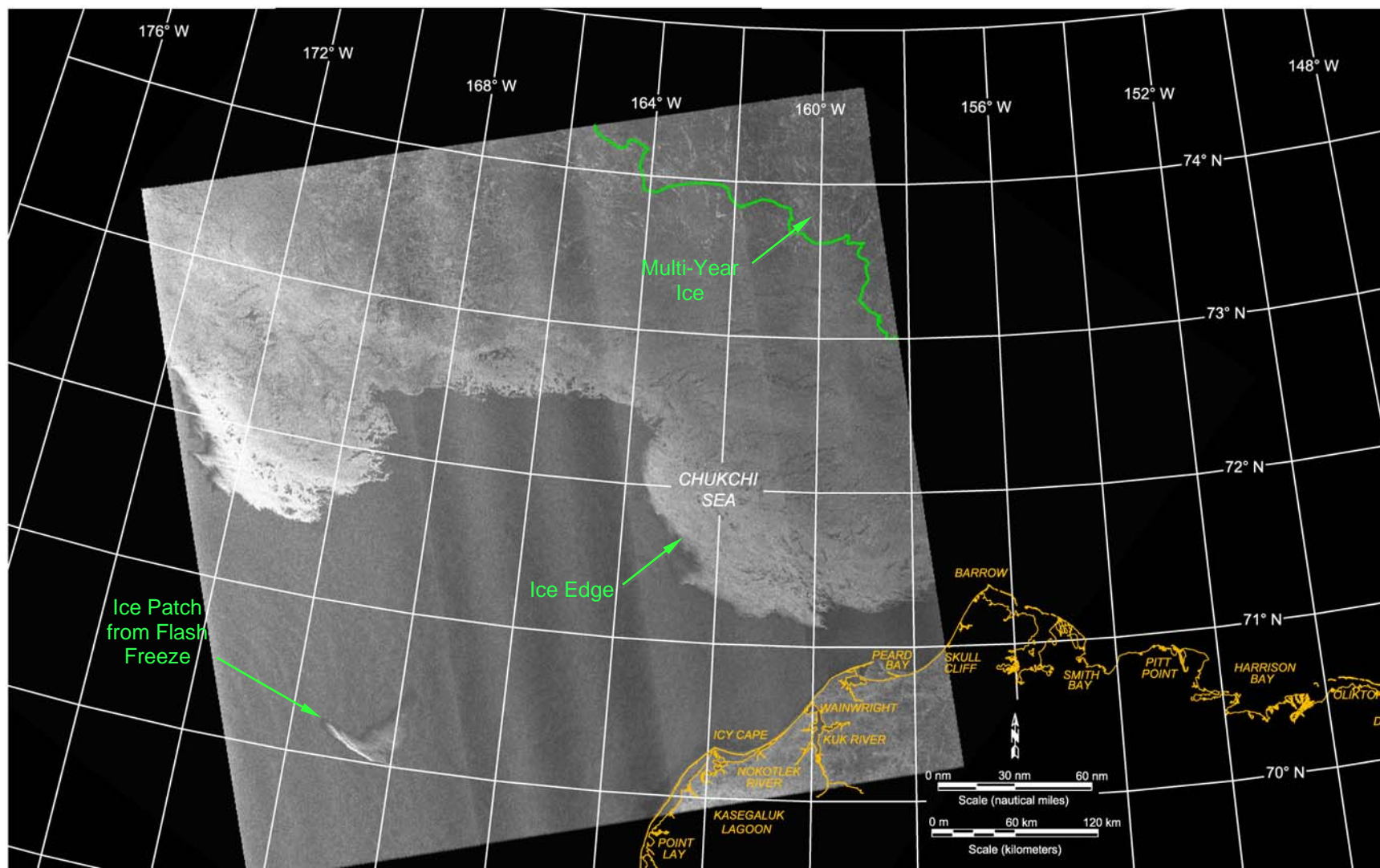
Figure 50 also displays a small patch of ice centered approximately 130 nm (241 km) west of Icy Cape that was created by a flash freeze event. Although much smaller than the patch which formed off Wainwright in October 2013 (Coastal Frontiers and Vaudrey, 2014), it nevertheless marked the second documented occurrence of flash freezing in the Chukchi Sea over the past five freeze-up seasons. Based on an analysis of the NIC ice charts (2014), it probably formed on November 12th when the low temperature at Barrow Airport sank to -3°F (-19°C).

During the second half of the month, the ice edge advanced rapidly to the south under the combined influence of colder air temperatures and winds from the northeast and northwest quadrants (Figure 49). Freeze-up in the nearshore region (defined for the present purpose as the region south of Point Barrow and east of the 163°W meridian, which passes through Point Lay) occurred on or about November 26th, when 697 FDD had accumulated at Barrow Airport.

The progress of freeze-up in each of the four Shell prospects (Hanna Shoal, Burger, Crackerjack, and West) was tracked using a combination of RADARSAT-2 images and NIC ice charts (2014). As shown in Table 14, the southerly advance of the pack ice that occurred in late October produced partial cover in the Hanna Shoal and Burger Prospects between October 22nd and 26th, and in the Crackerjack Prospects between the 26th and 30th. The coverage in these prospects decreased during the first half of November, reflecting the aforementioned retreat of the ice edge. During the third week of the month, however, the resumption of southerly pack ice movement produced complete cover in all four prospects.

Ice Thickness: The calculated thickness of undisturbed first-year ice increased from 18 cm at the beginning of the month to 45 cm at the end (Table 11).

Landfast Ice: In early November, landfast ice began to form in the semi-protected waters of Peard Bay, the Kuk River Inlet, and the Utukok River Inlet (Figure 51). Over the course of the month, the near-even split between easterly and westerly winds produced two extremely narrow, discontinuous strips of such ice: one extending from Barrow to Peard Bay, and a second from Wainwright to the vicinity of Point Lay.



Source: RADARSAT-2 Data and Products © MacDonald Dettweiler and Associates Ltd., 2013 – All Rights Reserved

Figure 50. RADARSAT-2 Image of Chukchi Sea Acquired on November 15, 2013

Table 14. Ice Cover in Shell's Chukchi Sea Prospects during Freeze-Up

Date	Ice Cover (%)			
	Hanna Shoal	Burger	Crackerjack	West
Oct 22 ¹	0	0	0	0
Oct 26 ²	30	30	0	0
Oct 30 ²	100	90	25	0
Nov 2 ²	90	20	0	0
Nov 7 ¹	100	50	0	0
Nov 15 ²	70	0	0	0
Nov 21 ¹	100	100	100	100
Nov 29 ²	100	100	100	100

Notes:

¹ Ice cover is estimated from NIC Ice Chart (2014).

² Ice cover is estimated from RADARSAT-2 image.

Ice Pile-Ups: During the aerial reconnaissance flight conducted on March 30th (Section 3.5), 22 ice pile-ups were observed on the coast of the northeast Chukchi Sea (Table 12; Drawing CFC-917-01-003). Three of these are likely to have formed when the wind shifted from southerly to northeasterly on November 21st and 22nd. Additional information will be provided in Section 5.6.5.

Multi-Year Ice: As in October, multi-year ice remained north of the 72° parallel throughout most of November (Figure 50). At the end of the month, however, a low concentration of multi-year floes moved as far south as the 71°30' parallel in the region between Point Barrow and the 160° meridian. Farther west, the southern boundary turned sharply to the north (Figure 52).

Ice Movement: Multi-year ice floes suitable for tracking first appeared in the RADARSAT-2 images of the Chukchi Sea available to this study in January 2014. As a result, no ice movement data are available for months of November and December.

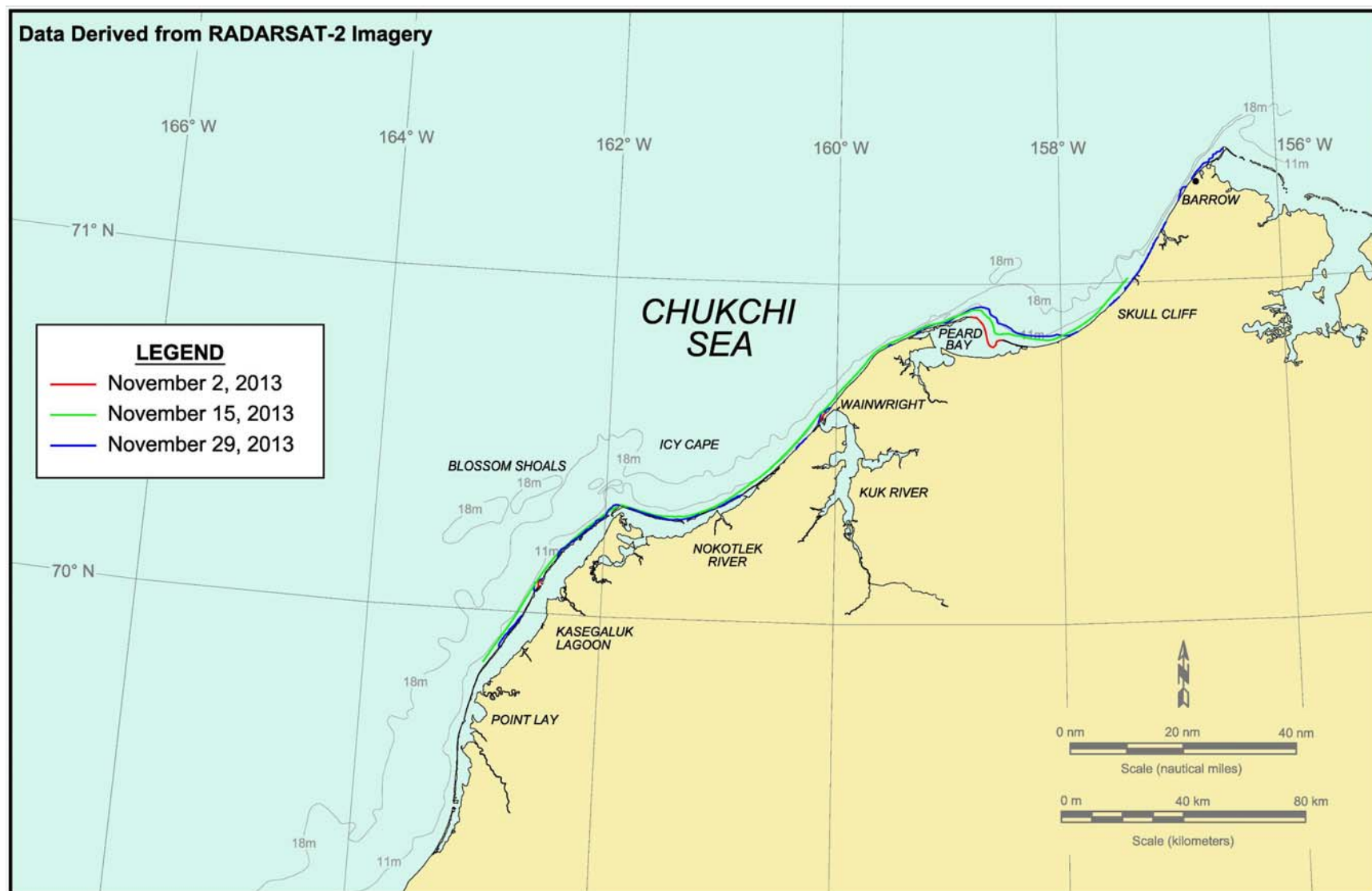
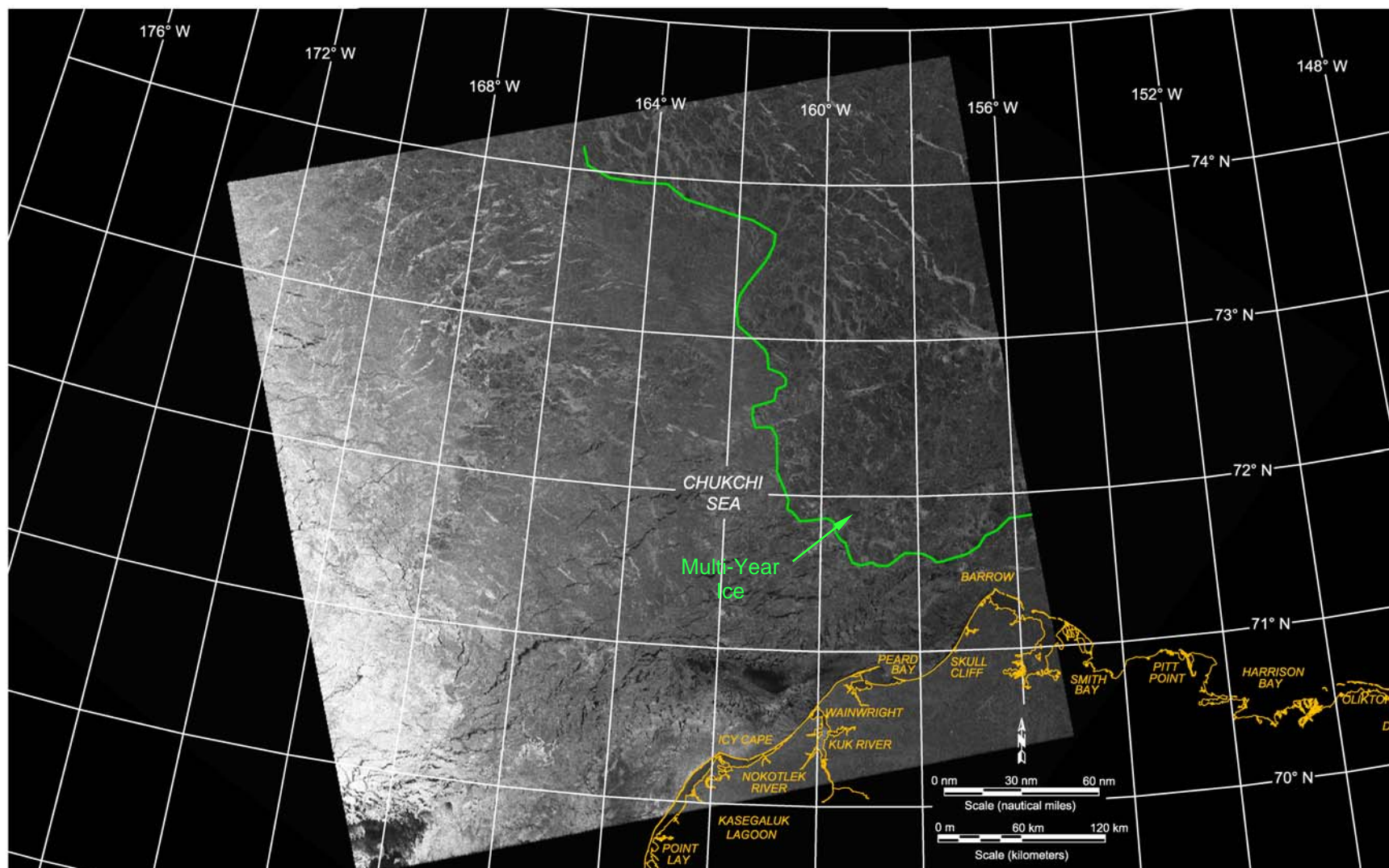


Figure 51. Chukchi Sea Landfast Ice Edge in November 2013



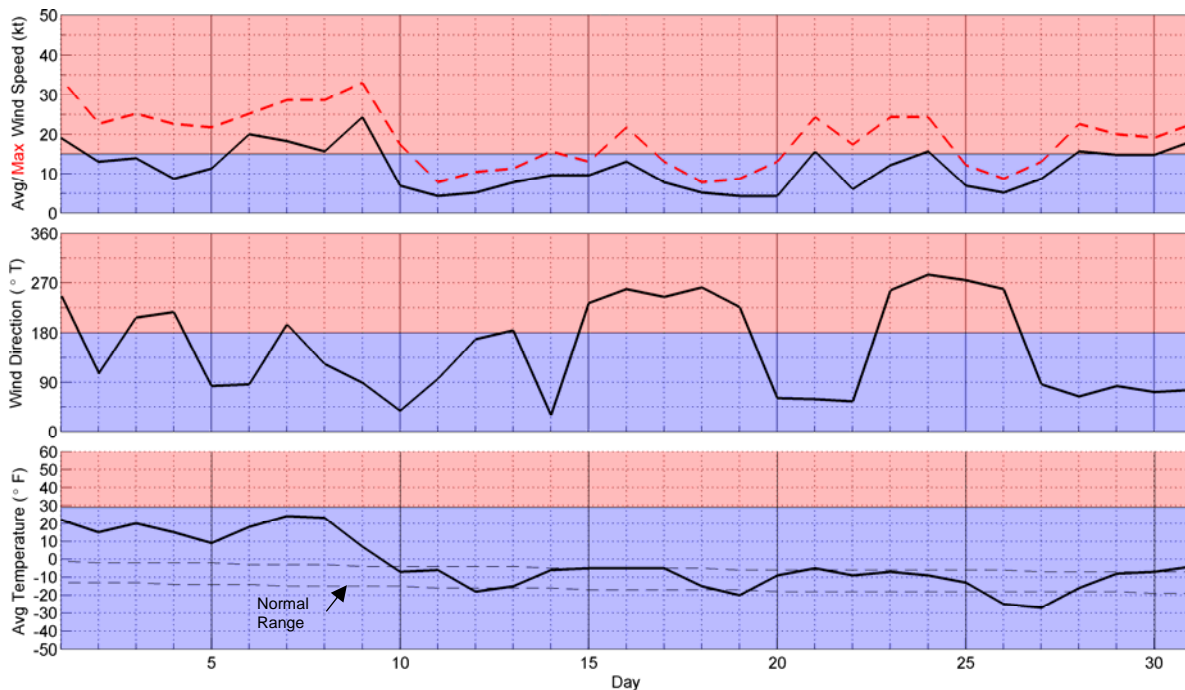
Source: RADARSAT-2 Data and Products © MacDonald Dettweiler and Associates Ltd., 2013 – All Rights Reserved

Figure 52. RADARSAT-2 Image of Chukchi Sea Acquired on November 29, 2013

5.4 Late Freeze-Up

5.4.1 December 2013

Meteorological Conditions: The wind and temperature data recorded at Barrow Airport in December 2013 are provided in Figure 53. During the first nine days of the month, the air temperatures were significantly warmer than normal. They returned to normal on the 10th, and remained close to normal thereafter.



Source: Weather Underground, 2014

Figure 53. Meteorological Conditions at Barrow Airport in December 2013

Continuing the pattern of slight easterly predominance established in November, easterly winds prevailed on 17 of the 31 days in December (Table 9). The average speed decreased from 14 kt (7 m/s) in November to 11 kt (6 m/s) in December. Six storm events, consisting of three easterlies and three westerlies, occurred over the course of the month. As indicated below, all were of short duration:

- Nov 30th-Dec 1st: two-day westerly with maximum speed of 19 kt (10 m/s);
- December 6th: one-day easterly with maximum speed of 20 kt (10 m/s);
- December 7th: one-day westerly with maximum speed of 18 kt (9 m/s);
- December 8th-9th: two-day easterly with maximum speed of 24 kt (12 m/s);
- December 21st: one-day easterly with maximum speed of 16 kt (8 m/s);
- December 24th: one-day westerly with maximum speed of 16 kt (8 m/s).

Ice Cover: From late November until mid-December, complete freeze-up in the region north of Cape Lisburne was delayed by the return of warm air temperatures and winds from the southeast and southwest quadrants (Figure 53). As shown in Figure 54, these conditions produced a tongue of open water that extended as far north as the 71° parallel and as far east as the 164° meridian (within 50 nm or 93 km of Icy Cape). The situation changed rapidly in mid-month, however, when cooler temperatures and light westerly winds produced a rapid expansion of the ice canopy into the remaining area of open water. Based on an analysis of daily AVHRR images (National Weather Service, 2013), complete ice cover in the Chukchi Sea occurred on December 14th (concurrent with the accumulation of 1002 FDDs at Barrow Airport).

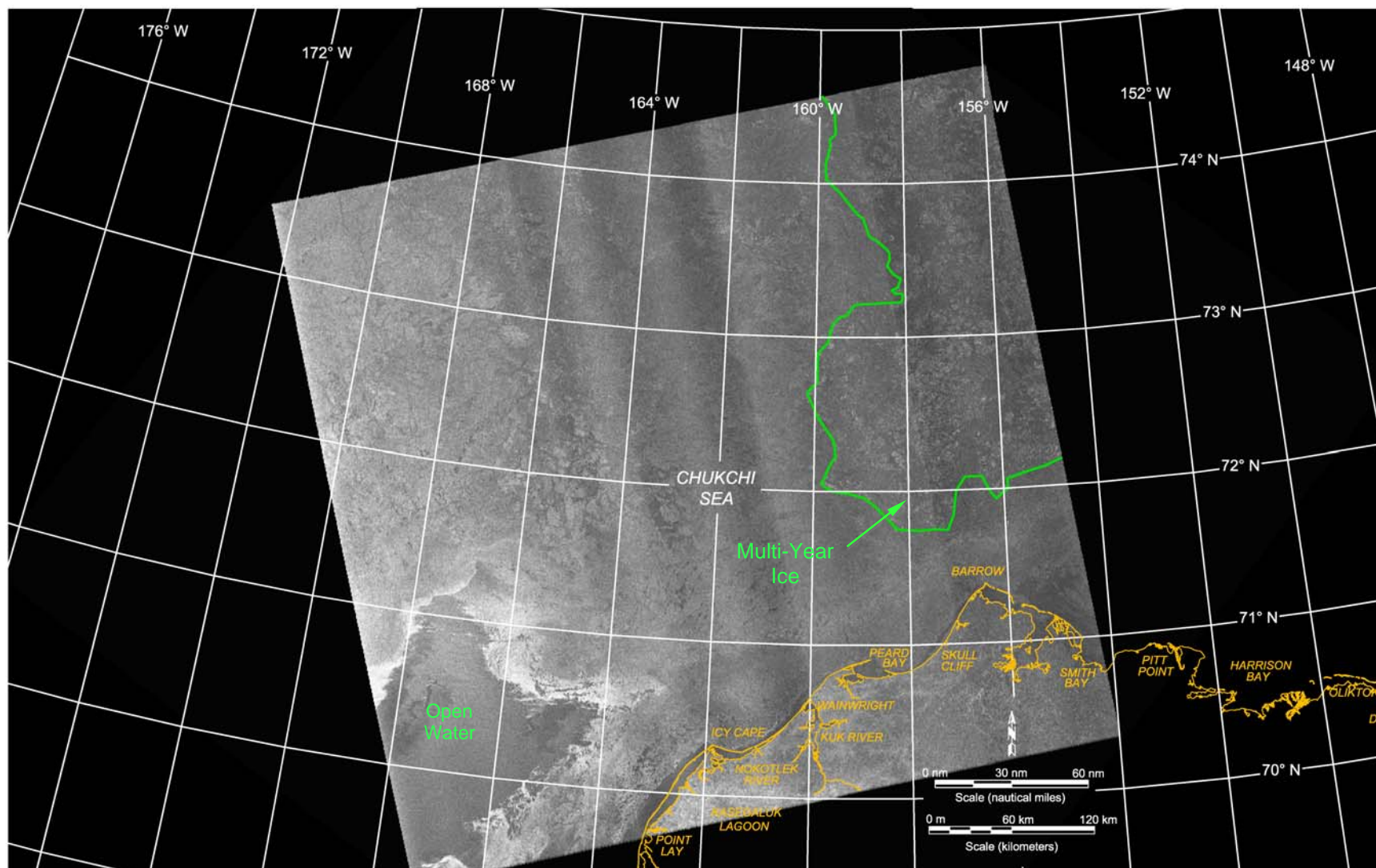
Ice Thickness: The calculated thickness of undisturbed first-year ice increased by 27 cm in December, from 45 to 72 cm.

Landfast Ice: The successive locations of the landfast ice edge were estimated from RADARSAT-2 images obtained on November 29th and December 6th, 13th, and 30th (Figure 55). Reflecting frequent wind shifts and an absence of prolonged westerly storms, the landfast ice zone remained extremely narrow and poorly-developed throughout the month. The sole exception was a significant increase in width to the east of Icy Cape – an expansion that apparently occurred when westward-moving ice became grounded on Blossom Shoals during the sustained easterly storm that began on December 28th (Table 10).

On December 30th, the width of the landfast ice zone was only 0.9 nm (1.7 km) off Barrow and Point Belcher, 0.7 nm (1.3 km) off Wainwright, and 1.0 nm (1.9 km) off Point Lay. To the east of Icy Cape, where the landfast ice was stabilized by Blossom Shoals, the maximum width was 7.8 nm (14.5 km).

Ice Pile-Ups: Nineteen of the 22 pile-ups observed during the aerial reconnaissance flight on March 30th (Section 3.5) are believed to have formed on December 7th, when the winds veered from easterly to westerly and freshened to 18 kt (9 m/s). Additional information will be provided in Section 5.6.5.

Coastal Flaw Lead: Based on analysis of AVHRR imagery (National Weather Service, 2013) and the three RADARSAT-2 images indicated above, the coastal flaw lead was present on twelve of the 25 days in December for which definitive information is available. The frequency of occurrence (48%) is virtually identical to that which occurred a year earlier, in December 2012 (47%; Coastal Frontiers and Vaudrey, 2013).



Source: RADARSAT-2 Data and Products © MacDonald Dettweiler and Associates Ltd., 2013 – All Rights Reserved

Figure 54. RADARSAT-2 Image of Chukchi Sea Acquired on December 6, 2013

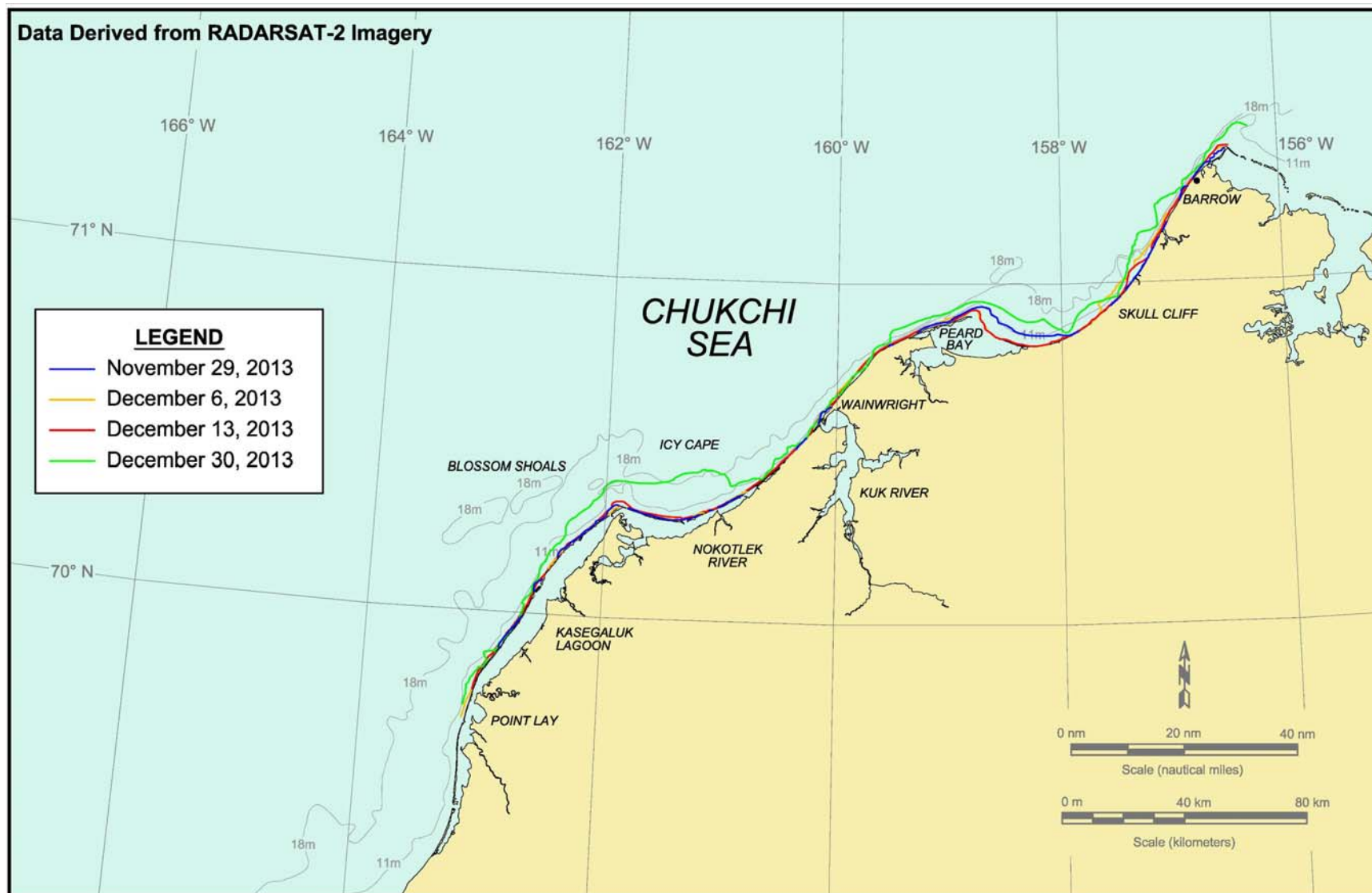
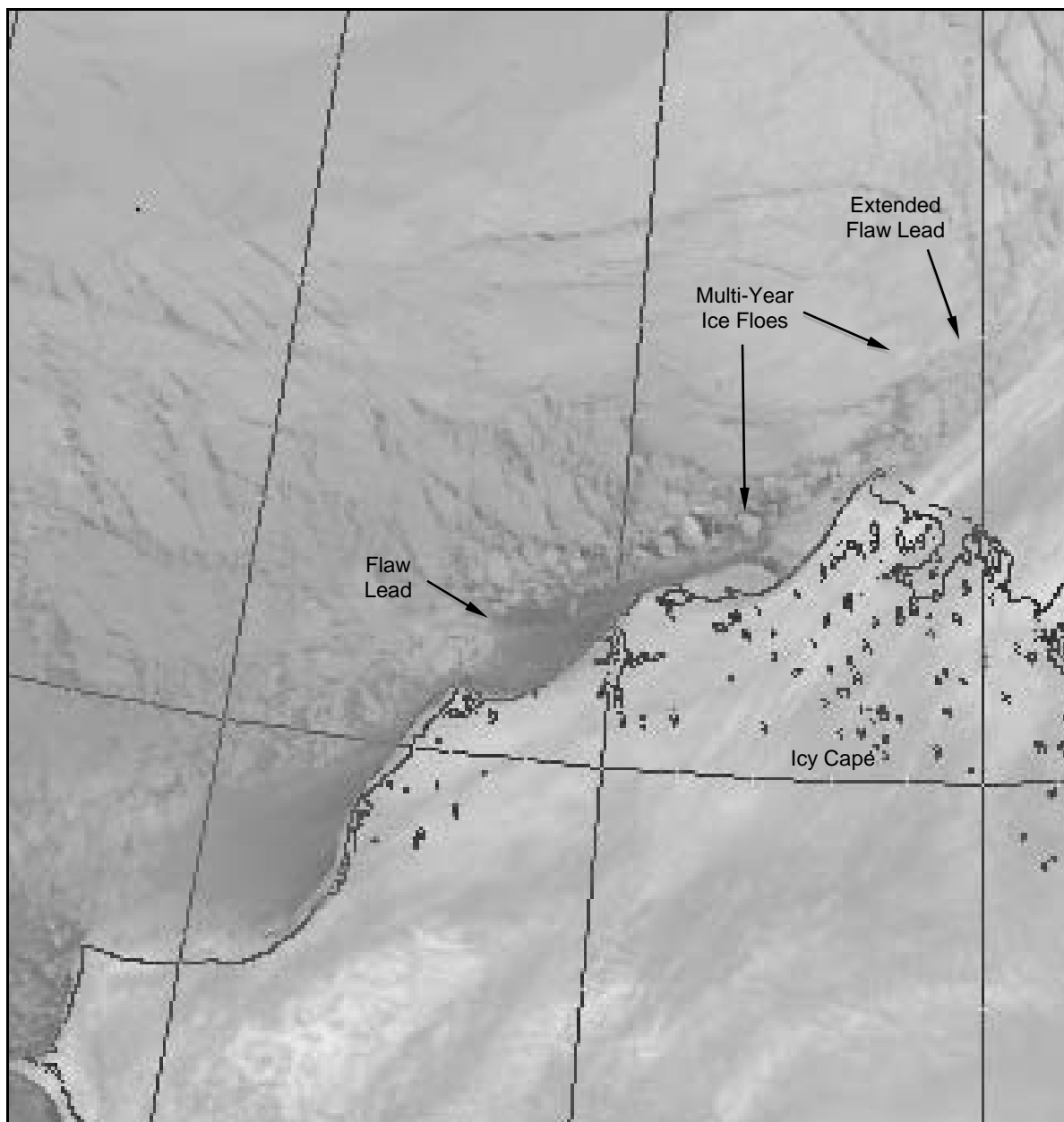


Figure 55. Chukchi Sea Landfast Ice Edge in December 2013

The flaw lead opened on four occasions in December for periods ranging from two to fourteen days (with ten of the fourteen days occurring in January). Its maximum length varied from 50 to 220 nm (93 to 408 km), while its maximum width varied from 12 to 60 nm (22 to 111 km). Figure 56 shows the lead that developed in response to a brief easterly storm on December 21st, and that produced the maximum dimensions noted in December (220 nm long and up to 12 nm wide).



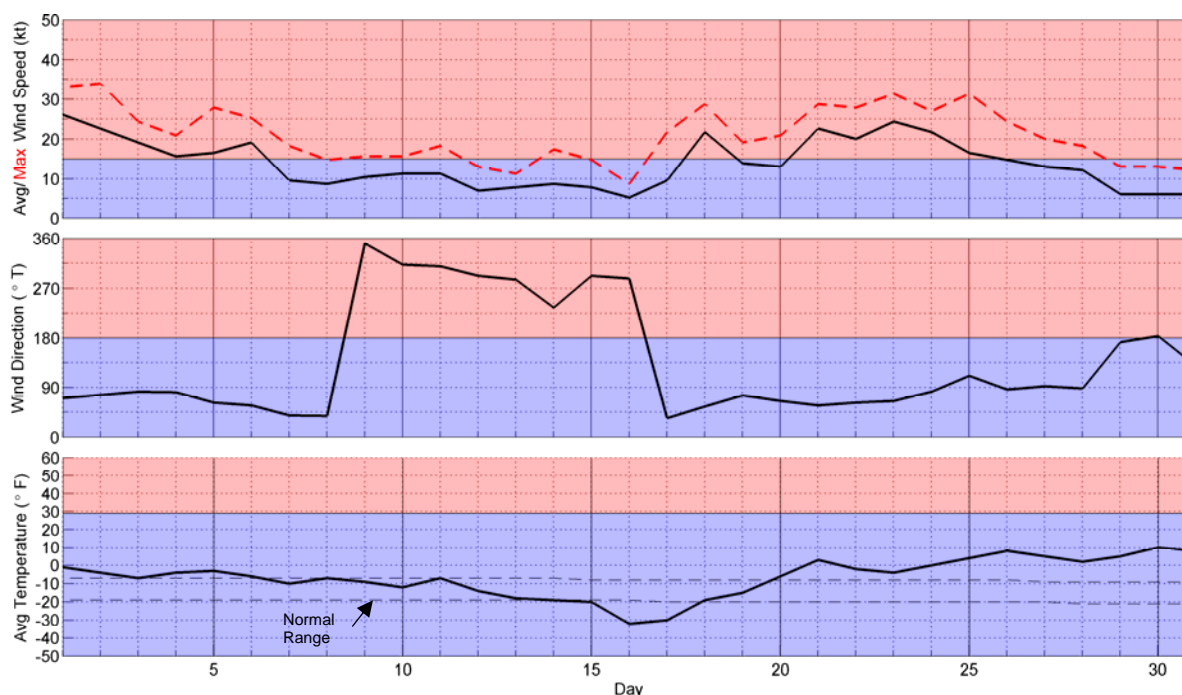
After: National Weather Service, 2014

Figure 56. AVHRR Image of Chukchi Sea Acquired on December 23, 2013

Multi-Year Ice: As in October and November, multi-year ice remained north of Point Barrow during the first three weeks of December. On December 23rd and again from December 30th through January 3rd, however, the flaw lead extended northeast of Point Barrow to such an extent that it intersected the southern boundary of the multi-year ice and channeled multi-year floes into the region south and west of Point Barrow (Figure 56). This cause-and-effect relationship between the extended flaw lead and multi-year ice invasions was first identified during the 2011-12 Freeze-Up Study (Coastal Frontiers and Vaudrey, 2012).

5.4.2. January 2014

Meteorological Conditions: Figure 57 presents the wind and temperature data recorded at Barrow Airport in January 2014. The air temperatures remained near normal during the first half of the month, dropped below normal for three days at mid-month, and then rose above normal for the last eleven days.



Source: Weather Underground, 2014

Figure 57. Meteorological Conditions at Barrow Airport in January 2014

Easterly winds prevailed more than 70 % of the time, occurring on 22 of the 31 days (Table 9). The westerlies tended to be light, and with one exception were confined to the period between the 9th and 16th. The easterlies were much stronger, producing an average monthly speed of 14 kt (7 m/s). Storm activity consisted of the following three events, two of which were of long duration:

- Dec 28th-Jan 6th : ten-day easterly with maximum speed of 26 kt (13 m/s);
- January 18th: one-day easterly with maximum speed of 22 kt (11 m/s);
- January 21st-25th: five-day easterly with maximum speed of 24 kt (12 m/s).

Ice Thickness: The calculated ice thickness increased from 72 cm at the beginning of the month to 96 cm at the end.

Landfast Ice: Figure 58 illustrates the locations of the landfast ice edge derived from RADARSAT-2 images obtained on December 30th and January 9th, 20th, and 26th. Between December 30th and January 9th, a period dominated by the ten-day easterly storm, the already-narrow landfast ice zone became even narrower and disappeared completely in some areas. A modest rebound followed between the 9th and 20th in response to light westerly winds, but the gain was quickly erased by the prolonged easterly storm that followed. On January 26th, one day after the storm ended, virtually all of the landfast ice to the north of the Nokotlek River Mouth had been removed. Farther west, in the vicinity of Icy Cape, a band of landfast ice up to 5 nm (9.3 km) remained aground on Blossom Shoals.

Coastal Flaw Lead: Of the 29 days for which useful data were identified, the coastal flaw lead was found to be present on 20 – a 69% frequency of occurrence. This high frequency, the largest recorded during the study, is consistent with the strong predominance of easterly winds that occurred in January (Figure 57).

The lead remained open from December 28th through January 10th, closed on the 11th in response to westerly winds, reopened on or about the 19th (Figure 59), and closed again on or about the 30th in response to light southerly winds. Its maximum length in January was 210 nm (389 km), while its maximum width was 60 nm (111 km).

Multi-Year Ice: As discussed above in Section 5.4.1, the multi-year ice invasion of the region south and west of Point Barrow that began on December 30th continued through January 3rd. A similar invasion took place from the 7th through 10th, when the flaw lead extended to the northeast, intersected the southern boundary of the multi-year ice in the vicinity of the 72° parallel, and diverted multi-year floes to the southwest (Figure 60).

Yet another invasion began on January 18th or 19th in response to an extended flaw lead that resulted from the easterly storm on the 18th (Table 10). As shown in Figure 59, the result was a significant southerly displacement of the discernible multi-year ice edge into the region south and west of Point Barrow. In contrast to the prior invasions, which were short-lived, this one persisted for the remainder of the study period (through the end of March).

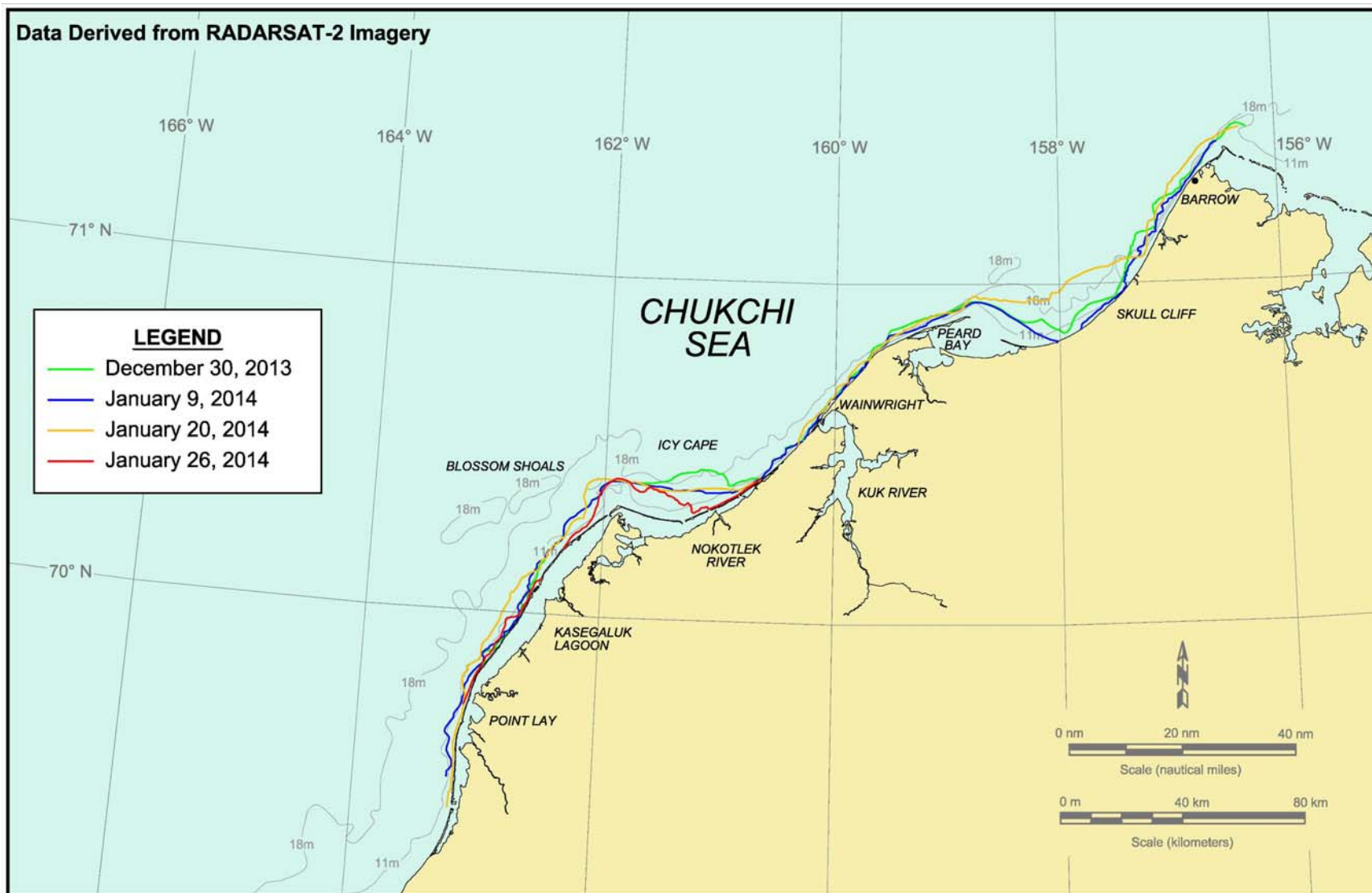
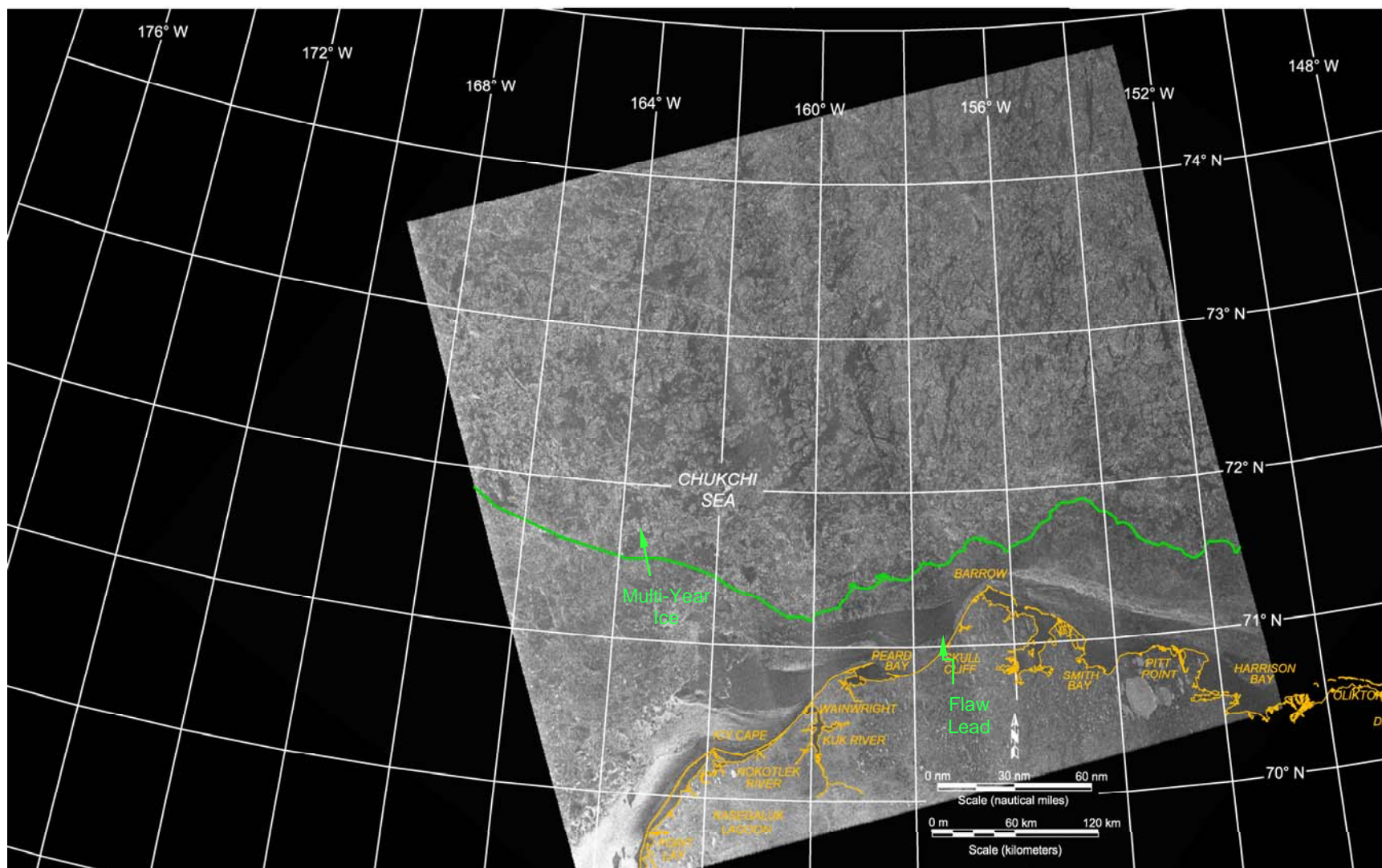
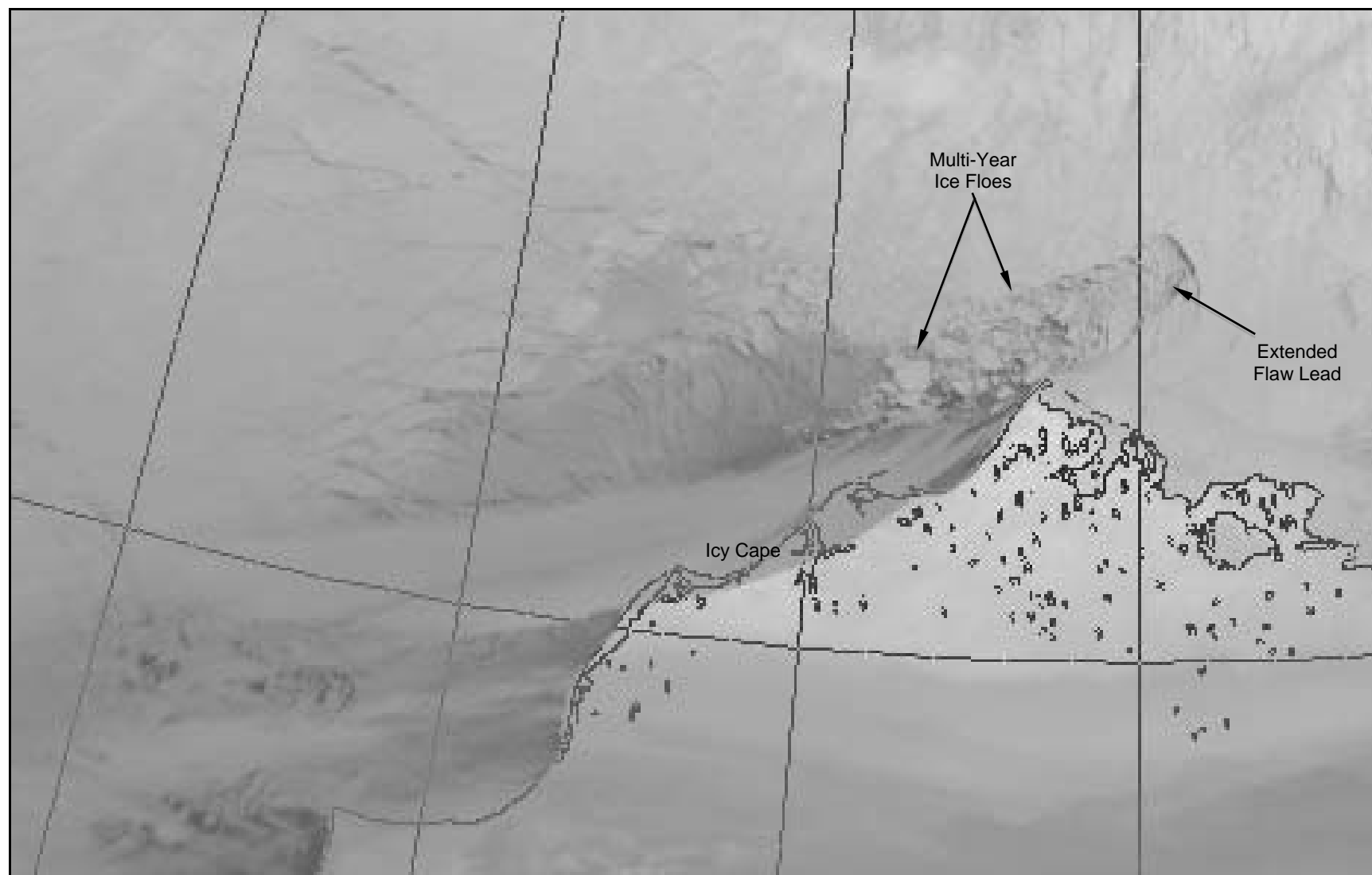


Figure 58. Chukchi Sea Landfast Ice Edge in January 2014



Source: RADARSAT-2 Data and Products © MacDonald Dettweiler and Associates Ltd., 2014 – All Rights Reserved

Figure 59. RADARSAT-2 Image of Chukchi Sea Acquired on January 20, 2014



After: National Weather Service, 2014

Figure 60. AVHRR Image of Chukchi Sea Acquired on January 7, 2014

Ice Movement: Floes B and E, which had been identified previously in the Beaufort, entered the Chukchi in late December or early January. Both were tracked in the Chukchi using the RADARSAT-2 images obtained on January 9th, 20th, and 26th, with the resulting trajectories shown in Figure 61.

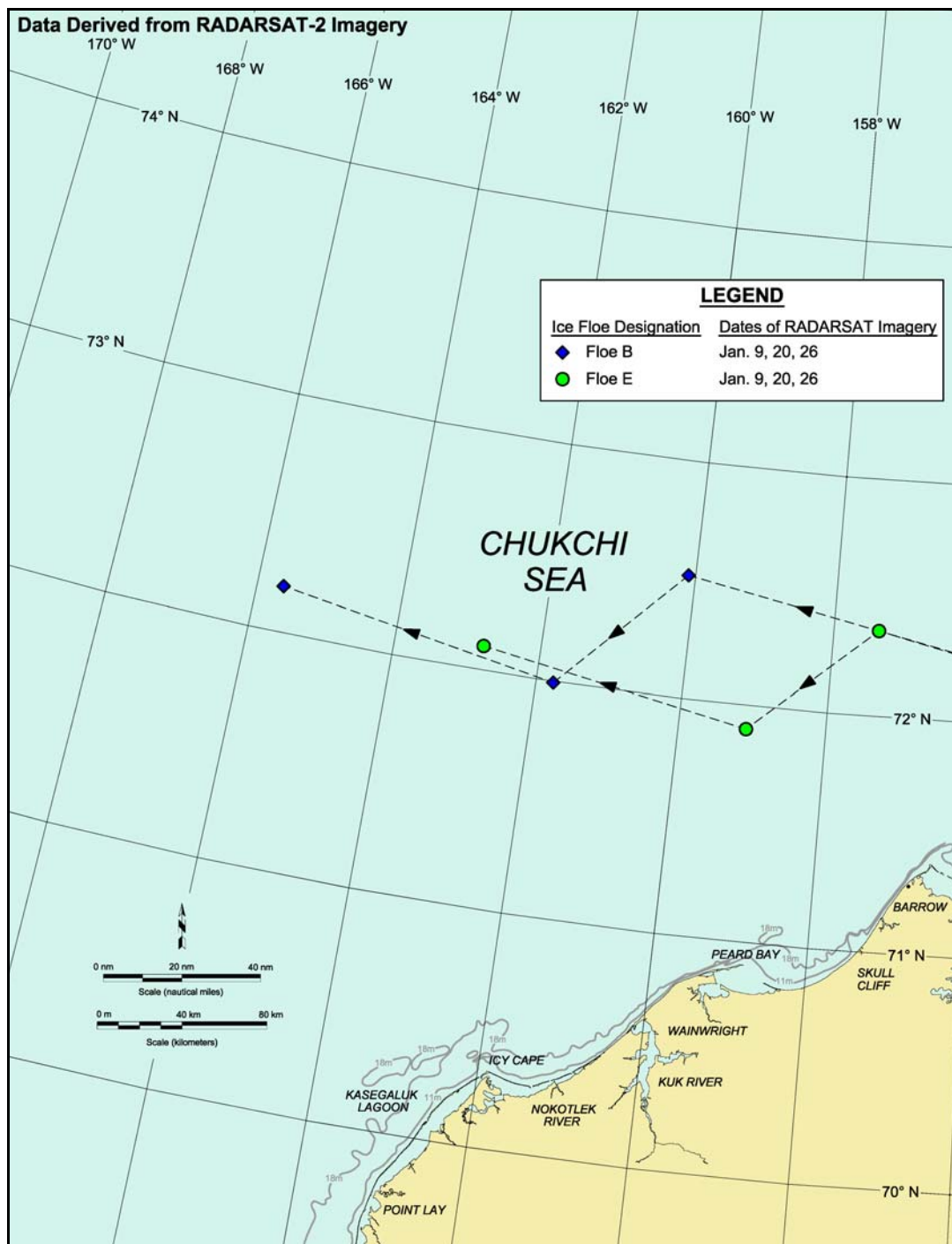


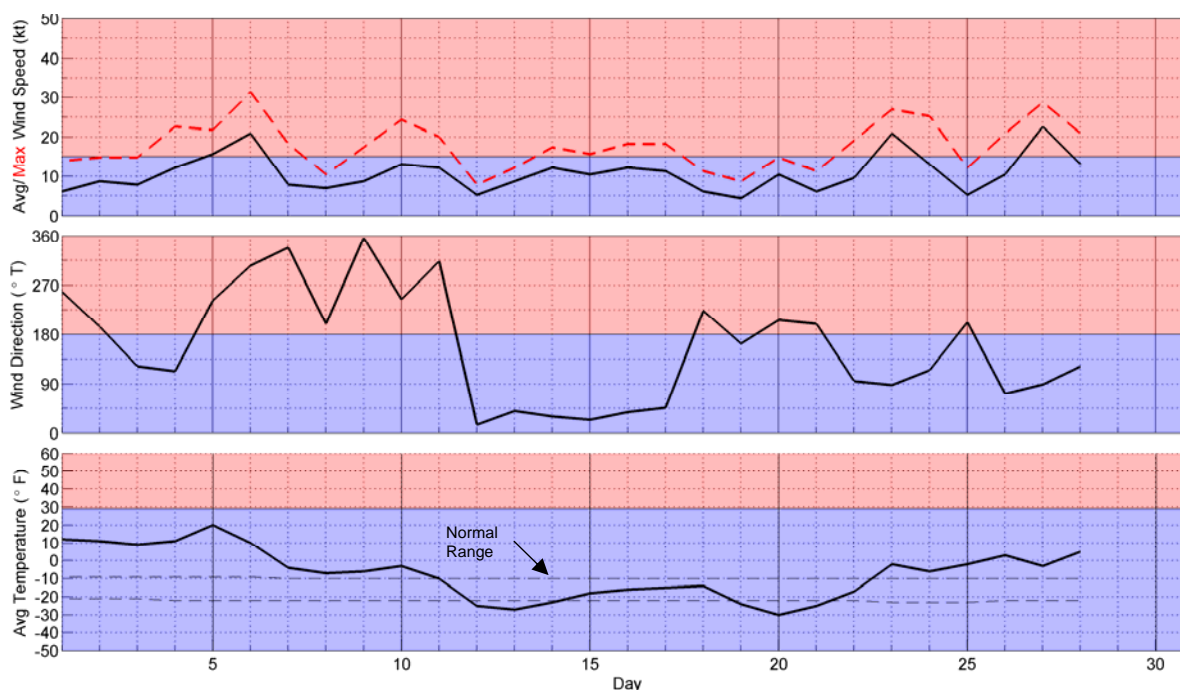
Figure 61. Chukchi Sea Multi-Year Ice Floe Displacements in January 2014

Between January 9th and 20th, a period dominated by light westerly winds but also containing a one-day easterly storm, both floes experienced modest displacements to the southwest at average speeds of about 4.0 nm/day (7.4 km/day). Rapid movement to the west-northwest followed between the 20th and 26th in response to the five-day easterly storm that prevailed from the 21st through 25th (Table 10). The floes attained speeds of 12.1 and 11.7 nm/day (22.4 and 21.7 km/day for Floes B and E, respectively) – the maximum values measured in the Chukchi during the study period. The average monthly speeds, computed on the basis of the net displacements between January 9th and 26th, were 6.1 nm/day (11.3 km/day) for Floe B and 5.9 nm/day (10.9 km/day) for Floe E.

5.5 Midwinter

5.5.1. February 2014

Meteorological Conditions: Wind and temperature data recorded at Barrow Airport in February 2014 are presented in Figure 62. The daily average air temperatures were unseasonably warm during the first ten days of the month, normal to slightly below normal during the next twelve days, and unseasonably warm again during the last six days.



Source: Weather Underground, 2014

Figure 62. Meteorological Conditions at Barrow Airport in February 2014

Easterly winds prevailed over westerlies by a narrow margin of 15 days to 13 days (Table 9). The average speed for the month, 11 kt (6 m/s), was 3 kt (2 m/s) lower than in

January. The storm population consisted of three events of shore duration, including the only westerly to occur after December 24th (Table 10):

- February 5th-6th: two-day westerly with maximum speed of 21 kt (11 m/s);
- February 23rd: one-day easterly with maximum speed of 21 kt (11 m/s);
- February 27th: one-day easterly with maximum speed of 23 kt (12 m/s).

Ice Thickness: The calculated ice thickness at the end of the month was 114 cm, representing 18 cm more than at the beginning.

Landfast Ice: Figure 63 presents the locations of the landfast ice edge derived from RADARSAT-2 images obtained on January 26th and February 16th and 26th. During the first of these two intervals, winds from the west and north-northeast re-established a continuous band of landfast ice from Barrow to Point Lay. The most significant change, an advance of up to 20 nm (37 km) in the embayment between Barrow and Point Franklin, probably occurred when ice moving to the southwest encountered Point Franklin during the north-northeasterly winds that began on the 12th. A similar but smaller increase (up to 10 nm or 19 km) occurred to the east of Icy Cape as a result of ice being trapped by Blossom Shoals.

During the second interval, from February 16th to the 26th, easterly winds and an easterly storm reversed most of the gains between Barrow and Point Franklin. South of Point Franklin, however, the landfast ice edge experienced only minor changes, suggesting that the ice had become sufficiently well-grounded to resist displacement.

Coastal Flaw Lead: Useful satellite images pertaining to the coastal flaw lead were identified for 26 days in February. The lead was present on sixteen days, representing a 62% frequency of occurrence. One-day openings occurred on the 4th and 9th, followed by an extended opening from February 15th through March 1st. The maximum length of 250 nm (463 km) occurred during the second and third openings and encompassed the entire stretch of coast between Point Barrow and Cape Lisburne. The maximum width of 100 nm (185 km), which occurred during the third opening, caused the lead to cover all of the Burger and Crackerjack Prospects and parts of the Hanna Shoal and West Prospects.

Multi-Year Ice: Multi-year ice persisted in the region to the south and west of Point Barrow throughout the month of February. Aided by another invasion that resulted from an extension of the flaw lead in mid-February (Figure 64), multi-year floes advanced farther to the south and closer to shore over the course of the month (Figure 65).

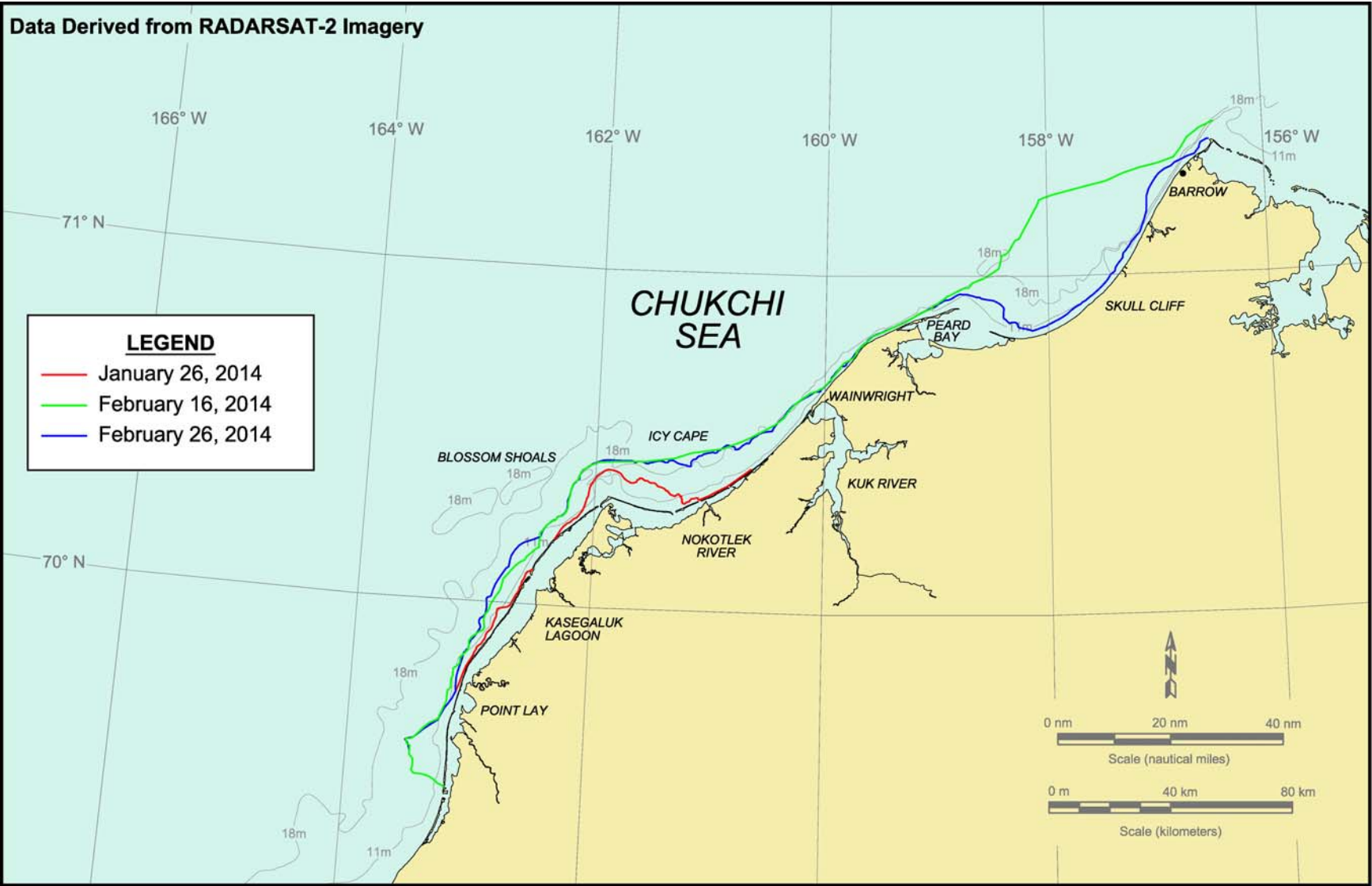
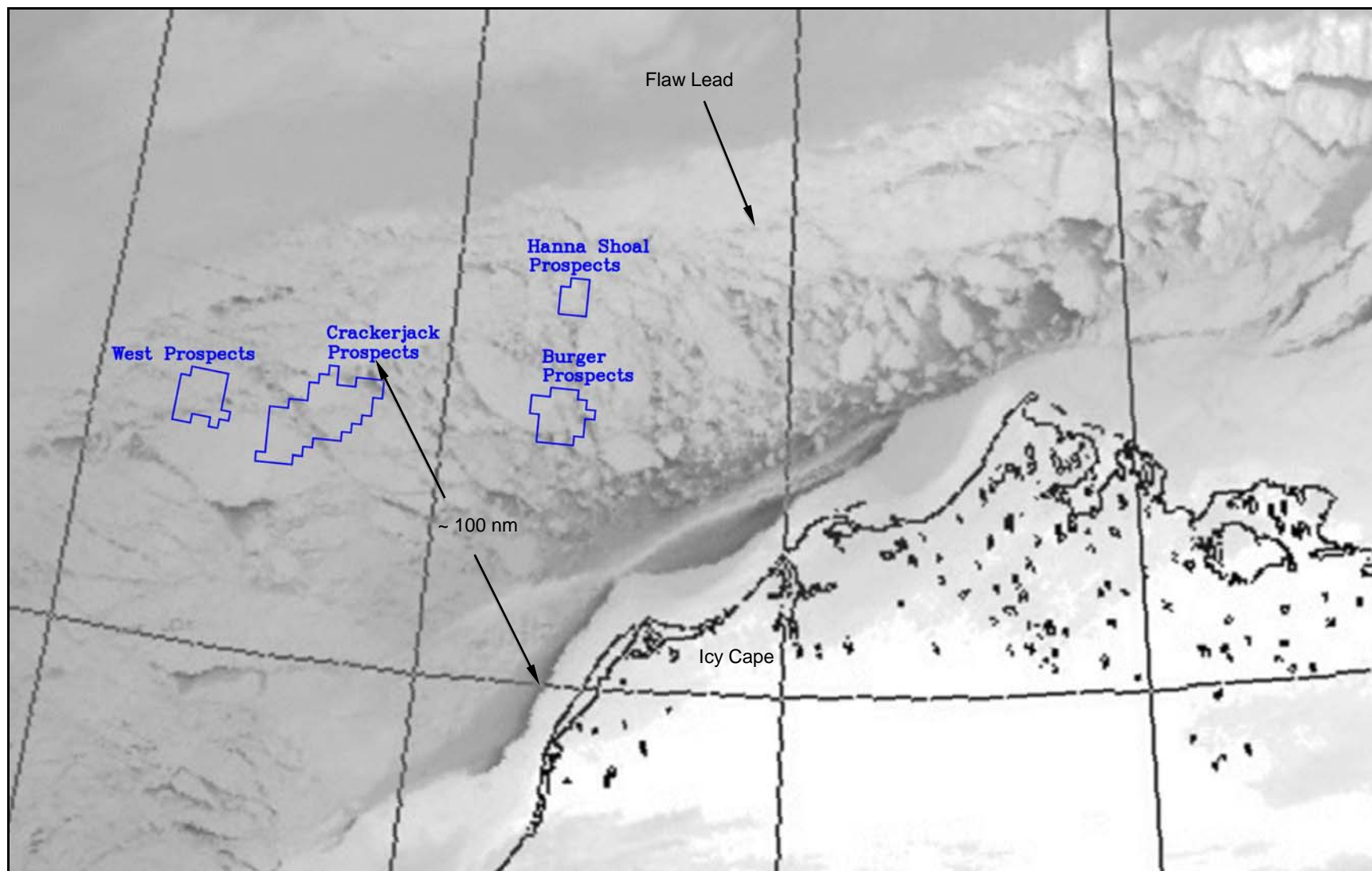
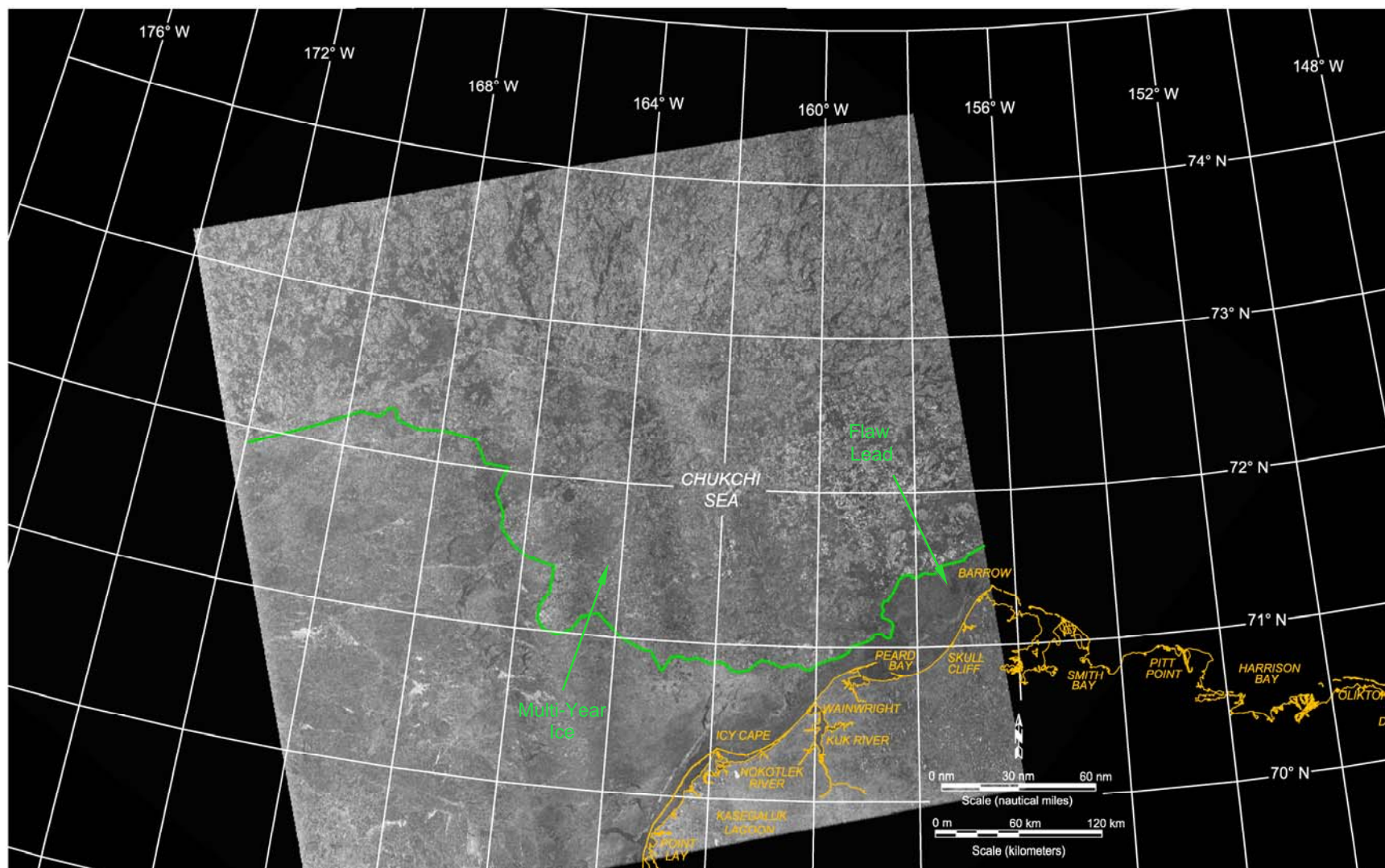


Figure 63. Chukchi Sea Landfast Ice Edge in February 2014



After: National Weather Service, 2014

Figure 64. AVHRR Image of Chukchi Sea Acquired on February 17, 2014



Source: RADARSAT-2 Data and Products © MacDonald Dettweiler and Associates Ltd., 2014 – All Rights Reserved

Figure 65. RADARSAT-2 Image of Chukchi Sea Acquired on February 26, 2014

Ice Movement: Ice movement rates were investigated using four multi-year floes that had been tracked previously in the Beaufort: Floe E, which entered the Chukchi in late December or early January (Section 5.4.2), and Floes C, D, and F, all of which entered the Chukchi in mid-February. The successive positions of these floes (Figure 66) were derived from RADARSAT-2 images acquired on January 26th (Floe E), February 16th (Floes C and E), February 18th (Floes D and F), and February 26th (all floes).

Between January 26th and February 16th, a period containing a near-equal split between easterly and westerly winds and a two-day westerly storm, Floe E experienced a net displacement of 19 nm (35 km) to the north. The average speed was only 0.9 nm/day (1.7 km/day). Subsequently, from the 16th/18th through the 26th, easterly winds along with a one-day easterly storm caused all four floes to move to the west at speeds that ranged from 2.2 to 4.7 nm/day (4.1 to 8.7 km/day). In the case of Floe E, the only feature tracked for more than sixteen days in February, the average monthly speed was a meager 1.0 nm/day (1.9 km/day).

Additional information on ice movement was obtained from telemetry buoys installed on three multi-year floes by the IABP (Section 3.4). Their tracks, which are plotted in Figure 67 based on the positions reported at midnight of each day, cover the brief period between installation on February 26th and month-end. On the 27th, when an easterly storm produced a daily average wind speed of 23 kt (12 m/s) at Barrow Airport, all three floes moved to the northwest at identical speeds of 0.72 kt (0.37 m/s). The associated wind factor, 3.1%, suggests that the floes were relatively unconstrained by the surrounding ice and therefore located in or adjacent to the flaw lead. The following day, 13-kt (7-m/s) southeasterly winds pushed the floes to the north at speeds that averaged 0.20 kt (0.10 m/s).

5.5.2. March 2014

Meteorological Conditions: Figure 68 presents the wind and temperature data recorded at Barrow Airport in March. The air temperatures exceeded the normal range on nineteen days, fell within the normal range on eleven days, and dropped below the normal range on only one day (March 10th).

Westerly winds occurred during the first nine days of the month, but easterlies prevailed thereafter. The end result was easterly predominance for the sixth consecutive month, with easterlies on nineteen days and westerlies on twelve (Table 9). The speeds remained low, with no storms and an average monthly value of only 8 kt (4 m/s).

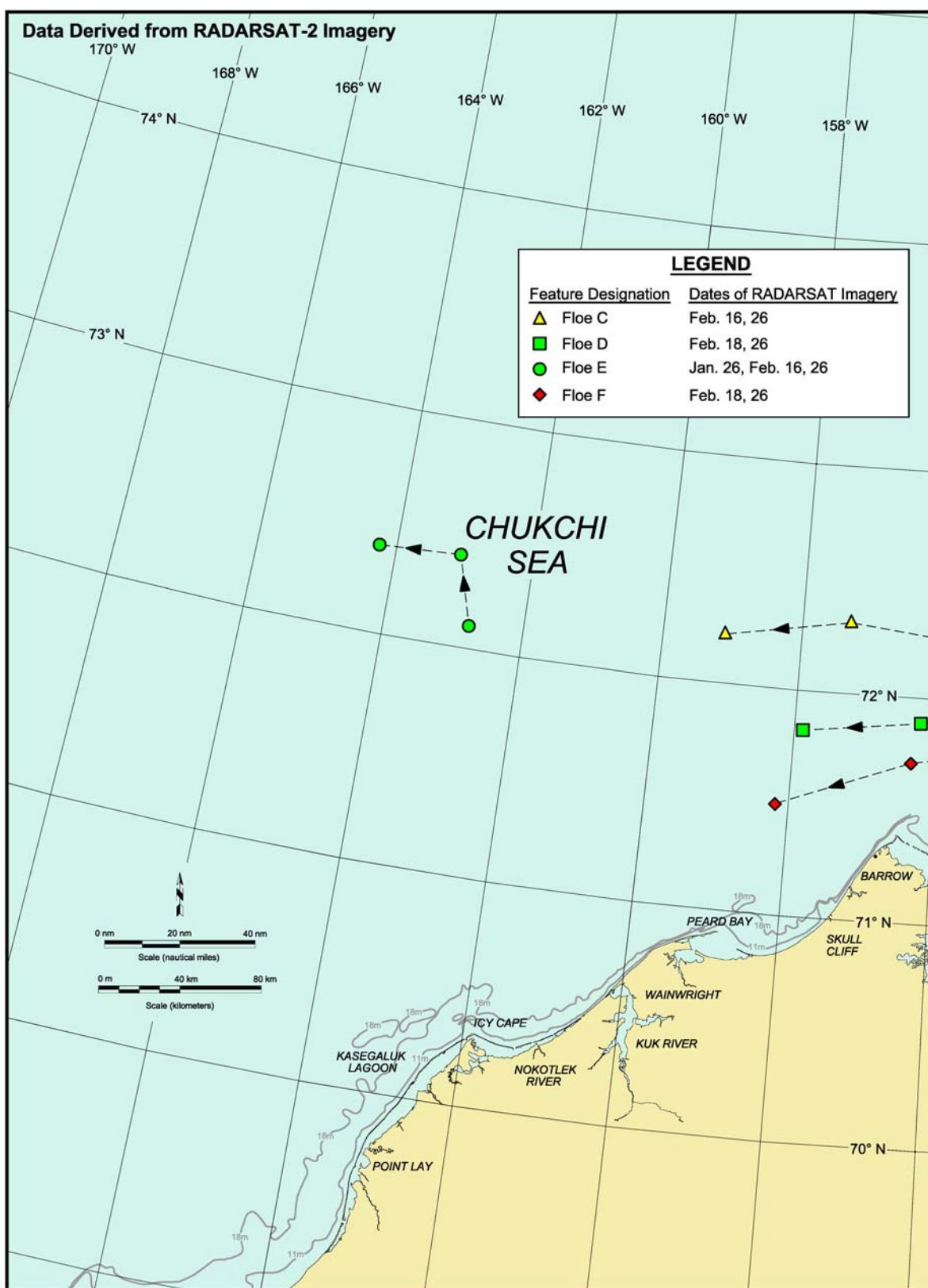


Figure 66. Chukchi Sea Multi-Year Ice Floe Displacements in February 2014

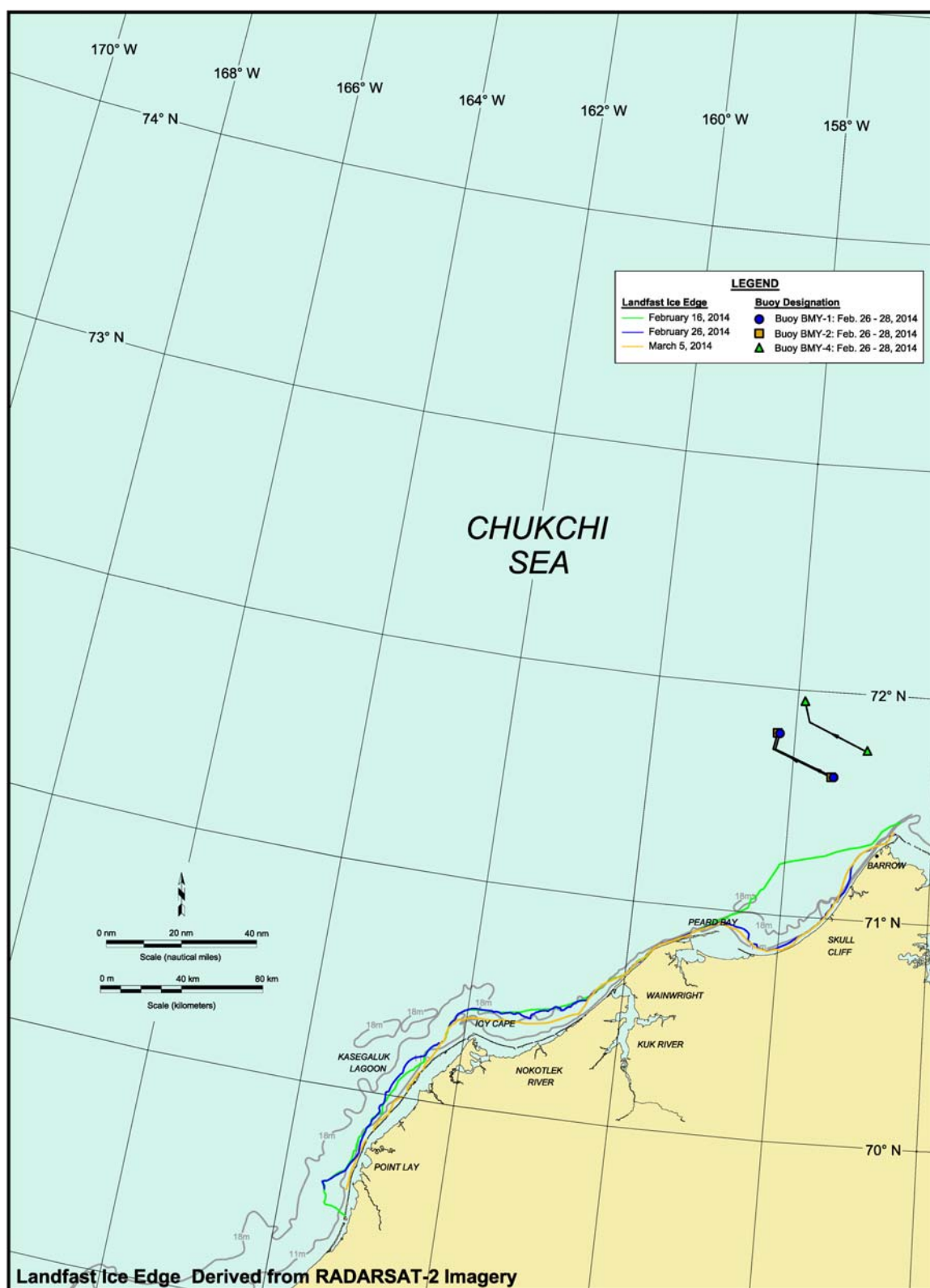
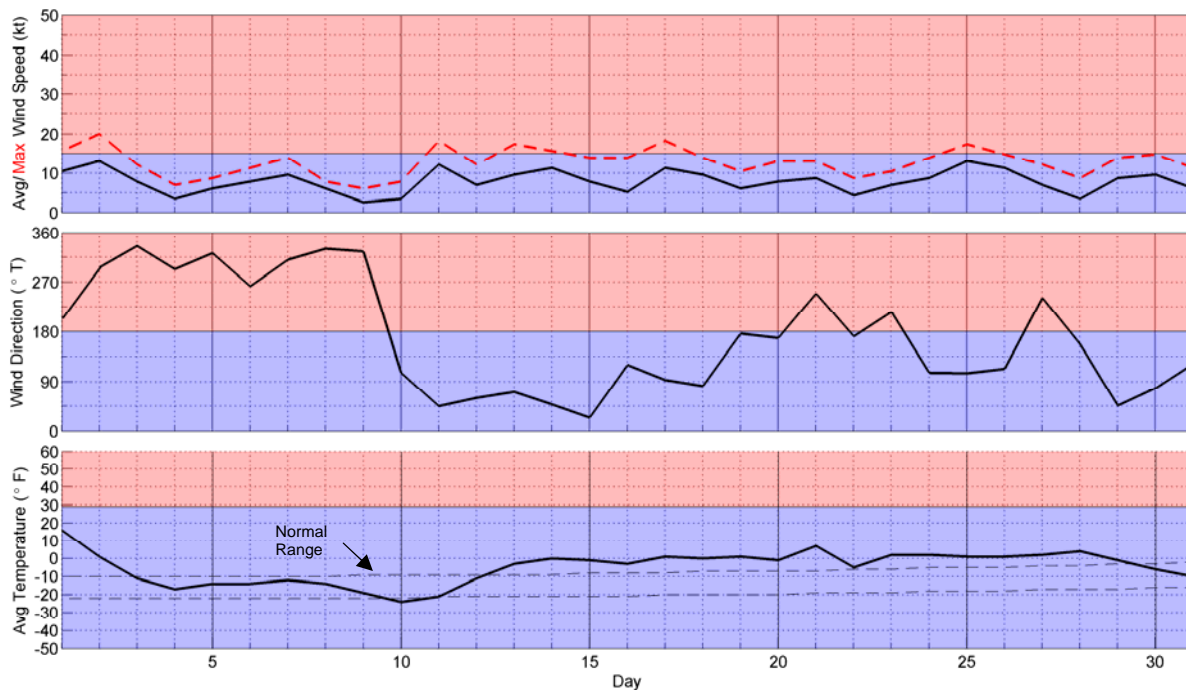


Figure 67. Chukchi Sea Landfast Ice Edge and Telemetry Buoy Tracks in February 2014



Source: Weather Underground, 2014

Figure 68. Meteorological Conditions at Barrow Airport in March 2014

Ice Thickness: The calculated thickness of undisturbed first-year ice at the end of March was 131 cm, an increase of 17 cm over the course of the month. The calculation was based on an accumulation of 4,945 FDD since the beginning of the freeze-up season. By comparison, the calculated ice thickness for the Beaufort (141 cm) was about 8% greater, based on 5,637 FDD.

Because the landfast ice zone was disturbed repeatedly during the freeze-up season by the opening and closing of the coastal flaw lead, much of the ice in this region probably failed to attain the calculated thickness of 131 cm at the end of March. Areas where the full thickness is likely to have developed include the protected waters of Kasegaluk Lagoon and Peard Bay.

Landfast Ice: Changes in the landfast ice zone that occurred between February 26th and March 29th are illustrated in Figure 69. Between February 26th and March 5th, the ice edge retreated off Peard Bay and on both sides of Icy Cape in response to the easterly storm that took place on February 27th. A substantial advance of up to 18 nm (34 km) followed between March 5th and 12th, a period dominated by light to moderate westerly winds. The advance occurred between Point Barrow and Blossom Shoals, producing an ice edge that approximated a straight line between these two points.

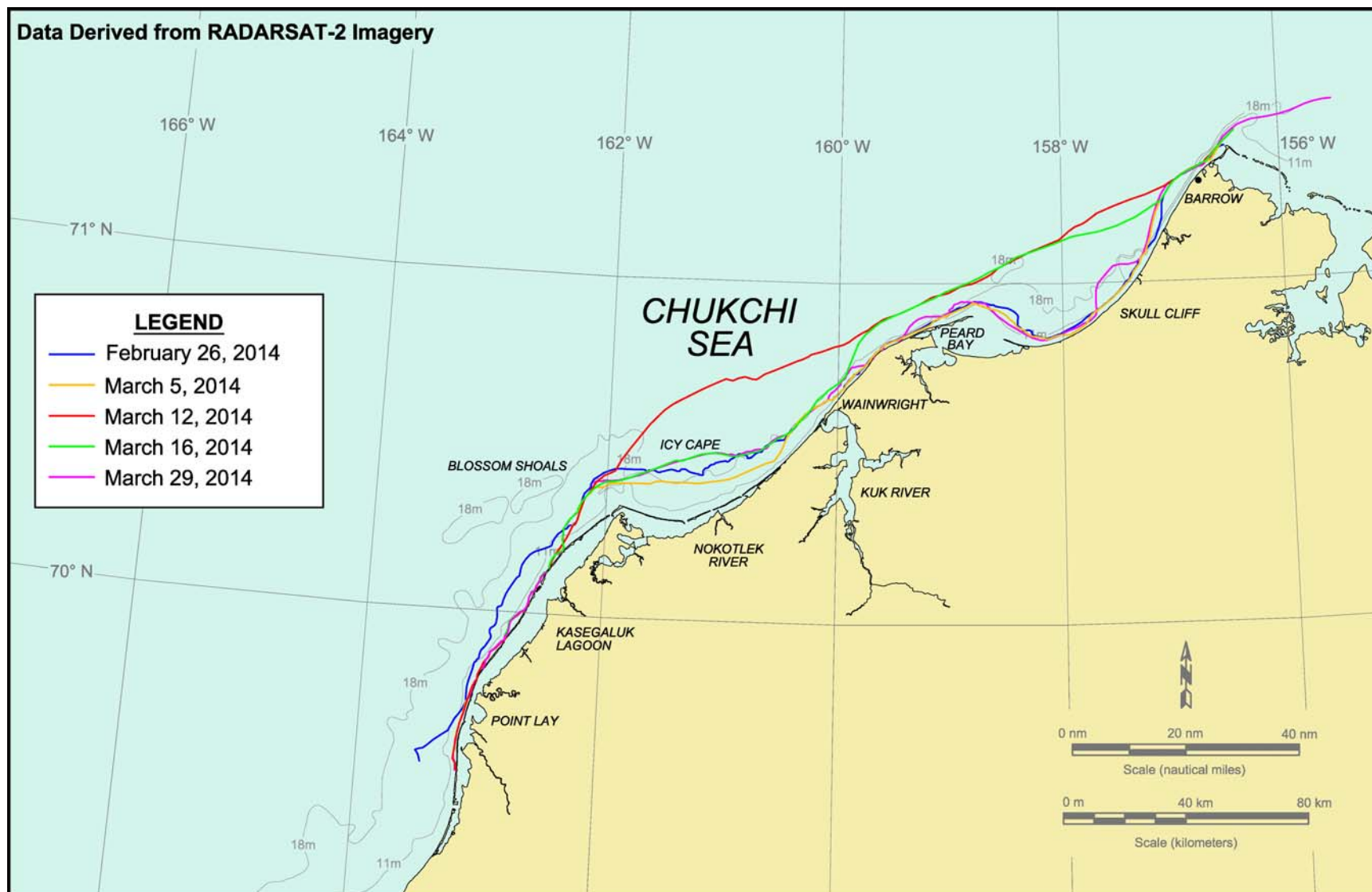


Figure 69. Chukchi Sea Landfast Ice Edge in March 2014

From the 12th to the 29th, a strong predominance of easterly winds removed most of the temporary landfast ice that had accumulated during the prior week. At month-end, the landfast ice zone between Point Barrow and Point Lay consisted of a continuous strip that was particularly narrow between Skull Cliff and Peard Bay, at Point Belcher, and from 15 nm (28 km) southwest of Icy Cape to Point Lay. The maximum width of 10 nm (18.5 km) was located to the east of Icy Cape, in the region stabilized by the ice grounded on Blossom Shoals.

Coastal Flaw Lead: Based on an analysis of satellite images covering all 31 days in March, the coastal flaw lead was open on three occasions:

- March 1st: continuation of the opening that began on February 15th;
- March 12th-18th: continuous easterly winds;
- March 25th-31st: predominance of easterly winds.

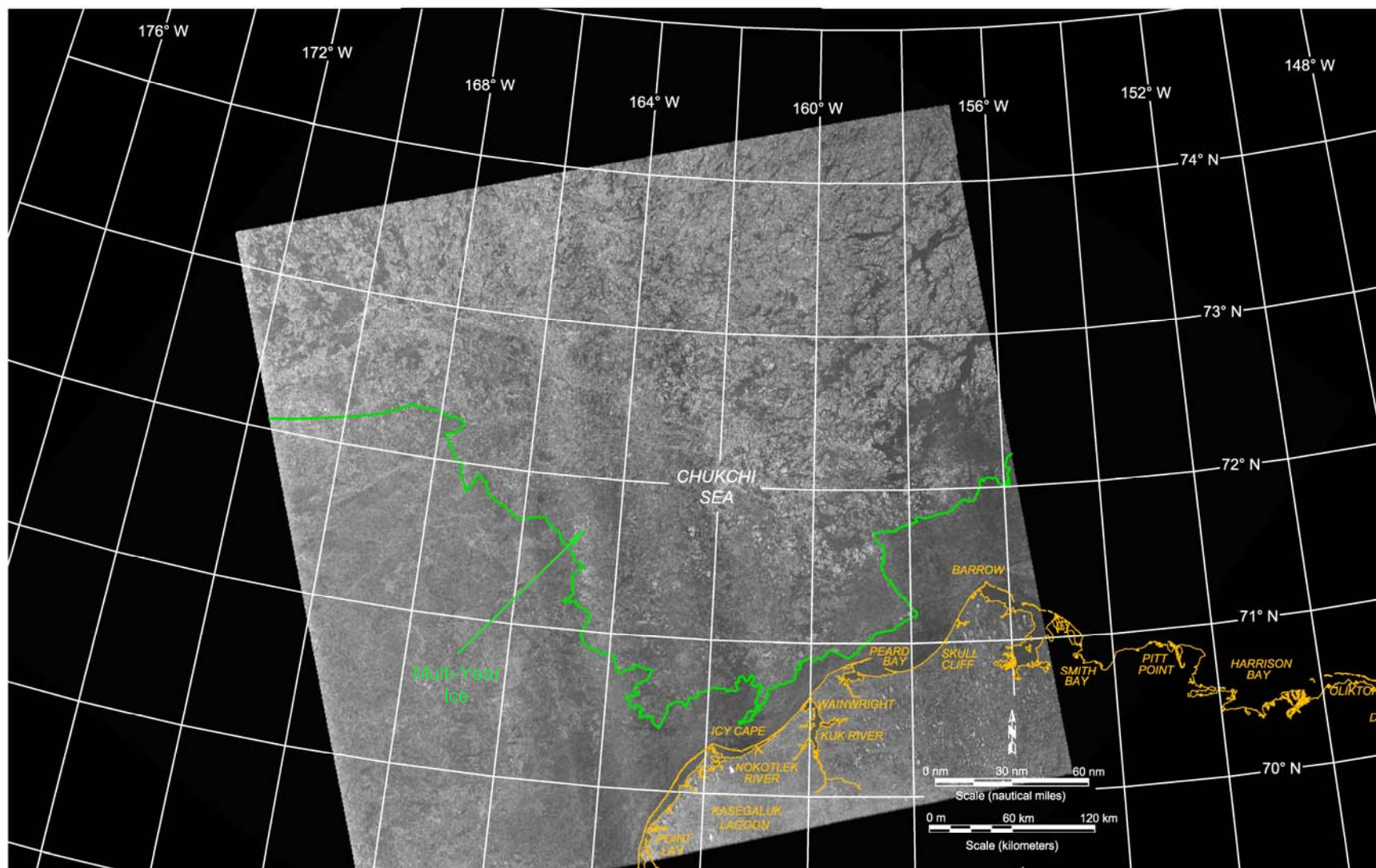
The frequency of occurrence, 48%, was relatively low despite a strong predominance of easterly winds. It probably reflects the absence of easterly storms with sufficient energy to push the ice away from the coast (Table 10).

The flaw lead attained a maximum length of 250 nm (463 km) during both the second and third openings. The maximum width, 30 nm (56 km) occurred during the second opening.

Multi-Year Ice: Although the flaw lead extended to the northeast of Point Barrow on a number of occasions, it did not open wide enough or long enough to initiate another multi-year ice invasion. Nevertheless, multi-year ice continued to occupy the region south and west of Barrow throughout the month of March. As shown in Figure 70, the southern boundary was located in the vicinity of Icy Cape at month-end.

Ice Movement: Ice movement rates in March were derived by tracking five multi-year floes in successive RADARSAT-2 images as well as seven telemetry buoys installed by the IABP (Section 3.4). The trajectories of the former are provided in Figure 71 while those of the latter appear in Figure 72.

The five multi-year floes consisted of three that had been tracked in the Chukchi in February (Floes D, E, and F), one that arrived from the Beaufort in Mid-March (Floe H), and one that was identified for the first time on February 26th (Floe I, with a diameter of 5 km). Floes D, F, and I were evident in five RADARSAT-2 images acquired on February 26th and March 5th, 12th, 16th, and 29th; Floe E was evident in all but the last of these images; and Floe H was evident in only the last two.



Source: RADARSAT-2 Data and Products © MacDonald Dettweiler and Associates Ltd., 2014 – All Rights Reserved

Figure 70. RADARSAT-2 Image of Chukchi Sea Acquired on March 29, 2014

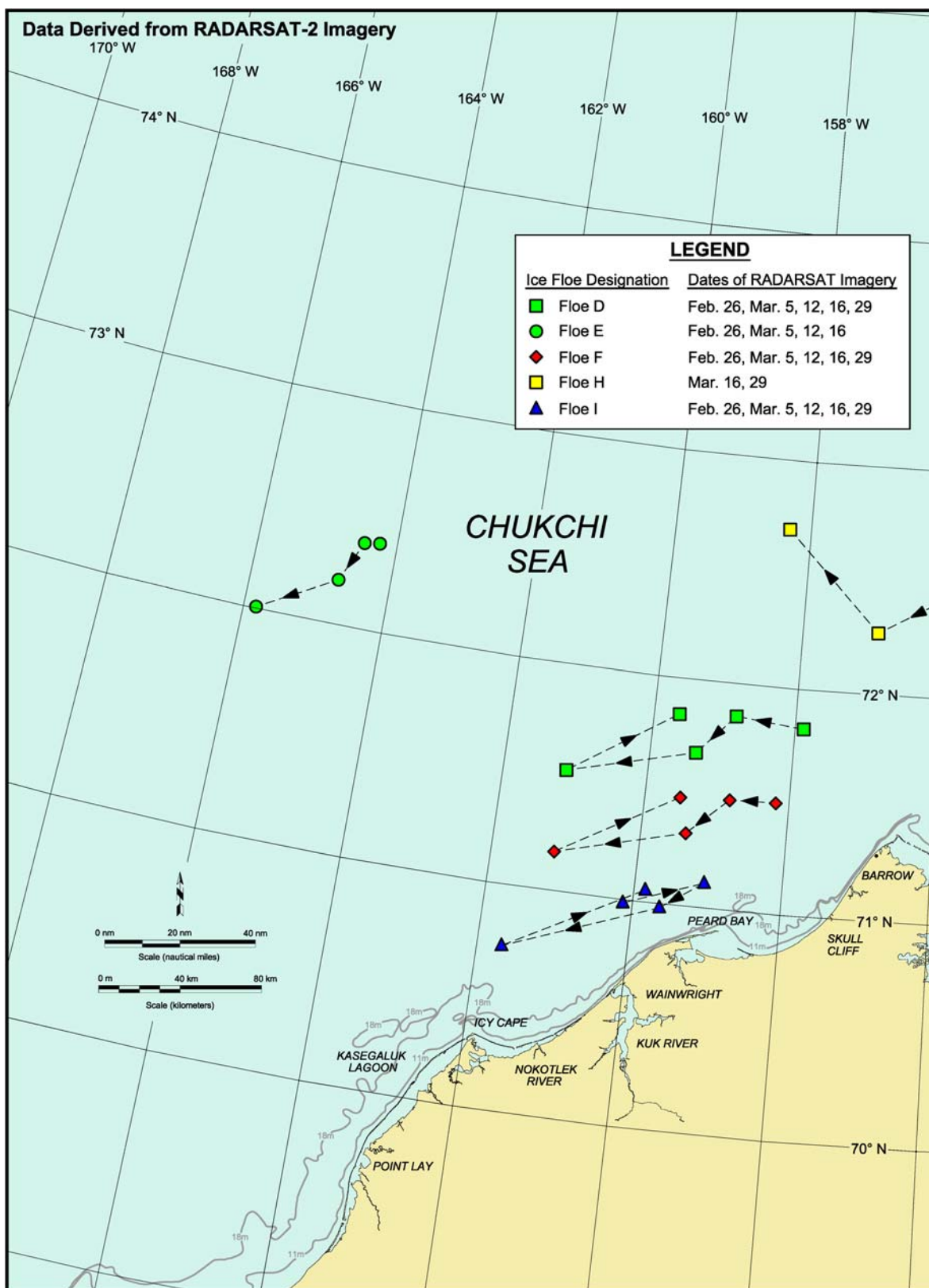


Figure 71. Chukchi Sea Multi-Year Ice Floe Displacements in March 2014

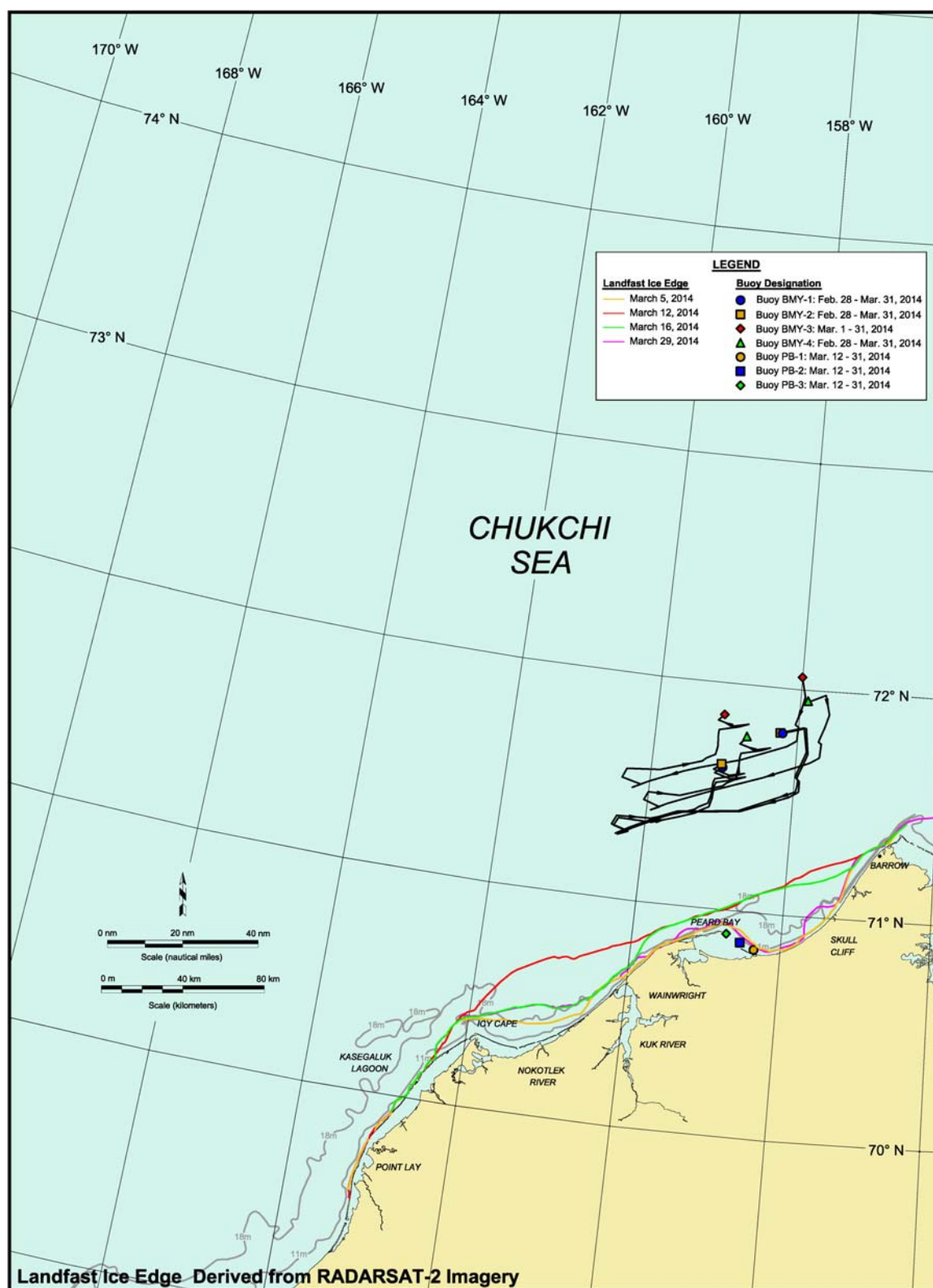


Figure 72. Chukchi Sea Landfast Ice Edge and Telemetry Buoy Tracks in March 2014

Floes D and F, which were located in the nearshore region subject to the influence of the flaw lead, described similar trajectories. Both moved to the southwest between February 26th and March 16th, with the highest speeds occurring during the last four days of this period in response to uninterrupted easterly winds (Figure 68) and an open flaw lead. Subsequently, between the 16th and 29th, the floes reversed direction and moved to the northeast at modest rates. The motive force was provided by winds from the southeast and southwest quadrants.

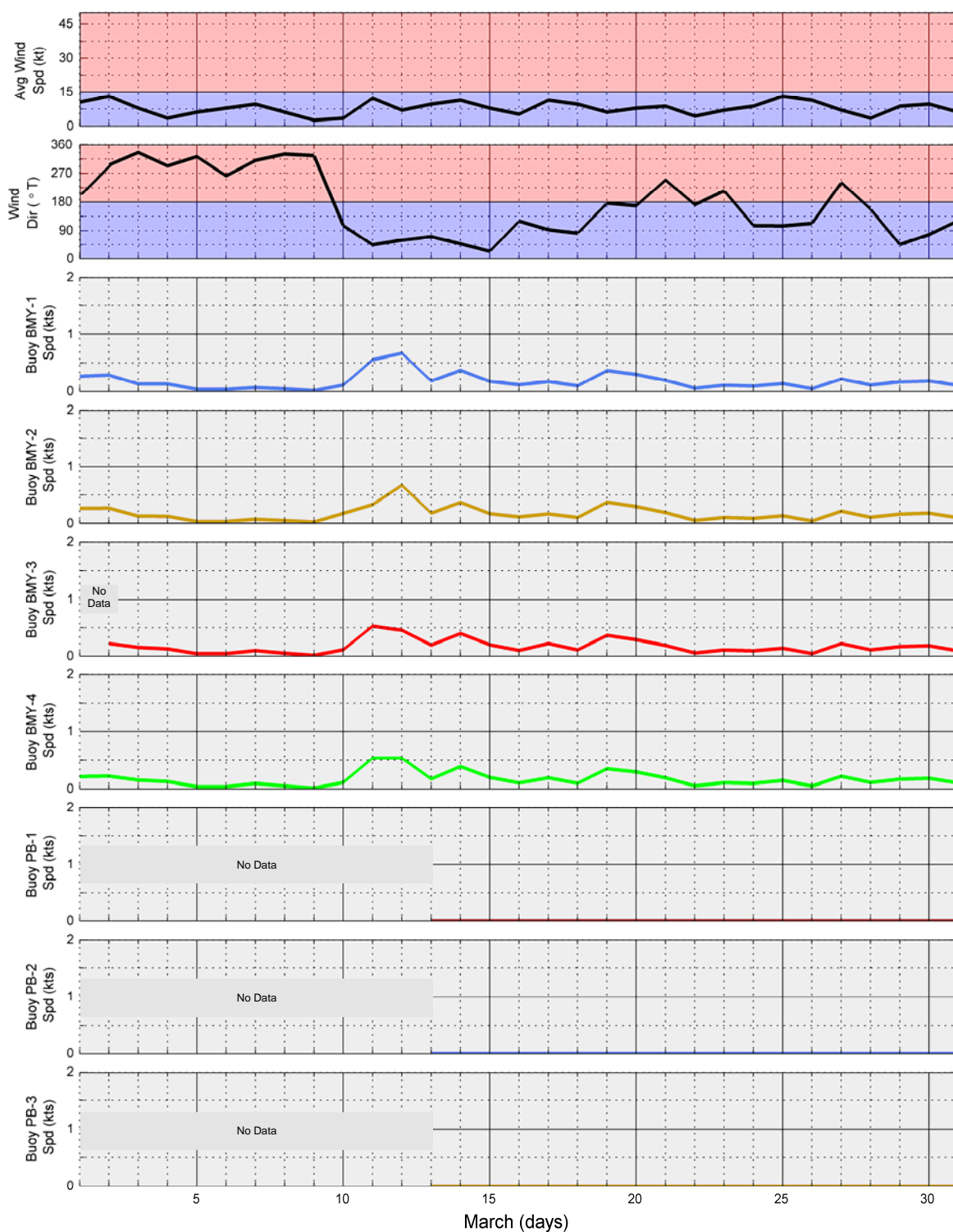
Floe I, which started and ended the tracking period within 15 nm (28 km) of Point Belcher, followed a trajectory similar to that of Floes D and F with one glaring exception: between February 26th and March 5th, it moved to the northeast rather than southwest. A possible explanation is that the floe was prevented from moving to the southwest by other ice during the first three days of this period, but moved freely to the northeast when the wind direction changed from easterly to westerly on March 1st.

Floe E followed a path similar to that of Floes D and F but moved at significantly lower speeds. The difference reflects the fact that it was located outside the flaw lead, and therefore subject to greater confinement by the surrounding pack ice. Floe H, which was tracked between March 16th and 29th, moved to the northwest when Floes D, F, and I moved to the northeast. A plausible explanation is that Floes D, F, and I were located in a region influenced by the northeast-southwest orientation of the flaw lead whereas Floe H was located in the pack ice north of Point Barrow in a region influenced by the Beaufort Gyre.

The speeds between successive positions ranged from 0.6 to 10.8 nm/day (1.1 to 20.0 km/day), with the maximum value attained by Floe I when it was located in the flaw lead between March 12th and 16th. The average monthly speeds varied between 0.2 and 1.9 nm/day (0.4 and 3.5 km/day).

Of the seven telemetry buoys from which data were received in March (Figure 72), three had been installed on multi-year floes in late February (BM-Y-1, -2, and -4; Figure 66), one was installed on another multi-year floe on March 1st (BM-Y-3), and three were installed on the landfast ice at the entrance to Peard Bay on March 12th (PB-1, -2, and -3). The Peard Bay buoys remained stationary through the end of the study period (March 31st).

The four buoys on multi-year floes were located in close proximity to one another and within the influence of the coastal flaw lead. Not surprisingly, they all followed trajectories that resembled those of Floes D, F, and I (Figure 71) with net displacements to the southwest during the first half of the month followed by net displacements to the northeast during the second. As illustrated in Figure 73, the highest average daily speed of 0.67 kt



Note: Wind data from Barrow Airport

Figure 73. Time Series of Telemetry Buoy Average Daily Speeds in Chukchi Sea, March 2014

(0.35 m/s or 16.1 nm/day) was attained by BMY-1 and -2 on March 12th when the average daily wind speed at Barrow airport was only 7 kt (4 m/s). Although the resulting wind factor of 9.6% is exceptionally high, it probably reflects a carry-over effect from the day before when the wind speed averaged 12 kt (6 m/s) and peaked at 21 kt (Figure 68). Nevertheless, the speeds attained by the multi-year floes under unexceptional wind conditions confirm the key role of the flaw lead in promoting rapid ice movement through loss of confinement.

5.6. March Reconnaissance Flights

Fixed-wing aerial reconnaissance missions were undertaken in the Chukchi Sea on March 30th and 31st. Chukchi Sea Flight No. 1 focused on the coastal and nearshore ice conditions between Barrow and Point Lay (Flight “C1” on Drawing CFC-917-01-003), while Chukchi Sea Flight No. 2 was used to observe the offshore region to the northwest and west of Barrow (Flight “C2” on the same drawing), including Hanna Shoal and Shell’s Hanna Shoal and Burger Prospects. It should be noted that the Hanna Shoal Prospects are centered approximately 25 nm (46 km) to the southwest of Hanna Shoal itself (Figure 4). A RADARSAT-2 image that illustrates the ice conditions on March 29th, just prior to Chukchi Sea Flight No. 1, is provided in Figure 70.

5.6.1. Lagoon Ice

As in each of the past four years, the ice in the protected waters of Kasegaluk Lagoon and Peard Bay was found to be flat and undeformed. The conditions in Kasegaluk Lagoon are shown in Plate 25.

5.6.2. Landfast Ice

The extent of the landfast ice zone observed on March 30th was virtually identical to that derived from the RADARSAT-2 image acquired on March 29th (Figure 69). Although the landfast ice was continuous over the entire length of the study area, it was extremely narrow off Skull Cliff, in the vicinity of Point Belcher, and along the 30-nm (56-km) stretch to the north of Point Lay. The width was estimated at 1.0 to 2.1 nm (1.9 to 3.9 km) off Barrow (depending on the location), 2.7 nm (5.0 km) off Wainwright, 4.4 nm (8.1 km) off Icy Cape, and 1.2 nm (2.3 km) at a site 15 nm (28 km) southwest of Icy Cape.

As shown in Plates 26 and 27, the landfast ice zone contained a mixture of flat and deformed ice. The ridge and rubble heights, which ranged from 1 to 5 m, were unexceptional. The most extensive rubble field was located on Blossom Shoals, where 5-m high rubble had been aground since the end of December (Figure 58, 63, and 69; Plate 28).



**Plate 25. Flat Ice in Kasegaluk Lagoon East of Icy Cape
(looking south on March 30, 2014)**



**Plate 26. Mixture of Flat and Deformed Ice in Landfast Ice Zone off Wainwright
(looking northeast on March 30, 2014)**

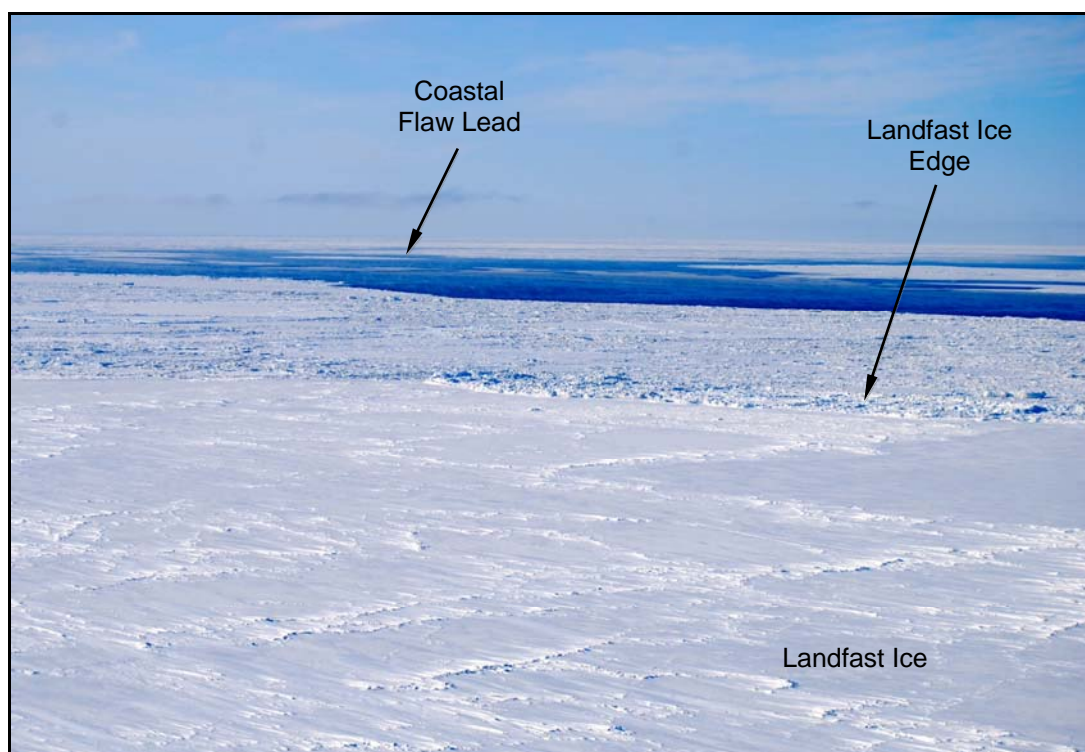


**Plate 27. Flat Ice Interspersed with Ridges Northwest of Icy Cape
(looking west on March 30, 2014)**



Plate 28. 5-m Rubble Grounded on Blossom Shoal (looking west on March 30, 2014)

5.6.3. Leads

As discussed in Section 5.5.2, the coastal flaw lead opened on March 25th and remained open through the end of March in response to easterly winds. It was clearly evident during the flights on the 30th and 31st, with the width increasing from about 5 m (9 km) off Barrow to 15 nm (28 km) off Point Lay. Representative views are provided in Plates 27, 29, and 30.

Additional leads were observed farther offshore, but they tended to be smaller and more widely dispersed. A representative example is provided in Plate 31, which shows a small refreezing lead near the southern boundary of the Burger Prospects.

5.6.4. Offshore Ice

Although the flaw lead was relatively narrow at the time of the flights, its influence was found to extend about 50 nm (93 km) offshore in the form of increased ice deformation. As illustrated in Plates 32 and 33, the ridge and rubble heights were nearly constant at 2 to 3 m between the flaw lead and the Burger Prospects, but the number of these features per unit area was markedly greater in proximity to the lead. Farther offshore, where the differential motion between individual floes was limited by the more consolidated nature of the ice canopy, the ridges and rubble were more widely spaced.

5.6.5. Ice Pile-Ups

Twenty-two ice pile-ups were observed on the Chukchi coast during the March 30th reconnaissance flight (Table 12). Based on the directions from which the ice had approached, it appeared that three formed on November 21st and 22nd when the wind shifted from southerly to northeasterly, and nineteen formed on December 7th when the wind shifted from easterly to westerly (Section 5.1). The highest concentration was located to the east of Icy Cape on the barrier islands that form the seaward boundary of Kasegaluk Lagoon.

The pile-up heights, which varied from 1 to 3 m above sea level, were the smallest encountered since the current series of freeze-up studies began in 2009. All 22 pile-ups encroached onto the subaerial beach, with the encroachment distances ranging from 5 to 20 m. The alongshore lengths varied from 100 to 7,800 m.

Representative examples are provided in Plates 34 and 35, respectively. The former shows a 3-m high pile-up that occurred on a barrier island 5 nm (9.3 km) east of Icy Cape when ice approached from the northeast. It was 1,900-m long and encroached 5 m onto the beach. The latter shows a 2-m high pile-up on a barrier island off the mouth of the



Plate 29. Coastal Flaw Lead off Barrow (looking north on March 31, 2014)



Plate 30. Coastal Flaw Lead off Point Lay (looking west on March 30, 2014)

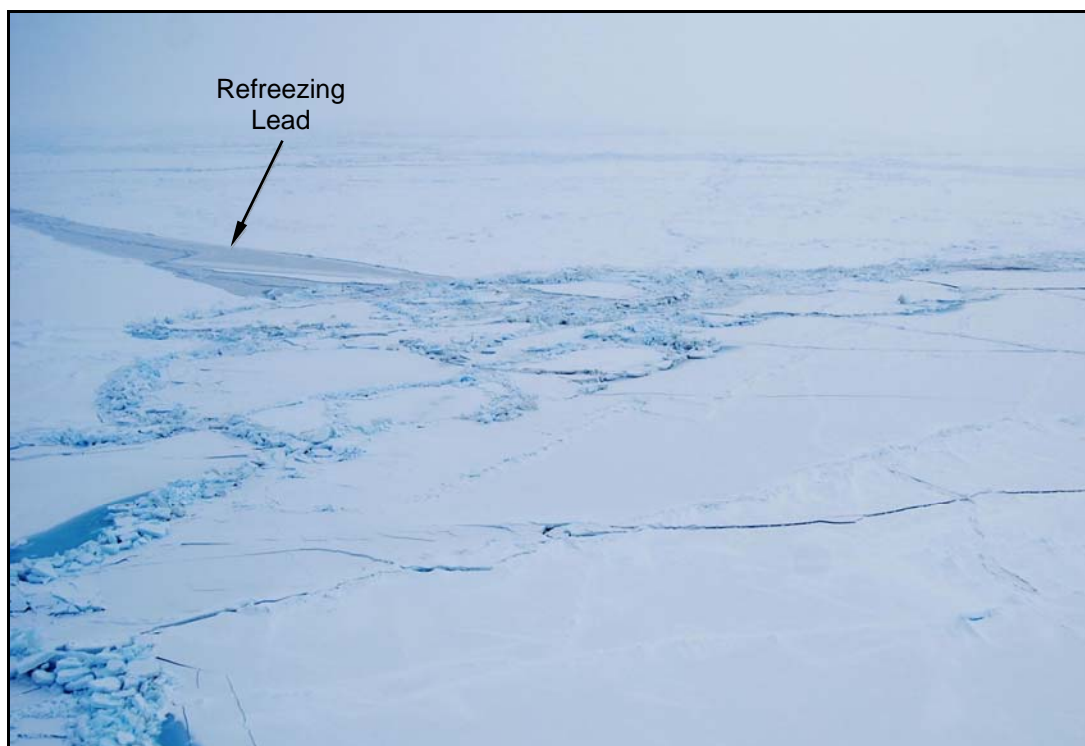
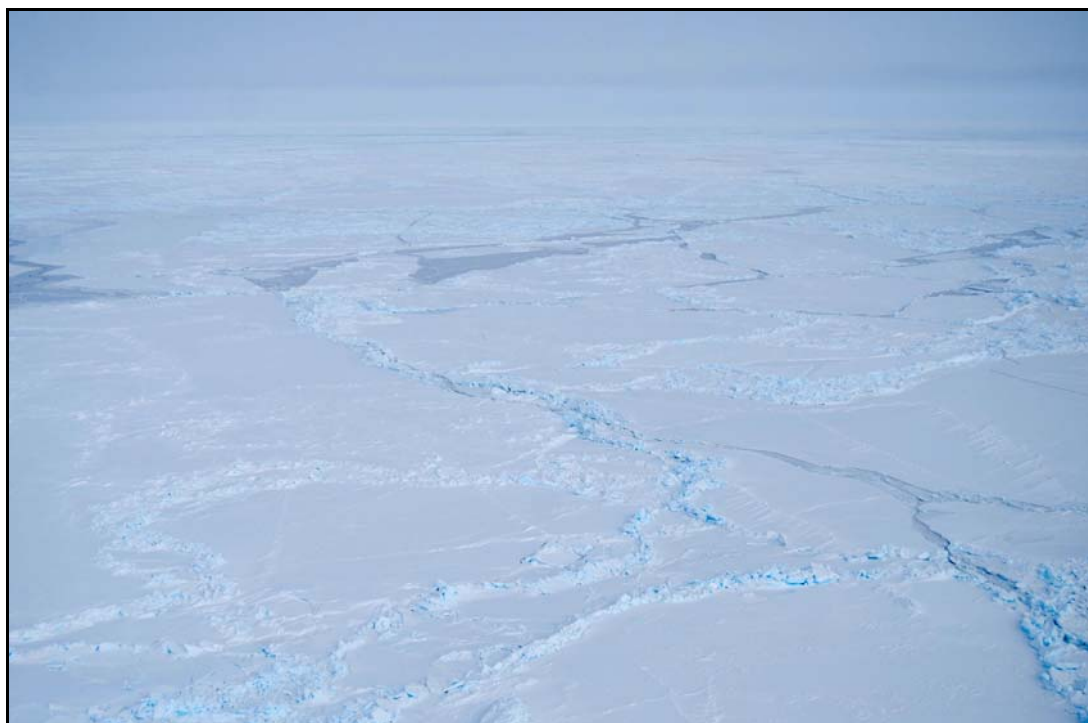


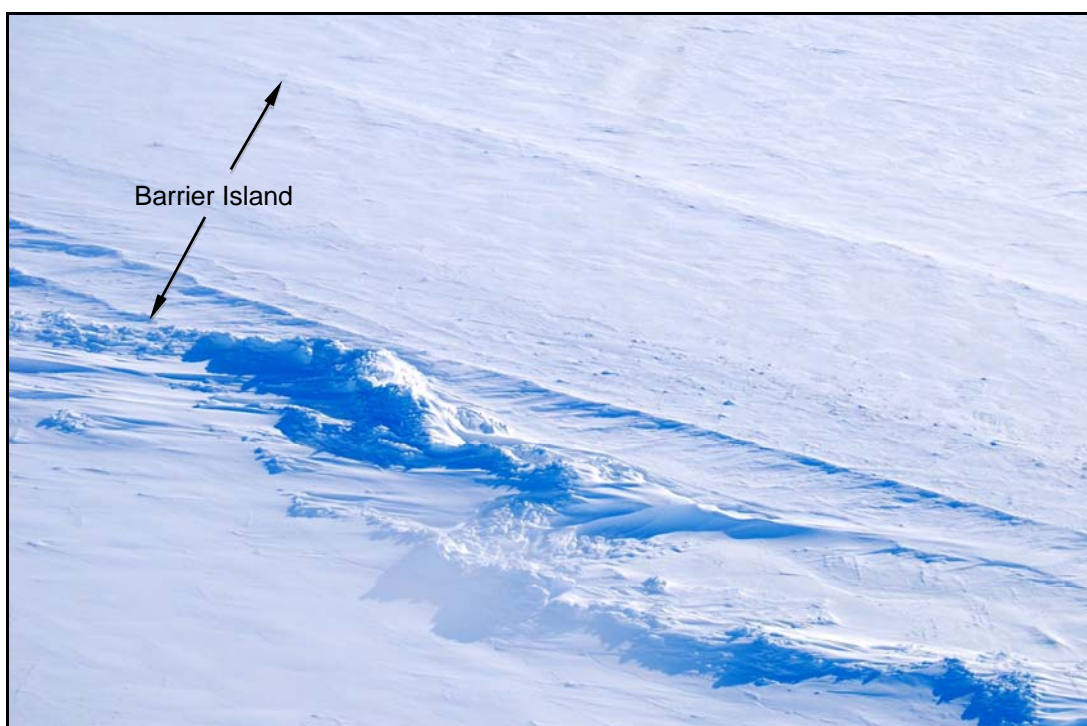
Plate 31. Small, Refreezing Lead in Burger Prospects (looking east on March 31, 2014)



Plate 32. Extensive Accumulation of 3-m Rubble 40 nm West of Barrow (looking northeast on March 31, 2014)



**Plate 33. Intermittent 3-m Ridges and Rubble 80 nm West of Barrow
(looking north on March 31, 2014)**



**Plate 34. 3-m Pile-Up on Barrier Island 5 nm East of Icy Cape
(looking southeast on March 30, 2014)**

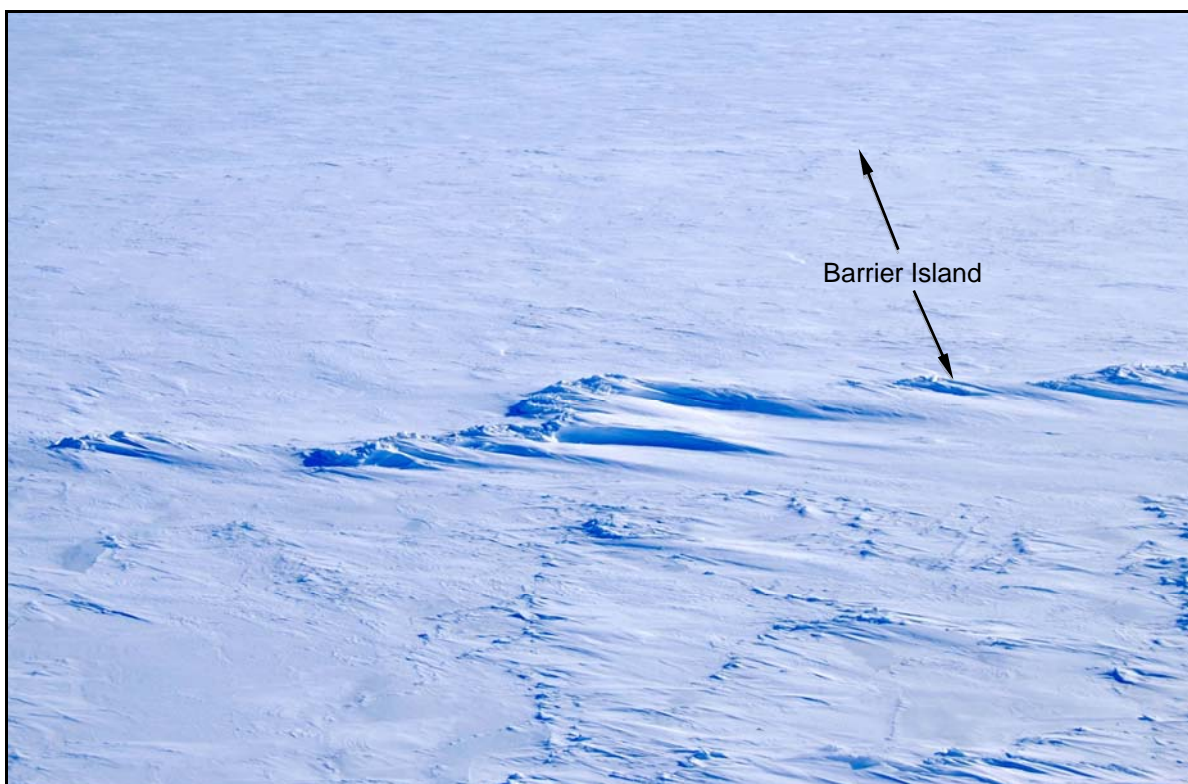


**Plate 35. 2-m Pile-Up on Barrier Island off Mouth of Nokotlek River
(looking southeast on March 30, 2014)**

Nokotlek River that was caused by ice arriving from the west. It was 1,800-m long and encroached 10 m onto the beach.

5.6.6. Multi-Year Ice

As anticipated from the RADARSAT-2 image acquired on March 29th (Figure 69), multi-year floes were sighted repeatedly during the two reconnaissance flights (Drawing CFC-917-01-003). The floe diameters ranged from less than 100 m to approximately 5 km, while the concentrations ranged from 10% to as high as 60%. Some of the larger floes contained embedded ridges with heights to 5 m (Plate 36), and others displayed cracks that appeared to have formed in the recent past (Plate 37). In keeping with the southern boundary shown in Figure 69, all of the floes were located to the north of Icy Cape.

An unanticipated finding was the presence of small multi-year floes in the landfast ice off Barrow. As illustrated in Plate 38, a number of such floes with diameters ranging from 100 to 300 m were spotted in close proximity to the shoreline. Based on the successive positions of the landfast ice edge shown in Figures 62 and 68, the floes arrived between January 26th and February 16th.

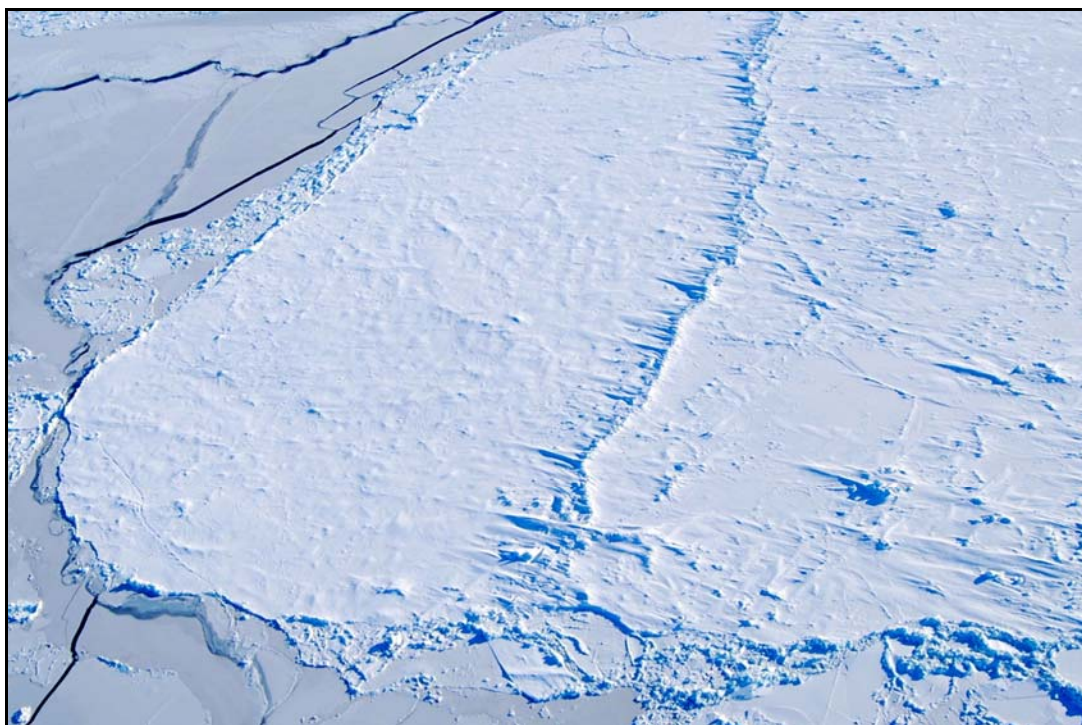


**Plate 36. Multi-Year Floe with 5-m Ridge 20 nm West of Wainwright
(looking southeast on March 30, 2014)**

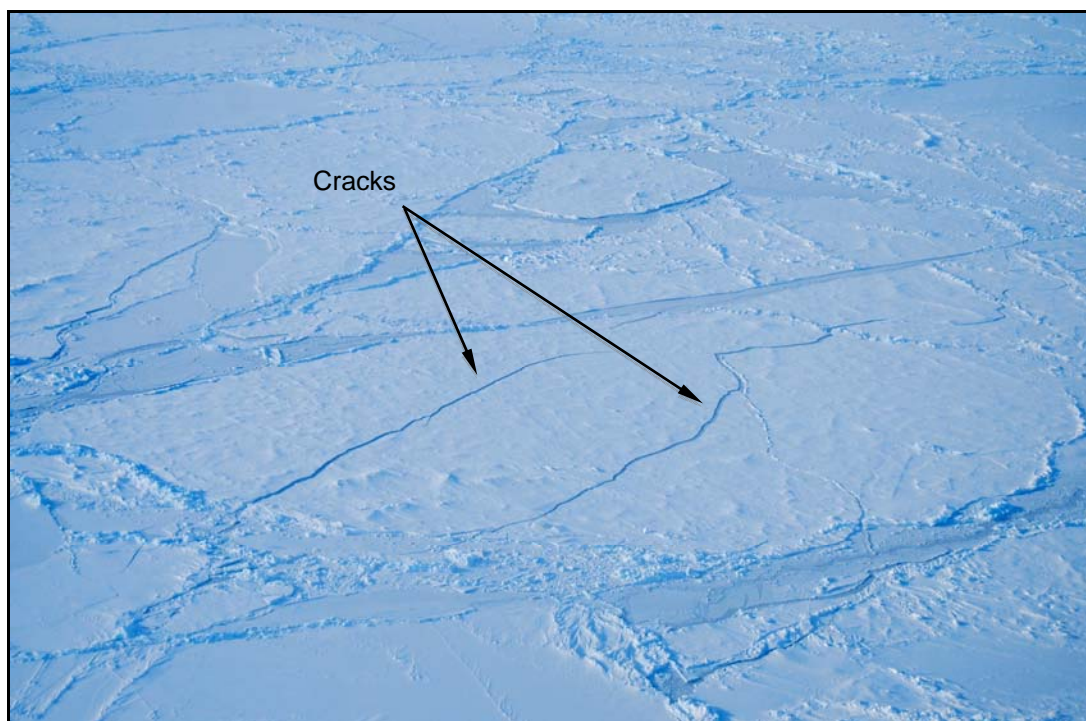


**Plate 37. Cracked Multi-Year Floe 80 nm West of Barrow
(looking southwest on March 31, 2014)**

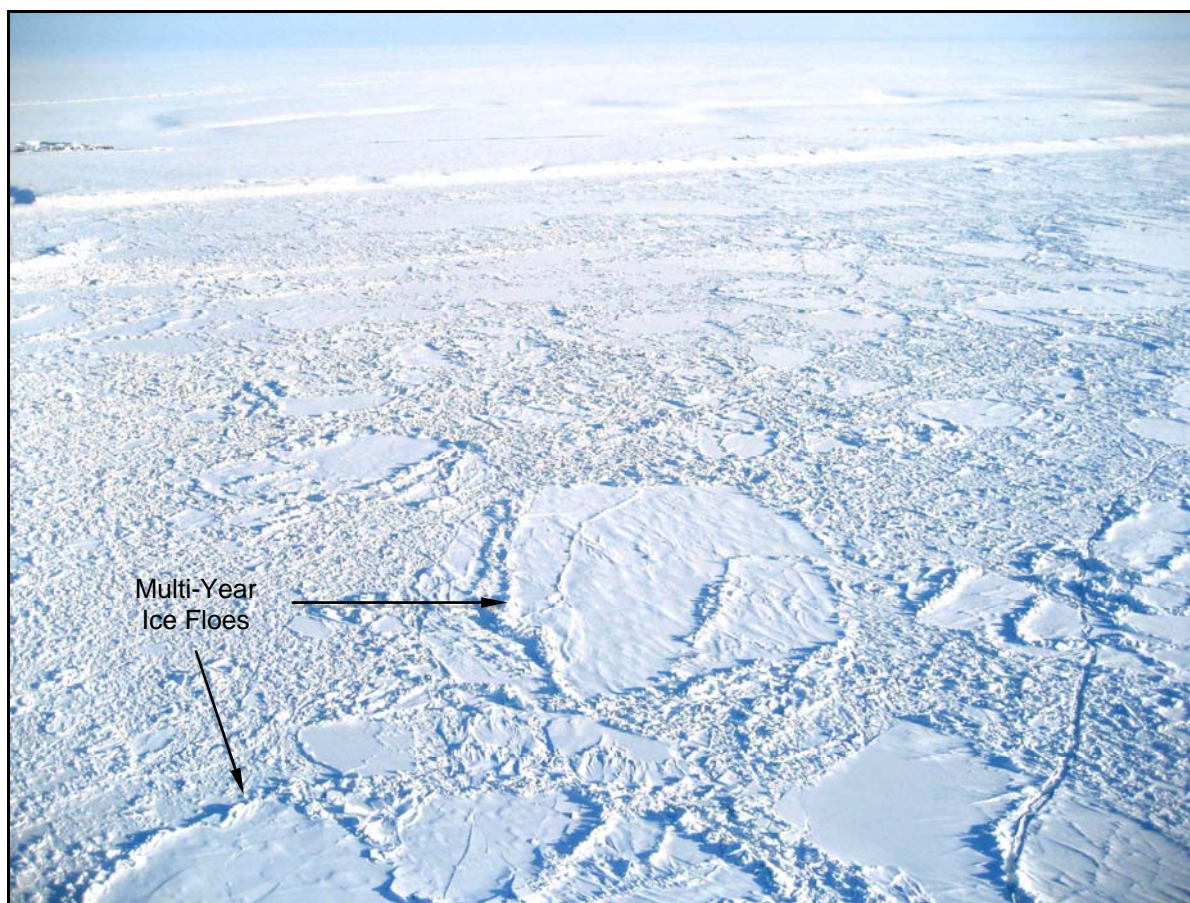


**Plate 38. Multi-Year Floes in Landfast Ice off Barrow
(looking southeast on March 30, 2014)**

5.6.7. Ice Conditions in Shell Prospects

In the central and eastern portions of Shell's Hanna Shoal Prospects, relatively flat first-year floes with diameters to 2 km were interspersed with occasional multi-year floes that constituted 10% of the ice canopy. Intermittent ridges and rubble with heights to 3 m were present among the first-year floes (Plate 39). The western portion of the Hanna Shoal Prospects was obscured by fog.

Observations in the Burger Prospects were hampered by fog that ranged from patchy to dense. In the areas that were visible, the ice consisted of flat, first-year floes with diameters ranging from less than 100 m to 3 km. Deformation was modest; as shown in Plate 40, the ridges and rubble were intermittent with typical heights of 2 to 3 m. Single and multiple leads, both open and refreezing, were noted in some areas along with broken ice (Plates 31 and 41). Although numerous multi-year floes were sighted to the east of the Burger Prospects, none were observed in the Prospect itself.



Plate 39. First-Year Ice with 3-m Ridges and Rubble at East Edge of Hanna Shoal Prospects (looking northwest on March 31, 2014)



Plate 40. First-Year Ice with Intermittent 3-m Ridges and 2-m Rubble in Southeastern Portion of Burger Prospects (looking east on March 31, 2014)



**Plate 41. Multiple Leads and Broken Ice in Central Portion of Burger Prospects
(looking east on March 31, 2014)**

5.6.8. *Katie's Floeberg*

Katie's Floeberg forms each winter when ice rubble accumulates on Hanna Shoal, which lies 110 nm (204 km) northwest of Barrow at 72°N, 162°W (Drawing CFC-907-01-003). The shallowest water depth on the shoal is about 12 m, while the surrounding depths exceed 30 m.

Katie's Floeberg was identified as early as 1966 using Nimbus satellite imagery (Kovacs, *et al.*, 1976). Its formation and growth have been described by a number of prior investigators, including Stringer and Barrett (1975), Kovacs, *et al.* (1976), Toimil and Grantz (1976), Barrett and Stringer (1978), and Vaudrey and Thomas (1981). In April 1980, the feature existed as a vast oval of grounded first-year and multi-year rubble (Plate 54) measuring 9 km long and 4.6 km wide (Vaudrey and Thomas, 1981). Its maximum elevation was 18 m above sea level. The long axis was oriented northeast-southwest, and the shallowest water depth was located at the southwest tip.

Similar characteristics were noted during the reconnaissance flight conducted on February 7, 2012: a mixture of first-year and multi-year rubble that was 10 km long, 5 km

wide, and up to 10 m above sea level (Coastal Frontiers and Vaudrey, 2012a). A year later, in February 2013, the feature was not present at the time of the reconnaissance flight and did not form until mid-March (Coastal Frontiers and Vaudrey, 2013).

When the 2014 reconnaissance flight was conducted on March 31st, Katie's Floeberg was clearly evident but somewhat smaller than the feature observed in 2012. It was estimated to be 8 km long and 4 km wide with the major axis oriented northeast-southwest (Plate 42). An open-water wake was present on the southwest (leeward) side. Approximately 20% of the floeberg consisted of multi-year floes with the remainder composed of first-year rubble (Plate 43). The highest rubble, which extended up to 8 m above sea level, was located on the northeast side.

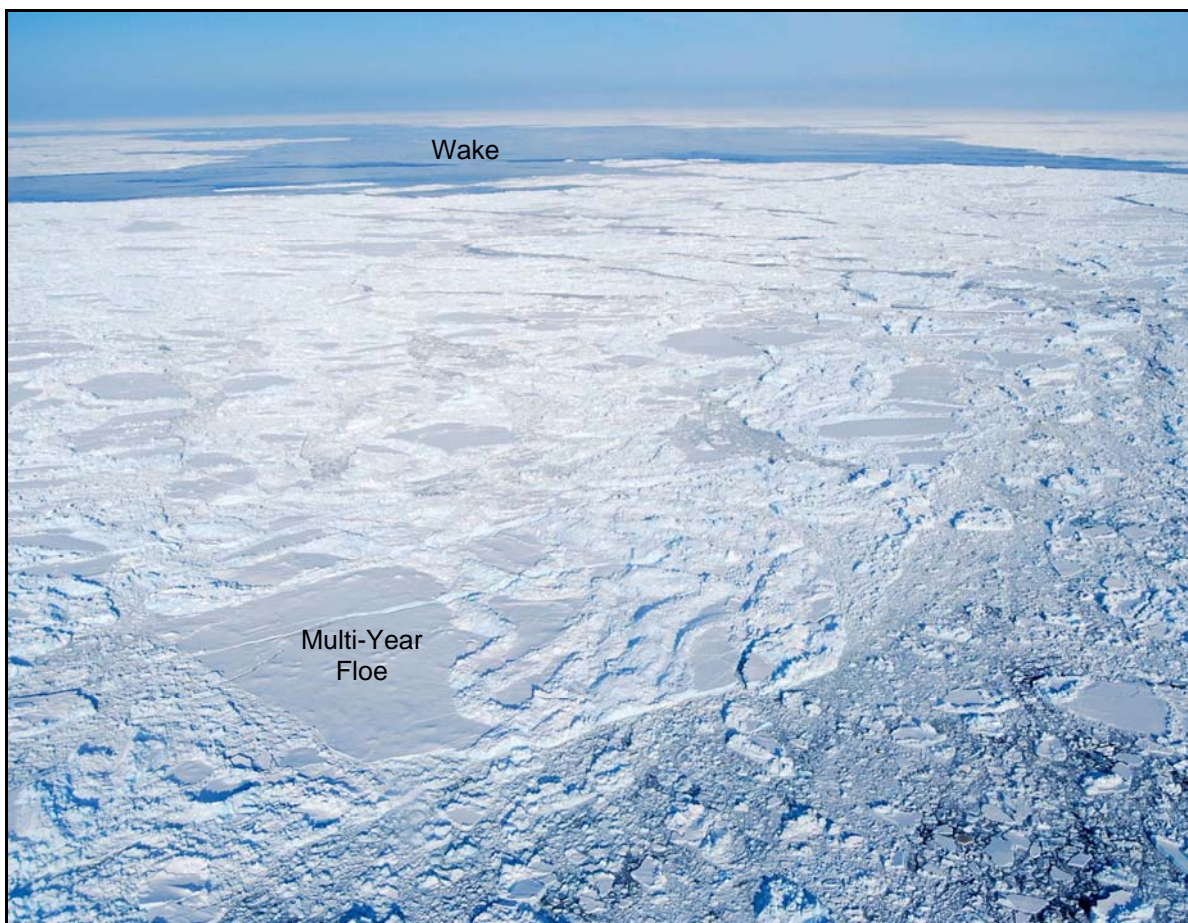


Plate 42. Mixture of First-Year Rubble and Multi-Year Floes Comprising Katie's Floeberg (looking northwest on March 31, 2014)



**Plate 43. 8-m Rubble on Northeast Side of Katie's Floeberg
(looking north on March 31, 2014)**

6. FREEZE-UP IN RECENT YEARS VERSUS THE 1980s

The primary objectives of this section are to characterize present-day freeze-up processes using the data acquired during the past five years (2009-10 through 2013-14), and to compare them with those documented from 1980-81 through 1985-86.

Two of the most important environmental influences on freeze-up are the air temperatures and wind conditions. Accordingly, the temperature and wind data acquired at Barrow Airport are analyzed to investigate perceived trends toward warmer conditions and higher storm frequencies. Both changes may make the sea ice more dynamic during freeze-up and midwinter (Walsh and Eicken, 2007).

Following the analysis of air temperatures and winds, six key aspects of the freeze-up season are evaluated: the timing of freeze-up, first-year ice growth, landfast ice development and stability, the coastal flaw lead in the Chukchi Sea, multi-year ice invasions, and ice movement. Based on comparisons with the 1980s, potential long-term trends in ice behavior are identified. It should be noted that the past five years constitute a relatively small sample of present-day conditions. As a result, the assessments presented below are subject to refinement as more data become available.

6.1. Air Temperatures

As discussed in Section 3.1, freezing-degree days (FDD) were computed as the difference between the freezing point of seawater (29°F; -2°C) and the mean daily air temperature, and then accumulated by month. Negative FDD (>29°F) that occurred after freeze-up had begun were subtracted from the total.

Table 15 presents the FDD accumulated at Barrow on a monthly basis for each winter season from 1970-71 through 2013-14. The values were computed using the daily mean air temperature. The table is divided into two parts, with the top portion showing the 20-year period from 1970-71 through 1989-90 and the bottom portion showing the subsequent 24-year period from 1990-91 through 2013-14. The column on the right side displays the rank of each winter over the entire 44-year period of record, with the highest ranking (No. 1) assigned to the warmest winter (fewest FDD at the end of the winter season) and the lowest ranking (No. 44) to the coldest (most FDD at the end of the winter season). The ten warmest winter seasons (Ranking Nos. 1 through 10) are shown in red type.

**Table 15: Accumulated Freezing-Degree Days (<29°F) at Barrow,
1970-71 through 2013-14**

Year	Sep	Oct	Nov	Dec	Jan	Feb	Mar	Apr	May	44-yr Rank
1970-71	129	1013	2009	3224	4727	6270	7734	8738	9098	43
1971-72	7	466	1351	2603	4004	5402	6912	7914	8252	39
1972-73	30	275	1103	2092	3410	4591	6135	7086	7393	23
1973-74	9	307	958	2024	3255	4859	6381	7488	7826	34
1974-75	18	725	1823	3546	5263	6453	7579	8584	8891	42
1975-76	155	893	2102	3677	5162	6667	8043	8976	9342	44
1976-77	12	486	1281	2689	3836	5107	6694	7756	8066	37
1977-78	0	272	1309	2444	3529	4738	5963	6785	7176	16
1978-79	17	696	1404	2734	3710	5082	6496	7393	7684	28
1979-80	0	310	895	2166	3496	4636	5891	6875	7247	17
1980-81	117	566	1586	2969	3896	5148	6384	7221	7389	22
1981-82	105	564	1452	2602	3845	4839	6122	7022	7407	24
1982-83	32	723	1896	3084	4578	5821	7136	7925	8300	40
1983-84	153	835	1666	2546	3919	5717	7128	8316	8700	41
1984-85	0	366	1479	2799	3925	5218	6517	7585	7780	31
1985-86	60	635	1424	2537	3901	4959	6407	7508	7784	32
1986-87	13	404	1262	2359	3661	5033	6295	7306	7579	27
1987-88	51	240	1272	2447	3672	4931	6224	7052	7337	20
1988-89	49	886	2164	3351	4994	5546	6637	7327	7687	29
1989-90	0	363	1611	2805	4417	5878	7131	7776	7903	36
Average	48	551	1502	2735	4060	5345	6690	7632	7942	
Std. Dev.	54	239	357	460	592	609	601	623	635	
Year	Sep	Oct	Nov	Dec	Jan	Feb	Mar	Apr	May	44-yr Rank
1990-91	25	400	1477	2863	4177	5499	6947	7718	7748	30
1991-92	27	384	1494	2883	4358	5788	6972	7818	8076	38
1992-93	154	666	1569	2737	4027	5150	6439	7114	7300	19
1993-94	27	210	924	2074	3252	4313	5776	6649	6972	12
1994-95	60	699	1827	3222	4493	5758	7175	7817	7898	35
1995-96	0	326	1076	2343	3463	4776	5849	6719	6830	11
1996-97	87	816	1431	2469	3911	5120	6425	7184	7473	25
1997-98	5	293	830	2089	3441	4661	5644	6178	6339	3
1998-99	0	132	1023	2275	3681	4860	6243	7179	7375	21
1999-00	18	371	1251	2657	3979	5263	6493	7337	7792	33
2000-01	31	392	1251	2300	3510	4388	5764	6584	7137	15
2001-02	39	638	1507	2654	4070	5371	6315	7127	7273	18
2002-03	0	175	849	1811	3028	4269	5483	6104	6329	2
2003-04	0	167	945	2061	3210	4703	6063	6897	7065	14
2004-05	9	243	1045	2205	3341	4501	5636	6436	6648	8
2005-06	8	237	1143	2156	3421	4475	5930	6908	7059	13
2006-07	0	102	790	1769	3160	4258	5615	6232	6599	6
2007-08	0	170	616	1525	2922	4387	5792	6428	6648	8
2008-09	3	195	933	1809	3109	4103	5492	6297	6438	5
2009-10	6	125	981	1988	3391	4479	5687	6312	6608	7
2010-11	7	199	739	1925	3121	4113	5216	6117	6388	4
2011-12	3	183	1059	2264	3814	5013	6588	7319	7556	26
2012-13	0	76	765	1959	3131	4463	5598	6451	6676	10
2013-14	34	161	799	1786	2889	3897	4945	5696	5775	1
Average	23	307	1097	2243	3537	4734	6004	6776	7000	
Std. Dev.	35	206	315	421	464	530	569	583	582	

Note: In 2013-14, FDD continued to accumulate through June 2nd. They are reflected in the total for May.

The most recent winter, 2013-14, proved to be the warmest in the entire 44-year period of record. Of the remaining four winters in the current round of freeze-up studies, three rank among the ten warmest: 2010-11 (4th), 2009-10 (7th), and 2012-13 (10th). The only exception is 2011-12, which was considerably colder and ranks 26th.

The accumulated freezing-degree days at the end of each winter season are plotted against time in Figure 74. A long-term warming trend is readily apparent, with freezing-degree days decreasing at an average rate of 44/yr since 1970-71. Although substantial deviations from the trend have occurred on numerous occasions, they tended to be short-lived with typical durations of one to three years. Also noteworthy is a modest decrease in interannual variability: the standard deviation during the past 14 years (1990-91 through 2013-14), 582 FDD, was about 8% lower than that during the prior two decades (1970-71 through 1989-90).

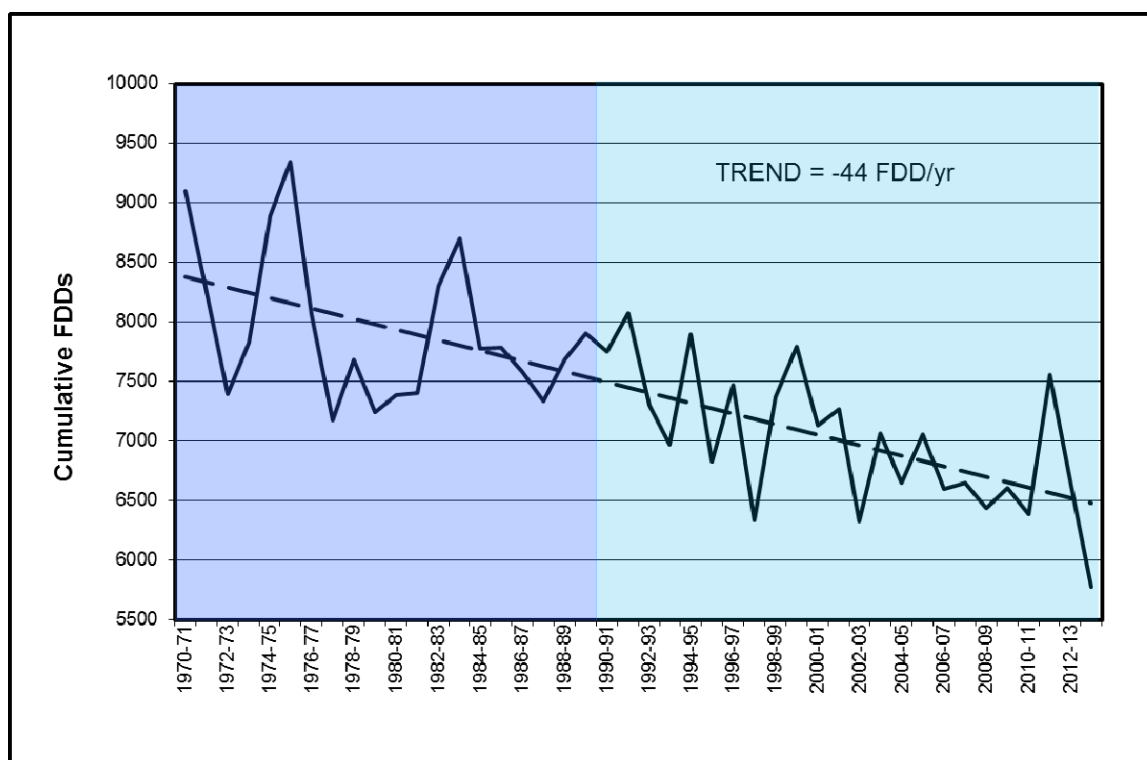


Figure 74. Annual Cumulative Freezing-Degree Days (<29°F) at Barrow, 1970-71 through 2013-14

Melling and Riedel (2005) found a similar but more gradual warming trend in the air temperatures at Tuktoyaktuk over the 30-year period from 1975 through 2004. They determined that the number of freezing-degree days decreased at a rate of 3.3% per decade, somewhat less than any of the decadal rates computed for Barrow. Based on the data

presented in Table 15, the average annual accumulated freezing-degree days declined by 3.8% from the 1970s to the 1980s, 5.2% from the 1980s to the 1990s, 8.1% from the 1990s to the 2000s, and an additional 2.7% during the past four winters. The total decline from 1970s to the most recent 5-year period (which encompasses the freeze-up studies) was 18.5%.

Additional information on the increase in winter air temperatures is provided in Figure 75, which compares the monthly average values at Barrow over the past five years with the long-term average values from 1971-72 through 1999-2000. The differences between the monthly values in 2013-14 and the long-term average values also are shown. The monthly average during the past five years exceeded the long-term value in each of the nine months that comprise the winter season. The divergence was greatest in the fall, peaking at 10°F in October followed by 6°F in November. For the entire nine-month period, the average temperature was 4°F higher than the long-term average value.

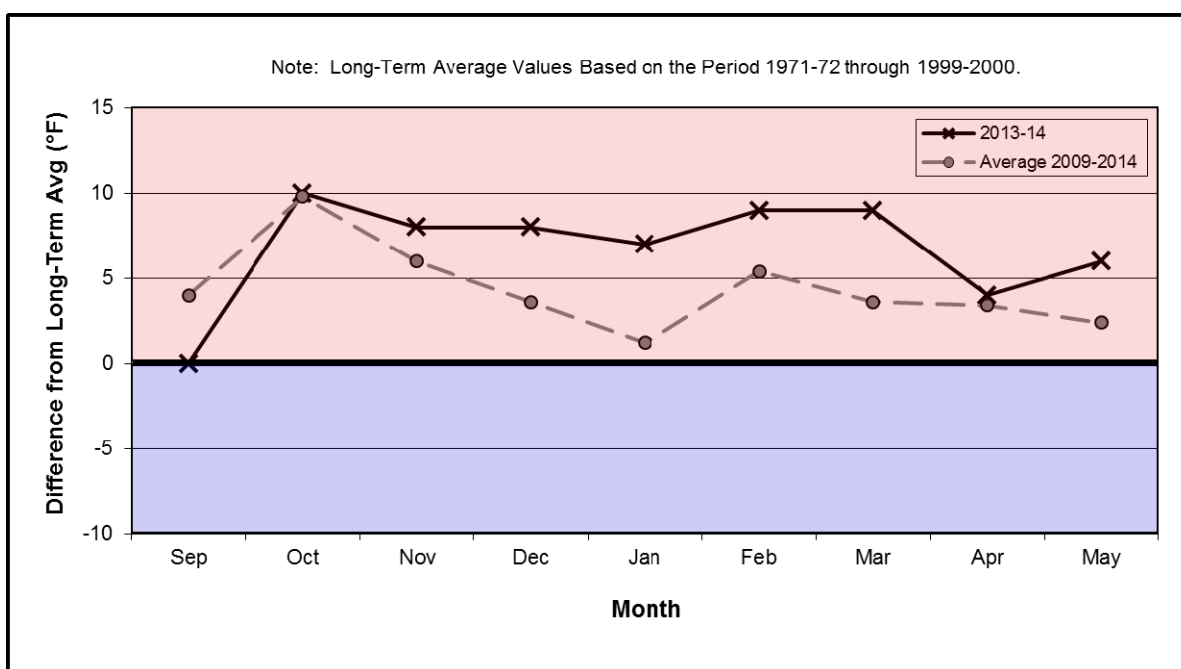


Figure 75. Differences between Recent Monthly Air Temperatures and Long-Term Average Values at Barrow

Trend: Since the 1970s, progressively warmer winter seasons have caused the number of freezing-degree days at Barrow to decline at an average rate of 44 per year. The greatest increases in temperature have occurred during the months of October and November.

6.2. Winds

The wind directions that prevailed at Deadhorse and Barrow Airports during each of the past five freeze-up seasons (October through March) are summarized in Tables 16 and 17. Notwithstanding the common perception that easterlies predominate in the Beaufort Sea, westerlies occurred slightly more often, with the frequency ranging from a low of 50% in 2010-11 to a high of 60% in 2011-12. The average value was 55%, with a standard deviation of 4%.

Easterlies predominated at Barrow, where the frequencies varied between 61% in 2013-14 and 71% in 2011-12. The average frequency was 67%. As in the Beaufort, the standard deviation was 4%.

The storms that occurred at Deadhorse and Barrow Airports during each of the past five freeze-up seasons are summarized in Tables 18 and 19. Both the number of discrete storm events and the total number of days with storm conditions (“storm days”) are shown. As in the case of Sections 4 and 5, a storm is defined as an event during which the daily average sustained wind speed exceeds 15 kt (8 m/s).

In the Beaufort (Table 18), eighteen storm events occurred on average during each freeze-up season. The total was divided equally between easterlies and westerlies. The easterlies tend to be of longer duration, however, yielding an average of 24 storm days versus eighteen for westerlies. During the past year (2013-14), nine easterly storms produced 23 storm days while eleven westerly storms produced 20 storm days.

In the Chukchi (Table 19), the easterly dominance in wind direction was clearly reflected in the storm population. Over the past five freeze-up seasons, the annual averages consisted of eleven easterly storm events producing 31 storm-days versus only five westerly storm events producing nine storm-days. In 2013-14, twelve easterly and seven westerly storms produced 29 and thirteen storm days, respectively.

Unfortunately, data from the 1980’s suitable for direct comparison with those in Tables 18 and 19 are not available. However, an indication of storm conditions in that era was developed by Dickins and Vaudrey (1994), who compiled mid-winter wind data (January through April) at Barrow for the 18-year period beginning in 1977 and ending in 1994. They defined a storm as having a sustained wind speed exceeding 15 kt (8 m/s) for a period exceeding 12 hr. The six winters from 1981 through 1986 were excerpted from this database in order to compare the mid-winter storm frequency in the early 1980s with that which occurred from 2010 through 2014.

Table 16. Beaufort Sea Wind Directions, 2009-10 through 2013-14

Month	2009-10 Days		2010-11 Days		2011-12 Days		2012-13 Days		2013-14 Days	
	East	West	East	West	East	West	East	West	East	West
October	20	11	25	6	23	8	6	25	15	16
November	19	11	15	15	7	23	4	26	10	20
December	15	16	13	18	15	16	14	17	13	18
January	7	24	16	15	3	28	18	13	18	13
February	16	12	8	20	19	10	21	7	11	17
March	11	20	14	17	7	24	20	11	11	20
Total Days	88	94	91	91	74	109	83	99	78	104
Frequency	48%	52%	50%	50%	40%	60%	46%	54%	43%	57%

Note: Table 16 is based on the average daily wind directions recorded at Deadhorse Airport.

Table 17. Chukchi Sea Wind Directions, 2009-10 through 2013-14

Month	2009-10 Days		2010-11 Days		2011-12 Days		2012-13 Days		2013-14 Days	
	East	West	East	West	East	East	East	West	East	West
October	23	8	29	2	28	3	10	21	22	9
November	21	9	18	12	16	14	13	17	16	14
December	22	9	22	9	27	4	21	10	17	14
January	13	18	21	10	14	17	29	2	22	9
February	22	6	10	18	23	6	25	3	15	13
March	24	7	18	13	22	9	28	3	19	12
Total Days	125	57	118	64	130	53	126	56	111	71
Frequency	69%	31%	65%	35%	71%	29%	69%	31%	61%	39%

Note: Table 17 is based on the average daily wind directions recorded at Barrow Airport.

Table 18. Beaufort Sea Storms, 2009-10 through 2013-14¹

Freeze-Up ²	Storm Events			Storm-Days		
	Easterly	Westerly	Total	Easterly	Westerly	Total
2009-10	10	5	15	24	13	37
2010-11	8	11	19	19	22	41
2011-12	8	6	14	16	18	34
2012-13	10	10	20	35	16	51
2013-14	9	11	20	23	20	43
Average	9	9	18	23	18	41

Notes:

- ¹ Table 18 includes all storm events with a daily average sustained wind speed exceeding 15 kt (8 m/s) at Deadhorse Airport.
- ² The period of record extends from October 1st through March 31st.

Table 19. Chukchi Sea Storms, 2009-10 through 2013-14¹

Freeze-Up ²	Storm Events			Storm-Days		
	Easterly	Westerly	Total	Easterly	Westerly	Total
2009-10	14	3	17	37	4	41
2010-11	10	8	18	27	13	40
2011-12	8	3	11	21	6	27
2012-13	12	4	16	42	7	49
2013-14	12	7	19	29	13	42
Average	11	5	16	31	9	40

Notes:

- ¹ Table 19 includes all storm events with a daily average sustained wind speed exceeding 15 kt (8 m/s) at Barrow Airport.
- ² The period of record extends from October 1st through March 31st.

Whereas Dickins and Vaudrey computed an average of 8.5 storm events per mid-winter season in the early 1980s, an analysis of the wind data recorded over the past five years produced a nearly-identical average of 8.6 storm events per season (ten in 2010, ten in 2011, seven in 2012, nine in 2013, and seven in 2014). This finding suggests that the storm frequency in mid-winter has not changed significantly since the 1980s.

A cyclical trend in storm frequency is evident in the data compiled by Walsh and Eicken (2007), who tabulated the number of storm events during the open-water and freeze-up seasons at Barrow from 1950 through 2004 (Figure 76). The storm count during freeze-up increased from the mid-1950s through early 1960s, declined from the early 1960s through mid-1970s, rose again from the mid-1970s through early 1990s, and remained nearly static from the early 1990s through 2004. The criteria used to identify storm events are not specified, but the data nevertheless indicate that the rise in storm frequency that began in the mid-1970s was sustained through the mid-2000s. Although other wind characteristics such as direction, intensity, and duration also influence ice dynamics, the rise in the number of storm events during freeze-up relative to the mid-1970s could cause an increase in wind-driven ice movement.

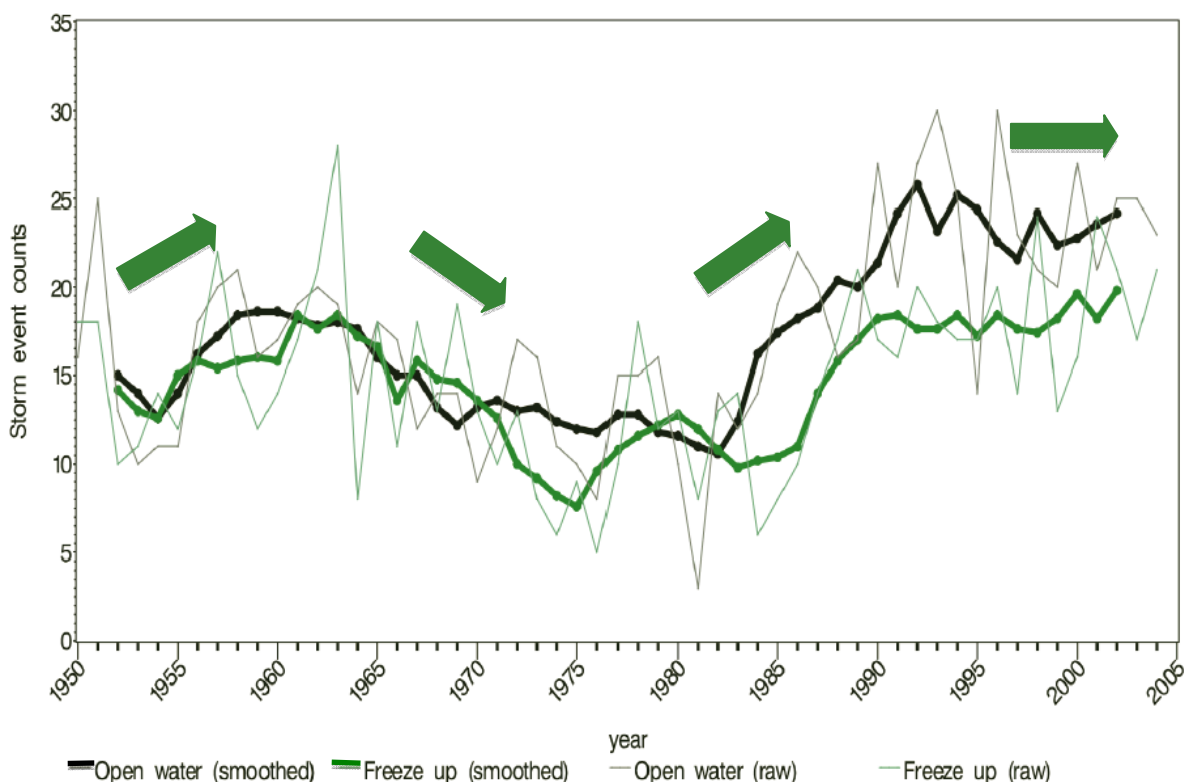


Figure 76. Yearly Storm Count at Barrow during the Open-Water and Freeze-Up Seasons, 1950-2004 (after Walsh and Eicken, 2007)

Trends: Since the mid-1970s, the frequency of storm events during freeze-up has increased by more than 50%. In contrast, the frequency of mid-winter storm events (January through April) is nearly identical to that in the early 1980s.

6.3. Timing of Freeze-Up

During the past five freeze-up seasons (2009-10 through 2013-14), the average monthly air temperatures at Barrow have exceeded the long-term averages for the period from 1971-72 through 1999-2000 by 4°F in September, 10°F in October, and 6°F in November (2°, 6°, and 3°C, respectively). These warmer temperatures in late summer and early autumn have contributed to, and in turn been intensified by, a decline in the extent of the pack ice (Section 4.2) and an increase in the temperature of the sea surface. The end result of this feedback loop (warmer air temperatures → reduced ice cover → warmer sea surface temperatures → warmer air temperatures) has been a significant delay in the onset of freeze-up in the Beaufort and Chukchi Seas.

The chronology of freeze-up in the Alaskan Beaufort Sea during the past five years is presented in Table 20. The date of freeze-up in the nearshore region ranged from October 11th to November 5th. The average, October 24th, is four days later than the average from 2002 through 2006 (Vaudrey, 2007) and 20 days later than that determined from 11 years of on-site observations and satellite imagery acquired from 1980 through 1985 and 1987 through 1991 (Vaudrey, 1982a; 1983; 1984; 1985a; 1985b, 1986; 1988-92). The accumulated freezing-degree days (FDD) at the time of nearshore freeze-up varied widely, from 80 to 363, with a mean value of 170.

Table 20. Chronology of Freeze-Up in the Alaskan Beaufort Sea, 2009 through 2013

Year	First Ice ¹		Nearshore Freeze-Up ²		Complete Freeze-Up ³	
	Date	FDD	Date	FDD	Date	FDD
2009	Sep 28	15	Oct 22	106	Nov 9	412
2010	Oct 4	19	Oct 11	80	Nov 2	305
2011	Oct 12	14	Oct 26	102	Nov 1	201
2012	Oct 15	51	Nov 5	363	Nov 12	508
2013	Sep 24	19	Oct 26	197	Nov 20	678
Average	Oct 5	24	Oct 24	170	Nov 9	421

Notes:

¹ “First Ice” refers to the date on which ice began to form in protected waters.

² “Nearshore Freeze-Up” refers to the date on which ice covered the region typically occupied by landfast ice.

³ “Complete Freeze-Up” refers to the date on which ice covered the entire Alaskan Beaufort Sea.

Complete freeze-up in the Alaskan Beaufort Sea occurred between November 1st and 20th, with the latter occurring in 2013. The average was November 9th. As in the case of nearshore freeze-up, the number of FDD at complete freeze-up varied widely over the five-year period of record (201 to 678). This outcome confirms that air temperature alone cannot be used to predict the date of freeze-up, and that other factors such as the sea surface temperature, wind conditions, and salinity must be taken into account.

Freeze-up dates in the Chukchi Sea during the past five years are presented in Table 21. Nearshore freeze-up occurred between November 4th and 26th with an average of November 16th. Based on an assessment of landfast ice formation performed by Mahoney, *et al.* (2007), this date is about one month later than in the mid-1970s. A significant delay in the occurrence of freeze-up also is implied by the research of Rodrigues (2009), who found that the length of the ice-free season off the coast between Point Barrow and Point Lay has increased from approximately 30 days in the late 1970s to 125 days at present. The accumulated FDD at the time of nearshore freeze-up averaged 484 during the past five years but varied widely, from 265 to 697.

Table 21. Chronology of Freeze-Up in the Chukchi Sea, 2009 through 2013

Year	First Ice ¹		Nearshore Freeze-Up ²		Complete Freeze-Up ³	
	Date	FDD	Date	FDD	Date	FDD
2009	Oct 9	17	Nov 16	535	Nov 29	949
2010	Oct 7	16	Nov 4	265	Dec 7	959
2011	Oct 6	24	Nov 20	601	Nov 30	1022
2012	Oct 13	4	Nov 15	322	Nov 28	722
2013	Oct 2	39	Nov 26	697	Dec 14	1104
Average	Oct 7	20	Nov 16	484	Dec 4	951

Notes:

- ¹ “First Ice” refers to the date on which ice began to form in protected waters (excluding ice that formed but subsequently melted before freeze-up began in earnest).
- ² “Nearshore Freeze-Up” refers to the date on which ice covered the region south of Point Barrow and east of the 163°W meridian.
- ³ “Complete Freeze-Up” refers to the date on which ice covered the entire Chukchi Sea north of Cape Lisburne.

Complete freeze-up in the Chukchi Sea north of Cape Lisburne took place between November 28th and December 14th. The average was December 4th, corresponding to an

average of 951 FDD. In 2013, nearshore and complete freeze-up occurred later than in any of the prior four years. The associated numbers of FDD were the highest recorded to date.

Trend: Freeze-up in the nearshore region currently tends to occur during the fourth week in October in the Alaskan Beaufort Sea, and the third week in November in the northeastern Chukchi Sea. The former is about three weeks later than in the 1980s, while the latter is about one month later than in the 1970s.

6.4. First-Year Ice Growth

As discussed in Section 4.1, the growth of undeformed first-year ice can be estimated on the basis of freezing-degree days (FDD) using the relationship of Lebedev (Bilello, 1960). Table 22 presents the computed ice thickness on a monthly basis for each winter season from 1970-71 through 2013-14. The results were obtained using the FDD data for Barrow Airport compiled in Table 15, and are presented in a comparable format with the highest ranking (No. 1) assigned to the lowest predicted ice thickness and the lowest ranking (No. 44) to the highest thickness.

The warm air temperatures that prevailed during the 2013-14 freeze-up season produced the lowest computed ice thickness in the entire 44-year period of record by a wide margin: 143 cm versus a prior minimum of 151 cm in 2010-11, 2002-03, and 1997-98. Two of the remaining three years covered by the current round of freeze-up studies also produced ice thicknesses that ranked among the lowest in the database: 154 cm in 2009-10 (tied for 6th lowest) and 155 cm in 2012-13 (tied for 8th lowest). The only exception was 2011-12, with a computed thickness of 167 cm that tied for 26th among the 44 values shown in Table 22. Notwithstanding this relatively large value, the average thickness over the past five years, 154 cm, is 17 cm less than that computed for the six-year period from 1980-81 through 1985-86.

Additional perspective on the reduced growth of first-year ice is provided by Figure 77, which compares the computed thickness of undeformed first-year ice at the end of each month in each of the past five winter seasons with the corresponding average value for the period from 1970-71 through 1989-90. Even in the anomalously cold year, 2011-12, the ice failed to attain the average thickness that prevailed in the 1970s and 1980s.

The reduction in ice thickness attributable to warmer temperatures may be exacerbated by an increase in the depth of the snow cover. To quantify the relative importance of these and other factors, Brown and Cote (1992) investigated the interannual variability in the maximum ice thickness at four sites in the Canadian High Arctic between 1950 and 1989

Table 22. Computed Ice Thickness (cm) at Barrow, 1970-71 through 2013-14

Year	Sep	Oct	Nov	Dec	Jan	Feb	Mar	Apr	May	44-yr Rank
1970-71	16	52	77	102	127	150	169	182	186	43
1971-72	3	33	61	90	115	137	158	171	176	39
1972-73	7	24	55	79	105	125	148	161	165	21
1973-74	3	26	50	78	102	129	151	166	170	31
1974-75	5	43	73	108	135	152	167	180	183	42
1975-76	18	48	79	110	134	155	173	184	189	44
1976-77	4	34	60	92	113	133	156	169	173	37
1977-78	0	24	60	87	107	127	145	157	162	16
1978-79	5	42	63	93	110	133	153	165	169	28
1979-80	0	26	48	81	107	126	144	158	163	17
1980-81	15	37	67	97	114	134	151	163	165	21
1981-82	14	37	64	90	113	129	148	160	165	21
1982-83	7	43	75	99	125	143	161	172	176	39
1983-84	17	47	69	89	114	142	161	176	181	41
1984-85	0	29	65	94	114	135	153	167	170	31
1985-86	10	40	63	89	114	131	152	166	170	31
1986-87	4	31	59	85	110	132	150	164	167	26
1987-88	9	23	59	87	110	130	149	160	164	19
1988-89	9	48	81	104	131	139	155	164	169	28
1989-90	0	29	68	94	122	144	161	170	171	35
Average	7	36	65	92	116	136	155	168	172	
Std. Dev.	6	9	9	9	10	9	8	8	8	
Year	Sep	Oct	Nov	Dec	Jan	Feb	Mar	Apr	May	44-yr Rank
1990-91	6	30	65	95	118	139	159	169	169	28
1991-92	6	30	65	95	121	143	159	170	173	37
1992-93	17	41	67	93	116	134	152	161	164	19
1993-94	6	21	49	79	102	121	143	155	159	12
1994-95	10	42	73	102	123	143	162	170	171	35
1995-96	0	27	54	85	106	128	144	156	157	11
1996-97	13	46	64	87	114	133	152	162	166	25
1997-98	2	25	46	79	106	126	141	149	151	2
1998-99	0	16	52	83	110	129	149	162	165	21
1999-00	5	29	59	91	115	135	153	164	170	31
2000-01	7	30	59	84	107	122	143	154	161	14
2001-02	8	40	66	91	117	137	150	161	163	17
2002-03	0	19	47	73	98	120	139	147	151	2
2003-04	0	18	50	79	102	127	147	158	161	14
2004-05	3	23	53	82	104	124	141	152	155	8
2005-06	3	22	56	81	105	123	145	158	160	13
2006-07	0	14	45	72	101	120	140	149	154	6
2007-08	0	18	39	66	96	122	143	152	155	8
2008-09	2	20	50	73	100	117	139	150	152	5
2009-10	3	15	51	77	105	123	142	150	154	6
2010-11	3	20	43	76	100	117	135	148	151	2
2011-12	2	19	53	83	112	132	154	164	167	26
2012-13	0	12	44	76	100	123	140	152	155	8
2013-14	7	18	45	72	96	114	131	142	143	1
Average	4	25	54	83	108	128	147	157	160	
Std. Dev.	5	10	9	9	8	8	7	7	7	

Note: The computed ice thickness for May 2013-14 is based on FDD accumulated through June 2nd.

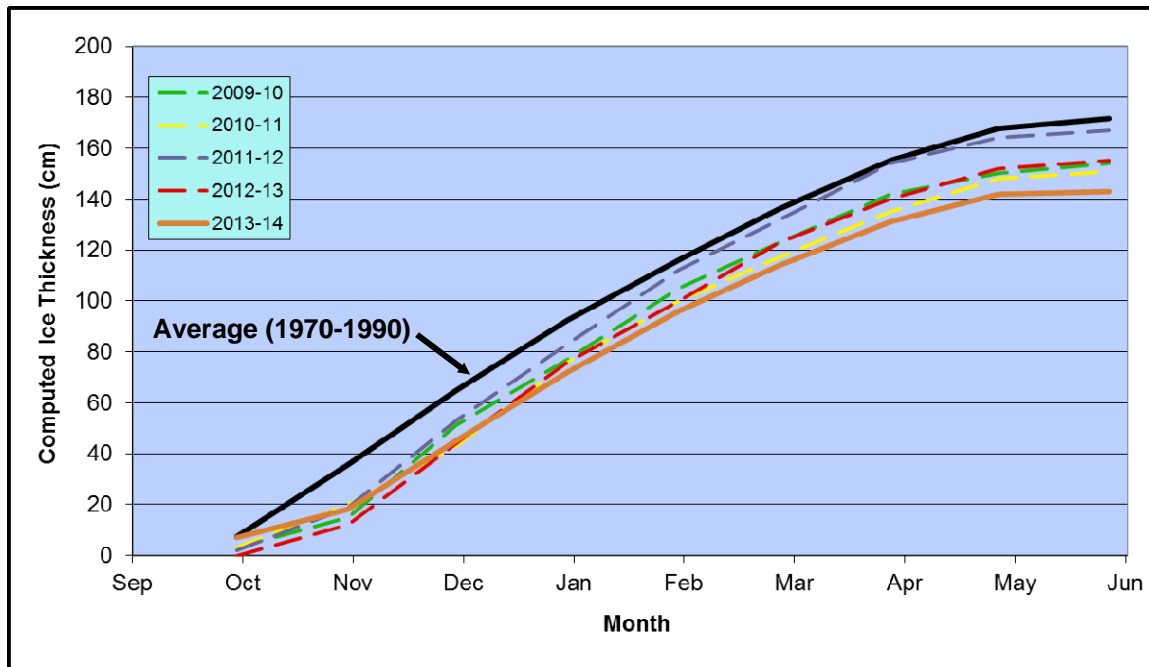


Figure 77. Computed Ice Thickness: Recent Winters vs. 1970s and 1980s

using a one-dimensional heat transfer model of ice growth. The depth of the snow cover was found to be the most important factor, explaining 30% to 60% of the variance in the maximum first-year ice thickness due to its insulating effect. Density fluctuations in the snow cover were estimated to explain an additional 15% to 30% of the variance. In contrast, annual variations in air temperature accounted for less than 4% of the variance in the maximum first-year ice thickness.

The average snowfall at Barrow during the six-month freeze-up season (October through March) has increased dramatically, from 34 cm in the 1980s to 64 cm in the 1990s and 93 cm in the 2000s (Figure 78). Despite a comparatively small accumulation of 89 cm in 2013-14, the average value over the past five freeze-up seasons has risen to 118 cm – nearly three and a half times larger than in the 1980s.

In addition to reducing the ice thickness, higher air temperatures tend to prolong the existence of leads and retard the production of new ice in those leads. Furthermore, higher temperatures and the insulating effect of heavier snowfall decrease the consolidation within ridges and rubble fields and reduce the overall strength of the ice canopy.

Trend: Based on air temperatures alone, the thickness of undeformed first-year ice attained during an average winter has decreased by nearly 10% (17 cm) since the early to mid-1980s. However, a significant increase in snowfall may be causing a greater reduction

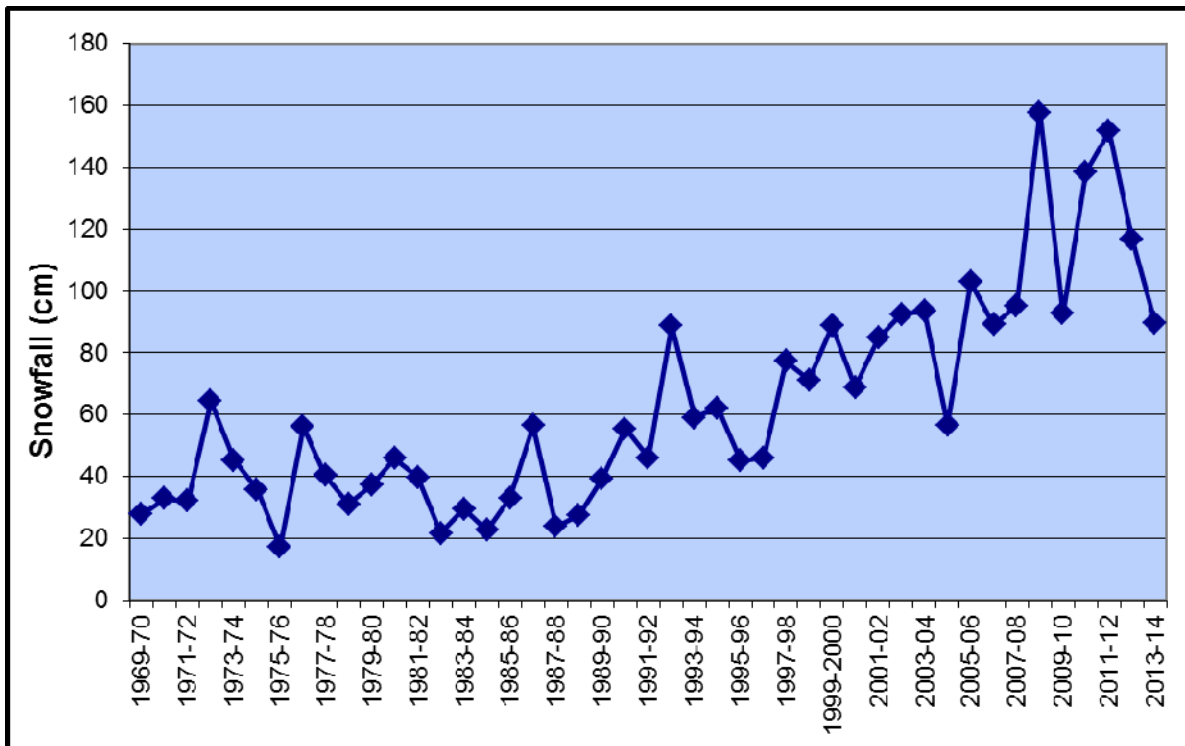


Figure 78. Annual Snowfall at Barrow during Freeze-Up (October 1 - March 31), 1969-70 through 2013-14

in the ice thickness due to its insulating effect. Other temperature-related factors, including reduced ice production in leads, decreased consolidation of ridges and rubble fields, and reduced ice strength, probably exert greater impacts on ice dynamics than reduced thickness.

6.5. Landfast Ice

Personal observations and data presented by investigators that include Barry, *et al.* (1979), Eicken, *et al.* (2006), and Mahoney, *et al.* (2012), indicate that characteristic patterns and features of the ice cover tend to recur. Such patterns include the distribution of landfast ice and the occurrence of leads and polynyas over the course of the winter. Factors that contribute to the recurring patterns include the seasonal cycles of meteorological and oceanographic conditions, the geometry of the shoreline and bathymetric contours, and the presence of shoals.

Beaufort Sea: The wind, which tends to be coast-parallel in the Alaskan Beaufort Sea, constitutes the dominant driving force for ice movement. Easterlies produce westerly ice motion with an onshore component, creating a stable landfast ice zone that ultimately extends to the vicinity of the 20-m isobath (Mahoney, *et al.*, 2012). The

western Beaufort between Point Barrow and Prudhoe Bay contains numerous shoals that are located up to 25 nm (46 km) offshore. The most prominent are Weller Bank, which lies off Harrison Bay, and Stamukhi Shoal, which lies off Pingok Island. The large grounded rubble piles that typically form on these shoals produce a significant seaward extension of the landfast ice. In contrast, water depths to the east of Prudhoe Bay increase more rapidly off the barrier islands from Cross to Flaxman and off the coast in the vicinity of Barter Island. In these areas, the landfast ice zone tends to be less than 5 nm (9 km) wide. An exception occurs in Camden Bay, where landfast ice can extend more than 10 nm (19 km) offshore.

During the 2009-10, 2011-12, 2012-13, and 2013-14 freeze-up seasons, warm air temperatures and a lack of strong, sustained easterly winds in the fall produced a narrow landfast ice zone that persisted into December. By late January, however, easterly storm activity had created a relatively wide landfast ice zone anchored by a grounded shear zone to the west of Prudhoe Bay that was reminiscent of the conditions observed in the early 1980s. Although substantial landfast ice development to the west of Prudhoe Bay also occurred in 2010-11, the formation of a securely-grounded shear zone was inhibited by a paucity of easterly storms and sustained easterly winds that persisted through mid-winter. As a result, the landfast ice zone remained narrower and less stable than in any of the other four years.

To the east of Prudhoe Bay, the contrast between the 1980s and the past five years encompasses not only the timing but also the extent of landfast ice development. A well-established, firmly-grounded shear zone formed off the barrier islands during five of the six freeze-up periods monitored in the 1980s. In three of the past five years, however, the ice in this region remained poorly-grounded and mobile throughout freeze-up and early winter. Exceptions occurred in each of the past two years, when prolonged easterly storms coupled with sustained easterly winds created a stable, grounded shear zone in January that persisted through March.

Chukchi Sea: As discussed in Section 5, easterly (offshore) winds and relatively steep slopes in the nearshore area limit the extent of the landfast ice in the Chukchi Sea to a narrow strip along the shoreline. The offshore edge typically lies within 5 nm (9 km) of the coast, but can retreat to the coast itself during breakout events triggered by easterly storms. Exceptions occur in the semi-protected areas to the east of Blossom Shoals and Point Franklin, where the landfast ice tends to be wider and more stable.

Due to its dynamic nature, particularly with respect to breakout events, the landfast ice zone in the Chukchi fails to exhibit the progressive expansion over the course of the freeze-

up season typically seen in the Beaufort. As a result, its maximum seaward extent is poorly correlated with water depth (Mahoney, *et al.*, 2012). In addition, the dynamic nature of the landfast ice zone increases the potential for ridge and rubble formation in the nearshore region and pile-ups at the shoreline.

The tendency toward a narrow, ephemeral landfast ice zone in the northeast Chukchi Sea was demonstrated in each of the past five freeze-up seasons. Instability was particularly prevalent in 2010-11 and 2012-13; in both cases, a continuous, well-grounded strip of landfast ice failed to materialize throughout freeze-up and early winter.

Trend: In the Alaskan Beaufort Sea, the extent of the landfast ice zone to the west of Prudhoe Bay is similar to that observed in the 1980s but the ice develops more slowly. To the east of Prudhoe Bay, a stable, well-grounded shear zone is far less likely to develop during freeze-up and early winter. In the Chukchi, the narrow, ephemeral nature of the landfast ice zone noted in the 1980s continues to prevail today.

6.6. Coastal Flaw Lead

Seaward of the landfast ice zone in the northeast Chukchi Sea, the ice is driven offshore during periods of easterly winds. The resulting flaw lead separates the mobile pack ice from the stationary landfast ice, and generates new ice throughout the winter as it experiences repeated cycles of opening, expanding, and either closing or refreezing. The width of the lead can vary substantially, depending on the duration and intensity of the easterly winds.

During the three freeze-up studies in the 1980s that included the Chukchi Sea, Vaudrey (1984; 1985; 1986) observed flaw lead widths of 1, 5, and 15 nm (2, 9, and 28 km) at the end of January 1984, 1985, and 1986, respectively. Substantially greater widths have been detected during the current freeze-up studies, with the maximum observed values ranging from 50 nm (93 km) in 2009-10 to 150 nm (278 km) in 2012-13 (Coastal Frontiers and Vaudrey, 2010; 2013). At least some of this disparity may be explained by the fact that Vaudrey's findings were obtained from reconnaissance flights conducted over short periods of time. Nevertheless, the order-of-magnitude difference prompted speculation that the flaw lead may attain greater widths and persist longer than in the 1980s (Coastal Frontiers and Vaudrey, 2013) – a trend that would be consistent with a more dynamic ice canopy subject to displacement at lower wind speeds.

A more detailed assessment of the flaw lead was undertaken during the past year in conjunction with a study of multi-year ice invasions sponsored by Shell. As reported by Ward, *et al.* (in press), satellite imagery covering the 21 winters from 1993-94 through

2013-14 was used to determine the number of days that the flaw lead existed during the five-month period from December through April. The findings suggest that, in contrast to the aforementioned hypothesis, the frequency of occurrence has not changed appreciably. The lead was present 51% of the time during the first ten winters and 49% during the last eleven. The frequency with which the flaw lead extends to the northeast of Point Barrow also appears to have remained constant; it averaged 35% during first ten years in the period of record, and 37% during the last eleven.

Trend: The frequencies with which the flaw lead and extended flaw lead occur off the Chukchi Sea coast have remained constant since the 1990s. Limited observations suggest that the width of the flaw lead may have increased since the 1980s, but the data are insufficient to confirm the existence of this trend.

6.7. Multi-Year Ice

Two types of “multi-year” or “old” ice can occur in the Beaufort and Chukchi Seas: (1) true multi-year floes from the permanent polar pack in the Arctic Ocean (“pack floes”), and (2) second-year ice formed in the nearshore zone and spared from melting and/or transport offshore during the ensuing summer by a combination of cold air temperatures, mild winds, and a preponderance of northerly or westerly winds. These “second-year floes” are fragments of first-year rubble fields or remnants of the shear zone that develops off the coast of the Beaufort Sea and in the Canadian archipelago. Such floes can be distinguished from pack floes by their more jagged appearance, with many embedded ridges, and by their greater thickness (6 to 9 m for second-year floes versus 3 to 5 m for pack floes).

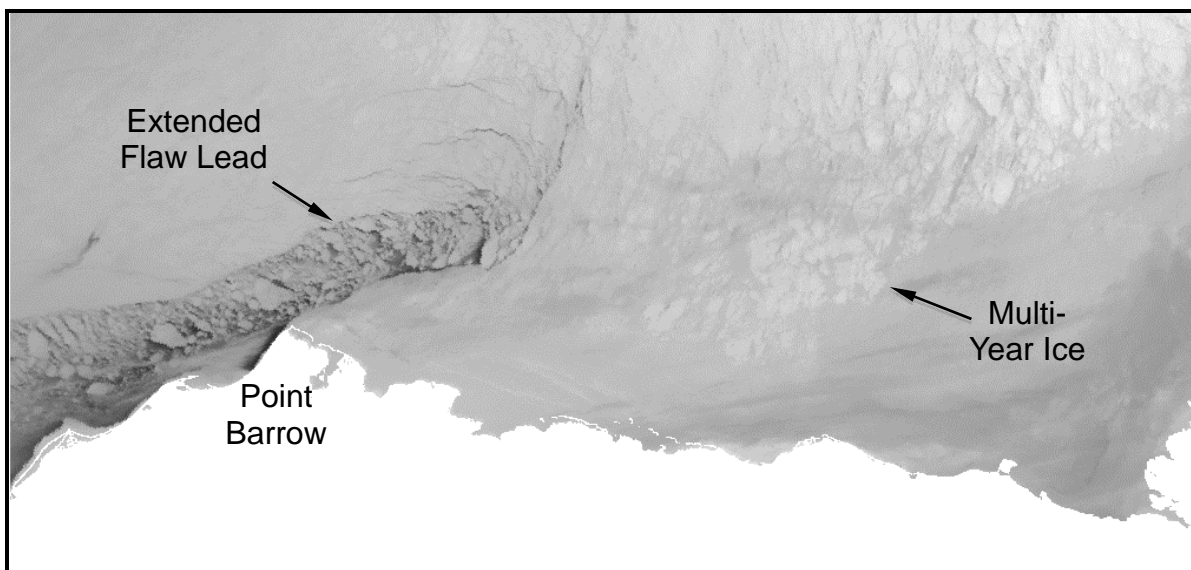
Beaufort Sea: When the initial round of freeze-up studies was conducted in the 1980s, large multi-year ice floes were present in the nearshore region of the Alaskan Beaufort Sea during three of the six freeze-up seasons studied: 1980-81, 1983-84, and 1985-86 (Vaudrey, 1981a, 1981b, 1982a, 1983, 1984, 1985a, 1986). Grounded multi-year fragments with diameters as large as 120 m were observed during the other three seasons (1981-82, 1982-83, and 1984-85).

In the nine years that preceded the resumption of freeze-up studies in 2009-10, large multi-year floes invaded the nearshore region on only one occasion: 2001-02, when a low concentration approached the coast in the western Beaufort and northern Chukchi during the initial stages of freeze-up. The next invasion occurred in 2009-10, when a high concentration of massive floes with embedded ridges entered the nearshore region of the Alaskan Beaufort from Canada, moved west to Point Barrow, and split into northern and southern branches in the Chukchi (Coastal Frontiers and Vaudrey, 2010). Although

grounded fragments of multi-year ice were observed on many of the barrier islands in 2010-11 (Coastal Frontiers and Vaudrey, 2011), large multi-year floes were absent from southern portion of the Alaskan Beaufort Sea not only in that year but also in the three that followed. Hence, during the past 14 years, such floes have entered the nearshore region on only two occasions.

Chukchi Sea: Multi-year ice was present in the Chukchi Sea during each of the three freeze-up seasons from 1983-84 through 1985-86 (Vaudrey, 1984, 1985, 1986) and also during the midwinter season of 1987 (Vaudrey, 1987). The invasions were characterized by concentrations up to 70% and southerly limits between 70.5° and 71°N.

In eight of the fourteen winters from 2000-01 through 2013-14, the extended flaw lead channeled large multi-year floes into the region south and west of Point Barrow: 2000-01, 2001-02, 2003-2004, 2005-2006, 2008-09, 2009-10, 2011-12, and 2013-14 (Ward, *et al.*, in press). The invasions followed a similar pattern, with an extended flaw lead that stretched well past Point Barrow (a configuration known as the “Barrow Arch”; Eicken, *et al.*, 2006) until it intersected the southern boundary of the multi-year ice. A representative example from March 2001 is provided in Figure 79.



After Eicken, *et al.*, 2006

Figure 79. AVHRR Image Acquired on March 12, 2001, Showing Multi-Year Ice Floes Entering Coastal Flaw Lead

In addition to the eight winters listed above, an analysis of AVHRR imagery revealed the presence of multi-year ice in the region south and west of Point Barrow at the beginning of December 2010 (Ward, *et al.*, in press). Although cloud cover prevented the acquisition

of useful AVHRR imagery in late November, a predominance of westerly winds during this period suggests that the ice drifted into the area as part of a broad-based advance of multi-year ice rather than via an extended flaw lead.

Trend: The probability of large multi-year ice floes invading the nearshore portion of the Alaskan Beaufort Sea in any given year is substantially less than in the 1980s. This trend may be explained in part by a reduction in the amount of multi-year ice comprising the permanent polar pack (Perovich, *et al.*, 2013) and an associated increase in the northerly retreat of the ice edge during the summer months, both of which have reduced the opportunities for pack floes to enter the nearshore area. In addition, warmer air temperatures and increased storm frequencies have decreased the likelihood that remnants of the shear zone will survive the summer melt season to become second-year floes. Nevertheless, as demonstrated in 2009-10, the possibility of multi-year ice encounters cannot be ruled out in the nearshore region of the Beaufort. Furthermore, fragments of old ice analogous to those observed in 2010-11 can be present even if large multi-year floes remain well offshore.

The probability of multi-year ice entering the Chukchi Sea to the south and west of Barrow also has decreased since the 1980s, but to a lesser extent than in the Beaufort. Although the factors that have reduced the probability of invasions in the Beaufort also apply to the Chukchi, their impact has been partially offset by the ability of the coastal flaw lead to extend past Point Barrow until it intersects the southern boundary of the multi-year ice.

6.8. Pack Ice Movement

Pack ice movement in the Beaufort and northern Chukchi Seas can be broken down into two categories: (1) long-term, steady-state movement caused by the relatively constant rotation of the Beaufort Gyre (Figure 1) and (2) short-term, transient movement caused by wind events. As the latter varies greatly depending on the wind conditions and degree of ice confinement, insufficient data exist to compare the short-term motions observed in recent years with those in the 1980s. It is worth noting, however, that a multi-year ice floe study conducted in the Alaskan Beaufort Sea during the 1984 open-water season arrived at the following conclusions: (1) the wind factor (ratio of floe speed to wind speed) for floes in the nearshore area is not constant, but varies as a function of wind speed, wind direction, water depth, and keel depth; (2) although the data exhibit considerable scatter, wind factors of 4 to 6% are typical during periods of strong winds (Tekmarine, *et al.*, 1985).

Long-term pack ice motion, often referred to as “ice flux” or “ice drift”, plays a key role in the design of fixed structures in that it governs the number of encounters with design

ice features (such as multi-year floes) that can occur over a specified period. Although detailed analyses of ice movement were omitted from the freeze-up studies conducted from 1980-81 through 1985-86, median ice drift values were derived from several ice motion buoy programs conducted in the mid- to late 1980s (Vaudrey, 1987a; 1988a; 1989a; 1989b) and from the successive positions of two large multi-year ice floes identified in AVHRR images in Fall 1988 (Vaudrey, 1989a). The results for the months of November and December, which are summarized by Vaudrey (2007), ranged from 4.9 to 6.3 nm/day (9.1 to 11.3 km/day).

In the current round of freeze-up studies, monthly drift rates were derived for multi-year ice floes in November and December using successive RADARSAT-2 images acquired in 2011, 2011, and 2013. The data from the Alaskan Beaufort Sea (where the floes are subject to the westward set of the Beaufort Gyre) are summarized in Table 23. The drift rates ranged from 1.2 to 9.9 nm/day (2.2 to 18.3 km/day) and averaged 5.2 nm/day (9.6 km/day)

Table 23. Beaufort Sea Ice Drift in November and December

Year	Monthly Drift Rate (nm/day)		
	Maximum	Minimum	Average
2010	9.9	5.5	7.3
2011	8.3	4.9	6.3
2013	3.4	1.2	1.9
Average			5.2

Note: Monthly drift rates were derived from the analysis of successive RADARSAT-2 images.

Although the data obtained from the recent studies are not suitable for direct comparison with those from the 1980s due to differences in the methods of acquisition and analysis, they nevertheless suggest that drift rates during the early stages of freeze-up have not changed appreciably. This finding runs counter to the hypothesis of Walsh and Eicken (2007), who suggested that reduced ice thickness and increased storminess may lead to increased ice movement.

Trend: Based on the limited data acquired in recent years, the average drift rate of pack ice in the Alaskan Beaufort Sea during the early stages of freeze-up is about 5 nm/day (9 km/day). This value is comparable to that which prevailed in the 1980s.

7. SUMMARY AND CONCLUSIONS

Findings for Entire Study Area

1. ***Air Temperatures:*** The air temperatures during the 2013-14 winter season were exceptionally warm. Based on the temperature data recorded at Barrow Airport, the past winter represented the warmest in the past 44 years.
2. ***First-Year Ice Growth:*** The computed thickness of undeformed first-year ice at the end of the 2013-14 winter season was 152 cm in the Alaskan Beaufort Sea and 143 cm in the Chukchi, based on accumulations of 6,425 and 5,775 FDD at Deadhorse and Barrow Airports, respectively. These thickness values represent the lowest recorded during the past five winters and, in the case of the Chukchi, the lowest in the past 44 years. The highest values in recent years, 176 cm in the Beaufort and 167 cm in the Chukchi, occurred in 2011-12.
3. ***Prediction of Freeze-Up:*** During the past five freeze-up seasons, the number of FDD at the time of freeze-up has varied widely in both the Beaufort and Chukchi Seas. This finding confirms that air temperature alone cannot be used to predict the date of freeze-up, and that other factors such as the sea surface temperature, wind conditions, and salinity must be taken into account.

Findings for Beaufort Sea

1. ***Late Summer:*** The ice cover in the Alaskan Beaufort Sea diminished throughout August and early September, 2013. The minimum extent of the pack ice occurred on September 13th. Although 50% larger than in 2012, it nevertheless represented the sixth lowest value since the acquisition of satellite-based data began in 1979.
2. ***Freeze-Up:*** Freeze-up commenced in late September, when ice began to form in the semi-protected waters adjacent to the coast. Complete ice coverage in the nearshore region occurred on October 26th, followed by complete coverage in the Alaskan Beaufort Sea on November 20th. During the past five years, the average date of nearshore freeze-up was October 24th, while that of complete freeze-up was November 9th.
3. ***Wind Regime:*** Based on the average daily wind directions recorded at Deadhorse Airport, westerlies prevailed more than 50% of the time in every month except January, and more than 60% of the time in November, February, and March. Over the entire

six-month study period, westerlies outnumbered easterlies by a ratio of 57% to 43%. The highest average monthly wind speed, 15 kt (8 m/s) occurred in January.

4. **Storm Events:** Storm events with average daily wind speeds exceeding 15 kt (8 m/s) occurred on twenty occasions encompassing 43 days. Nine of the events were easterlies, while eleven were westerlies. Both the total number of storms and total number of storm days were slightly higher than the average values over the past five freeze-up seasons (eighteen storms and 41 storm days).
5. **Landfast Ice:** The landfast ice zone remained narrow and poorly-developed until the end of December due to a predominance of westerly winds, a series of westerly storms, and a paucity of sustained easterly storms. The situation changed in January, when persistent easterly winds coupled with two prolonged easterly storms produced a substantial expansion past the 18-m isobath that extended from Point Barrow to Barter Island. In February and March, the landfast ice edge advanced in response to easterly winds and retreated in response to westerly winds but tended to retreat no farther than the 18-m isobath due to the existence of a well-grounded shear zone.
6. **Ice Pile-Ups:** Forty-six ice pile-ups occurred in central portion of the Alaskan Beaufort Sea during the 2013-14 freeze-up season. Thirty-nine were located on natural barrier islands, four on man-made facilities, and three on the mainland shore. The heights ranged from 1 to 8 m, the encroachment distances from 0 to 20 m, the alongshore lengths from 50 to 2,600 m, and the ice block thicknesses from 30 to 60 cm.
7. **Multi-Year Ice:** Multi-year ice was present in the offshore portion of the Alaskan Beaufort Sea throughout freeze-up and early winter, but remained absent from the nearshore region except in the immediate vicinity of Point Barrow. During the past fourteen freeze-up seasons (2000-01 through 2013-14), large multi-year floes have invaded the nearshore region on only two occasions, 2001-02 and 2009-10. This finding suggests that the probability of an invasion in any given freeze-up season is less than 15%.

Findings for Chukchi Sea

1. **Freeze-Up:** Freeze-up in the Chukchi Sea began during the first week in October but proceeded slowly due to unseasonably warm temperatures that persisted through mid-November. Complete ice coverage in the nearshore region occurred on November 26th, followed by complete coverage in the entire Chukchi Sea north of Cape Lisburne on December 14th. These dates are the latest recorded in the past five years, with each exceeding the corresponding average value for the five-year period by ten days.
2. **Flash-Freeze Event:** On or about November 12th, a flash freeze created a small patch of ice centered 130 nm (241 km) west of Icy Cape. Although much smaller than that

which formed off Wainwright in October 2013, it nevertheless marked the second documented occurrence of flash freezing in the Chukchi Sea over the past five freeze-up seasons.

3. **Wind Regime:** In sharp contrast to the Beaufort, easterly winds prevailed in the Chukchi in each month from October through March. Over the entire six-month period, easterlies outpaced westerlies by a margin of 61 to 39%. The highest average monthly speed, 14 kt (7 m/s), occurred in November and January.
4. **Storm Events:** Nineteen storm events were recorded from October through March. Twelve were easterlies, including five of the six storms that occurred after December 24th. The easterlies produced 29 storm-days, while the westerlies produced thirteen. Both the total number of storms and total number of storm days were slightly higher than the average values over the past five freeze-up seasons (sixteen storms and 40 storm days).
5. **Landfast Ice:** At the end of November, a narrow, discontinuous strip of landfast ice extended from Barrow to Peard Bay, and another narrow strip extended from Wainwright to the vicinity of Point Lay. The landfast ice zone remained narrow throughout December except for an advance to Blossom Shoals (off Icy Cape) that occurred at the end of the month. The ice remained grounded on this feature for the remainder of the study period. In mid-January, a prolonged easterly storm dislodged virtually all of the landfast ice north of the Nokotlek River Mouth. Subsequently, the ice waxed and waned in response to changing wind conditions, producing widths that ranged from negligible to 20 nm (37 km). At the end of March, the landfast ice was confined to a narrow strip that was located inside the 11-m isobath in most areas.
6. **Coastal Flaw Lead:** The distinctive flaw lead that opens off the Chukchi Sea coast in response to easterly winds was present on 57% of the days from December 2013 through March 2014. The frequency of occurrence peaked at 69% in January in response to a predominance of easterly winds and three easterly storms. The maximum width of 100 nm (185 km) occurred in February, at which time the lead encompassed all of the Burger and Crackerjack Prospects and parts of the Hanna Shoal and West Prospects. The maximum length, 250 nm (463 km), occurred on repeated occasions in February and March. The maximum persistence of 15 days took place from mid-February to early March.
7. **Nearshore vs. Offshore Ice Cover:** As in each of the past four years, a change in the nature of the ice canopy was noted on the seaward side of the coastal flaw lead during the aerial reconnaissance flights. Within about 50 nm (93 km) of the coast, where the

lead had caused a loss of confinement, the ice evidenced greater deformation indicative of collisions. Farther offshore, where the differential motion between individual floes had been limited by the more consolidated nature of the ice canopy, the ridges and rubble were more widely spaced.

8. ***Ice Pile-Ups:*** Twenty-two ice pile-ups were observed on the coast of the northeast Chukchi Sea during the 2013-14 freeze-up season. The highest concentration was located to the east of Icy Cape on the barrier islands that form the seaward boundary of Kasegaluk Lagoon. The pile-up heights, which varied from 1 to 3 m, were the smallest in the past five years. All 22 pile-ups encroached onto the subaerial beach, with encroachment distances ranging from 5 to 20 m, alongshore lengths from 100 to 7,800 m, and ice block thicknesses from 30 to 40 cm.
9. ***Multi-Year Ice:*** Multi-year ice remained north of Point Barrow until mid-December. During the month that followed, multi-year floes were channeled into the region south and west of the Point on four occasions by a northeasterly extension of the coastal flaw lead. The last invasion, which occurred in mid-January, produced a significant southerly displacement of the multi-year ice edge. The ice continued to advance slowly to the south in February and March, crossing the 71° parallel in late February and reaching the vicinity of Icy Cape in mid-March. Large multi-year ice floes have invaded the region south and west of Point Barrow in nine of the past fourteen freeze-up seasons: 2000-01, 2001-02, 2003-04, 2005-06, 2008-09, 2009-10, 2010-11, 2011-12, and 2013-14. This finding suggests that the probability of an invasion in any given freeze-up season is about 65%.

Freeze-Up in Recent Years versus the 1980s

1. ***Air Temperatures:*** Since the 1970s, progressively warmer winter seasons have caused the number of freezing-degree days at Barrow to decline at an average rate of 44 per year. The greatest increases in temperature have occurred early in the freeze-up season, in October and November.
2. ***Winds:*** Since the mid-1970s, the frequency of storm events during freeze-up has increased by more than 50%. However, the frequency of mid-winter storm events (January through April) is nearly identical to that in the early 1980s.
3. ***Freeze-Up:*** Freeze-up in the nearshore region currently tends to occur during the fourth week in October in the Alaskan Beaufort Sea, and third week in November in the northeastern Chukchi Sea. The former is about three weeks later than in the 1980s, while the latter is about one month later than in the 1970s.

4. ***First-Year Ice Growth:*** Based on air temperatures measured at Barrow Airport, the thickness of undeformed first-year ice attained during an average winter has decreased by nearly 10% (17 cm) since the early 1980s. However, a significant increase in snowfall may be causing a greater reduction in ice thickness due to its insulating effect. Other temperature-related factors, including reduced ice production in leads, decreased consolidation of ridges and rubble fields, and reduced ice strength, probably exert greater impacts on ice dynamics than reduced thickness.
5. ***Landfast Ice Development and Stability:*** In the Alaskan Beaufort Sea, the extent of the landfast ice zone to the west of Prudhoe Bay is similar to that observed in the 1980s but the ice develops more slowly. To the east of Prudhoe Bay, a stable, well-grounded shear zone is far less likely to develop during freeze-up and early winter. In the Chukchi, the narrow, ephemeral nature of the landfast ice zone noted in the 1980s continues to prevail today.
6. ***Coastal Flaw Lead:*** The frequencies with which the flaw lead and extended flaw lead occur off the Chukchi Sea coast have remained constant since the 1990s. Limited observations suggest that the width of the flaw lead may have increased since the 1980s, but the data are insufficient to confirm the existence of this trend.
7. ***Multi-Year Ice in the Alaskan Beaufort Sea:*** The probability of large multi-year ice floes invading the nearshore portion of the Alaskan Beaufort Sea in any given year is substantially less than in the 1980s. This trend may be explained in part by a reduction in the amount of multi-year ice comprising the permanent polar pack and an associated increase in the northerly retreat of the ice edge during the summer months, both of which have reduced the opportunities for pack floes to enter the nearshore area. In addition, warmer air temperatures and increased storm frequencies have decreased the likelihood that remnants of the shear zone will survive the summer melt season to become second-year floes. Nevertheless, as demonstrated in 2009-10, the possibility of multi-year ice encounters cannot be ruled out for developments in the nearshore region.
8. ***Multi-Year Ice in the Chukchi Sea:*** The probability of multi-year ice entering the Chukchi Sea to the south and west of Barrow has decreased since the 1980s, but to a lesser extent than in the Beaufort. Although the factors that have reduced the probability of invasions in the Beaufort also apply to the Chukchi, their impact has been partially offset by the ability of the coastal flaw lead to extend past Point Barrow until it intersects the southern boundary of the multi-year ice.
9. ***Pack Ice Movement:*** Based on the limited data acquired in recent years, the average drift rate of pack ice in the Alaskan Beaufort Sea during the early stages of freeze-up is about 5 nm/day (9 km/day). This value is comparable to that which prevailed in the 1980s.

8. REFERENCES

- Barrett, S.A., and W.J. Stringer, 1978, "Growth Mechanisms of Katie's Floeberg", *Arctic and Alpine Research*, Vol. 10, No. 4, pp.775-783.
- Barry, R.G., R.E. Moritz, and J.C. Rogers, 1979, "The Fast Ice Regimes of the Beaufort and Chukchi Sea Coasts", *Cold Regions Science and Technology*, Vol. 1, pp. 129-152.
- Bilello, M., 1960, "Formation, Growth, and Decay of Sea Ice in the Canadian Arctic Archipelago", SIPRE Research Report 65, Hanover, New Hampshire.
- Brown, R. and P. Cote, 1992, "Interannual Variability of Landfast Ice Thickness in the Canadian High Arctic 1950-89", *Arctic*, Vol. 45, No. 3, pp. 273-284.
- Canadian Ice Service, 2014, <http://ice-glaces.ec.gc.ca/app/WsvPrdCanQry.cfm?subID=2003&Lang=eng>.
- Coastal Frontiers Corporation, 2013, "Bathymetric Survey at the Site of a Grounded Ice Feature in the Chukchi Sea", Joint Industry Project performed for Shell International Exploration and Production, Inc., Statoil, and the Bureau of Safety and Environmental Enforcement, U.S. Dept. of the Interior, Chatsworth, California 43 pp.+ appen.
- Coastal Frontiers Corporation and Vaudrey and Associates, Inc., 2010, "2009-10 Freeze-Up Study of the Alaskan Beaufort and Chukchi Seas", Joint Industry Project performed for Shell International Exploration and Production, Inc., and the U.S. Minerals Management Service, Chatsworth, California, 100 pp. + appen.
- Coastal Frontiers Corporation and Vaudrey and Associates, Inc., 2011, "2010-11 Freeze-Up Study of the Alaskan Beaufort and Chukchi Seas", Joint Industry Project performed for Shell Offshore, Inc., and the Bureau of Ocean Energy Management, Regulation, and Enforcement, U.S. Dept. of the Interior, Chatsworth, California, 149 pp. + appen.
- Coastal Frontiers Corporation and Vaudrey and Associates, Inc., 2012a, "2011-12 Freeze-Up Study of the Alaskan Beaufort and Chukchi Seas", Joint Industry Project performed for Shell International Exploration and Production, Inc., and the Bureau of Safety and Environmental Enforcement, U.S. Dept. of the Interior, Chatsworth, California, 182 pp. + appen.
- Coastal Frontiers Corporation and Vaudrey and Associates, Inc., 2012b, "Ice Encroachment in the Alaskan Beaufort Sea", Joint Industry Project performed for Shell Exploration and Production Company, and the Bureau of Safety and Environmental Enforcement, U.S. Dept. of the Interior, Chatsworth, California, 78 pp. + appen.

- Coastal Frontiers Corporation and Vaudrey and Associates, Inc., 2013 (revised January 2014), “2012-13 Freeze-Up Study of the Alaskan Beaufort and Chukchi Seas”, Joint Industry Project performed for Shell Gulf of Mexico Inc. and Shell Offshore Inc., Statoil Petroleum AS, and the Bureau of Safety and Environmental Enforcement, U.S. Dept. of the Interior, Moorpark, California, 175 pp. + appen.
- Dickins, D. and K. Vaudrey, 1994, “Phase III Ice Conditions, ANS Gas Commercialization Study: Marine Export Facilities”, prepared for Arco Alaska Inc., BP Exploration (Alaska) Inc., and Exxon Company, USA, prepared by DF Dickins Associates Ltd., Salt Spring Island, British Columbia, and Vaudrey & Associates Inc., San Luis Obispo, California.
- Eicken, H., L. Shapiro, A. Gaylord, A. Mahoney, and P. Cotter, 2006, “Mapping and Characteristics of Recurring Spring Leads and Landfast Ice in the Beaufort and Chukchi Seas”, OCS Study MMS 2005-068, U.S. Department of the Interior, Mineral Management Service, Alaska Outer Continental Shelf Region, Anchorage, Alaska.
- Kovacs, A., A. Gow, and W. Dehn, 1976, “Islands of Grounded Sea Ice”, CRREL Report 76-4, Hanover, New Hampshire.
- MacDonald, Dettweiler and Associates Ltd., 2013 and 2014, <http://gs.mdacorporation.com/>.
- Mahoney, A., H. Eicken, A. Gaylord, and L. Shapiro, 2007, “Alaska Landfast Sea Ice: Links with Bathymetry and Atmospheric Circulation”, *Journal of Geophysical Research*, Vol. 112, C02001.
- Mahoney, A., H. Eicken, L. Shapiro, R. Gens, T. Heinrichs, F. Meyer, and A. Graves, 2012, “Mapping and Characterization of Recurring Spring Leads and Landfast Ice in the Beaufort and Chukchi Seas”, Final Report, OCS Study BOEM 2012-067, University of Alaska Fairbanks, Fairbanks, Alaska, 154 pp.
- Melling, H. and D. Riedel, 2005, “Trends in the Draft and Extent of Seasonal Pack Ice, Canadian Beaufort Sea”, *Geophysical Research Letters*, Vol. 32, L24501.
- NASA, 2014a, Status of LANCE Rapid Response MODIS Images, <https://earthdata.nasa.gov/about-eosdis/news/status-lance-rapid-response-modis-images>.
- NASA, 2014b, <http://rapidfire.sci.gsfc.nasa.gov/subsets/>.
- National Ice Center, 2014, http://www.natice.noaa.gov/products/weekly_products.html.
- National Ocean Service, 2013 and 2014, <http://tidesandcurrents.noaa.gov>.

- National Snow & Ice Data Center, 2012, “Arctic sea ice settles at record seasonal minimum”, Arctic Sea Ice News and Analysis, <http://nsidc.org/arcticseaicenews/2012/09/arctic-sea-ice-extent-settles-at-record-seasonal-minimum/>.
- National Snow & Ice Data Center, 2013a, “Arctic sea ice reaches lowest extent for 2013”, Arctic Sea Ice News and Analysis, <http://nsidc.org/arcticseaicenews/2013/09/draft-arctic-sea-ice-reaches-lowest-extent-for-2013/>.
- National Snow and Ice Data Center, 2013b, “A better year for the cryosphere”, Arctic Sea Ice News and Analysis, <http://nsidc.org/arcticseaicenews/2013/10/>.
- National Weather Service, Alaska Region Headquarters, 2013 and 2014, <http://www.arh.noaa.gov/poes.php>.
- Perovich, D., S. Gerland, S. Hendricks, W. Meier, M. Nicolaus, J. Richter-Menge, and M. Tschudi, 2013, “Arctic Report Card, Update for 2013”, Sea Ice, NOAA, http://www.arctic.noaa.gov/reportcard/sea_ice.html.
- Polar Science Center, 2014a, “International Arctic Buoy Programme”, Applied Physics Laboratory, University of Washington, <http://iabp.apl.washington.edu/index.html>
- Polar Science Center, 2014b, “USIABP BeaCON Real Time Data”, Applied Physics Laboratory, University of Washington, http://psc.apl.washington.edu/UpTempO/NEWLY_DEPLOYED/USIABP_BeaCON_2014/RealTimeNEW.html
- Reece, A.M., 2009, personal communication, Shell International Exploration and Production, Inc., Houston, Texas.
- Rodrigues, J., 2009, “The Increase in the Length of the Ice-Free Season in the Arctic”, *Cold Regions Science and Technology*, Vol. 59, pp. 78-101.
- Shell Ice & Weather Advisory Center, 2014, <http://www.siwac.com>
- Stringer, W. and S. Barrett, 1975, “Ice Motion in the Vicinity of a Grounded Floeberg”, *Proceedings POAC-75*, Fairbanks, Alaska.
- Tekmarine, Inc., Polar Alpine, Inc., and Offshore and Coastal Technologies, Inc., 1985, 1984 Beaufort Sea Multiyear Ice Floe Tracking Study, AOGA Project No. 280, Sierra Madre, California, 233 pp. + appen.
- Toimil, L. and A. Grantz, 1976, “Origin of a Bergfield in the Northeastern Chukchi Sea and its Influence on the Sedimentary Environment”, *AIDJEX Bulletin* 34, December, 1976.

- Vaudrey, K.D., 1981a, "1980 Freezeup Study of the Barrier Island Chain and Harrison Bay", AOGA Project No. 129, Vaudrey & Associates, Inc., Missouri City, Texas, 32 pp. + appen.
- Vaudrey, K. D., 1981b, "Beaufort Sea Multiyear Ice Features Survey, Volume I: Field Study", AOGA Project No. 139, Vaudrey & Associates, Inc., Missouri City, Texas, 36 pp. + appen.
- Vaudrey, K.D., 1982a, "1981 Freezeup Study of the Barrier Island Chain and Harrison Bay", AOGA Project No. 160, Vaudrey & Associates, Inc., Missouri City, Texas, 30 pp. + appen.
- Vaudrey, K.D., 1982b, "Ice Cracking in Stefansson Sound during the Winter of 1981-82", Memorandum prepared for ARCO Alaska and Shell Oil Company, San Luis Obispo, California.
- Vaudrey, K.D., 1983, "1982 Freezeup Study of the Barrier Island Chain and Harrison Bay Region", AOGA Project No. 200, Vaudrey & Associates, Inc., San Luis Obispo, California, 32 pp. + appen.
- Vaudrey, K.D., 1984, "1983 Freezeup Study of the Beaufort and Upper Chukchi Seas", AOGA Project No. 246, Vaudrey & Associates, Inc., San Luis Obispo, California, 48 pp. + appen.
- Vaudrey, K.D., 1985a, "1984 Freezeup Study of the Beaufort and Upper Chukchi Seas", AOGA Project No. 282, Vaudrey & Associates, Inc., San Luis Obispo, California, 44 pp. + appen.
- Vaudrey, K.D., 1985b, "Historical Summary of the 1980-82 Freezeup Seasons and 1981-83 Breakup Seasons (Volume 1 of 2)", AOGA Project No. 275, Vaudrey & Associates, Inc., San Luis Obispo, California, 79 pp.
- Vaudrey, K.D., 1986, "1985 Freezeup Study of the Beaufort and Upper Chukchi Seas", AOGA Project No. 327, Vaudrey & Associates, Inc., San Luis Obispo, California, 49 pp + appen.
- Vaudrey, K.D., 1987, "1986-87 Chukchi Sea Ice Conditions", AOGA Project No. 346, Vaudrey & Associates, Inc., San Luis Obispo, California, 68 pp + appen.
- Vaudrey, K. D., 1987a, "1985-86 Ice Motion Measurements in Camden Bay (Vol. 1 of 2)", AOGA Project 328A, Vaudrey & Associates, Inc., San Luis Obispo, California, 70 pp + appen.

- Vaudrey, K., 1988, “1987 Summer and Freeze-Up Ice Conditions in the Beaufort and Chukchi Seas Developed from Satellite Imagery”, AOGA Project No. 360, Vaudrey & Associates, Inc., San Luis Obispo, California.
- Vaudrey, K.D., 1988a, “1987 Ice Motion Measurements in the Eastern Beaufort Sea”, prepared for Amoco Production Company and Unocal Corporation, prepared by Vaudrey & Associates, Inc., San Luis Obispo, California.
- Vaudrey, K.D., 1989a, “1988-89 Ice Motion Measurements in the Dease Inlet – Smith Bay Region Using ARGOS Buoys”, prepared for Mobil Research and Development Corporation, prepared by Vaudrey & Associates, Inc., San Luis Obispo, California.
- Vaudrey, K. D., 1989b, “Statistical Analysis of Ice Movement in the Beaufort and Chukchi Seas using 1979-87 ARGOS Buoy Data”, prepared for Unocal Science and Technology Division, prepared by Vaudrey & Associates, Inc., San Luis Obispo, California.
- Vaudrey, K., 1989c, “1988 Summer and Freeze-Up Ice Conditions in the Beaufort and Chukchi Seas Developed from Satellite Imagery”, AOGA Project No. 370, Vaudrey & Associates, Inc., San Luis Obispo, California.
- Vaudrey, K., 1990, “1989 Summer and Freeze-Up Ice Conditions in the Beaufort and Chukchi Seas Developed from Satellite Imagery”, AOGA Project No. 372, Vaudrey & Associates, Inc., San Luis Obispo, California.
- Vaudrey, K., 1991, “1990 Summer and Freeze-Up Ice Conditions in the Beaufort and Chukchi Seas Developed from Satellite Imagery”, AOGA Project No. 381, Vaudrey & Associates, Inc., San Luis Obispo, California.
- Vaudrey, K., 1992, “1991 Summer and Freeze-Up Ice Conditions in the Beaufort and Chukchi Seas Developed from Satellite Imagery”, AOGA Project No. 386, Vaudrey & Associates, Inc., San Luis Obispo, California.
- Vaudrey, K., 2007, “Effects of Recent Climate Change on Sea Ice Conditions in the Alaskan Beaufort and Chukchi Seas”, prepared for Shell International Exploration and Production, Inc., prepared by Vaudrey & Associates, Inc., San Luis Obispo, California.
- Vaudrey, K. and B. Thomas, 1981, “Katie’s Floeberg – 1980”, report prepared for the Kopanoar Partners by Gulf Research and Development Company, Houston, Texas.
- Walsh, J. and H. Eicken, 2007, “Sea Ice Changes Affecting Alaska: Offshore Transportation, Coastal Communities, Marine Ecosystems”, presented at Symposium on the Impact of an Ice-Diminishing Arctic on Naval and Maritime Operations, sponsored by National Ice Center and U.S. Arctic Research Commission, 10-12 July 2007, Washington, DC.

Ward, E.G., C. Leidersdorf, J. Coogan, and K. Vaudrey, in press, “Multi-Year Ice Incursions into the Chukchi Sea”, *Proc. Arctic Technology Conference 2015*, Copenhagen, Denmark, 13 pp.

Weather Underground, 2014, <http://www.wunderground.com>.